Regulation and function of S100 proteins in pancreatic carcinoma

Qais Ibraheem Ismaeel

Abstract

Pancreatic cancer (PC) is one of the leading causes of cancer-related death worldwide with the survival rate less than 5% because of late diagnosis. Development of PC is complex, it is promoted by the tumour microenvironment and often accompanied by inflammation. Epithelial mesenchymal transition (EMT) is an embryonic genetic program reactivated in cancer. EMT is implicated in the escape from senescence, tumour cell invasiveness, cancer metastasis, and drug resistance. EMT encompasses global reorganisation of the gene expression profiles, loss of epithelial markers and activation of mesenchymal genes. Among the genes affected during EMT are those coding for the members of the S100 protein family. Regulation and function of these genes in PC are, however, insufficiently studied.

To link S100 proteins with EMT programs in PC, expression of eleven S100 proteins, a number of epithelial and mesenchymal markers, and several EMT-inducing transcription factors was analysed in a panel of the PC cell lines and clinical samples. I found that two S100 family members, namely S100A4 and S100A6 are induced during EMT in PC. In contrast, S100A14 expression was repressed by EMT-inducing transcription factors. Consistent with this observation, S100A4&A6 and S100A14 respectively activated and repressed invasion of PC cells in zebrafish xenografts. Exosomes isolated from the actively migrated MIA PaCa-2 cells contained high levels of S100A4&A6 proteins, stimulated invasion of the slowly migrating BxPC-3 cells. In a cohort of PC samples, it was observed a trend towards enhanced expression of S100A4 protein in most aggressive tumours. The mechanism of S100A4 activation was investigated in PC. Our data show that in the course of an EMT" mesenchymal" genes, S100A4 and S100A6 are induced via IL-6 and IL-11/STAT3 pathway. Treatment of cells with the STAT3 inhibitor, Stattic, inhibited expression of these genes, and blocked cell invasion in zebrafish xenografts. It has been proposed that uncoupling inflammatory IL/STAT3 signalling from the activation of S100A4 and S100A6 genes may decrease the mortality rate of PC patients.

I

Acknowledgement

Table of Contents

III

VII

List of Figures

List of Tables

List of Abbreviations

BSA	Bovine serum albumin
cDNA	Complementary deoxy nucleic acid
CHX	Cycloheximide
Ct	Cycle threshold
DAPI	4',6-diamidino-2-phenylindole
DMEM	Dulbecco's Modified Eagle Media
DMSO	Dimethyl sulfoxide
DNA	Deoxyribose nucleic acid
DOX	Doxycycline hyclate
dpf	Day post fertilization
ECL	enhanced chemiluminescence
ECM	Extracellular matrix
EDTA	Ethylenediaminetetraacetic acid
EGF	Epidermal growth factor
EMT	Epithelial Mesenchymal Transition
EMT-TFs	EMT-Transcriptional factors
FBS	Foetal bovine serum
FGF	Fibroblast growth factor
GAPDH	Glyceraldehyde 3-phosphate dehydrogenase
GFP	Green fluorescence protein
h	Hours
hpi	Hour post injection
hpf	Hour post fertilisation
IF	Immunofluorescence
IHC	Immunohistochemistry
IL	Interleukin
JAK	Janus Kinase
kDa	kilo Dalton
KRAS	Kristen rat sarcoma virus
MAPK	Mitogen activated protein kinas
Mdm2	Mouse double minute 2 homology

MET	Mesenchymal epithelial transition
mins	Minutes
mir	microRNA
mJ	Megajoules
MMP	matrix metalloproteinases
MTT	3-(4 5-dimethylthiazol-2-yl)-2 5-diphenyltetrazoliumbromide
MVB	Multivesicular bodies
NF-κ B	Nuclear factor kappa B cells
p	Phosphorylation
PanIN	Pancreatic Intraepithelial Neoplasms
PBS	Phosphate buffer saline
PC	Pancreatic Cancer
PCR	polymerase chain reaction
PDAC	Pancreatic ductal adeno carcinoma
PenStrep	Penicillin/Streptomycin
PTU	N-phynylthiourea
qPCR	quantitative realt time polymerase chain reaction
RAGE	Receptor advanced glycation end products
RNA	ribonucleic acid
RNAi	RNA interference
rpm	Revolution per minute
RPMI	Roswell Park Memorial Institute Medium 1640
RT	Room temperature
RT-PCR	reverse transcription polymerase chain reaction
SDS-PAGE	Sodium dodecyl sulphate-polyacrylamide gel electrophoresis
sec	Seconds
Ser	Serine
siRNA	Small interfere RNA
STAT	Signal transducer and activator of transcription
TBE	Tris borate EDTA
TBS	Tris buffered saline
TBST	Tris Buffered Saline- Tween 20

TE	Trypsin/Ethylenediaminetetraacetic acid
TEM	Transmission electron microscopy
TEMED	N,N,N',N'-tetramethylethylenediamine
Tet	Tetracycline
TGF-β	Transforming Fibroblast growth factor beta
UK	United Kingdom
UV	Ultraviolet
V	Voltage
w/t	Wild type
WB	Western blot
ZEB1	Zinc finger E-box-binding homeobox 1
ZEB2	Zinc finger E-box-binding homeobox 2

Chapter 1: Introduction

1.1 Pancreatic Cancer

1.1.1 An overview of pancreatic cancer

Pancreatic Cancer (PC) is considered to be the fourth leading cause of cancer-related mortality, and the tenth most common cancer in the UK (Cancer Research UK, 2016). The lethality of PC is higher in industrialized countries, and approximately 80% of these diseases occur after the age of 60 years, with the disease being rare before the age of 45 years (Figure 1.1) (Cancer Research UK, 2016). Generally, PC is more common in men, with a male to female ratio of 1-0.6 (Ilic and Ilic, 2016). Despite advances in medical research, the overall survival rate for patients diagnosed with this neoplasia averages less than 5% (Liu et al., 2017c). According to the American Cancer Society 2016, there are expected to be some 53,000 new cases of PC in the USA. Additionally, it is also predicted to be the second leading cause of death in the USA by 2030 (Rahib et al., 2014).

There are many contributory factors that serve to make PC a life-threatening disease, such as the high dissemination of tumour cells, a lack of symptoms and diagnostic markers, diagnosis at a late stage and resistance to chemo and radio-therapy (Giovannetti et al., 2017). Many factors have been identified as major risk factors for PC including; cigarette smoking, which is the most consistent factor and accounts for about 30% of cases, while chronic pancreatitis contributes to an 18 fold increased risk (Nunes and Lobo., 2007). Hereditary pancreatitis is also associated with a 50-70 fold increased risk and PRSSI, SPINK1 and CFTR are the most common gene mutations correlated to hereditary pancreatitis. Less strong contributory factors include an unhealthy diet, alcohol consumption, obesity and other diseases such as pernicious anaemia, cholelithiasis and previous gastric surgery (Vincent et al., 2011).
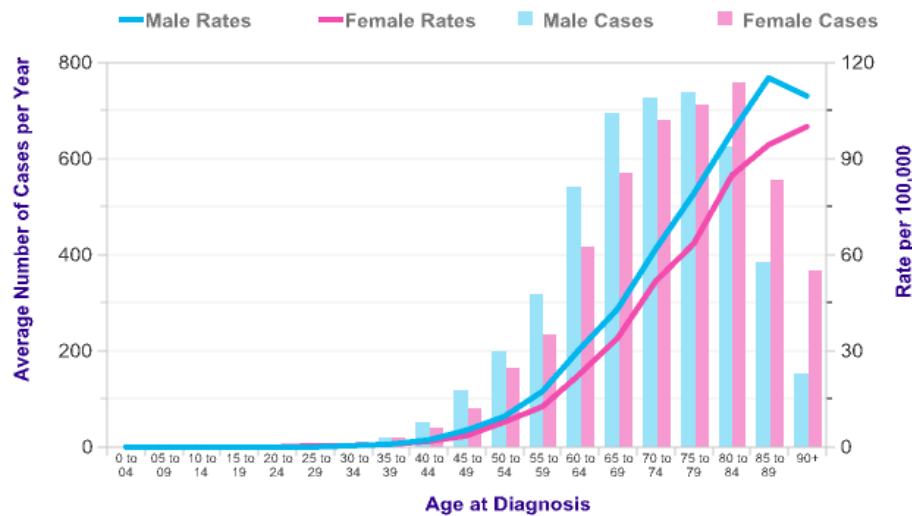
Figure 1.1 Pancreatic cancer incidences by age.

PC incidence is significantly associated with age, with increasing incidence rate in males compared to females (Cancer Research UK, 2016).

1.1.2 Diagnosis and staging of pancreatic cancer

The diagnosis of PC is usually detected at an advance stage of disease, when the tumour spreads and invades distant organs. The late diagnosis is usually due to the fact that patients with PC do not exhibit any clinical symptom at early stages of the disease (Bruenderman and Martin, 2015). Clinically, the main signs of PC may include abdominal and back pain, depending on the tumour location (e.g. the tail or head of pancreas), jaundice, indigestion, nausea and vomiting, fever, weight loss and depression (Schober et al., 2015).

Once PC has been suggested by clinical symptoms, different modern diagnosis tests are useful to confirm the diagnosis. High resolution tomography imaging, such as MRI and CT scans, are most frequently used to diagnose the pancreatic tumour and its metastasis into other organs (Robert, 2014). Additionally, a number of serum tumour markers such as DUPAN2 antibody, CAM17.1 antibody and macrophage inhibitory cytokines 1 (MIC-1) can be useful to detect PC, especially in the early stages, (Bunger et al., 2011). Detection of an elevated serum level of CA 19-9 marker is commonly used to monitor the diagnosis of patients with PC.

Nevertheless, this analysis does involve potential error because levels of CA19-9 also rise other diseases such as cholestasis and chronic pancreatitis (Duffy et al., 2010).

The staging of PC has been thought of as a key factor in selecting treatment options and monitoring a patient's outlook. It has been graded into T1, T2, T3 and T4 tumours according to the American Joint Committee on Cancer Tumour-Node-Metastasis (TNM) classification, which classifies patients histopathologically on the basis of primary tumour size (T), the number of lymph nodes involved (N) and distant metastasis (Table1.1) (Bilimoria et al., 2007). T1, T2 and T3 tumours are considered to be respectable, whilst T4 tumours are unrespectable, which affect the superior mesenteric artery or celiac axis (Hidalgo, 2010).

Table 1.1 Stages of pancreatic cancer

Stage	Tumor grade	Nodal Status	Distant Metastasis	Median survival	Characteristics
IA	T1	N0	M0	24.1	Tumor limited to the pancreas, ≤2 cm in its longest dimension
IB	T2	N0	M0	20.6	Tumor limited to the pancreas, >2 cm in its longest dimension
IIA	T3	N0	M0	15.4	Tumor extends beyond the pancreas but does not involve the celiac axis or superior mesenteric artery
IIB	T1, T2, T3	N1	M0	12.7	Regional lymph-node metastasis
III	T4	N0 or N1	M0	10.6	Tumor involves the celiac axis or the superior mesenteric artery
IV	all T's	N0 or N1	M1	4.5	Distant metastasis

1.1.3 Types of pancreatic tumours

Generally, PC can be classified into two main categories; exocrine and endocrine tumours. The exocrine tumours originate from the exocrine part of the pancreas, and represent more than 95% of pancreatic tumours (Gilliland et al., 2017). Pancreatic Ductal Adeno Carcinoma (PDAC) is the most common type of exocrine tumour, accounting for 90% of exocrine cancers (Giovannetti et al., 2017).

The less common types of exocrine tumours are acinar cell carcinomas (4%) and Cystadenocarcinomas (1%) (Tobias and Hochhauser, 2015), while adenosquamous carcinomas, signet ring cell carcinomas, hepatoid carcinoma, colloid carcinomas, undifferentiated carcinomas and undifferentiated carcinomas with osteoclast-like giant cells are also all examples of exocrine tumours (Hong et al., 2011). The endocrine tumours, meanwhile, are rare and start in the small cluster of cells producing hormones, known as Islets of Langerhans cells. These tumours are therefore called islet cell or neuroendocrine tumours (Klimstra et al., 2010).

1.1.4 Histological development of pancreatic cancer

Histologically, PC develops from the ductal epithelium, and multiple precursor lesions, and progresses to aggressive PDAC. These lesions are known as Pancreatic Intraepithelial Neoplasms (PanIN) (Hruban et al., 2000); although they can also arise from other lesions, including Mucinous Cystic Neoplasms (MCN) and Intraductal Papillary Mucinous Neoplasms (IPMN) (Cowley et al., 2013) (Figure 1.2). PDAC is the most common type of PC, representing about 90% of all malignant pancreatic tumours (Giovannetti et al., 2017). The majority of PDAC developed from PanIN lesion and it may be came from other lesions (Alexakis et al., 2004).

Sixty five percent of PDAC arises in the head of the gland, 15% and 10% in head and tail respectively, and the remaining are multifocal (Nunes and Lobo, 2007). Microscopically, PDAC can be marked as a small or tubular gland lined by small columnar-mucus secreting cells with polymorphism nuclei (Winter et al., 2006). The degree of gland formation depends on the development stages of the cancer, ranging from infiltrating single cells to well-formed gland in well differentiated cancer (Capella et al., 2011).
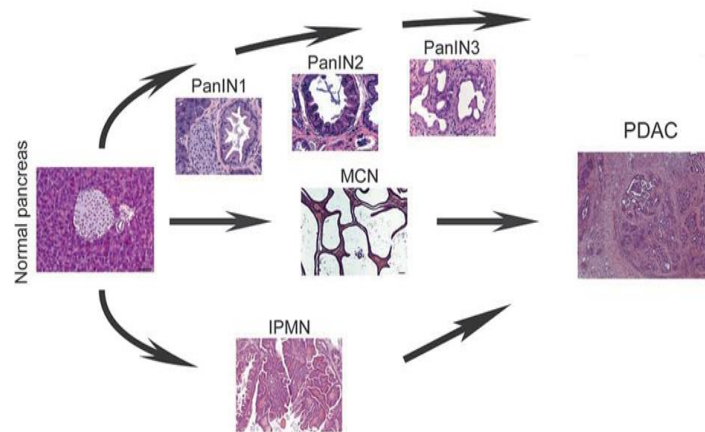
Figure 1.2 Schematic representing the progression of pancreatic ductal adenocarcinoma.
Normal tissue develops multiple precursor lesions including PanINs, MCN and IPMN, and thus, in turn becomes less differentiated to develop finally into aggressive PDAC. Adapted from (Mazur and Siveke, 2012)

1.1.5 Molecular pathology of pancreatic cancer

The molecular basis of PC is complex, and a large number of genetic alterations occur along the way of development, which make PC resistant to treatment and more lethal than other cancers. KRAS mutations is one of the most frequently event in the early stages of development and have a fundamental role in progression of PC. It occurs in up to 30 % of low grade of PanIN lesion and approximately in up to 90% of all PC cases (Hezel et al., 2006).

Telomere shortening is also considered as an early event which occurs in 91 % of PanIN (van Heek et al., 2002). Telomere is a hexameric repetitive of DNA sequences (TTAGGG) at the end of the chromosomes, which prevents fusion of the end of chromosomes and protect chromosomal stability (Moyzis et al., 1988). With each cell division, the telomeres become shorter, subsequently lose their function, termed telomere crisis. Therefore, shorter telomeres may have contributed to increase in chromosomal instability and malignant phenotype in new generation of cells (Skinner et al., 2012).

These molecular alteration is followed by inactivation of tumour suppressor gene (P16 INK4) in 85% of the moderate stage of precursor lesions, followed by inactivation of P53 (50–75%) and SMAD4 (55%) in the advanced stage of progression.

 Similarly, inactivation of BRCA2 seems to be present in 10% of late stage of PDAC (Hahn et al., 2003), (Figure 1.3).
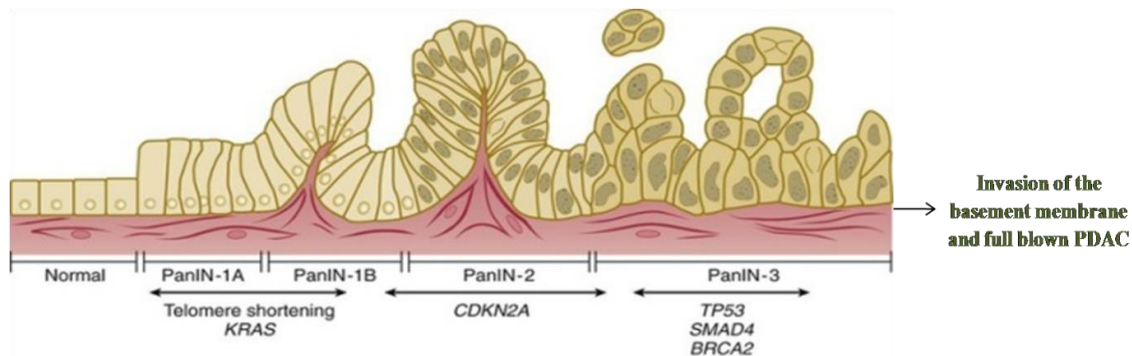
Figure 1.3 Scheme of genetic alteration involved in pancreatic cancer development.

Normal tissue develops PanINs that becomes less differentiated leading to fully development of PC. The predominant genetic events which associated with the development stages of PC are shown. Modified from (Hruban et al., 2000).

1.1.6 Pancreatic cancer metastasis

Metastasis is considered the most critical factor for PC lethality and associated strongly with poor outcome (Le Large et al., 2017). Many studies have focused on PC as an ideal tumour type to study cancer progression and metastasis for many reasons. Firstly, up to 90% of PC patients develop metastasis, mainly in the liver (76-94%), peritoneum (41-56%), lymph nodes (41%) and lung (45-48%) (Le Large et al., 2017).

Secondly, understanding of the molecular biology and genetics alterations associated with PC development is quite well defined, and patients with metastatic PC continue to maintain the primary cancer *in situ* until the time of death, making it easier to compare primary metastasis tissues within the one individual (Sohn et al., 2000). Thirdly, pancreatic tumour is characterised by the presence of highly dense desmoplastic stroma, which comprises Extracellular Matrix (ECM) and numerous cells leading to form a complex network of the tumour associated microenvironment (Jung et al., 2009, Pang et al., 2015).

Fourthly, the intracellular communication between cancer cells and the tumour associated microenvironment may responsible for high metastasis of PC (Rucki and Zheng, 2014). Recently, there is a growing body of evidences that recognises the importance of exosomes in intracellular communication and the pathology of PC.

7

Exosome cargo contains various oncogenic proteins and nucleic acid which influence cancer metastasis; including promotion of EMT, migration, invasion, chemotherapy resistance and metastasis (Robinson et al., 2016).

Finally, the majority of PC undergoes the EMT process as an essential step towards metastasis. Therefore, there are prospects for researchers to study all aspects of this process in more detail within the one type of cancer (Karamitopoulou, 2013, Castellanos et al., 2013). Figure 1.4 presents an overview of promoting related factors of PC metastasis and the most common metastatic organs.
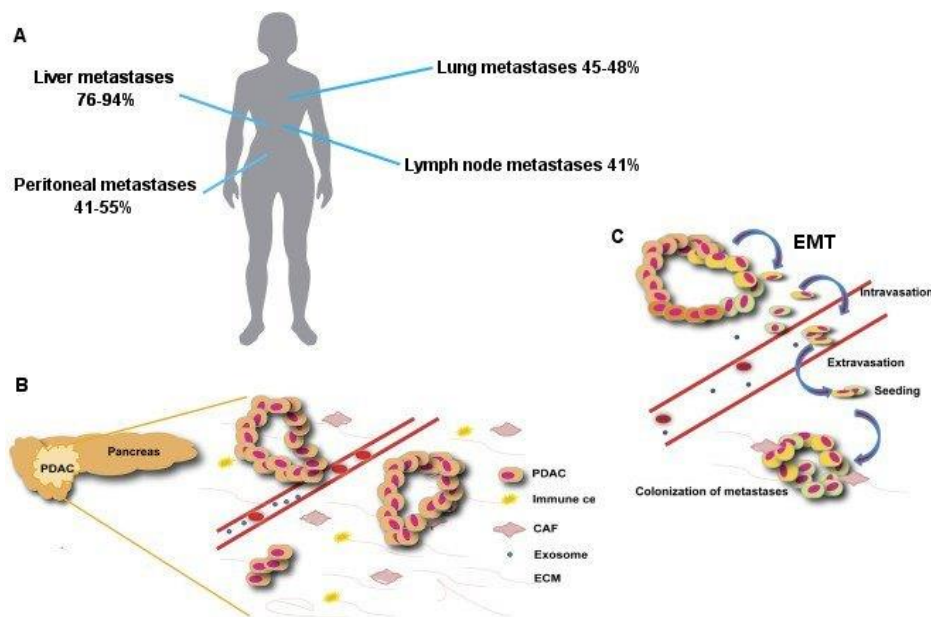
Figure 1.4 Predominant metastatic organs and promoting related factors of PC metastasis.
(**A).** Liver, lung, lymph node and peritoneal are the predominant organs for PC metastases. (**B).** Tumour associated microenvironment comprises ECM, exosomes, immune cells and cancer associated fibroblast (CAF), and the intracellular communication between these components and cancer cells essential for high metastasis of PC. (**C).** Cells that undergo EMT invade nearby tissues, intravasion into blood vascular, disseminate through blood stream and extravasation to colonize at distance site. Modified from (Le Large et al., 2017).

1.1.7 Inflammation fostering pancreatic cancer development

The last years have seen growing observations regarding the role of inflammation in development of all steps towards cancer progression including tumour initiation, invasion, migration, metastasis and formation of secondary metastasis (Hanahan and Weinberg, 2011).

It is well known that approximately 20% of all cancer cases are linked to enduring infection and chronic inflammation, and even those tumour that are not caused by chronic inflammation, are characterized by the presence of inflammatory infiltrates cells with high cytokines expression in their surrounding microenvironment which referred to "tumour elicited inflammation" (Taniguchi and Karin, 2014).

Pancreatic tumour is characterised by the presence of high dense desmoplastic stroma, which comprises of ECM and numerous other cells types including, fibroblast cells, endothelial cells, stellate cells, inflammatory cells which secret chemokines and cytokines. These immune cells and their secretion form a complex network of tumour associated inflammation which involve in development of pro-tumorigenic effect (Rucki and Zheng, 2014).

However, chronic pancreatitis could be a contributing factor to increased risk of PC and the link between the inflammation and the progression of PC has been long recognized (Holmer et al., 2014). For example, chronic pancreatitis induced by caerulein accelerate PDAC development in transgenic mice models, and the inflammation contribute to initiate EMT, invasion and metastasis in these animal models (Guerra et al., 2007, Carriere et al., 2009)

1.2 Cytokines as triggering factor in cancer development

1.2.1 Overview of IL-6 family of cytokines

Cytokines are low molecular weight secreted proteins produced by different cell types such as fibroblasts, macrophages, T helper cells, endothelial cells, Schwann cells and mast cells. These proteins have different biological functions including cell-cell communication, proliferation, differentiation, apoptosis, cell migration, metastasis and immune response. Additionally, cytokines are involved in tumour associated inflammation and anti-tumoural modulation (Zhang and An, 2007). Elevated levels of IL-6 family of cytokines have been found to be associated with poor survival and cancer progression in different tumour such as adamantinomatous craniopharyngioma cells (Zhou et al., 2017b), liver (Lanton et al., 2017), breast cancer (Barajas-Gomez et al., 2017), Cervical Cancer (Song et al., 2016), prostate cancer (Huang et al., 2016b) and lung adenocarcinoma (Tao et al., 2016).

The existing studies on tumour associated inflammation are extensive and focus particularly on some cytokines such as IL-6 family members as a major factors linking inflammation to tumour progression (Ernst and Putoczki, 2014).

The IL-6 family is one of the best well known tumour association cytokines and comprises nine soluble members including; IL-6, IL-11, IL-27, IL-31, cardiotrophin-1, cardiotrophin like cytokine, oncostatin, leukemia inhibitory factor and ciliary neutrophic factor (Garbers et al., 2012).

This group of cytokines share the same receptor subunit gp130. In both IL-6 and IL-11, gp130 shows homo dimerization (Howlett et al., 2009). It may be therefore expected that both IL-6 and IL-11 have similar or even identical biological function (Xu et al., 2016a). The binding of IL-6 and IL-11 to their unique alpha receptor subunits on the plasma membrane can result in formation of a dimeric complex which associated with gp130, generating a hexameric complex consisting of 2 molecules of ligand (IL-6 or IL-11), 2 molecules of alpha receptors (IL-6R or IL-11R) and 2 molecules of gp130 subunit (Howlett et al., 2009). Following formation of IL-ligand/IL-receptor/gp130 complex, activation of downstream signalling pathways can be fostered including JAK/STAT, MAP kinas/ PI3K/Akt, thus, in turn involve in regulation of multistep of cancer progression (Hamada et al., 2016, Bharti et al., 2016, Hideshima et al., 2001) (Figure 1.5).
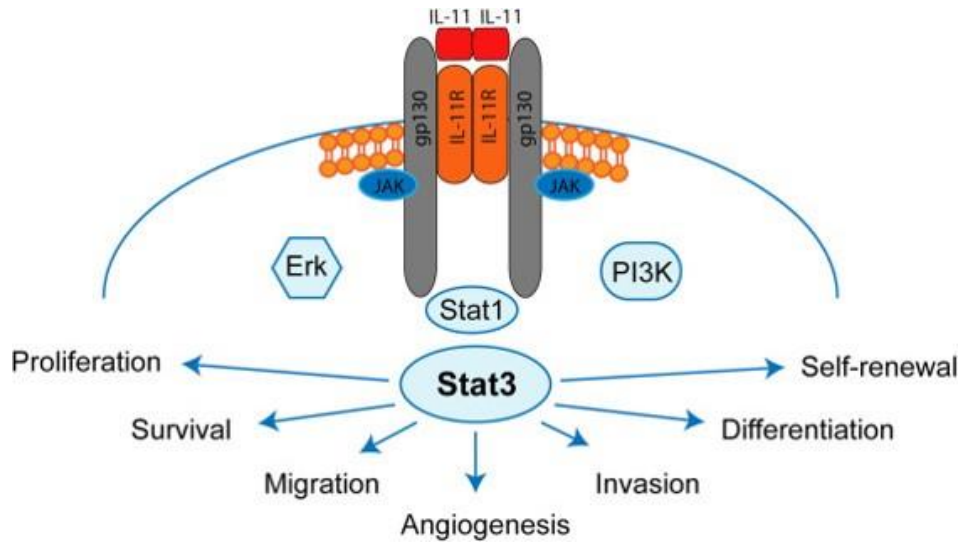
Figure 1.5 Pro-oncogenic effect of IL-11 through the IL-11/gp130/STAT3 signal transduction cascade.

IL-11 binds to its specific receptor to form a dimeric complex which associated with gp130 dimerization leading to hexameric complex formation consisting of one gp130 homodimer and two IL-11/IL-11R. Following formation of IL-ligand/IL-receptor/gp130 complex, activation of downstream signal pathway can be fostered which involve in regulation of multistep of cancer progression (Johnstone et al., 2015)

1.2.2 IL-6 family mediated activation of STAT signalling

Signal transducer and activator of transcription is a group of transcription factor proteins which regulate the expression of different gens involving in many biological and pathological process. The STAT proteins family consist of seven functional proteins including STAT1, STAT2, STAT3, STAT4, STAT5A, STAT5B and STAT6 (Mali, 2015).

Although all members of the STAT family have the same structure, each STAT protein is encoded by a different gene. Generally, the protein structure comprises of a DNA binding domain, a N- terminal domain, a coiled -coiled domain, a Src homology 2 (SH2) domain and a linking domain (Furtek et al., 2016).

STAT3 was first recognized as a DNA binding factor interacting with enhancer elements of acute phase gene promoters in hepatocytes cells stimulated by IL-6 (Akira et al., 1994). Later, it was revealed that all IL-6 family members are implicated in activation of STAT3 (Yu et al., 2009).

The first evidence describing the oncogenic role of STAT3 in human cancer came from the observation that activation of STAT3 is required for development of head and neck cancer (Grandis et al., 1998). STAT3 are regulatory activated by phosphorylation in the tyrosine 705 residue located in the SH2 domain in response to IL-6 family of cytokines and growth factors (Furtek et al., 2016).

However, Janus Kinases and transducer and activators of transcription JAK/STAT3 signalling is recognized as the main signal pathway which is initiated by the 1L-6 family and play a vital role in oncogenesis. Subsequently, activation of JAK kinases results in phosphorylation of five tyrosine residues in the intracellular domain of gp130 (Y759,Y767,Y814,Y905 and Y915), generating docking sites for STAT1, STAT3, suppressor of cytokine signalling (SOCS3) and tyrosine phosphatase (SHP-2) proteins. Phosphorylated STAT molecules will then translocate to the nucleus regulating transcription of target genes involving in control cellular process (Taniguchi and Karin, 2014), (Figure 1.6).
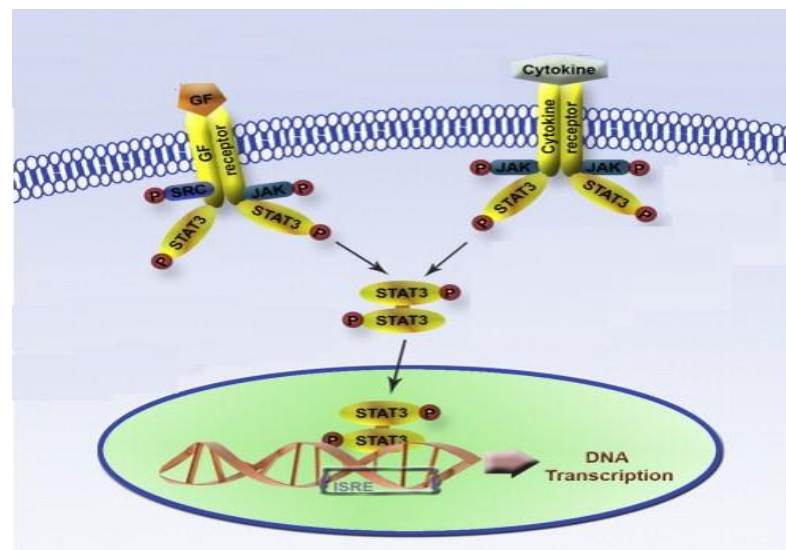
Figure 1.6 Schematic representing activation of STAT3 signalling.

Binding the IL-6 family members or growth factors to their specific receptors resulted in transmit STAT3 signalling a cross cell membrane, leading to phosphorylation, dimerization, nucleus translocation and DNA binding, thereby regulating transcription of target genes. Modified from (Siveen et al., 2014).

1.2.3 Oncogenic effect of IL-6/STAT3 signalling in pancreatic cancer development

It is well known accepted that pro-oncogenic effect of the IL-6 family are associated with activation of JAK/STAT3 signalling (Landskron et al., 2014). For example, IL-11 mediate activation of STAT3 promotes metastasis potential for hepatocellular carcinoma (Zheng et al., 2016) and drive tumorigenesis of gastric cancer (Balic et al., 2017). Evidences from numerous studies revealed that persistent activation of STAT3 pathway is important to regulate apoptosis associated genes, tumour growth, angiogenesis, and metastasis (Yu et al., 2009). Additionally, hyper activity of the JAK/STAT3 signalling is able to provide a suitable pro-inflammatory microenvironment, facilitating tumour initiation and development (Wang et al., 2017c).

Moreover, IL-6 expression mediated STAT3 activation have been found to be associated positively with EMT induction. In small lung carcinoma, IL-6 with combination to CCL2 are capable of inducing EMT via activation of STAT3 pathway. Interestingly, high expression level of IL-6 was detected in area which were expressed high level of Vimentin and low level of E-Cadherin in tumour tissue specimens (Chen et al., 2015a, Zhao et al., 2014).

STAT3 activation has been reported to be associated with development of different tumour such as breast (Aghazadeh and Yazdanparast, 2017), prostate (Jianwei et al., 2017), colorectal cancer (Zhang et al., 2017a), liver (Xia et al., 2017) and ovarian cancer (Zhu et al., 2017), and its activation detected nearly in 70% of human malignancies (Narindar et al., 2014).

The link between IL-6/STAT3 signalling and PC development is supported by animal studies, showing that IL-6 mediated activation of STAT3/SOCS3 is required to develop PC progression. Myeloid cells release significant amount of IL-6 in tumour stoma which activate STAT3 signalling and promoting PanIN development into PDAC in mice model. Inhibition STAT3 activation or IL-6 blockade attenuated PanIN progression (Lesina et al., 2011). Corcoran et al. support this finding when they found that STAT3 plays a critical role in the progression of PanINs. They also found high expression levels of IL-6 and gp130 in human PC tissue compare to normal tissue. High expression level of IL-6 family was observed in serum patients with PDAC and associated with developmental stages of tumour and lymph node metastasis (Corcoran et al., 2011).

Additionally, it has been demonstrated that JAK/STAT3 activation by IL-6 trans-signalling produced by pancreatic stellate cells promoted invasion and migration of PC through induce expression of mesenchymal proteins (Wu et al., 2017).

Fukuda et al. study found that IL-6/STAT3 activation associated with cell proliferation and MMP7 production during KRAS driver PanIN progression following chronic pancreatitis in KRAS-driven mouse model of pancreatic ductal adenocarcinoma. Produced MMP7 promote tumour growth and metastasis in mice (Fukuda et al., 2011).

Taken together, this evidence indicates the important role of STAT3 activation induced by IL-6 family in PC development.

1.2.4 Therapeutic targeting IL-6/STAT3 signalling

Due to the complexity of the pancreatic tumour environment and high metastatic feature, the effectiveness of drugs in treating PC is unsatisfactory. However, there is a large number of evidences describing the strong correlation between IL-6 family signalling pathways especially JAK/STAT3 and initiation and progression of different human cancer. Therefore, targeting activation of signalling pathways induced by IL-6 family can be considered as an excellent therapeutic target in cancer therapy (Taniguchi and Karin, 2014).

However, different approaches have been used to suppress STAT3 activation including; blocking ligand-receptor interaction, blocking upstream kinas such as JAK which are involved in phosphorylation and inhibiting STAT3 phosphorylation, proteins dimerization and transcriptional activity (Mali, 2015).

Stattic is a small non peptide molecule which selectively inhibit STAT3 activation by direct binding to SH2 domain (Schust et al., 2006), leading to supressed STAT3 phosphorylation, dimerization and DNA binding activity (Kraskouskaya et al., 2013). Stattic has displayed anti-cancer efficacy by inducing apoptosis and reducing cell proliferation. JAK/STAT3 activation was observed in endometrial cancer cells when co-cultured with cancer-associated fibroblasts. Treatment of cells with Stattic and AD412, leading to significant decreases in tumour cell proliferation (Subramaniam et al., 2016).

Exposure of gastric cancer stem cells to Stattic in the presence of IL-17 supressed the activation of STAT3 signalling and reversed STAT3 induced EMT-associated properties of gastric stem cells (Jiang et al., 2017c). In prostate cancer, Stattic mediated suppression activation of STAT3 significantly reduced the prostate cancer capacity to initiate progression of prostate adenocarcinoma and impaired tumour growth in mice mode (Han et al., 2014).

STAT3 activation in non-invasive PC cells induced via IL-6 secreted by pancreatic stellate cell enhance cell invasion and migration. Targeting of IL-6 and JAK/STAT3 signalling using IL-6 antibody or AZD1480 impaired activation of STAT3 signalling mediated tumourgenecity and tumour growth (Nagathihalli et al., 2016). Similarly, JAK/STAT3 inhibitor, AZD1480 alone or in combination with gemcitabine markedly reduced pancreatic tumour growth in mice model (Nagathihalli et al., 2015).

1.3 S100 proteins

S100s belong to a family of calcium-binding proteins which consists of more than 20 members with a low molecular weight of around 10-12kDa (Marenholz et al., 2004). The first members of the S100 family were detected in bovine brain by Moore in 1965 and are so named because they are soluble in 100% ammonium sulphate (Moore, 1965). The members of this family are present exclusively in vertebrates and their expression has been proven in a wide range of tissues. The nomenclature of S100 proteins is very complicated and there are several names for each individual protein (Salama et al., 2008).

Accordance with the established nomenclature (Schafer et al., 1995), S100 genes which clustered on chromosomes 1q21 are designated by S100A symbol followed by consecutive Arabic numbers (S100A1-S100A16). Whilst genes on other chromosomal region are designed by placing single letter behind the S100 symbol (S100P, S100Z, S100G and S100B). Only CALB3 is an exception because it was first identified as a member of the calbindin group which consist of vitamin D-dependent calcium binding proteins (Marenholz et al., 2004).

At present, it has been found that sixteen of S100 genes (S100A1-S100A16) cluster on chromosome 1q21 which are known as the epidermal differentiation complex. The remaining genes (100G, 100Z, S100B and S100P) are located on chromosomes X, 5, 21 and 4, respectively (Gross et al., 2014), (Figure 1.7).
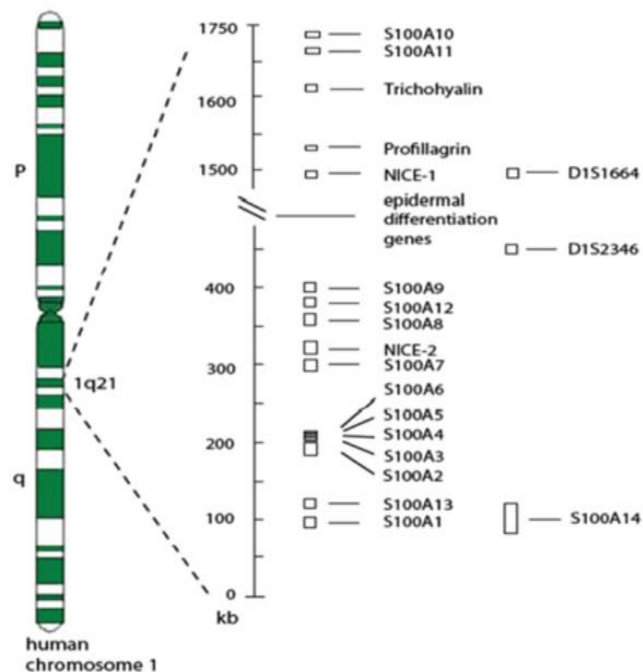
Figure 1.7 S100 genes clustered organization on chromosome 1q21.
Modified from (Heizmann et al., 2002).

1.3.1 S100 proteins structure and function

S100 proteins have two EF-calcium binding motifs and they are characterized by their ability to form heterodimers, homodimers, and oligomers. (Marenholz et al., 2004). The first EF hand motif (pseudo' or 'S100' EF-hand) is located on the N terminal and composed of 14 amino acids. This motif is specific for the S100 proteins family and arranged as helix I, loop and helix II. Whereas the second EF-hand motif (canonical EF-hand) is common to all calcium binding proteins and located on the C terminal and consist of helix III, loop and helix IV with 12 amino acids. Both motifs are held together by a short hinge region (Figure 1.8) which represent the crucial region for target interaction and consist of 10-12 residues (Gross et al., 2014).

16

The structure and functional regulation of the S100 proteins depends on calcium binding, resulting in conformational changes that reorient helix III to expose a hydrophobic cleft, forming binding site for target proteins which allow them to interact with a wide range of target proteins (Liriano et al., 2012).

Generally, calcium binding to the N terminal EF motif is weaker than binding to the C terminus motif (Rezvanpour and Shaw, 2009). Moreover, it has been shown that the biological activity of some S100 members can be regulated by binding to $Cu2+$ and $Zn2+$ rather than $Ca2+$ (Sedaghat and Notopoulos, 2008).

However, as a result of the interaction of S100 proteins with many effector proteins, they have been involved in the control of many intracellular and extracellular processes (Bresnick et al., 2015). Intracellular S100 proteins exert their activities on regulation of many cellular process including calcium homeostasis, phosphorylation, regulation of transcriptional factors, dynamics of cytoskeleton proteins, and enzyme regulation (Ji et al., 2014). Extracellularly, they act as chemo-attractants (Ambartsumian and Grigorian, 2016) or in a cytokine-like manner by binding to many transmembrane receptors such as Toll-like receptors and advanced glycation end products (RAGE), leading to the activation of specific signalling pathways, thereby regulating cellular processes such as cell cycle, differentiation, cell growth and apoptosis (Chen et al., 2014).
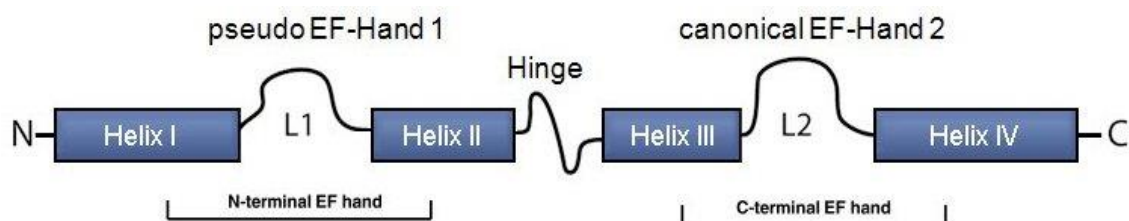
Figure 1.8 Schematic represents S100 protein structure.

Members of S100 proteins have two EF calcium binding motifs, and held together by hinge region. The first one is pseudo motif on N terminal comprise helix I, loop (L1)and helix II, while other is canonical motif which arranged as helix III, loop (L2) and helix IV on C terminal. Modified from (Rohde et al., 2010)

1.3.2 S100 proteins regulation

The expression of S100 proteins is regulated either by epigenetic mechanisms or by transcriptional activity resulting in activation of many signal pathways. Evidence suggest that DNA methylation is among the most important epigenetic mechanism which regulates the expression of many members of the S100 proteins (Lindsey et al., 2007).

The most obvious indication for this comes from the notion that treatment of non-expressing cells with methyltransferase inhibitors such as 5-aza- cytidine can lead to reactivated synthesis of certain S100 proteins. For example, re-expression of S100A2 and S100A6 was detected upon treatment with 5-aza-cytidine in both tumour-derived mammary epithelial cells (Lee et al., 1992) and HepG-2 cells (Lesniak et al., 2000) respectively. Expression of other members of the S100 proteins family such as S100A3, S100A11 and S100P have also been detected in medulloblastoma cell post DNA demethylation (Lindsey et al., 2007).

Additionally, expression of S100 proteins also regulated by activation of many signalling transduction pathways in response to different ligands. For example, S100A4 is activated downstream of many cytokines and growth factors such as TGF-β (Wang et al., 2014) , FGF (Ryan et al., 2003), EGF (Poeter et al., 2013) and IL-1β (Franco-Barraza et al., 2010). Activation of JAK/STAT3 pathways via IL-6 regulates the expression of S100A4 in rhomboid-phenotype pulmonary arterial smooth muscle cells (Liu et al., 2012) and S100A9 in Colonic Epithelial Cells (Lee et al., 2012). Similarly, IL-7 stimulates chondrocyte secretion of S100A4 via activation of JAK/STAT signalling (Yammani et al., 2009).

In colon cancer, expression of S100A4 is regulated by activation of Wnt–β-catenin pathways (Sack and Stein, 2009), whilst, S100P expression is activated as a consequence of activation of prostaglandin E2 (PGE2) receptor (Chandramouli et al., 2010). Expression of S1008 and S100A9 transcriptionally regulated in response to activation of NF-κB signalling (Nemeth et al., 2009).

Moreover, it has been found that different members of S100 proteins including S100A2 (Tan et al., 1999), S100A4 (Parker et al., 1994) and S100B (Lin et al., 2004) transcriptionally regulated by tumour suppressor P53.

Finally, expression of some S100 proteins may modulate via activation of other members of the S100 family resulting in feedback loops. For instance, in skin carcinogenesis, S100A8 and S100A9 bind to RAGE receptors and activate downstream signalling, thereby upregulating expression of these proteins resulting in a loop (Gebhardt et al., 2008).

1.3.3 The potential role of S100 proteins in cancer progression

There is a growing body of literature that recognises the importance of S100 proteins and their association to a number of human diseases such as cardiac disease, inflammation, neurological disorder as well as neoplasia (Lukanidin and Sleeman, 2012). Most notably, the relationship between S100 protein members and cancer progression has been widely investigated, since dysregulation of S100 proteins has presence in different forms of cancer.

One of the observations which linked the S100 proteins to cancer progression is the high affinity of several members to interact with receptors for RAGE. The interaction of S100 proteins with RAGE results in activation of many cellular pathways downstream of RAGE such as mitogen-activated protein (MAP) kinases, phosphatidylinositol 3-kinase (PI3K), nuclear factor NF-κB and JAK/STAT, consequently, regulating many cellular process which are implicated in cancer progression (Xie et al., 2013),(Figure 1.9).

For example, extracellular S100A4 and S100A7 proteins promote metastasis of melanoma and breast cancer via interaction with RAGE receptor (Nasser et al., 2015b, Herwig et al., 2016).

Likewise, it has been demonstrated that interaction exists between P53 and S100 protein members such as S100A4 and S100B, thus, regulating the transcriptional activities of P53 mediated differentiation, proliferation and apoptosis (Chen et al., 2014). Both S100A4 and S100B inhibit the tumour suppressor activity of P53 by inhibiting its phosphorylation (Rustandi et al., 2000, Grigorian et al., 2001), in contrast, S100A2 enhance transcriptional function of P53 (Mueller et al., 2005).

It has also been found that S100 proteins are involved in tumour metastasis through interaction with the cytoskeleton network including microtubules, actin filaments, microfilaments, tropomyosin and myosin which are proven to be mainly responsible for cell migration (Ji et al., 2014).

As previously reported that most of S100 genes cluster on chromosome lq21, the genes in this locu can be recognized easily and interfere with S100 genes during development of tumours. For that reason, abnormal expression of S100 protein has often be observed in developing stages and advanced metastasis (Marenholz et al., 2004).

Finally, it is now well established that S100 proteins are among many molecules in the tumour environment which exert their effect either by requirement of inflammation cells at tumour's site or by the activation in many cells of the synthesis of different inflammation association molecules (cytokines and chemokines), acute phase proteins and extracellular matrix molecules (Ambartsumian and Grigorian, 2016).
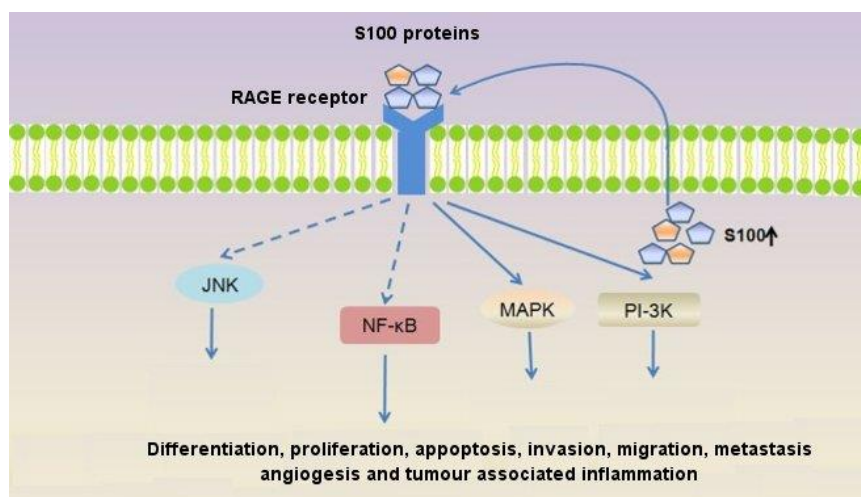
Figure 1.9 RAGE signalling triggered by S100 proteins family members.

S100 proteins secrete into extracellular space and bind to RAGE receptors, resulting in transmit signal a cross cell membrane, leading to activation downstream signal pathway such as MAPK, PI-3K, JNK and NF-kB which involve in modulating many aspects of cancer features. Modified from (Chen et al., 2014)

1.3.3.1 S100 proteins in tumour metastasis

S100 proteins are implicated in the control of many steps of tumour metastasis and some of them have been detected as metastasis markers such as s100A4. For example, siRNA mediated silencing S100A2 decreased the invasion ability of laryngeal cancer cells HEp-2 cells *in vivo* (Zha et al., 2015). Immunohistochemical analysis of 109 tumour specimens of patients with lung cancer showed that the expression level of S100A2 was significantly associated with lymph node metastasis (Wang et al., 2017b).

There is convincing evidence which show a strong correlation between S100A4 and cell invasion and metastasis in different malignant tumours. S100A4 promotes cell motility by interaction with the C-terminal domain and organizes the phosphorylation of the myosin heavy chain (Kriajevska et al., 1998) as well as disassembly of myosin filaments (Ford et al., 1997). S100A4 can also interact with annexin II and speed up the formation of plasmin, which in turn, leads to increase tumour metastasis (Semov et al., 2005).

Natarajan et al. demonstrated that S100A4 can be recognized as a potential biomarker for metastasis and recurrence in oral squamous cell carcinoma, since upregulation of S100A4 has been significantly correlated with tumour stages, metastasis and pattern of invasion and recurrence (Natarajan et al., 2014).

In another study regarding the functional role of S100A4 in cancer, Yuan et al. overexpressed S100A4 in two gastric cell lines AGS and SCM-1, and found that this expression significantly increased the invasive activity for these cells. While silencing S100A4 expression in MKN-45 and TMK-1, which displayed high levels of endogenous S100A4, resulted in decrease the migration rate but without any effect on cell survival (Yuan et al., 2014).

Defects in the expression of S100A6 led to an increase or decrease in the migration capacity of osteosarcoma cells (Luu et al., 2005, Luo et al., 2008). It has also been suggested that the ability of S100A6 to induce migration is dependent on its interaction with the tropomyosin-actin complex (Golitsina et al., 1996).

S100A7 has also been identified as a major contributing factor in inhibiting migratory behaviour in many cancer cells. For example, in aggressive triple-negative breast cancer (TNBC) cells, S100A7 was considered the proinflamatory ligand which is bound to RAGE leading to activate ERK, and NF-κB pathways' cascade and promoting cell migration and metastasis (Nasser et al., 2015b).

Like other S100 protein members, S100A8/A9 also exhibit a fundamental role during cancer progression, since Hiratsuka et al. found that lung carcinoma cells treated with a combination of S100A8 and S100A9 activated the mitogen protein kinase P38, and this caused morphological changes in cytoskeleton components which can result in formation of cell membrane extensions, possibly pseudopodia, at the leading edge of cells (Hiratsuka et al., 2006).

S100A10 may play a vital role in bringing about rearrangement of the actin complex and increasing migration of epithelial squamous carcinoma cell lines, where knockdown of the expression of this protein via siRNA approach can give rise to defects in the organization of actin filaments and thus decrease cell dissemination (Jung et al., 2010).

The results from (Liu et al., 2015) study suggest that silencing of S100A11 in HO8910 ovarian cancer cell elevate expression of E-Cadherin and downregulate Snail expression, therbey inhibit cell growth and metastasis. Recently, it has been demonstrate that S100A11 play a fundamental role in plasma membrane repair and survival of migrated tumour cells. A complex of S100A11 and Annexin A2 have the ability to facilitate the migration of cancer cell by excising the damage part of plasma membrane via polymerization of cortical F-actin (Jaiswal et al., 2014).

The extracellular activity of S100A14 has been observed in promoting cell migration through regulating the expression MMP-2 depending on activity of P53 (Chen et al., 2012). Co expression of S100A14 and S100A16 was detected immunohistochemically in human breast cancer tissues, and siRNA mediated knockdown of S100A14 and S100A16 inhibited the migration capacity of both MCF7 and SK-BR-3 breast cancer cells *in vivo* (Tanaka et al., 2015).

S100P is generally seen as a factor strongly related in promoting metastasis formation. The most likely cause of the role of S100P in cancer progression is its direct interaction with components of cytoskeleton proteins such as F-actin and non-muscle myosin IIA, subsequently increasing the migratory and invasive capabilities of tumour cells (Du et al., 2012). S100P was elevated in triple-negative breast cancer and this elevation was markedly associated with clinopotholigical stages including pattern of invasion, recurrence events and distance metastasis (Maierthaler et al., 2015).

The effective role of S100A16 in cancer progression elucidated in prostate cancer, where overexpression of S100A16 markedly increased invasion and metastasis of tumour cells via activation of AKT and ERK signalling pathways and inhibition of tumour suppressors p21 and p27, effecting their downstream factors (Zhu et al., 2016).

However, the oncogenic effect of S100 proteins family members is not limited only on promoting cancer cells migration and metastasis but also they have ability to regulate other malignant phenotypes of cancer which include aberrant cells differentiation and proliferation and abnormal apoptosis (Chen et al., 2014). Figure1.10 represents an overview of the role of members of S100 family in many aspects of cancer progression.
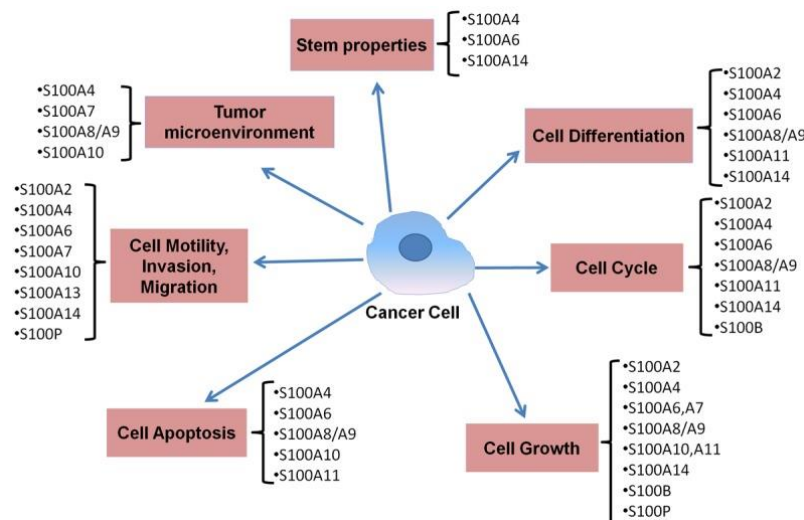
Figure 1.10 Functional role of S100 proteins family in cancer progression.

S100 proteins family members may have been important factors in regulation multistep of cancer development including cancer cells proliferation, differentiation, apoptosis, invasion, metastasis, stemness and tumour microenvironment modulation (Chen et al., 2014).

1.3.3.2 Evidence of the role of S100 proteins in pancreatic cancer progression

Several studies thus far have linked many S100 protein members with PC progression via different roles in cell proliferation, invasion, angiogenesis and metastasis, thus indicating that these proteins may be an excellent therapeutic target in PC (Ji et al., 2014).

It has been found that S100A2 can be used as a poor prognostic marker in the pathogenesis of PC (Ji et al., 2014). Analysis of data from paraffin-embedded samples concluded that expression levels of S100A2 was higher in tissue from patients with an overall survival rate higher than 1000 days than in patients with overall survival rate less than 1000 days (Ohuchida et al., 2007).

Another member of S100 proteins which has been found to be implicated in PC progression is S100A4. Many studies have demonstrated that expression of S100A4 upregulated significantly in PC compared to adjacent normal tissues, and its expression was significantly higher in poor differentiated and metastasis PC tissues than those in well differentiated and non-metastasis tissues (Rosty et al., 2002, Tsukamoto et al., 2013).

Surveys such as that conducted by Oida et al. found that 78% of surgical specimens of PC expressed high levels of S100A4 and less than 43% showed positive expression of E-Cadherin (Oida et al., 2006). This finding has been further supported by Li et al. who found that silencing with S100A4-siRNA led to a marked elevation in E-Cadherin expression and decreased PC migration properties (Li et al., 2012)

Meta-analysis of 474 patients with PC collected from the PubMed database only from studies reporting the association between expression of S100A4 and clinicopathological features after inclusive literature search, showed that expression of S100A4 is considered as a potential biomarker for lymph node metastasis and prognosis factor for patients with PC (Huang et al., 2016a).

Both S100A6 and S100P show a gradual increase in their expression to accompany the development of PC, from intraepithelial neoplasia (PanIN) precursor lesions to PDAC (Shekouh et al., 2003, Dowen et al., 2005, Vimalachandran et al., 2005).

It has been reported that S100P expression tends to be specific to PC cells and it has not been observed in chronic pancreatitis, an inflammatory disease, and this specificity can be exploited as a biomarker for early detection of PC (Ohuchida et al., 2006a). Surveys such as that conducted by (Dakhel et al., 2014) showed that S100P promote differentiation in PC cell BxPC-3, and also has ability to induce IκBα phosphorylation and matrix metalloproteinase 9 (MMP-9) secretion , thereby increasing cell migration.

S100A6 is as important as S100P in terms of its active role in the development of PC. PC cells display high frequency and intensity of S100A6 expression (Crnogorac-Jurcevic et al., 2003), whilst down regulation of its expression has a negative impact on migration and invasiveness behaviour of PC.

S100A6 can promote PC cells invasion and migration via activation of β-catenin and subsequently inducing EMT. It has been revealed that S100A6 enhances upregulation of mesenchymal markers, N-Cadherin and Vimentin, and downregulation of epithelial marker, E-Cadherin (Chen et al., 2015b).

Manipulating expression levels of S100A7 using siRNA or constructed plasmid have an effective role in PC cells invasion and metastasis. Moreover, in the same study, the immunostaining analysis of S100A7 proteins for 126 pancreatic tumour tissues and 114 adjust normal tissues showed expression of S100A7 associated with local invasion and advance tumour growth (Liu et al., 2017c).

S100A11 is considered a potential prognostic markers for patients with PC, and high expression of S100A11 in PC specimens was associated with lymph node metastasis and such expression was significantly higher than in normal tissues. (Xiao et al., 2012). It also has been found that expression of this protein upregulated during the early stages and then downregulated as cancer progressed (Ohuchida et al., 2006b).

Collectively, these studies indicate a critical role for S100 proteins in pathogenesis of PC.

1.3.3.3 S100 proteins, link between inflammation and cancer

Existing research recognizes the critical role played by the tumour microenvironment in cancer development. Generally, tumour is composed of malignant and non-malignant cells as well as extracellular component. Non-malignant cells include different types of inflammatory cells which derive from hematopoietic cell such as macrophages, neutrophils, myeloid cells and mast cells, and also other non-malignant cells such as fibroblasts, endothelial cells and stellate cells (Felix and Gaida, 2016). The cross talk between tumour cells and microenvironment components play a major role in tumour invasion and metastasis (Chikina and Aleksandrova, 2014).

The inflammatory cells release different pro-inflammatory factors such as cytokines, chemokines and S100 proteins which activate many signalling pathways involving in sequences steps of cancer progression including angiogenesis, invasion, metastasis and colonization at distant organs where secondary tumour develop (Ambartsumian and Grigorian, 2016), (Figure 1.11).

It is now well established from a variety of studies that S100 proteins are among many molecules in tumour environment which have a fundamental role in cancer progression. Numerous studies have attempted to explain the role of S100A4 in tumour environment. S100A4 is secreted by a variety of cells in tumour microenvironment including both tumour and stoma cells such as macrophages, fibroblasts, lymphocytes and myeloid cells (Chen et al., 2014). Upon releasing, this protein exerts its effect either by moving the inflammation cells into tumour's site or by activation many cells to synthesis different inflammation associated molecules (cytokines and chemokines), acute phase proteins and ECM molecules (Ambartsumian and Grigorian, 2016).

RAGE, Toll like receptor (TLR4), EGFR are considered to be the main receptors which associated with the inflammation role of S100A4. Extracellular S100A4 interacts with these receptors and activates MAPK (Dahlmann et al., 2014) and JAK/STAT (Dmytriyeva et al., 2012) pathways which represented the main proinflamatory signal transduction in cells. Furthermore, S100A4 has as strong effect on the activation of NF-κB the major inflammatory transcription factors (Zhang et al., 2014, Kim et al., 2017).

S100A7 has also been found to be involved in modulating tumour microenvironment. A study by (Nasser et al. has linked the functional role of S11A7/RAGE to inflammation and development of breast cancer. They found that interaction between RAGE receptors and S100A7 resulted in modulation of tumour microenvironment by recruitment of tumour-associated macrophages which expressed high levels of MMP9 (Nasser et al., 2015b).

S100A8/9 is one of the most frequently found proteins in tumour microenvironment which often exert their effect either by creating pro-inflammatory condition or recruiting tumour cells to the site of tumour (Foell et al., 2007, Ehrchen et al., 2009)**.** Like other members of S100 proteins, S100A8/A9 interact with RAGE receptors resulting in activation of many transduction pathway such as MAPK and NF-κB, leading to infiltrating of inflammatory cells and tumour metastasis (Turovskaya et al., 2008, Ichikawa et al., 2011)

Overall, these finding strengthens the idea that S100 proteins drive inflammation and thus enhance cancer progression.
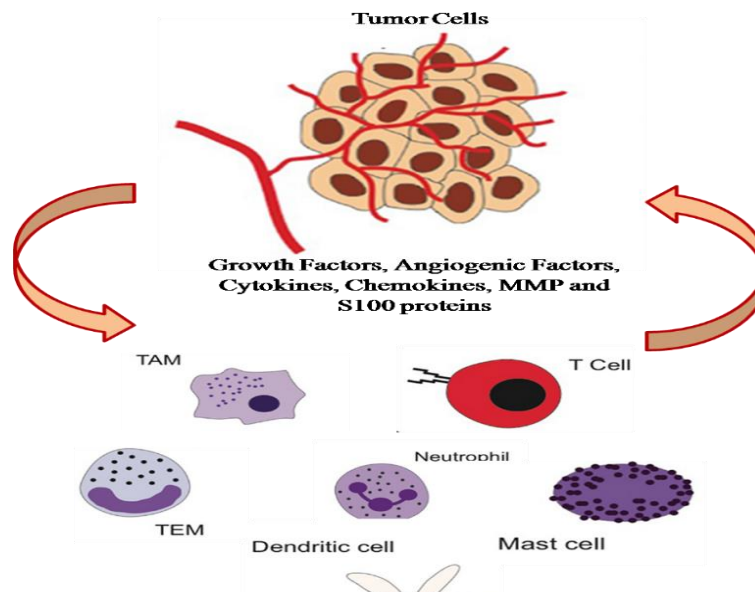
Figure 1.11 Schematic represents cross talk between tumour cells and tumour microenvironment.

Tumour associated microenvironment comprises different inflammatory and immune cells such tumour associated macrophages (TAM), mast cells, neutrophils … etc. These cells release different angiogenic and pro-inflammatory factors such as cytokines, chemokines and S100 proteins to form a complex network of tumour associated microenvironment which involve in development of pro-tumorigenic effect

1.4 Epithelial Mesenchymal Transition (EMT)

Epithelial cells differ from mesenchymal cells in many functional and phenotypical properties. Epithelial cells appear as a columnar or polygonal phenotype, arrested on the basement membrane and joined tightly to neighbouring cells by specialized membrane structures such as adherent junctions, tight junctions and desmosomes to form sheets of cells. However, under normal conditions, epithelial cells cannot escape from the layer or move away. Moreover, epithelial cells display apical–basolateral polarization and a well-organized cytoskeleton which give this type of cells their specific architecture (Schock and Perrimon, 2002).

On the other hand, mesenchymal cells have a fibroblast-like shape, anterior-posterior polarization, contact neighbouring cells only focally and also exhibit strong migratory and invasive behaviour. Epithelial cells can transform into mesenchymal cells under a process known as Epithelial–Mesenchymal Transition (EMT) (Thompson et al., 2005). EMT is a process whereby epithelial cells lose their characteristics, undergo radical changes in cytoskeleton organization and gain a mesenchymal phenotype with migratory ability (Aparicio et al., 2015).

EMT was first recognized by Elizabeth Hay in the early 1960s during embryogenesis (Hay, 1968) and according to Cold Spring Harbor Laboratory meeting in 2008 about EMT, the scientist classified EMT on the basis of biological context into three subtypes, type 1 which usually occur during developmental stages of embryo, type 2 is associated with wound healing in response to tissue repair and type 3 EMT which implicate in tumour progression and responsible for cells invasiveness and migration (Kalluri and Weinberg, 2009). Recently, attention has been paid to this phenomenon especially after revealing that more than 85% of carcinoma exhibited EMT, contributing to major steps in cancer progression including angiogenesis, invasion, dissemination and metastasis (Ribatti, 2017).

There are many molecular mechanisms that are involved in EMT induction and enable it to reach accomplishment. These include activation of many signalling pathways, forced expression of EMT-transcriptional factors (EMT-TFs), changes in cytoskeleton organization, dysregulation expression of cell-surface proteins and induced expression of extracellular matrix degrading enzymes (Kalluri and Weinberg, 2009), (Figure 1.12).
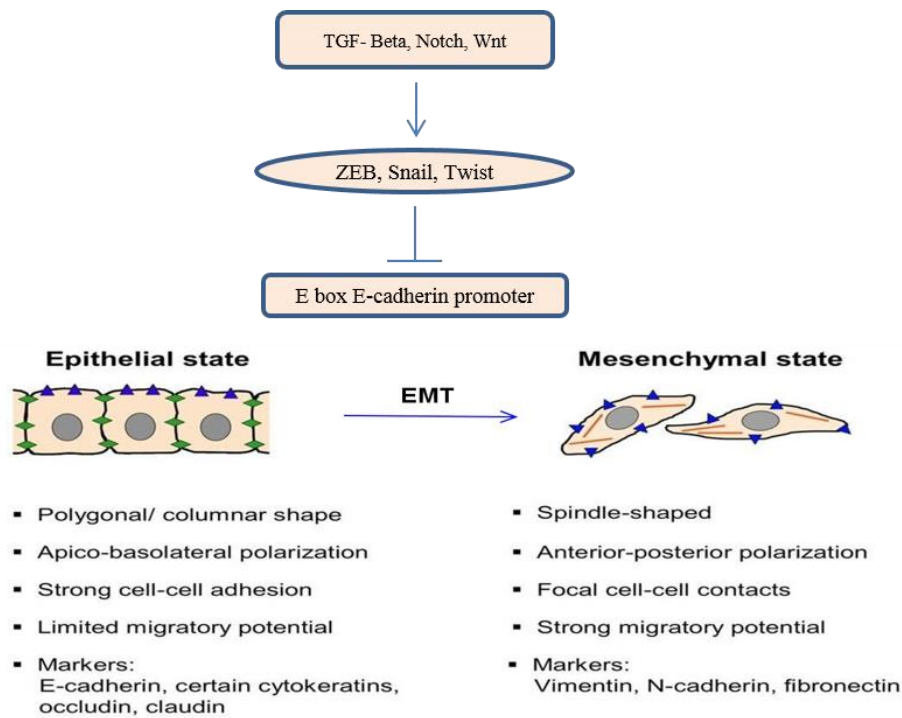
Figure 1.12 Scheme of the EMT process.

TGF-β and other signalling pathways increase expression of transcriptional repressors of E-Cadherin (ZEB, Snail, Twist) which leads to stimulation of the expression of mesenchymal markers (Vimentin, N-Cadherin, Fibronectin) and down-regulation of epithelial markers (E-Cadherin, Occludin, Claudin). Modified from (Maier et al., 2010)

1.4.1 E-Cadherin loss is an essential step for EMT

As previously described, EMT is characterised by the loss of epithelial cells and their adhesion and polarization in relation to neighbouring cells and the gaining of motile features. E-Cadherin is a transmembrane glycoprotein which acts as a central adhesion molecule between epithelial cells by interaction with E-Cadherin from adjacent cells and also associates with actin cytoskeleton via β-catenin and α-catenin (Ouyang et al., 2010) (Figure 1.13). This modulation of E-Cadherin mediated cell-cell adhesion is required for organization of cytoskeleton, maintenance of epithelium architecture, and thus prevention of cell dissemination (Yilmaz and Christofori, 2009).

Loss of E- Cadherin is one of the most important hallmarks in EMT and is accomplished by the diminished levels of the epithelial proteins (P-cadherin, ZO-1, claudins and occludins) and upregulated mesenchymal markers (Vimentin, N-cadherin and Fibronectin) (Teng and Li, 2014), (Figure1.12).

Functional loss of E-Cadherin is regulated by different mechanisms such as gene mutations, hyper-methylation and EMT-TFs (ZEB, Snail and Twist families) (Kurahara et al., 2012). Frixen et al. studied the role of E-Cadherin in a series of human cancer cell lines, including breast, lung and PC, and demonstrated that cells which were not invasive appeared to have epithelial characteristics and expressed normal levels of E-Cadherin. In contrast, those which displayed a mesenchymal phenotypes and invasive ability had reduced expression of E-Cadherin (Frixen et al., 1991). Thus far, a number of studies have revealed a strong correlation between the functional loss of E-Cadherin and tumour progression in ovarian cancer (Mise et al., 2015) prostate (Abdelrahman et al., 2017), renal cell carcinoma (Zhang et al., 2017b) and colorectal cancer (Yusup et al., 2017).
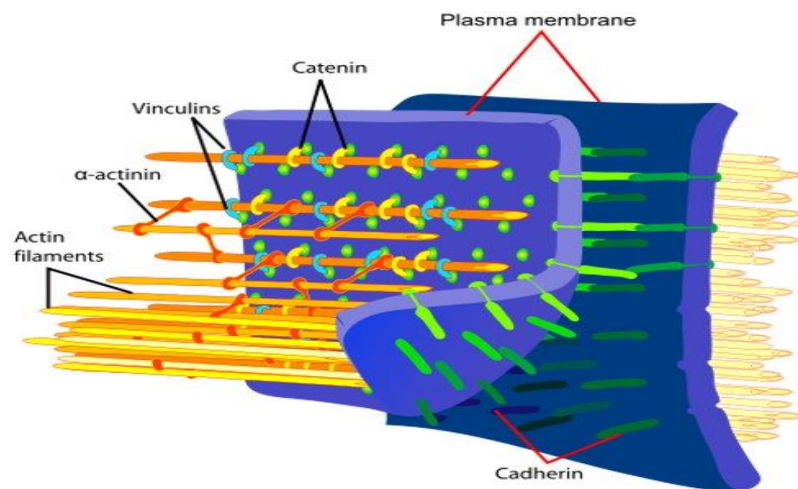
Figure 1.13 E-Cadherin mediated cell-cell adhesion.

E-Cadherin acts as a central adhesion molecule between epithelial cells by interaction with E-Cadherin from adjacent cells and associates with the actin cytoskeleton via β-catenin and α-catenin. (Modified from https://en.wikipedia.org/wiki/Cadherin)

1.4.2 EMT is a key driver for cancer metastasis

The vast majority of cancer related deaths (90%) are not the result of growth in the primary tumour, but as a result of the spread of tumour cells to distant organs, followed by formation of secondary tumours, in a process known as metastasis (Luo et al., 2017). Despite the considerable amount of research into the concept of cancer progression, patients still ultimately die due to metastatic disease (Peela et al., 2017). Metastasis can be defined as a multistep process that entails malignant cells escaping from the primary tumour, their invasion of surrounding tissues, intravasation into the vasculature, dissemination through the circulation, and finally extravasation to form macroscopic secondary tumours (Massague and Obenauf, 2016), (Figure 1.14).

The majority of tumours arise from epithelial tissue, and for malignant cells to escape from the primary tumour and gain invasive ability they have to lose their adherence to adjacent cells and the ECM, detach from the underlying basement membrane, rearrange the cytoskeleton, and eventually invade surrounding tissues. All these processes are defined under the EMT mechanism (Teng and Li, 2014). The role of EMT is not just confined to the primitive steps of cancer progression, but rather is proven to be a fundamental step at other stages, such as intravasation and extravasation (Gupta and Massague, 2006)

Tumour cells which have underwent EMT have high mobility through the tumour environment due to lose of adhesion junctions and gain migratory properties (Aparicio et al., 2015). Invasion is considered to be the second step in metastasis formation, during which tumour cells follow a chemo-attractive path across the extracellular matrix and basement membrane of surrounding tissues.

 The cells that undergo EMT begin to produce large quantities of a specific matrix degradation enzyme called matrix metalloproteinase (MMP) (Hotary et al., 2006). Activation of this enzyme facilitates invasion of tumour cells into blood vessels (intravasation) which attach directly to the tumour mass or close to the leading edge (Lentini et al., 2013).

The invasion cells which enter the blood stream gain specific futures such as express of VE-cadherin, allowing them to interact with endothelial cells and require passage through an endothelial cell junctions to exit into a new tissue (through extravasation) (Labelle et al., 2008).

For effective macro metastasis at distant sites, tumour cells undergo Mesenchymal Epithelial Transition (MET) to change back from a mesenchymal to an epithelial phenotype, which allows cells to adhere to the new tissue and develop into secondary tumours (Hugo et al., 2007).
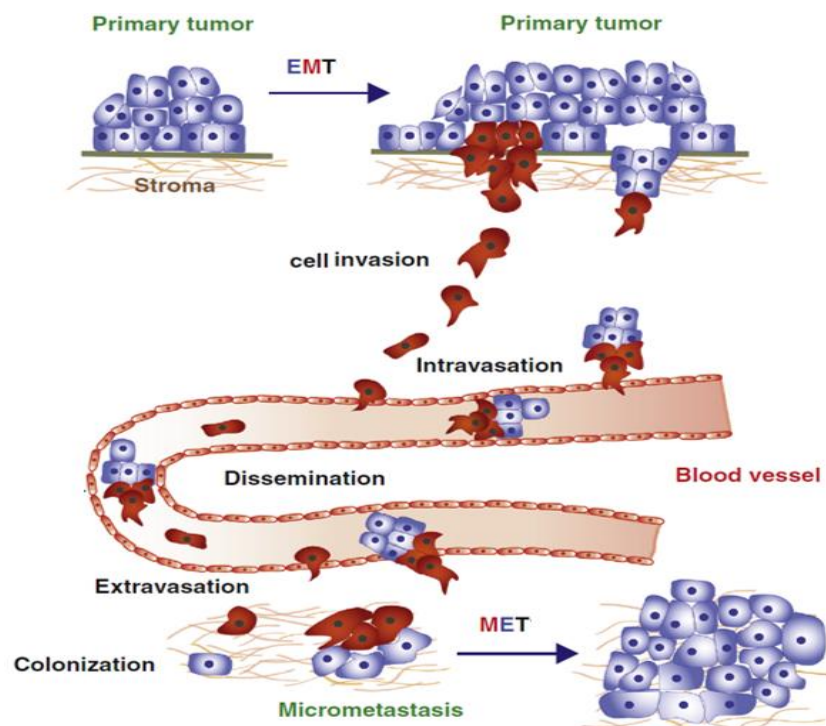
Figure 1.14 Scheme represents multistep of metastasis cascade.

Cells released from the primary tumour and invade nearby tissues, intravasasion into blood vascular, disseminate through blood stream and extravasation to form micro metastasis at distance site. Adapted from (Diepenbruck and Christofori, 2016).

1.4.3 EMT-Triggering factors and signalling pathways

EMT can be triggered either by intrinsic stimuli that arise from activation of different oncogenes such as K-RAS mutation (Edme et al., 2002) and overexpression of proto-oncogene receptor tyrosine-protein kinase (c-erbB2) (Jenndahl et al., 2005) or by extrinsic factors that emerge from microenvironment (Shih and Yang, 2011). Activation of receptor-mediated signalling occur in response to ligands in surrounding microenvironment which representing by soluble and growth factors (TGF-β, EGF, Hedgehog and Wnt) inflammatory cytokines (interleukin and tumour necrosis factor), and extracellular matrix component (e.g. hyaluronic acid and collagen) (Thiery et al., 2009). The majority of these signalling cascades can result in activation of EMT-TFs which mediate repression of epithelial cell adhesion proteins such as E-Cadherin or β-Catenin (Cervantes-Arias et al., 2013).

1.4.4 EMT-Transcriptional factors (EMT-TFs)

Many genes which involved in regulation of cell-cell contact, mesenchymal differentiation and cell invasion and migration are altered transcriptionally during EMT process (Yang and Weinberg, 2008). There are two well-studied EMT-TFs including zinc finger proteins (Snail, Slug, ZEB1 and ZEB2) and basic helix loop helix (Twist1 and Twist2) (Smit and Peeper, 2010). Activation of these EMT-TFs mediated by activation of EMT-related signalling in response to different ligands such as TGF-β, cytokines and hypoxia (Samatov et al., 2013). ZEB1 and Snail families of transcriptional factors exert their effect by repressing the expression of the central adhesion molecule E-Cadherin via interaction with specific sequences (E-box) of the E-Cadherin promoter while promoting the expression of genes involved with cell motility and migration (Ouyang et al., 2010), (Figure1.12). The activity of these genes in inducing EMT is not only restricted to repression of E-Cadherin but have also been shown to downregulate other proteins of the adherent junctions, such as desmoplakin, occludin, crunbs3, connexions 26 and desmoglein (Savagner et al., 1997, Vandewalle et al., 2005). Unlike other transcriptional factors, Twist represses E-Cadherin expression indirectly by binding to a second bHLH to form a dimer and then interacting with the E-box of the E-Cadherin promoter (Rose and Malcolm, 1997)

There is a large volume of published studies describing the role of these factors in the pathologies of malignant forms of many cancers. For example, upregulation of RPB5-mediating protein and downregulation of connexion 32 facilitate cell invasion and metastasis of hepatocellular carcinoma by modulation the expression of Snail (Yang et al., 2017). High expression level of Slug have been found to be implicated in cancer cells invasion and migration, metastasis, high tumour grade and poor survival in oral squamous cell carcinoma and glioma (Xue et al., 2017, Zhang et al., 2017c).

qPCR analysis of RNA extracted from tissue specimen from 35 patients with bladder cancer showed high expression level of ZEB1 in tumour tissues compared to healthy adjacent tissues, and its expression significantly associated with tumour size (Mahdavinezhad et al., 2017). On the other hand, over expression of ZEB2 was closely related to metastasis, high tumour grade and poor prognosis in many cancers, including oral squamous cell carcinomas (Maeda et al., 2005), pancreatic cancer (Kurahara et al., 2012), colorectal cancer (Kahlert et al., 2011), non-small cell lung cancer (Miura et al., 2009) and hepatocellular carcinoma (Cai et al., 2012a).

Twist expression has been found to be strongly related to EMT development, metastasis and cancer growth in colorectal cancer (Abdelmaksoud-Dammak et al., 2017), thyroid cancer (Anelli et al., 2017), non-small cell lung cancer (Zhou et al., 2017a), prostate cancer (Lyu et al., 2017) and breast cancer (Jiang et al., 2017b).

1.4.5 The role of EMT in pancreatic cancer progression

The ability of PC cells to disseminate and metastasise in the early stage is the main cause for their lethality. There is much evidence to suggest that this phenomenon may be due to the ability of cells to undergo EMT (Karamitopoulou, 2013, Castellanos et al., 2013). It has been found that more than 70% of primary pancreatic tumours which display mesenchymal properties can metastasise into another organs such as the liver and lung (Rasheed et al., 2010, Dangi-Garimella et al., 2012).

Moreover, overall poor diagnosis and undifferentiated phenotypes of PC have also been linked to the presence of EMT (Masugi et al., 2010). Research focused on elucidating the correlation between PC and EMT have shown forced expression of EMT markers such as ZEB1 (Krebs et al., 2017), Twist (Chen et al., 2016), N-Cadherin (Li et al., 2016b), and Vimentin (Lahat et al., 2014) in the tissue of patients with PC but not in normal pancreatic tissues.

Interestingly, the vast majority of PC cells have been shown to express at least one of the EMT-TFs. One major study found that 78% and 50% of resected PDAC specimens displayed positively to Snail and Slug respectively, and their expression appear to be strong mediators of E-Cadherin repression, metastasis enhancement and drug resistance (Hotz et al., 2007). In a survey to study the expression profile of EMT associated markers and their correlation with the clinicopathological features for patients with PC, it was found that high expression levels of Snail, ZEB1 and Twist mRNA in tumour cells at the invasive front of cancer was correlated with distance metastasis (Galvan et al., 2015).

To provide more clarification about the role of EMT in the prognosis of PC, a study conducted by Yamada et al. 2013 in which E-Cadherin and Vimentin staining were performed on 174 surgical specimens, found that patients with epithelial tumours had an overall survival of 40.2 months compared to 13.7 months for patients with mesenchymal tumours (Yamada et al., 2013). Furthermore, in mutant K-RAS and P53 mouse model, ZEB1 played a critical role in formation of precursor lesion and metastasis of PC. Depletion of ZEB1 expression correlated with downregulation of other EMT markers such as ZEB2, Snail and Slug and reduce grading, migration and distance metastasis of PC (Krebs et al., 2017).

Recently, various steps which mediate cancer formation and metastasis of PC, such as increased motility, angiogenesis and metastasis, have been associated with activation of Twist. For example, Twist expression status analysis by immunostaining and immunoblot for PC tissues and cells showed that more that 70% of tissues were stained positive for Twist and expression levels of Twist protein associated with tumour node metastasis and advance stages (Li et al., 2016a).

P-Cadherin is among well-known genes which strongly activated in the vast majority of PDAC (Taniuchi et al., 2005). In some tumours, P-Cadherin act as a tumour suppressor such as melanoma and hepatocellular carcinoma, while has opposite effect in other tumours like, bladder and prostate (Vieira and Paredes, 2015). Immunolabelling showed that approximately 50% of pancreatic tumour tissues were stained positive for P-Cadherin, and knockdown its expression by siRNA reduced invasion and migration of PC cells (Sakamoto et al., 2015). In contrast to Taniuchi et at. study, they revealed that overexpressed of P-Cadherin in P-Cadherin-deficient cell increased the migration ability of cells (Taniuchi et al., 2005).

In case of E-Cadherin, immunohistochemical analysis of invasive murine PanIN lesions derived from KRAS mouse model showed high expression levels with cell membrane-localization of E-Cadherin in 3 and 9 months old mice. Additionally, forced expression of E-Cadherin was detected in PanIN invasive cell lines derived from mice, and its expression correlated negatively with Slug expression (Stark et al., 2015).

In general, therefore, there seems to be a strong association between the presence of EMT factors and PC and the present study will provide additional evidence with respect to this correlation.

1.4.6 EMT modulates the expression of S100 proteins

In recent years, it has been hypothesized that a relationship exists between S100 protein members and the EMT process. The first systematic study to connect the two strategies was derived from a study by Strutz et al. on renal fibrosis, in which S100A4 was detected as an active Fibroblast-Specific Protein and it subsequently became known as FSP (Strutz et al., 1995). Since then it has been revealed that transfection of the epithelial cells lining the proximal tube in the human kidney with S100A4 leads to induction of EMT. In addition, when S100A4 expression was downregulated via RNA interference, these cells could not complete cytokine-induced EMT (Schneider et al., 2008).

Much evidence has emerged from previous research to indicate that there is association between S100 proteins and EMT. Firstly, remodelling of cytoskeletal dynamics which occur during EMT and the subsequent increase in migration and invasive behaviour in many cells systems are a result of interaction of S100 protein members such as S100A4, S100A6, S100A7, S100A8/9, S100A10 and S100P with cytoskeleton proteins (Kriajevska et al., 2000, Golitsina et al., 1996, Hiratsuka et al., 2006, Jung et al., 2010, Du et al., 2012).

Secondly, an inverse correlation has been identified between E-Cadherin and members within the S100 family including S100A2 (Naz et al., 2014), S100A4 (Garrett et al., 2006, Zhai et al., 2014), S100A6 (Li et al., 2014) , S100A14 (Wang et al., 2015b) and S100A16 (Zhou et al., 2014).

Thirdly, given the assumption that TGF-β is the major inducer for EMT, members of the S100 family such as S100A2 and S100A4, which mediate TGF-β signalling pathways, can lead to conversion of epithelial cells into mesenchymal cells through regulation of the expression of E-Cadherin (Naz et al., 2014, Techasen et al., 2014).

To date, there are few studies that have investigated the association between S100 family members and EMT process. S100A6 can promote PC cell invasion and migration via activation of β-catenin and subsequently induction EMT. It was showed that S100A6 enhanced upregulation of mesenchymal markers, N-cadherin and Vimentin, and downregulated the epithelial marker E-Cadherin (Chen et al., 2015b).

A study by Zhou et al. revealed that over expression of S100A16 induced EMT and enhanced invasion of breast cancer MCF-7 in Notch1-dependent manner (Zhou et al., 2014). The results from Liu et al. study suggests that silencing of S100A11 in HO8910 ovarian cancer cell elevated expression of E-Cadherin and downregulated Snail expression, consequently inhibiting cell growth and metastasis (Liu et al., 2015).

An implication of this is the possibility that there could be a strong correlation between the S100 protein family and EMT.

1.5 Exosomes: biogenesis, internalisation and composition

Exosomes are small cell derived membrane vessels (30-100nm dimeter) secreted by almost all cells and present in virtually all body fluid including urine, semen, blood, saliva and cerebrospinal fluid (Whiteside, 2016). Exosomes were first identified in immature red blood cells, reticulocytes by Trams et al. in the early 1980 (Trams et al., 1981). Exosomes are formed from inward budding from multivesicular bodies (MVB), and release to extracellular space in exocytosis manner when MVB fuse with plasma membrane (Fu et al., 2016). Secretion of exosomes to extracellular space are regulated by different factors such as calcium signalling, P53 and ceramide synthesis (Yu et al., 2015).

Upon release, exosomes may be fused with nearby cells or transferred through systemic transport to distance recipient cells where they may mediate activation of signalling pathways and different biological activities such as immunregulation, cancer progression and drug resistance (Syn et al., 2016).

The uptake of exosomes by target cells could be through different mechanisms including direct interaction with cell surface receptors, direct fusion with the cell membranes and endocytosis by phagocytosis (Zhang et al., 2015b), (Figure 1.15).

Exosome cargo include various biomolecules such as proteins, nucleic acid, micro RNA, lipids, genetic material and non-coding RNA which can be transmitted with exosomes to the target cells (could be deleted).

Proteins are the most prominent molecules in exosomes which include different sets of proteins such as; cytoplasmic proteins (Heat shock proteins), membrane associated proteins (CF63, CD81, tetraspanin families of proteins), proteins required for transportation and fusion (Rab, GTPases, Alix), cytoskeleton proteins (myosin, tubulin) and proteins that involved in activation of signalling pathways (Wnt and Notch) (Azmi et al., 2013), (Figure 1.15).

Additionally, exosome cargo is enriched with various cell specific proteins which depend on cellular origin. For example, exosome derived from dendritic cells and B lymphocytes contain both class of major histocompatibility complex antigens (MHC) (Denzer et al., 2000), and those from T cells carry Fas ligand which is associated with apoptotic program of T-cells (Cai et al., 2012b).
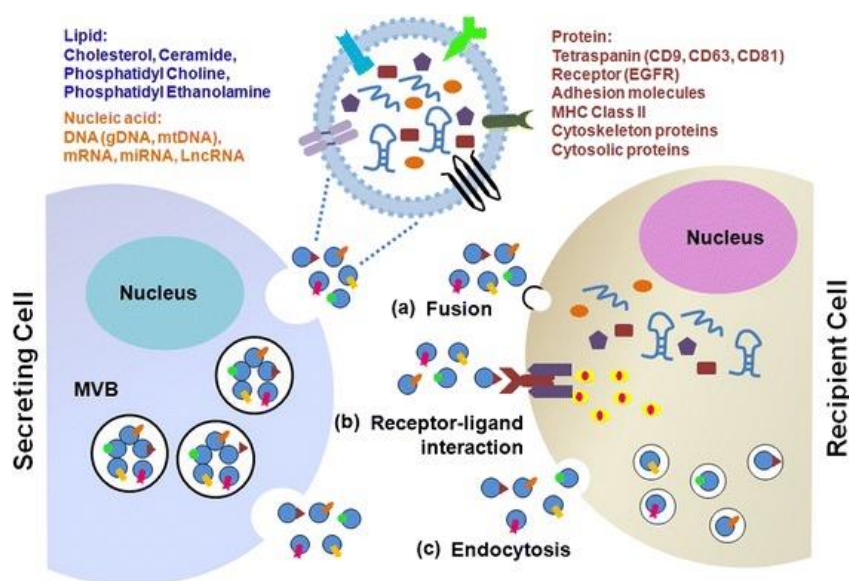
Figure 1.15 Biogenesis, composition and internalisation of exosomes.

Exosomes are formed from inward budding from MVB, and release to extracellular space when MVB fuse with plasma membrane. Shedding exosomes transmit a various biomolecules such as lipids, proteins, nucleic acids soluble factors and proteins associated signalling to recipient cells. Uptake of exosomes by recipient cells could be through different mechanisms including; direct interaction with cell surface receptors, direct diffusion with the plasma membrane and endocytosis by phagocytosis (Zhang et al., 2015b).

1.5.1 The emerging roles of exosomes in tumour progression

There is a growing body of evidences that recognises the importance of exosomes in cancer pathology. Exosome cargo contains various oncogenic proteins and nucleic acids which modulate the activity of target cells and thus influence a multistep of cancer progression including promotion of EMT, differentiation, migration, angiogenesis, metastasis and chemotherapy resistance (Robinson et al., 2016). For example, exosomes derived from KRAS mutated colon cancer cells carry various cancer promoting proteins such as KRAS, EGFR and integrin to healthy recipient cells, leading to perverse activation of KRAS in recipient cells (Demory Beckler et al., 2013).

There are many mechanism highlighting the role of exosomes mediated tumour progression. Firstly, tumour derived exosomes induce EMT process in tumour epithelial cells by providing autocrine and paracrine signal within tumour microenvironment, thereby facilitating cells invasion and intravasasion into blood circulation.

Secondly, exosomes are transmitted to distance organs and initiate pre-metastatic niche where migratory cells extravasate and colonise. Finally, exosomes activate inflammation response elements and modulate tumour associated inflammation (Syn et al., 2016).

Recently, it has been demonstrated that exosomes carry appreciable amount of EMT driver factors such as MMPs, miR-100, Notch, hypoxia inducible factors, soluble factors and cytokines and diverse transcriptional factors which regulate EMT-related morphological and molecular changes (Vella, 2014). Treatment of nasopharyngeal cancer cells with MMP-13 containing exosomes purified from the same cell line induced EMT in an autocrine manner with evidence increasing expression of Vimentin and N-Cadherin and reducing expression of E-Cadherin, thus facilitating cancer cell migration (You et al., 2015). Similar finding for EMT induction and increasing the migration of cells was observed in oesophageal cancer cells after treatment with irradiated oesophageal carcinoma-infiltrating T- Cell exosomes (Min et al., 2017).

Exosomes could be a contributing factor to stimulate many signalling pathways by transferring required proteins for signal activation such Wnt (Gross et al., 2012) and Notch-4 (Sheldon et al., 2010) in both tumour and stroma cells.

Exosomes derived from tumour cells have ability to drive recipient cells to secret multiple proinflamatory cytokines and growth factors, which are the necessary components for stimulation or impairment immune and inflammatory cells. Exosomes released by prostate cells underwent hypoxia carry proinflamatory cytokines IL-6 and tumour necrosis factor (TNF) and MMP2 and MMP9 enzymes which promote cancer cell invasion and metastasis (Ramteke et al., 2015).

In term of drug resistance, exosomes derived from cancer associated fibroblasts after treatment with gemcitabine increase proliferation and chemoresistance of recipient cells by inducing expression of Snail. Exposure of gemcitabine-treatment cancer associated fibroblasts to exosomes release inhibitor, GW4869, supress survival in co-cultivated epithelial cells (Richards et al., 2017).

In case of PC, data from several sources have identified the role of exosome in PC progression. For example, exosomes containing CD44 promoted soluble matrix formation which induced cancer metastasis and settlement in lung and lymph node in transgenic rat pancreatic adenocarcinoma BSp73ASML (Jung et al., 2009). Similar, exosomes with high level of miR-155 may have contributed to promote cancer invasiveness by promoting conversation of normal pancreatic fibroblasts to tumour associated fibroblasts (Pang et al., 2015).

In a recent survey published in nature cell biology journal, Costa-Silva and his colleagues, demonstrated that pancreatic ductal adenocarcinoma derived exosomes promoted pro-metastatic niche formation in liver. PDAC-derived exosomes were uptake by - kupffer cells leading to increase secretion of TGF-β, which in turn induced hepatic stellate cells to secret fibronectin into extracellular space. This fibronectin recruited neutrophils and bone marrow derived macrophages to produce tumour associated cytokines, thus promoting pre metastatic niche formation in the liver (Costa-Silva et al., 2015).
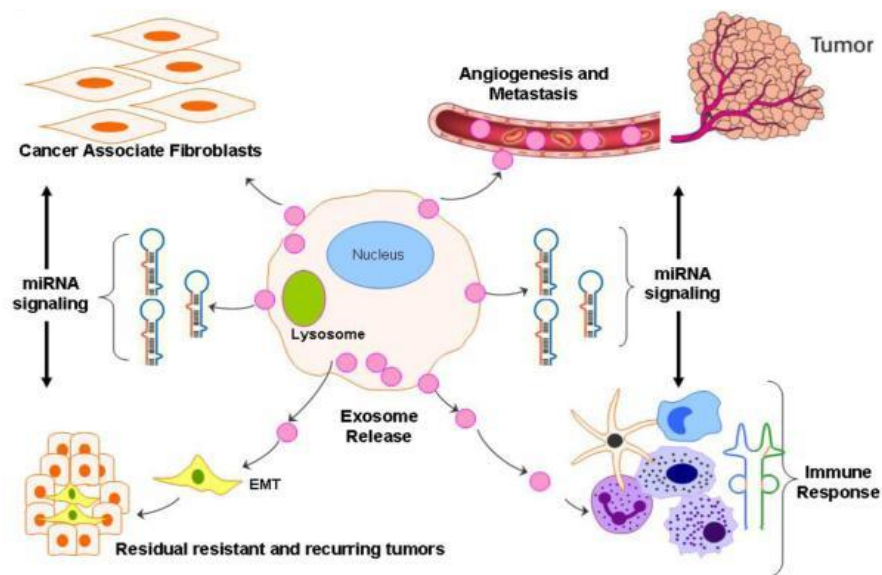
Figure 1.16 Exosome mediates tumour growth from EMT to escape from immunosurveillance.

Exosomes play a vital role in intracellular communication and they transfer functional cellular components to recipient cells resulting in activation many signalling pathways which involved in EMT promotion, invasion, angiogenesis, and metastasis and drug resistance. Additionally, exosomes could also modulate and interact with immune and stromal cells, leading to tumour escape from immune surveillance (Azmi et al., 2013).

1.6 Tumour suppressor P53

P53 is a transcription factor which act as a tumour suppressor. The activation of P53 resulting from cellular condition stress such as hypoxia and DNA damage, a consequence of this activation is regulate the transcription of different genes such as BAX, Cyclin G, p21, PUMA, Mdm2 which contribute to regulate many cellular process including; cell cycle, apoptosis, repairing DNA and cellular metabolism (Ko and Prives, 1996). P53 mutations has been reported in more than 50 % of all human malignancies (Hollstein et al., 1994), and the most frequent mutation is missense that occur in a single allele which companied with the loss of other allele (Rozenblum et al., 1997).

In PC, P53 mutations were detected in 50-75% of PDAC (Redston et al., 1994, Pellegata et al., 1994). Immuhistochemical analysis of P53 demonstrated that more than 12 % of histological advanced lesions appeared to be positive for P53 overexpression compared to low grade lesions which were negative. This observation indicated that P53 mutation is one of the late molecular event during PC development (DiGiuseppe et al., 1994).

Stabilization of P53 protein is one of the most important mechanism for regulating the functional role of P53. The main key to this process is E3 ubiquitin-protein ligase mouse double minute 2 homolog (Mdm2) which interact with and suppress the transcriptional function of P53 (DiGiuseppe et al., 1994). Additionally, P53 can be stabilized via posttranslational modifications such as acetylation, methylation and SUMOylation, phosphorylation (Olivos and Mayo, 2016). For instance, P53 stabilization occur via phosphorylation of the N-terminus at amino acid site Ser^{15}, Ser^{20}, Ser^{33}, Ser^{37}, Ser^{46}, Thr^{18} and $Th^{81,}$ thus blocking the interaction of P53 with Mdm2.

The functional role of P53 binding DNA can also be activated by phosphorylation in C-terminus at Ser^{315} and $Ser^{392.}$ Furthermore, SUMOylation at Lys^{386} and Acetylation at Lys^{320}, Lys^{373} has also been detected at this terminus (Barak et al., 1993, Moll and Slade, 2004).

Several members of S100 proteins family such as S100A2 (Mueller et al., 2005), S100A4 (Grigorian et al., 2001), S100A6, S100A14 (Chen et al., 2012) and S100B (Wilder et al., 2010) have been found to interact with Mdm2. S100A4 (Berge and Maelandsmo, 2011) and S100B (Wilder et al., 2010) interact directly with P53 and promote its degradation.

It is notable that P53 binding sites have been detected in promoter region of several members of S100 proteins suggesting that implication of S100 proteins in promoting cancer metastasis may be contributed to their interaction with P53-dependent apoptosis. This may explain why expression of some members of S100 proteins increased in tumour cells with compared to normal cells (Maletzki et al., 2012).

1.6.1 Contribution of P53 to EMT

P53 inactivation has been found to be associated with modulation of stemness in undifferentiated and embryonic cells (Spike and Wahl, 2011). In term of cancer, P53 is linked to EMT and cancer stemness (Mizuno et al., 2010). Regulatory connection between tumour suppressor P53 and family members of miRNA mediated EMT has been investigated (Dong et al., 2013). Kim et al. study showed that P53 unregulated the expression of miR-200 and miR-192 family members in hepatocellular carcinomas cell lines; thus, in turn repress ZEB1 and ZEB2 activation (Kim et al., 2011).

Similarly, wild type (w/t) P53 regulate expression of miR-200 and miR-34 transcriptionally, generating reciprocal feedback loops to suppress EMT-transcriptional factors ZEB1 and Snail (Chang et al., 2011, Kim et al., 2011). Furthermore, Twist can suppress $p19^{ARF}$ transcription which mediate P53 activation by inhibition of Mdm2.

Twist is also able to modulate P53 by the transcriptional repression of tumour suppressor p19ARF, which regulate apoptotic pathway responding to Myc (Maestro et al., 1999).Regulation of the expression of P53 related proteins has also been found to be associated with EMT program. Expression of P63 which is a member of the P53 family is downregulated in squamous cell carcinoma during Snail induced EMT (Higashikawa et al., 2007).

1.7 Zebrafish as an innovative animal model for human cancer

Over the past few years, visualising tumour progression *in vivo* has been routinely performed in mouse models. Recently, xenotransplantation of human tumour cells into zebrafish provided an exciting opportunity to advance the understanding of tumour proliferation (Zoni et al., 2017), invasion and metastasis (Zhong et al., 2017), angiogenesis (Zhang et al., 2016), tumour-host cells interaction (Vazquez Rodriguez et al., 2017) and cancer stemness (Chen et al., 2017)

Zebrafish embryos possess many morphological and physiological features which distinguish this animal from other conventional animal models making them as excellent *in vivo* model for cancer research (Figure 1.17).

For example, the visual clarity of zebrafish embryo can be exploited by the use of fluorescently labelling cancer cells and advance imaging technique to visualise cancer progression in the living animal (Blackburn and Langenau, 2014). Lack of a fully developed immune system which not develop until the third week post fertilization, avoiding rejection of allograft (Lam et al., 2004). Zebrafish have about 70% genetic homology to human (Howe et al., 2013). Additionally, it is easy to keep a large number of zebrafish in the lab due to their small size and low cost feeding requirements. Zebrafish are also characterised by their short life cycle of about 90 days, and one female can lay a hundred eggs per day providing a reasonable number for experimental analysis (Zhao et al., 2015).

Zebrafishhas the ability to survive for 3-4 days in the absence of functioning circulation (Weinstein, 2002). Finally, huge number of fish can be engrafted in one experiment which prove the viability of statistical analysis (Tobia et al., 2013). All of these factors render zebrafish embryos as a useful *in vivo* models for cancer research.

The first systematic study of the ability of tumour cells to disseminate and metastasise, using zebrafish, was reported in 2005 by (Lee et al., 2005). They transplanted melanoma cells into the zebrafish embryo and showed that these cells could remain alive and exhibit the ability to spread and metastasise 48h after injection. Then, in 2006, Haldi et al. performed a similar series of experiments to observe the formation of tumour-like cell masses in zebrafish embryo after injection with melanoma cells (Haldi et al., 2006).

Subsequently, numerous studies have attempted successively to increase knowledge about the behaviour of tumour cells in zebrafish. For example, Marques and his colleagues injected PC cells from a patient with gastrointestinal tumours into zebrafish embryos and found that these cells disseminated rapidly and formed micrometastases within 24 hours. The same group later used small interfering RNA-mediated knockdown of LIM kinase-1 and LIM kinase-2 in human Panc-1 PC cells and observed that this led to decreased invasion and metastasis (Marques et al., 2009).

In more recent , a large volume of published paper showed that zebrafish have been exploited as a tool for *in vivo* studies of the oncogenic behaviour of different human cancer cells such as melanoma (Sacco et al., 2016), non-small lung carcinoma (Zhong et al., 2017), breast cancer (Itou et al., 2017), prostate (Butler et al., 2017), colon (Gnosa et al., 2016), glioblastoma (Gnosa et al., 2016) and pancreatic cancer (Guo et al., 2015).
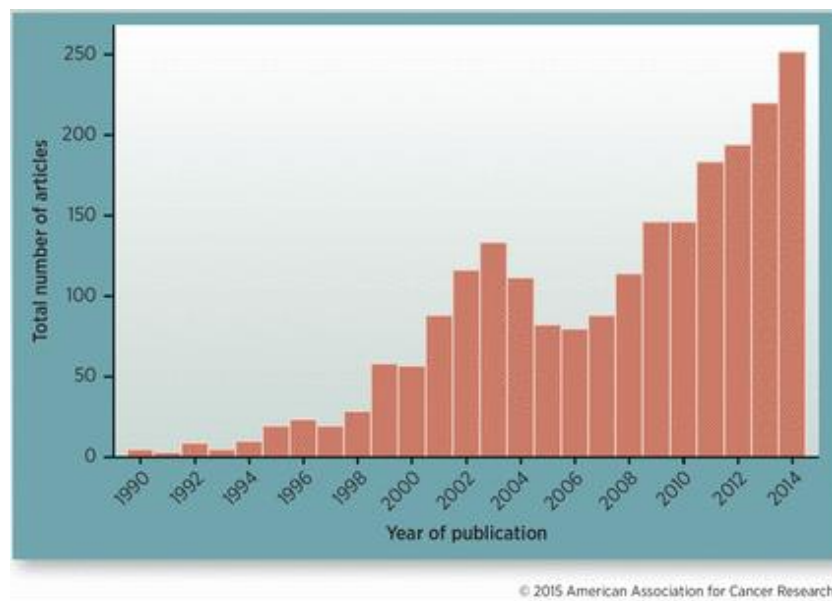
Figure 1.17 Number of published articles per year using zebrafish as animal model for cancer research (Barriuso et al., 2015).

1.7.1 Transgenic zebrafish xenografts as a powerful tool for identifying oncogenic drivers

Understanding the molecular mechanism and tumour microenvironments which involve in tumour metastasis remain a major challenge that require new models. Therefore, generating florescence and transplantable transgenic zebrafish lines has become a main priority to open new horizons for cancer researchers to track metastasis process.

Most cancer researchers which used zebrafish as a model to study cells migration behaviour emphasized the use of the wild type strain "*Danio rerio*". Pigmentation in wild type usually starts 30 hpf (Hill et al., 2005) and pigment cells become fully differentiated during few hours which reduce visualisation through epidermis layers. Generally, three distinct types of pigment cells contribute to transparency of zebrafish, iridophores, melanophores and xanthophores (Rawls et al., 2001)

There are two basic approaches currently being adopted in research to reduce zebrafish pigmentation. One is the use of chemical agents which prevent melanin synthesis, and the most common one is 1-phenyl-2-thiourea (PTU), and the other is mutation in pigmentation related genes (Antinucci and Hindges, 2016). Recently, (White et al., 2008) developed a new strain of mutant zebrafish, known as *Casper*, which fully lack both melanophores and iridophores and was generated by crossing two pigmentation mutant lines, *nacre (*Lister, et al, 1999), which lack completely melanocytes and the *roy orbison* line, exhibiting a loss of iridophores pigmentation cells (White et al., 2008). Data from the same study demonstrated that optical clarity of *Casper* during florescence microscopy permits high resolution imaging, deep into the tissue allowing clear observation to follow migration behaviour of tumour cells. *Nacre* is another mutant of zebrafish which is slightly different from *Casper* in pigmentation features (Lister, et al, 1999).

Additionally, transgenic approaches enables the generation of new strains of zebrafish by crossing *Casper* fish with fluorescent reporter fish lines. A well-known example of these lines is tg(*fli1:eGFP*) which expresses green fluorescent protein in endothelial cells under control of specific promotors (Lawson and Weinstein, 2002). Other available reporter lines with fluorescence markers of immune cells include tg(*mpx:eGFP*) with green fluorescent neutrophil (Renshaw et al., 2006) and tg(*mpeg:Cherry*) with red macrophage (Ellett et al., 2011).

Recently, these new transgenic of zebrafish have been applied in numerous studies, including multistep of cancer progression (Yang et al., 2013). Additionally, these animals represent a unique model for visualisation of tumour-host cell interaction and innate immune cells mediate experimental metastasis. For instance, (Liu et al., 2017a) used tg (*Fli1:eGFP*) zebrafish as a model to discover a novel mechanism of cancer associated fibroblast-mediated cancer metastasis when co-implantation with different cancer cells.

1.7.2 Zebrafish xenotransplantation as tools for *in vivo* validation of anticancer therapies

Zebrafish also can be used as experimental tractable animal model in anti-cancer drug screening to identify promoting and suppressing factors involving in tumour growth and metastasis. The technology of gene silencing which are involved in cancer progression directly or through activation of signal transduction using inhibitor or RNAi approach have been applied in zebrafish (Zhao et al., 2015).

For instance, activation of TGF-β signalling induced breast cancer cell migration. Therefore, targeting proteins mediating activation of this signalling pathway by chemical agents and siRNA impaired metastasis in zebrafish embryos (Li et al., 2015). Epidermal growth factor receptor inhibitors SKLB-178 treatment has been reported to suppress the invasion, migration and metastasis of non-small lung cancer in zebrafish embryo (Zhong et al., 2017). Sal-like4 a transcriptional factor which is required for maintaining fibroblast like morphology, promoted breast cancer cells migration. siRNA mediated knockdown SALL4 diminished implanted cancer cells migration in 2dpf *fli1-eGFP* zebrafish embryos (Itou et al., 2017).

Additionally, Guo et al. studied the xenotransplantation model of zebrafish to test the inhibitor effect of U0126 targeting KRAS pathway on migration behaviour of human PC cells. They found that UO126 treatment significantly reduced MIA PaCa-2 cells proliferation and migration in zebrafish (Guo et al., 2015).

Together these findings provide important insights into engrafting mammalian cancer cells in zebrafish can be employed to be as promising tools for anti- cancer drug screenings.

1.8   Hypothesis

S100 proteins regulate invasion in pancreatic cancer and can be considered as potential diagnostic markers.

1.9   Aim and objectives

The overall goal of this project is to analyse the role, regulation and function of S100 proteins in pancreatic cancer progression; and to characterise their relationship to the EMT programs in this cancer type.

Objectives of the study are:

• To analyse patterns of S100 proteins expression in pancreatic cancer cell lines, exosomes and in tumour samples;

• To investigate expression of the S100 proteins during EMT in cell models, and to correlate their expression with EMT markers in pancreatic cancer specimens;

• To establish zebrafish xenograft PC cancer models and to evaluate an effect of S100 proteins on the invasion of PC cells;

• To study regulation of S100 proteins by inflammatory signalling and, in particular, a role for interleukin/STAT axis in their regulation.

Chapter 2: Material and Methods

2.1 Materials
2.1.1 Tissue cultures
2.1.1.1 Cell lines

A431-ZEB2 and MCF-7-ZEB1 were taken from lab stock, and all pancreatic cell lines were a gift from Dr Berditchevski, School of Cancer Studies/University of Birmingham, UK. AsPC-1 cells were purchased from American Tissue Culture Collection (ATCC).

Table 2.1 Description of cell lines

Cell lines	Description	References
A431-ZEB2	Human epidermoid carcinoma derived from 85-year old female	(Mejlvang et al., 2007)
AsPC-1	Derived from a 62-year-old woman with adenocarcinoma and metastases to several abdominal	(Chen et al., 1982)
BxPC-3	Derived from a 61-year-old woman with adenocarcinoma	(Tan et al., 1986)
CAPAN-1	Derived from a 40-year-old male with adenocarcinoma and metastases to liver	(Kyriazis et al., 1982)
HPAF-II	Derived from a 44-year-old male with adenocarcinoma and metastases to liver	(Metzgar et al., 1982)
HPDE	Immortalized epithelial cell derived from normal human pancreatic duct epithelial cells	(Furukawa et al., 1996)
MCF-7-ZEB1	Derived from a 69 year old women with breast adenocarcinoma, Transformed to express GFP tagged ZEB1 in the presence of Doxycycline	Created in our Lab by Eugene Tulchinsky and Youssef Alghamadi
MIA PaCa-2	Derived from a 65-year-old man with adenocarcinoma	(Yunis et al., 1977)
SU.86.86	Derived from a 57-year-old woman with adenocarcinoma	(Drucker et al., 1988)

Table 2.2 Tissue culture materials

Materials	Sources	Catalogue Number
100X Penicillin/Streptomycin (P/S)	Gibco, UK	15070-63
10X Trypsin EDTA (TE)	Gibco, UK	15400-054
CO_2-independent medium	Gibco, UK	18045-054
Dilc12 dye	Invitrogen, UK	354218
Dimethyl sulfoxide (DMSO)	Sigma-Aldrich, UK	D5879
Doxycycline(DOX)	Sigma-Aldrich, UK	D-9891
Dulbecco's Modified Eagle's Media (DMEM) with high glucose	Lonza, UK	BE-12-604F
Ethylenediainetetraaceticacid (EDTA)	Sigma-Aldrich, UK	E5134
Fetal Bovine Serum (FBS)	Seralab, UK	EU-000F1
Iscove's Modified Dulbecco's Medium (IMDM)	Gibco, UK	12440-053
Keratinocyte serum free media with glutamine	Gibco, UK	17005-034
PCR mycoplasma test kit I/C	PromoKine, UK	DK-CA91-1024
Phosphate Buffered Saline (PBS)	Oxoid Ltd, UK	BR0014G
Rosewell Park Memorial Institute 1640 (RPMI-1640)	Lonza, UK	BE-12-702F

2.1.1.2 Transfection work

Table 2.3 List of siRNA, reagents and kits

Items	Sources	Catalogue number
JetPRIME kit	JetPrime, France.	114-01
Mirus Buffer (Ingenio® Electroporation solution)	Bio Ingenio, UK	51023799
Non-Targeting siRNA	Dharmacon, UK	D-001810-01-05
S100A11-siRNA	Sigma-Aldrich, UK	4192015
S100A4-siRNA	Dharmacon, UK	L-004792-00
S100A6-siRNA	Dharmacon, UK	L-013463-00
Silencer select S100A14	Ambion, UK.	4392421
Silencer select S100A2	Ambion, UK	4392420
STAT3-siRNA	Dharmacon, UK	L-003544-00-0005 5

2.1.1.3 Plasmids

Table 2.4 List of plasmid used in this study

Plasmid name	Origin	Sources	Use
GFP	pmaxGFP	Amaxa, UK	Positive control to check the efficiency of transfection
pEGFP-C1	pEGFP-C1	Clontech, UK	Control of transfection efficiency and a positive control for gene expression
pEGFP-C1-ZEB1	pEGFP-C1	In lab	Induction of ZEB1 expression

2.1.2 Proteins analysis

Table 2.5 Proteins quantification and Sodium Dodecyl Sulphate-Polyacrylamide Gel Electrophoresis (SDS-PAGE) materials

Materials	Sources	Catalogue number
20% Sodium Dodecyl Sulphate solution (SDS)	Fisher Scientific, UK	BP1311-1
30%acrylamide/bis acrylamide	Proto Gel, UK	EC-890
Ammonium Persulfate (APS)	Sigma-Aldrich, UK	A3678
Bovine Serum Albumin (BSA)	Fisher Scientific, UK	9048-46-8
Bromophenol Blue	Sigma-Aldrich, UK	13-8026
Glycerol	Sigma-Aldrich, UK	G5516
Glycin	Sigma-Aldrich, UK	G7126
Hydrochloric Acid	Fisher Scientific, UK	J/4270117
Methanol	Fisher Scientific, UK	M/3950117
N,N,N',N'-Tetramethylethylenediamine (TEMED)	Sigma-Aldrich, UK	T9281
Pierce BCA Protein Assay Kit	Thermo Scientific, UK	23227
Pierce ECL western blotting substrate	Thermo Scientific, UK	32106
Ponceau-S	Sigma-Aldrich, UK	D-3504
Pre-stained protein ladder	Thermo Scientific, UK	26619
Sodium Chloride Na Cl_2	Sigma-Aldrich, UK	57653
Super signal west Dura Extended Duration Pierce ECLsubstrate	Thermo Scientific, UK	34075
Tris base	Fisher Scientific, UK	BP152-1
Tween-20	Sigma-Aldrich, UK	P2287
β-mercaptoethanol	Sigma-Aldrich, UK	M3148

2.1.3 Immunostaining

Table 2.6 Immunofluorescence and immunohistochemistry materials

Materials	Sources	Catalogue number
Citric Acid	Sigma-Aldrich, UK	251275
Cover slips	VWR, USA	631-0135
DAPI	Thermo Scientific, UK	66248
Hematoxylin Solution, Mayer's	Sigma-Aldrich, UK	MHS1
Novolink Polymer detection kit	Leica, UK	RE7150-CE
Paraformaldehyde (PFA) 4%	Fisher Scientific, UK	30525-89-4
Triton	Sigma-Aldrich, UK	T-8787

2.1.4 Antibodies

Table 2.7 The description of primary antibodies

Antibody	Species	Clone	Dilution	Catalogue number	Sources
Calgranulin A (S100A8)	Mouse	Monoclonal	WB 1:500	sc-48352	Santa Cruz Biotechnology, Inc, USA
Cyclin D1	Rabbit	Polyclonal	WB 1:1000	2922	Cell signalling, UK
E-Cadherin	Mouse	Monoclonal	WB 1:4000 IHC 1:6000	610181	BD transduction laboratories, UK
p.STAT3	Rabbit	Monoclonal	WB 1:25	9131	Cell signalling, UK
P53 (wild type and mutant)	Mouse	Monoclonal	WB 1:1000	OP43	Calbiochem, UK
P-Cadherin	Mouse	Monoclonal	WB 1:1000 IHC 1: 500	610227	BD transduction laboratories, UK
P-Histone H2A.X	Rabbit	Polyclonal	WB 1:1000	05-636	EMD Millipore, UK
p-P53	Rabbit	Polyclonal	WB 1:1000	9284	Cell signalling, UK
S100A11	Goat	Monoclonal	WB 1:1000	AF4874	R&D,UK
S100A14	Rabbit	Polyclonal	WB 1:1000 IF 1:1000 IHC 1: 2000	HPA027613	Sigma-Aldrich, UK
S100A2	Rabbit	Polyclonal	WB 1:1000 IHC 1: 1500	HPA062451	Sigma-Aldrich, UK

S100A4	Mouse	Monoclonal	WB	1:1000 IF	1:10	P26447	Developmental Studies Hybridoma Bank (DSHB),USA
S100A4	Rabbit	Polyclonal	IHC	1:1500	05-1-AP	Proteintech, UK
S100A6	Mouse	Monoclonal	WB	1:1000 IF	1:500	WH0006277M10	Sigma-Aldrich, UK
S100A6	Rabbit	Polyclonal	IHC	1: 500	10245-1-AP	Proteintech, UK
S100A9	Rabbit	Polyclonal	WB	1:150	HPA004193	Atlas antibodies, UK
S100P	Rabbit	Polyclonal	WB	1:1000	HPA019502	Sigma-Aldrich, UK
Slug	Rabbit	Polyclonal	WB	1:1000 IHC 1: 100	9585S	Cell signalling, UK
Snail	Rabbit	Polyclonal	WB	1:1000	3879P	Cell signalling, UK
STAT3	Rabbit	Polyclonal	WB	1:1000	2922	Cell signalling, UK
Tubulin	Mouse	Monoclonal	WB	1:30000	T6074	Sigma-Aldrich, UK
Twist	Mouse	Polyclonal	WB	1:50	50887	Abcam, UK
Twist	Rabbit	Polyclonal	IHC	1:100	ABD29	EMD Millipore, UK
Vimentin	Mouse	Monoclonal	WB 1:2000 IHC 1:1000	550513	BD transduction laboratories, UK
ZEB1	Rabbit	Polyclonal	WB 1:250 IHC 1:200	Sc-25388	Santa Cruz Biotechnology, Inc, USA
ZEB2	Rabbit	Monoclonal	WB 1:5000	Homemade (our lab)	Dr Eugene Tulchinsky (University of Leicester)

Table 2.8 The description of secondary antibodies

Antibody	Species	Clone	Dilution		Catalogue Number	Sources
Alexa Fluor® 488 Anti–Mouse IgG	Donkey	Polyclonal	IF	1:500	A21202	Invitrogen, UK
Alexa Fluor® 594 Anti–Rabbit IgG	Donkey	Polyclonal	IF	1:500	A21207	Invitrogen, UK
Anti-Goat IgG/HRP	Donkey	Polyclonal	WB	1:2000	Sc-2065	Santa Cruz Biotechnology, Inc, USA
Anti-Mouse IgG/HRP	Goat	Polyclonal	WB	1:3000	P0448	Dako,Denmark
Anti-Rabbit IgG/HRP	Goat	Polyclonal	WB	1:3000	P0447	Dako, Denmark

2.1.5 DNA oligonucleotides

Table 2.9 List of PCR primers designed using NCBI/Primer-BLAST program

Primer name	Primer sequences		Tm (ºC)	Cycle number
	Forward Primer	Reverse Primer		
ZEB1	GATGACCTGCCAACAGACCA	CTTTCACTGCTCCTCCCTGG	60	40
P-Cadherin	ACCAACCATCATCCCGACAC	GTTAGCCGCCTTCAGGTTCT	59	40
E-Cadherin	ATGGCTGAAGGTGACAGAGC	TGCATTCCCGTTGGATGACA	62	40
Vimentin	CTCTGGCACGTCTTGACCTT	GCCATCAACCTCTTCGTGGA	60	40
S100A2	CCAGCTTTGTGGGGGAGAAA	TGAGTGCCAGGAAAACAGCA	60	40
S100A4	CTAAAGGAGCTGCTGACCCG	TGTCCCTGTTGCTGTCCAAG	62	40
S100A6	GAAGGAGCTCACCATTGGCT	CACCTCCTGGTCCTTGTTCC	60	40
S100A7	ACCTCGCCGATGTCTTTGAG	CCATGGCTCTGCTTGTGGTA	58	40
S100A8	AAGGGGAATTTCCATGCCGT	AGGACACTCGGTCTCTAGCA	60	40
S100A9	GCTGGTGCGAAAAGATCTGC	TGTGTCCAGGTCCTCCATGA	60	40
S100A10	AAAAGACCCTCTGGCTGTGG	AATGGTGAGGCCCGCAATTA	58	40
S100A11	GGTGTCCTTGACCGCATGAT	AGGAAGGAGTCATGGCAAGC	62	40
S100A13	ATCTGCTCAAGGATGTGGGC	GCCAGCTCCCCAATCAATCT	60	40
S00A14	CGCAGAGGATGCTCAGGAAT	GTAGCTCAGAAGGGGTCAGC	60	40
S100P	GCTCAAGGTGCTGATGGAGA	CAGCCACGAACACGATGAAC	60	40
P53	AGTCACAGCACATGACGGAG	ACCATCGCTATCTGAGCAGC	58	40
GAPDH	GTCAAGGCTGAGAACGGGAA	CAGCCACGAACACGATGAAC	60	40

2.1.5.1 PCR amplification

Table 2.10 RNA extraction, cDNA and PCR amplification materials

Materials	Sources	Catalogue number
50X Acitate Borate EDTA	Thermo Scientific, UK	B52 67-66-3
Agarose Hi-Res Standard	Thermo Scientific, UK	A4-0700
Chloroform	Sigma-Aldrich, UK	67-66-3
Ethanol	Fisher Scientific, UK	64-17-5
Fast SYBR Green Master Mix	Applied Biosystems, USA	438612
Isopropanol	Fisher Scientific, UK	67-63-0
ReverAid H minus First strand c DNA synthesis kit	Thermo Scientific, UK	K1622
RNeasyPlus mini Kit	QIAGEN,UK	74134
TRIZOL	Invitrogen, UK	15596-018

2.1.6 Zebrafish work

Table 2.11 Zebrafish care and microinjection materials

Materials	Sources	Catalogue number
CalciumChloride $CaCl_2$	Sigma-Aldrich, UK	C1016
Ethyl 3-aminobenzoate methanesulfonate (MS222)	Sigma-Aldrich, UK	E10521
Ocean® Sea Salt	PetSmart, UK	36-17999
KCl	Sigma-Aldrich, UK	P9333
Low-melt agarose	Sigma-Aldrich, UK	A9414
Magnesium Chloride $MgCl_2$	Sigma-Aldrich, UK	M8266
N- Phynylthiourea (PTU)	Sigma-Aldrich, UK	P-7629

2.1.7 General equipment

Table 2.12List of general equipment

Equipment	company	Catalogue number
Amaxa® Nucleofector® electroporation device	Lonza, UK	
Borosilicate glass capillary needles1.0mm OD, 0.78mm ID	Harvard apparatus, USA	300040
Centrifuge 5415R machine	Eppendorf, UK	
CL-XPosure film	Thermo Scientific, UK	34089
Cover Glass 22 x 22 mm	VWR International, UK	831-0124
Disposable Neubauer haemocytometers (C-CHIPs)	DigitalBio, Korea	DHC-N01
fine surgical forceps 0.1 x0.06mm	Fine Science Tools Inc. Canada	11251-20
Immobilon-P polyvinylidene fluoride (PVDF) membrane	Millipore, Bedford, USA	IPVH-00010
Microloader 20ml	Eppendorf, UK	5242 956-003
micropipette puller Sutter instrument co.	Sutter instrument, USA	P-1000
NanoDrop ND-1000 Spectrophotometer	Thermo Scientific, UK	
Picospritzer III injection apparatus	Parker, USA	051-0500-900
Pipettes	Gilson, USA	
Polysin Slides	Thermo Scientific,UK	J2800AMNZ
Protein gel electrophoresis apparatus	BioRad, UK	
Sigma Compact Centrifuge 2-5	SciQuip, UK	
StepOnePlus ™ Real-Time PCR Systems	Applied Biosystems, UK	
Transfection cuvettes, 2mm	GeneFlow, UK	E6-0060
Transfection cuvettes, 4mm	GeneFlow, UK	E6-0070
Whatman Filter paper	Whatman, UK	3030917

2.1.8 Buffers and solutions preparation

Loading Buffer 1X
2.5ml Tris HCL 1M pH 6.8, 5ml 20%SDS, 5ml 100% Glycerol topped up with 100 ml distilled water

Running buffer 10X
30g Tris base, 144g 99% Glycine and 10g 20%SDS, topped up with 1L distilled water

Running buffer 1X
100 ml 10X running buffer, 200 ml methanol, made up to 1 L with distilled water.

Transfer buffer 10X
30g Tris base and 144g 99% Glycine, topped up with 1L distilled water

Transfer buffer 1X
100ml 10X transfer buffer topped up with 900ml distilled water

TBST buffer
1.8ml Tween 20, 36ml TrisHCl 1M pH 8 and 49 ml NaCl 5M, topped up with 1L distilled water

Tris-borate-EDTA 1X (TBE)
20 ml 50X Tris borate-EDTA topped up with 980 ml distilled water
40g of Instant Ocean® Sea salt dissolved in 1L distilled water

Stock Salts
40g of Instant Ocean® Sea salt dissolved in 1L distilled water

Egg water
1.5ml stock salt solution made up to 1L distilled water.

Evans solution
2.9mM KCl, 134mM NaCl, 1.2mM $MgCl_2$, 2.1mM $CaCl_2$, and 10mM HEPES dissolved in 10 L distilled water. pH and osmolality to be adjusted to 7.8, 280-290 respectively.

0.02% MS-222
0.04g Ethyl 3-aminobenzoate methanesulfonic acid (MS-d222) dissolved in 200ml Evans solution

0.1% Ponceau S dye
1g Ponceau S dissolved in 50 ml acetic acid and topped up to 1 L with distilled water

Blocking solution
5g Marvel milk dissolved in 100 ml TBST, or 5g BSA dissolved in 100 ml TBST.

Protein Loading Buffer
1 part 0.4% Bromophenol blue mixed with 1 part 50% v/v β-mercaptoethanol.

Trypsin/ EDTA 1X
500μl/ml Trypsin and 0.22 mg/ml EDTA top up with 45ml PBS

N- Phynylthiourea (PTU)
0.002g PTU dissolved in 100ml egg water

Citric Acid
22g citric acid topped up to 500ml distilled water

Paraformaldehyde (PFA) 4%
4g paraformaldehyde dissolved in 100ml distilled water

2.2 Methods
2.2.1 Cell culture technique
2.2.1.1 Cell resuscitation

All tissue culture procedures were carried out under a sterile conditions in a laminar flow cabinet and all cells were incubated under the same conditions, 37 °C with 5% CO_2. All media used for cell maintained were adjusted to contain 10% Foetal Bovine Serum (FBS) and 1% of Penicillin/Streptomycin.

For cells resuscitation, cell lines were taken from liquid nitrogen and warmed up directly in a water bath at 37°C to be thawed completely. Cell suspensions were then transferred into a tube containing 10ml indicated media and thoroughly re-suspended. After centrifugation at 1000rpm for 5 minutes (mins), the supernatant was discarded; the pellet was re-suspended again with 5ml fresh media, transferred into T-75 flask and topped up with 15ml media.

2.2.1.2 Cell culture

Culture media and Trypsin/ EDTA (TE) were stored at 4°C and warmed up to 37°C before using. A431-ZEB2, MCF-7-ZEB1, HPAF-II and MIA PaCa-2 cells were grown in Dulbecco's Modified Eagle's Media (DMEM) with high glucose and L-glutamine. AsPC-1, BxPC-3 and SU.86.86 were cultured in Rosewell Park Memorial Institute 1640 media (RPMI-1640) with glutamine, while CAPAN-1 were maintained in Iscove's Modified Dulbecco's Media (IMDM) and HPDE cell line were grown in keratinocyte free serum media

2.2.1.3 Cells passaging

Cells were passaged when confluence reached approximately 70-80% and they were not sub-cultured more than twenty times. Cell passaging was performed by aspirating media from the flask, washing with Phosphate Buffer Saline (PBS) twice, and incubating at 37°C for 10 to 15mins with 1X TE to detach monolayer cells from the surface. After that, trypsin was neutralised by adding a fresh media, transferred into 15ml tube and pelleted at 1000rpm for 5mins. The cell pellet were re-suspended with 1ml complete media and seeded at the required density in the correct sized flask and media added (Table 2.13).

Table 2.13 Recommended volumes (ml) of PBS, TE, resuspension media and total volume of media required for cell passaging

Tissue culture vessels	PBS	Trypsin	Resuspension media	Total volume of media
6 well plates or 35mm	2	0.25	1	2
T-25 or 60mm	5	1	4	5
T-75 or 100mm	10	2	8	15
T-175	15	4	11	25

2.2.1.4 Cell counting

Cells were re-suspended with complete media after washing with PBS and trypsinisation with TE. 10µl of cell suspension were drawn up and placed in one chamber of haemocytometer gridlines. Cells were counted in all 4 sets of 16 corner squares and the average number of cells was calculated and then multiplied by 10,000 or any dilution factor depending on experiment to arrive at the total concentration of cells/ml.

2.2.1.5 Mycoplasma test

The mycoplasma test was carried out using a PCR mycoplasma test kit. Cells were grown to 80% confluency in media-free antibiotic for two passages. To prepare samples for PCR reaction, 1ml of supernatant from culture media was transferred into a sterile Eppendorf tube and heated at 95°C for 10mins. Meanwhile, test reaction tubes were prepared in the same number as the samples, in addition to negative and positive control tubes. 23µl of rehydration buffer was placed in each tube (sample, negative and positive control) to rehydrate the lyophilized components. 2µl of the samples was added to the test tubes while 2µl of DNA-free water was added for each negative and positive control tube to make these up to 25µl as a final volume. The total volume was mixed gently and left at room temperature (RT) for 5mins. The tubes were placed in a thermal cycle and the programme set up as follows (initial denaturation at 95°C for 2mins, denaturation at 95°C for 30 second (sec), annealing at 55°C for 30sec, extension at 72°C for 40sec and cool down to 4-8°C (40 cycle).

For gel electrophoresis, 1.5% Tris Borate EDTA Buffer (TBE) gel electrophoresis was used to analyse the bands by adding 1.5g of gel powder to 100ml 1XTBE and this was boiled until fully dissolved. The gel was left to cool at room temperature and 2µl Ethidium Bromide (EtBr) was added before pouring into a gel electrophoresis tank. 10µl for each reaction including positive, negative controls as well as DNA ladder were loaded into separate wells and run at 100V for 30 mins.

Gel evaluation was conducted according to the appearance of distinct bands, as shown in figure 2.1. PCR mycoplasma test for all cell lines used in this study showed that all cells tested negative for mycoplasma.
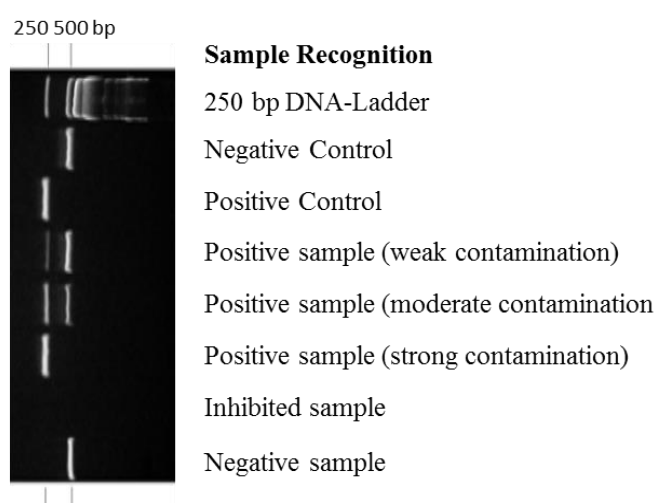
Figure 2.1 Typical agarose gel picture for mycoplasma test.

2.2.1.6 MTT assay

The MTT (3-(4, 5-dimethylthiazol-2-yl)-2, 5-diphenyltetrazolium bromide) is a colorimetric assay used to assess cell viability depends upon a mitochondrial dehydrogenase acting upon MTT to produce blue-purple formazan crystal (Price and McMillan, 1990). PC cell lines (BxPC-3, SU.86.86 and MIA PaCa-2) were seeded in 200µl complete media into 96 well plates at specific cell densities. After 24h, the media was replaced with serum free media and cells left for further 24h. The plates then were incubated an additional 48h with Stattic inhibitor using 5 fold serial dilutions starting from 10 to 0.6µM. At the endpoint of the experiment, 20µl MTT solution was added to each wells for 72h at 37°C.

The media then were replaced with 200µl of DMSO, incubated 10mins, and gently agitated for further 10mins. The absorbance in each well was measured using BioTek ELx808 Absorbance Microplate Reader at wavelength of 560nm. The assay- was repeated in triplicate for each cell line. To get IC50 values, the obtained results were analysed using Graphpad Prism 7 software.

2.2.1.7 Cells treatment

2.2.1.7.1 Doxycycline (DOX) treatment

MCF-7-ZEB1 and A431-ZEB2 cells express ZEB1 and ZEB2 respectively in the presence of DOX. To induce ZEB1 and ZEB1 expression, cells were grown in the presence of DOX (2µg/ml) on the day of seeding and left for 48 or 72h before harvesting.

2.2.1.7.2 Cytokines treatment

Cells were seeded in 60mm dishes in complete media. After 24h, the media was replaced with serum free media and cells left for further 24h. The dishes then were incubated an additional 48h with 200ng/ml of cytokines before harvesting.

2.2.1.7.3 Stattic treatment

Cells were seeded in 60mm dishes in complete media to 50% confluency. The media was replaced with serum free media and cells left for 24h. The dishes then were incubated an additional 48h with 200ng/ml of cytokines and Stattic inhibitor dissolved in DMSO at indicated concertation for required experiments.

2.2.1.7.4 Cycloheximide (CHX) treatment

Cells were seeded in 60mm dishes in complete media. After 24h, cells were treated with 50µg/ml CHX at various time points before harvesting for protein analysis.

2.2.1.7.5 Exosomes treatment

BxPC-3 cells were seeded in T-25 flask in complete RPMI media to 60% confluency. The cells were washed 3 times with PBS and maintained overnight in serum free media. The cells then were incubated with 100µg of purified exosomes from MIA PaCa-2 or SU.86.86 cell lines for 24h for required experiments.

2.2.1.7.6 Cells irradiation

To activate p-P53 in response to DNA damage, MCF-7-ZEB1 cells were seeded in 6 well plates and treated with DOX for 72h. While BxPC-3 and SU.86.86 cells were transfected transiently with GFP-ZEB1 plasmid or GFP control vector for 48h. At the time of irradiation, the media were removed, washed with PBS and irradiated with $50mJ/cm^2$. The media then were added to wells and left to recover in the incubator for 0, 2 and 4h before harvesting for protein analysis.

2.2.1.8 Freezing cells for long-term storage

The cells were grown to 80% confluence in a large flask (T-175). The cells were then trypsinised and re-suspended with freezing media which consisted of 80% complete media in addition to 10% FBS and 10% Dimethyl Sulfoxide (DMSO). 1ml from the suspension was aliquoted into individual CRYO vials and frozen at -80°C to then be stored in liquid nitrogen.

2.2.1.9 Transfection

2.2.1.9.1 Transfection with Ingenio® Electroporation solution

Transfection is a process of inserting the nucleic acids, DNA or RNA into the mammalian cells to study the role of specific gene and protein expression. siRNA and plasmids were transiently transfected in cell lines using Ingenio® Electroporation solution. For that purpose, the cells were grown to 80% confluence and the medium was placed two hours prior to transfection.

The cells were washed twice, trypsinised, re-suspended with fresh media and spun down at 1000rpm for 5mins. The plate was then re-suspended with 10ml PBS, counted as earlier described and centrifuged at 1000rpm for 5mins.

The pellet was re-suspended again in 1ml PBS and 2×10^6 cells of cell suspension was used for each transfection and transferred into an Eppendorf tube containing 0.5ml PBS to be centrifuged at 1000rpm for 5mins. The existing plate was re-suspended with 60µl Ingenio® Electroporation solution and appropriate volume of siRNA or DNA plasmid was added. The final suspension was transferred into 2mm electroporation cuvette and placed in Amaxa® device and subjected to proper programs (T-020 or A-020...etc.). Otherwise, the suspension was transferred into 4mm cuvette and eloctroporated using Gene PulserX cell electroporator which was set at 250V and 250µF.

After that, the transfected cells were re-suspended with 1ml fresh media and maintained in growth media ready for the required experiment after 48h.

2.2.1.9.2 Transfection with jetPRIME

Transfection with jetPRIME was carried out using (Polyplus jetPRIME Kit) according to the manufacturer's protocol. Briefly, one day prior to transfection, cells were seeded in 6 well plates containing 2ml growth media. At the time of transfection, 2µl of target siRNA, 200ml of jetPRIME buffer and 4µl jetPRIME reagents was mixed thoroughly by pipetting, vortex for 10sec, spun down quickly and incubated for 10mins at RT.

The transfection mixture was then added into the wells that contained seeded cells, drop wise, to be ready for required experiment

2.2.1.9.3 Time-lapse microscopy

Time lapse microscopy is a technique used to image biological dynamic events in real time. For that purpose, cells were seeded in 6 well plate and grown to the required density. At the time of imaging, the media was replaced with fresh media and cells were placed in inverted Nikon TE2000 chamber (Nikon Instruments Ltd., Japan) which supplied with standard condition for cell growth including temperature 37°C and CO_2. The microscope software programme was set up to choose 3 position for each samples and image were taken automatically with 10x objective lens every 15mins controlled by Micromanager software (Micromanager, Version 1.3). Images stacking and analysis were processed with ImageJ software.

2.2.2 Manipulation of proteins
2.2.2.1 Protein lysates

Cells were grown to 80% confluence in small flasks (T-25). Media was aspirated from the flask and washed once with PBS. Approximately 300µl (Depending on the cell density in flask) of 1X Laemmli buffer was added; cells were scraped gently and transferred into 1.5ml Eppendorf tubes. Cells were then boiled at 95°C for 10mins to deactivate degradation enzyme and sonicated for 30sec to homogenise and lysate them. The product was kept at -20°C to use further for determination of protein quantification.

2.2.2.2 Protein quantification

The protein concentration was measured via Pierce BSA protein assay kit according to the manufacturer's protocol. Briefly, 96 well plate was set up using 200µl of BCA reagent for each sample, consisting of 50 parts reagent A to 1 part reagent B. Furthermore, a series of protein standards was included (range 2µg/µl -25ng/µl) of BSA. The colorimetric reaction commenced with the addition of 5µl of pre-boiled protein sample or protein standard. A blank sample was also included, whereby the protein sample was replaced with Laemmli buffer. The plate was incubated at 37°C for 30mins and absorbance reading was taken at 562nm using BioTek ELx808 Absorbance Microplate Reader.

The absorbance value for the blank sample was subtracted from values for the protein samples and standards. The unknown protein samples was determined by generating standard curve for protein standards.

2.2.2.3 Sodium Dodecyl Sulphate-Polyacrylamide Gel Electrophoresis (SDS-PAGE)

Sodium dodecyl sulphate-polyacrylamide gel electrophoresis (SDS-PAGE) was used to determine the expression of a target protein. The percentage of resolving gel depends on the molecular weight of the antigen and ranges from 6 to 15% (Table 2.14) (Harlow and Lane, 1988). The final volume of these solutions was poured into assembled glass plates for gel apparatus and water saturated butanol applied to the top of gel to avoid bubbles, and then left for 10-15mins to solidify.

After setting up the gel, the butanol was removed and washed with water and dried. 5ml of stacking gel (5%) was made by mixing (3.4ml water, 0.8ml acrylamide mix, 1.25 ml 1M Tris-HCl (pH 6.8), 0.01ml Ammonium Persulfate (APS) and 0.01ml N,N,N',N'-Tetramethylethylenediamine (TEMED) and poured on top of the resolving gel. A 15 well comb was inserted directly into the stacking gel before it became solid. After polymerisation, the gel was transferred into a BioRad tank running tank, filled with 1X running buffer and the comb was removed. In the meantime, samples were boiled at 95°C for 5mins. A known volume of sample mixed with 0.0016 % bromophenol blue and 4% ß-mercaptoethanol, and 4µl of ladder were loaded separately into each well and the gel was run at 140V for 90mins.

Table 2.14 Volume (ml) of components required to prepare 10ml of resolving gel with different concentrations

Gel %	Water	30% Acrylamide mix	1.5 M Tris (pH 8.8)	10% Ammonium persulfate	TEMED
6	5.3	2	2.5	0.1	0.008
8	4.6	2.7	2.5	0.1	0.006
10	4	3.3	2.5	0.1	0.004
12	4.4	4	2.5	0.1	0.004
15	2.3	5	2.5	0.1	0.004

2.2.2.4 Transfer of SDS-PAGE gels onto PVDF

After completion of the running process, the proteins were transferred onto polyvinylidene fluoride (PVDF) membrane. To this end, transfer components, including filter papers and sponges, were soaked with 1X transfer buffer and the PVDF membrane was activated in absolute methanol. All these components in addition to the gel were arranged according to the indicated order shown in figure 2.2, to make a transfer cassette. The cassette was then placed in a tank filled with 1X transferring buffer and set up at 25V overnight.

2.2.2.5 Western blotting and immunodetection

After transferring the protein, the PVDA was removed from the cassette, soaked in 0.1% Ponceau S dye for 10mins to visualise the protein bands and rinsed with water three times to clean the membrane from the dye. For blocking, the membrane was placed in a small pot that contained blocking buffer and rotated for 50mins at RT. The membrane was washed with three times (5mins rotation each time) and incubated with target primary antibody for 1h at RT or 24h at 4°C.

 It was then washed again with TBST three times and incubated with secondary antibody for 1h at RT. In the final step, Pierce Enhanced chemiluminescence (ECL) western blotting substrate kit was used to visualise the protein bands. The membrane was incubated with ECL reagent (1:1 of solution A and B) for one min at RT and placed between two light in a radiography cassette and visualised using the CL-XPosure Film in the dark room or films were scanned with a Canon LIDE 60 scanner.
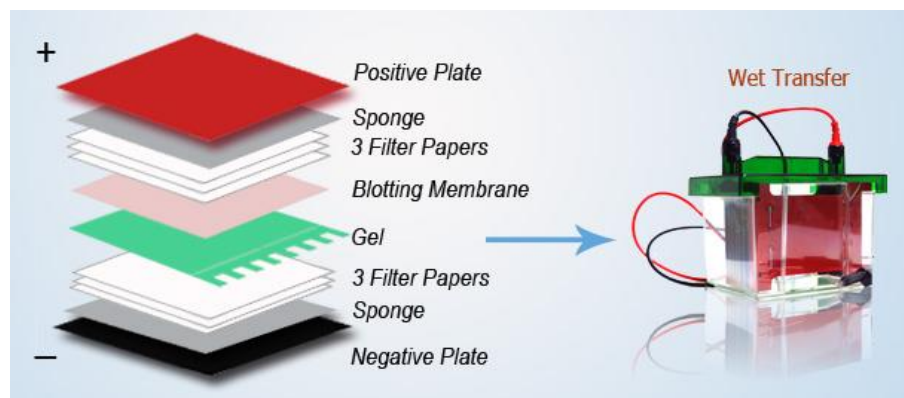
Figure 2.2 Scheme explains assembly of transfer components according to indicated order to make a transfer cassette.

http://www.western-blot.us/western-blot-protocol/wet-western-blot.

2.2.3 Exosomes purification works
2.2.3.1 Exosomes isolation from pancreatic cancer

Exosomes isolation for mass spectrometry analysis and all other experiments were performed by ultracentrifugation according to (Thery et al., 2006) with a slight modification in time and speed of centrifugation. Briefly, the cells were grown in complete media to 70-80% confluency and then the media was replaced with media free serum for 48h.

The condition media was collected and spun down at 400g for 5mins followed by 2000g for 10mins to pellet dead cells and cellular debris. The supernatant was transferred to ultracentrifugation tubes and spun down at 15000g for 60mins at 17°C to pellet microparticles. The supernatant was transferred into new ultracentrifugation tubes and spun down at 100000g for 80mins at 4°C to pellet exosomes. The supernatant was discarded and pellet was re-suspended with 100ml PBS, and PBS was added to fill the tube completely and centrifuged at 100000g for 1h at 4°C to wash exosomes pellet. Finally the supernatant was discarded, the pellet was re-suspended with PBS and kept at -20 until required analysis.

2.2.3.2 Coomassie blue staining

Coomassie blue dye is used to stain and visualised exosome protein band in SDS-PAGE gel. 100µg of protein exosome and 10µl of ladder were loaded separately into each well of SDS-PAGE gel and run at 140V for 90mins. After running, the gel was rinsed with water and soaked in Coomassie stain over night with gentle agitation.

The gel was then destained with at least 3 washes of destain solution until the background is nearly destained and the images were taken by a Canon PowerShot digital camera (Canon UK Ltd.).

2.2.3.3 Mass spectrometry analysis

To prepare sample for mass spectrum, the total protein concentration of exosomes was measured by BCA protein assay kit. 100µg of exosome protein were loaded into 15% polyacrylamide linear gradient gels (Bio-Rad). After running, the gel was stained with Coomassie Blue. Distinct bands were visualised and these bands were excised from the gel for mass spectrum analysis which carried out in proteomic facility centre, University of Leicester.

2.2.3.4 Transmission Electron Microscopy (TEM)

Exosome size and particle number were confirmed and analysed using electron microscopy. To this end, 3µl of sample was adsorbed onto glow discharged pioloform carbon coated copper mesh grids for 5minutes. Grids were then washed with 2 drops of distilled de-ionised water, immediately followed by 2X 4µl drops of 0.5% aqueous uranyl acetate.

Excess stain was removed using filter paper and the grids left to air dry before observation in the TEM. Samples were viewed on the JEOL JEM 1400 TEM with an accelerating voltage of 80kV. Images were captured using Megaview III digital camera with iTEM software (Electron Microscopy Facility, Centre for Core Biotechnology Services, University of Leicester).

2.2.4 RNA extraction, cDNA and PCR amplification

2.2.4.1 RNA extraction from cancer cell lines

RNA was extracted from cell lines using the TRI Reagent®method (Chomczynski and Sacchi, 2006) and the RNeasy® Plus Mini Kit. Basically, the media was aspirated from the plates or flasks that contained the growing cells and washed twice with PBS. Trizol was added to each plate (1ml per 10cm^2), and the samples were pipetted several times (up and down) and transferred into a 2ml Eppendorf tube. After incubation for 5mins at RT to allow for dissociation of nucleoprotein complexes, 200µl chloroform was added, shaken vigorously and centrifuged at 12000g for 15mins. After centrifugation, three phase solution were generated including upper, interface and lower phase which referred to RNA, DNA and proteins respectively.

Approximately 500µl of the aqueous solution (upper phase) was removed, placed in gDNA eliminator column provided with the RNeasy® Plus Mini Kit and spun down at 8000g for 30sec. The column was discarded and approximately 500µl of 75% ethanol was added to flow through and mixed gently. Up to 700µl of the sample (flow through mixed with ethanol) was transferred into an RNeasy tube and centrifuged at 8000g for 15sec. The flow through was discarded and the RNeasy tube was washed by adding 700µl of RW1 and centrifuged at 8000g for 15sec. The flow through was discarded and the tube washed twice with 500µl RPE buffer at 8000g for 15sec and 2mins respectively. After that, the RNeasy tube was placed in a new collection tube and spun down at 12000g for 1min to completely dry the column from existing ethanol. At the final step, the tube was transferred into new collection tube, RNA was eluted by adding 50µl RNase free water and spun down at 8000g for 1min. The concentration of isolated RNA was determined using a Nano drop device and stored at -80°C until required.

2.2.4.2 Determination of RNA concentration

RNA concentration was determined using the Nano Drop ND-1000 Spectrophotometer. The pedestal was cleaned firstly by optical instrument cleaner. The program was initialized with ultra-pure water and blanked with RNase free water. The purity of sample was determined by applying 1.2µl of sample onto pedestal and monitoring the absorbance reading at 280nm.

2.2.4.3 cDNA synthesis

cDNA synthesis for RNA collected from cell lines was performed using a ReverAid H minus First strand cDNA synthesis kit. Usually 1µg RNA was used for each reaction; this was made up to 11µl with RNase free water. Then 1µl of random primer was added, mixed thoroughly and centrifuged briefly. Samples was incubated at 65°C for 5mins and placed on ice whilst adding: 4µl 5XRxn buffer, 1µl Ribo Lock RNase inhibitor, 2µl 10mM dNTP mix and 1µl Revert Aid Reverse Transcriptase in the indicated order, with a final volume of 20µl per reaction. Negative and Positive control GAPDH RNA were conducted in the meantime to verify the quality of the first strand synthesis. For negative control, the reaction contain all reagents which used with sample except for the reverse transcriptase, while positive control was prepared as shown in table 2.15. Both samples and control were mixed gently, centrifuged, incubated at 25°C for 5mins followed by 42°C for 1h and then stored at -80°C for long term storage.

Table 2.15 GAPDH RNA (Positive control) components

Components	Volume (µl)
Control GAPDG RNA (50ng/ml)	2µl
Primer	1µl
5x Rxn buffer	4µl
RiboLockRNase inhibitor	1µl
10Nm Dntp MIX	2µl
RevertAid Reverse Transcriptase	1µl
Nuclease free water	9µl
Total	20µl

2.2.4.4 Real-Time Quantitative Reverse Transcription (qPCR)

Real-time quantitative reverse transcription (qPCR) was conducted with Fast SYBR green PCR master mix to compare relative gene expression in different cell lines. Glyceraldehyde-3-phosphate dehydrogenase (GAPDH) was used as the endogenous gene control. Before applying the experiments to detect expression level of genes, the genes of interest and the GAPDH gene was determined to have high amplification efficiency.

To this end, preliminary experiments were performed using serial dilutions of cDNA sample including, 1:1, 1:10, 1:50, 1:75 and 1:100. Sample with 1:10 dilution was selected as the standard sample in the subsequent experiments. Additionally, a standard curve for target genes and the reference gene was constructed to determine the gene- specific PCR efficiencies using 8 fold serial dilutions starting from stock solution and then 20ng to 0.31ng. The slope values was obtained from the standard curve, and the efficiency (E) of PCR was calculated according to the equation $E = 10^{\wedge} (-1/slope)$ (Ruijter et al., 2009). The PCR reaction was performed with triplicate in 96 well plate, and each reaction contain 10μl Fast SYBR green PCR master mix, 2μl cDNA, 0.5μl of forward and reverse primers(10μM) and this was made up to 20μl as a final volume with RNase-free water. The templates were amplified in StepOnePlus™ System (Applied Biosystems, USA) with the following cycle condition: one cycle holding stage at 95°C for 20mins and 40 cycle of 3sec at 95°C for melting and 30sec at 60°C for annealing and extension. The data were analysed using comparative relative gene expression Ct method also termed the '$2^{-\Delta\Delta C_T}$ method' according to (Schmittgen and Livak, 2008), which measure the transcription level of samples normalized to the expression of endogenous control representing ΔCt value ($\Delta Ct = Ct^{reference} - Ct^{target}$).

2.2.5 Immunostaining
2.2.5.1 Immunofluorescence (IF)

Immunofluorescence is a wide used technique to determine the localization and endogenous expression of target proteins. The principle of this technique deepened on using fluorescent-labelled antibodies to determine specific target antigens.

For staining, the cell were seeded on cover slips (18×18mm; thickness no.1; borosilicate glass) placed in 6 well plate or ibidi dish 48h prior to staining to reach the required density. The media was aspirated and cells were rinsed twice with PBS (the washing in all steps were conducted gently on a shaker for 5mins in each time). The cells were fixed by adding 1ml 4%paraformaldhyde and incubation for 15mins at RT. After fixation, the cells were washed twice with PBS and 1ml of 0.5% Triton was added for 5mins to membrane permeabilization.

Then, the cells were washed again twice with PBS and incubated with 100μl primary antibodies diluted in 3% BSA/PBS for 1h at RT in dark place. The cells were then washed three times with PBS, 100μl fluorescent-conjugated secondary antibody was applied and incubated for 1h at RT.

The cells were rinsed three times and 1ml of 0.5μg/ml 4', 6-diamidino-2-phenylindole (DAPI) was applied for nuclear staining and incubated 5mins at RT. After DAPI staining, the cover slips were washed twice and mounted into glass slide contained mounting media or 90% glycerol in PBS with the cells facing down on the slides. The excess liquid was removed and the edge of cover slip was sealed with polish nail to prevent drying and movement under microscope. Confocal microscopy was used to visualise and analyse the images

2.2.5.2 Immunohistochemistry (IHC)

The immunohistochemistry is the most practical method for assessing the change and localization of protein expression and detecting functionally important post-translational protein modifications, such as phosphorylation in diagnostic histopathology depending on antigen-antibodies interaction. In this study, the IHC was carried out using the Novolink™ Polymer Detection Systems. Before applying the experiments to detect expression level of target proteins, the optimal primary antibodies dilutions was determined using a series of dilutions in a titration experiment applied on normal pancreatic tissues and normal tonsil sections to minimize background.

Moreover, negative slides which were not treated with primary antibodies was performed with each experiment as negative control to exclude any non-specific background staining. Tissue section slides were arranged in staining rack and heated to 65°C for 10mins in oven before being deparaffinised by submerging the slide in xylene (2 changes X 3mins). The sections were rehydrated by immersing them in 99% ethanol (2 changes x 3minutes) and then transferred once to 95% ethanol for 3mins. The slides were rinsed with tap water for 5mins and they kept in water until ready to perform antigen retrieval.

 For antigen retrieval, the slides were removed from tap water, transferred into microwaveable vessel containing 500ml of citric acid buffer and placed in microwave set up to full power for 20mins.

After that, the container was removed from microwave and cold tap water was run into it for 15mins. Then the slide were transferred into a humidified chamber to neutralize endogenous peroxidase activity by adding drops of peroxidase block providing that cover entire sections for 5mins at RT. The slides were rinsed with tow changes PBS, 5mins for each and subsequently protein block was applied as the same way for 5mins at RT to block non-specific protein binding, followed by 2 changes X 5 mins PBS washes. Optimal primary antibodies diluted in 3%BSA/PBS was applied and incubated over night at 4°C.

The slides were rinsed twice with PBS (5mins for each) before adding drops of a post primary block for 30mins at RT. The sections were rinsed again with PBS and the polymer buffer was applied for 30mins at RT followed by watching once with PBS for 5mins. Appropriate amount of 3, 3 – diaminobenzidine (DAB) substrate solution (100µl) which made freshly by mixing 1volume of chromogen with 20 volume substrate (1:20) was applied for 5mins at RT and washed with tape water for 5mins. For counter stained, the slides were immersed in Mayer's haematoxylin for 30sec followed by washing with tap water. The slides were dehydrated and cleaning by submerging them through a serial solutions including; ethanol 95% (once for 5mins), ethanol 99% (2change X 2mins) and xylene (2 changes X 3mins) and a proper cover slips were mounted over tissue sections using DPX. The sections were kept to dry for 30mins at RT before microscopy analysis.

2.2.5.3 Evaluation and analysis of tissue sections

Evaluation of pancreatic pathology specimens was performed by two independent pathologists; Dr Peter Greaves and Catherine Moreman. The intensity of staining was assessed for each section on a four point scale: negative = -, + = minimal, ++ = moderate and +++ intense staining. All slide images were viewed and captured using Hamamatsu Slide Scanner rm 315 microscope. The staining was performed in parallel with a negative control, which was not applied with the primary antibody to exclude any nonspecific background staining. Samples varied considerably with respect to the number of carcinoma cells, degree of fibrosis and presence of other tissues. Stroma was evaluated primarily on the staining characteristics of the cytoplasm of spindle or fibroblast-like cells. Some very pale staining was evident in some cases, although these were assessed as +.

As the number of tumours was relatively small, the immunostaining was grouped into two groups for analysis as the numbers were too small to allow any meaningful analysis if divided into three/four groups. For some markers there is just one comparison (e.g. no stain vs. positive stain). For markers where there were reasonable numbers in the different staining brackets, analyses performed around two different cut-off points. Where only 1-2 cases were negative (e.g. S100A6), there is no point analysing negative vs. positive (as it will never show significance).

Table 2.16 The cut-off points used for the different marker

Marker	Notes	Categories 1	Categories 2
S100A2	7 positive cases	0 vs. any	
S100A4	Even spread across score 0-3	0 vs. any	0-1 vs. 2-3
S100A6	One scored 0. One scored 1. Five scored 2	0-1 vs. 2-3	0-2 vs. 3
S100A14	Two score 0. None score 1. Nine score 2.	0 vs. 2-3	0-2 vs. 3
Vimentin	Only 6 positive cases.	0 vs. any	
P-Cad	None scored 0. Nine scored 1.	1 vs. 2-3	1-2 vs. 3
E-Cad	None scored 0. Two scored 1.	1 vs. 2-3	1-2 vs. 3
Slug	Fourteen scored 0. One scored 2.	0 vs. 1-2	
Twist	Two score 0. Three score 1. Eight score 2	0-1 vs. 2-3	0-2 vs. 3
ZEB1	Eight score 1. One scores 2. Others 0.	0 vs. 1-2	
P53	Two score 0. Ten score 1. Others 2-3.	0-1 vs. 2-3	0-2 vs. 3

2.2.6 Zebrafish Handling

2.2.6.1 Zebrafish care and breeding

Fluorescent reporter fish lines including *fli1:eGFP* (green vasculature), *mpx:GFP* (green neutrophil) and *mpeg:Cherry* (red macrophage) was provided by professor Stephen Renshaw, University of Sheffield. While other strains including *"Casper"*, *"Nacre"* and wild type *"Danio rerio"* by Dr Jonathan McDearmid, department of neuroscience, psychology and behaviour, University of Leicester. The fish were maintained under special conditions (28°C and steady day light cycle, 10h dark and 14h light) (Hurd et al., 1998).

A few of the fish were paired for breeding in a special aquarium, fertilized embryo were transferred into new containers every morning and kept in egg water at 28°C which contained methylene blue to avoid any contamination, until they developed to required stage (2days post-fertilisation) (dpf). To prevent pigmentation in wild type, 24 hour post fertilisation (hpf) fish was kept in 0.002% PTU.

2.2.6.2 Labelling cells for microinjection

Cells were trypsinised, counted and $2x10^6$ cells seeded in T-75 flask two days before preparation for injection. To label cells fluorescently, the media was aspirated and replaced with 10ml new media containing 5μl of Dilc12 dye dissolved in DMSO (5mg/ml). After 1h of incubation, cells were washed with PBS, detached with TE, re-suspended in fresh media and counting. Meanwhile the cell suspension was spun down at 1000rpm for 5mins and after discarding the supernatant, the plate was kept in appropriate volume of CO_2 independent media supplemented with 10% FBS and 1% Penicillin/Streptomycin to make up a concentration of $2x10^6$cells/ml to be ready for microinjection.

2.2.6.3 Fish Preparation for microinjection

Twenty four hours-post fertilisation, the embryos were collected and placed in a small dishs. Using fine surgical forceps, the embryos were released from their chorion (dechorionated) under a stereo-microscope. The fish were then transferred into a new dishs, anaesthetised in 0.02% Tricaine solution (ethyl 3-aminobenzoate methanesulfonate or MS222) and immobilised by adding 1% low melting agarose. Then, the fish were directly orientated in one direction for the purpose of facilitating the process of injection and imaging (Figure 2.3).
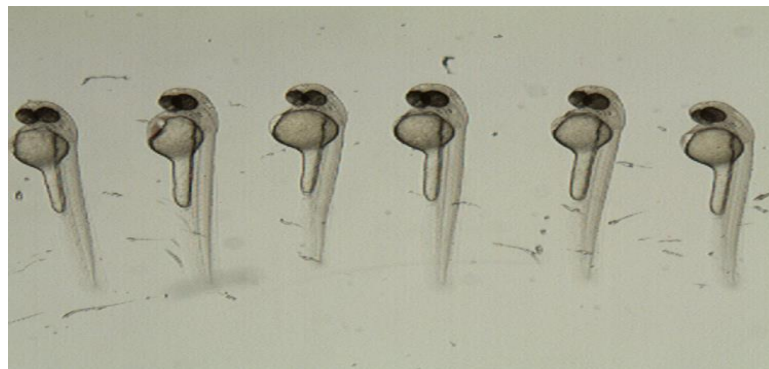
Figure 2.3 Two dpf zebrafish embryos immobilised and orientated in one direction for the purpose of facilitating the process of injection and imaging.

2.2.6.4 Microinjection protocol

Borosilicate glass capillary needles were designed by micropipette puller and 10μl of cell suspension which had earlier been labelled was loaded into the needle and fixed into an injection instrument set at a pressure of 500-1000 hPa and time of 0.3-0.8sec. About 100-200 cells were injected manually into the perivitelline cavities of the zebrafish (Figure2.4). The fish were kept for 1h at 33°C and then checked using a fluorescence microscope (Nikon TIRF microscope) to determine the success of the injection process. After screening, the embryos were cut out from agarose using forceps and kept in egg water at 33°C after excluding all fish with cells outside the injection site. 48 hour post injection (hpi), the fish were mounted in agarose again as described previously and imaging was conducted using fluorescent microscopy. Image montage and analysis of cell migration were carried out using image J software program.
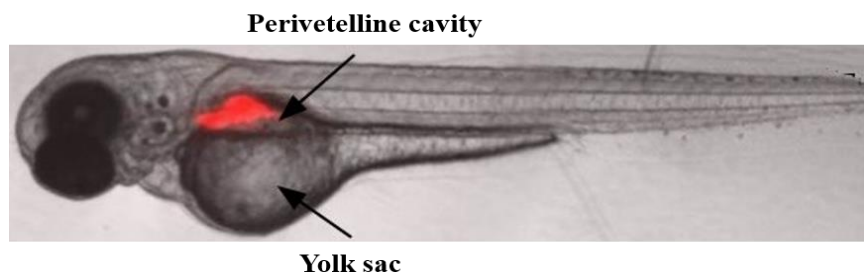
Figure 2.4 Two dpf zebrafish embryos were injected in the perivetelline cavity

2.2.7 Statistical analysis

All experiments were performed in triplicate. A t-test, one way ANOVA and two way ANOVA were used to compare data using GraphPad Prism Version 7.0, and P values < 0.05 were considered as significant.

All statistical analysis for immunohistochemical data were performed by Dr. Christopher Paul Neal (Department of Health Sciences, University of Leicester) using Statistical Package for the Social Sciences 20.0® (SPSS, Chicago, Illinois, USA). Associations between different proteins were determined using person correlation coefficient. Results from this test produced a correlation coefficient, indicating the strength and direction of the association, and a P value, indicating the significance.

If the coefficient is positive then both variables increase together. If the coefficient is negative then the variables are inversely related. The Chi-squared and Fisher's exact tests were used to analyse for significant associations and differences between subgroups within the cohort. Univariate prognostic significance of variables was determined by means of univariate Cox regression analysis, Kaplan-Meier analysis and application of the log-rank test. The comparison in protein expression between cancer and normal tissue was performed by using Wilcoxon Signed Ranks Test. Statistical significance was defined as P < 0.05.

Chapter 3: The expression pattern of S100 proteins in a model of epithelial-mesenchymal transition

3.1 Introduction

Epithelial Mesenchymal Transition (EMT) is a process whereby epithelial cells lose their characteristics and gain a mesenchymal phenotypes, allowing them to escape from the primary tumour, invade surrounding tissues and migrate to distant sites (Spano et al., 2012, Teng and Li, 2014). Such changes in cell phenotype are reflected in upregulation of mesenchymal markers (i.e., S100A4, N-Cadherin and Vimentin) and downregulation of the epithelial markers (e.g., E-Cadherin, claudins and occludins) (Peinado et al., 2007, Teng and Li, 2014).

It is now well established that a relationship exists between small calcium binding S100 proteins and the EMT process. The expression of members of the S100 proteins is altered during EMT and their expression is correlated with EMT-associated factors, although little is known regarding their functional effects during EMT (Chen et al., 2015b, Xu et al., 2016b). Additionally, S100 proteins are implicated in modulating many steps of tumour metastasis and some of them, such as S100A4, have been used as metastatic markers (Boye and Maelandsmo, 2010).

The intrinsic invasive abilities of cancer cells are important in the process of metastatic dissemination. Traditionally, studies on the metastatic potential of human tumour cells are performed in mice, but, recently, transparent zebrafish embryos have become popular as a model system in cancer research (Zhang et al., 2015a). One of the aims of this study, therefore, was to establish zebrafish xenografts as a tool for *in vivo* studies of cancer cell migration.

The main goal of this chapter was to study the role of S100 proteins in the EMT process, and also to use human epidermoid carcinoma A431 cells to estimate the extent to which S100s have the ability to increase the metastatic potential of an EMT cell model.

3.1.1 EMT cell models

Different cancer cell lines have been used as models to study the features of the EMT process, including tumour cell lines in which transcriptional repressors of E-Cadherin are downregulated, such as Slug (Bolos et al., 2003), ZEB2 (Mejlvang et al., 2007) and Twist (Yang et al., 2004). For this study, human epidermoid carcinoma A431 cells with Tet-On inducible expression of ZEB2, a master regulator of EMT, were used. Doxycycline (DOX) is a tetracycline derivative that regulates gene expression through the Tet system. DOX interacts with the rtTA transcription factor, allowing it to bind DNA at the target gene promotor. Growing these cells using DOX, therefore, initiates expression of the ZEB2 transcription, thereby inducing EMT (Mejlvang et al., 2007).

3.2 Results

3.2.1 ZEB2 expression promotes morphological changes and modifies the profile of gene expression in A431 cells

3.2.1.1 ZEB2 expression initiates EMT in the A431 cell line

ZEB2 is one of the major transcription factors that represses E-Cadherin expression and induces EMT. To induce EMT, A431 cells were grown in the presence and absence of DOX for 0, 24, 48 and 72h with phase-contrast images of cells being taken at each time point so as to observe the phenotypical changes in the cells during activation of ZEB2. Cells which were grown without DOX displayed an epithelial phenotype and formed large clusters whereas, after 24h of treatment with DOX, small cores appeared within the clusters as a prelude to scattering and the initiation of a fibroblastic phenotype. After 48h, only a few small clusters remained and most of the cells had become individual, exhibiting small protrusions. After 72h, cells exhibited a fully-scattered mesenchymal phenotype with the large lamellipodial protrusions that are a pre-requisite for cell migration (Figure 3.1A).

In order to achieve more precise estimates of the EMT induced during ZEB2 activation, A431-ZEB2 cell lysates were prepared for Western blotting to analyse the expression of EMT-associated proteins ZEB2, Vimentin, E-Cadherin and P-Cadherin at different time points (0, 24, 48 and 72h).

The expression of ZEB2 was detected at the 24h time point, increasing markedly, until 72h post DOX treatment. In parallel, expression of the Vimentin mesenchymal marker was absent in non-treated cells but in treated cells it was activated after 24h and remained stable until 72h. In contrast, expression of the epithelial markers P-Cadherin and E-Cadherin was detected at high levels in non-treated cells and then decreased slightly after 24h (Figure 3.1B). Together, the morphology changes and the downregulation of epithelial markers and upregulation of mesenchymal markers were an indicator of the transformation of epithelial cells to mesenchyme cells and induction of the EMT process.
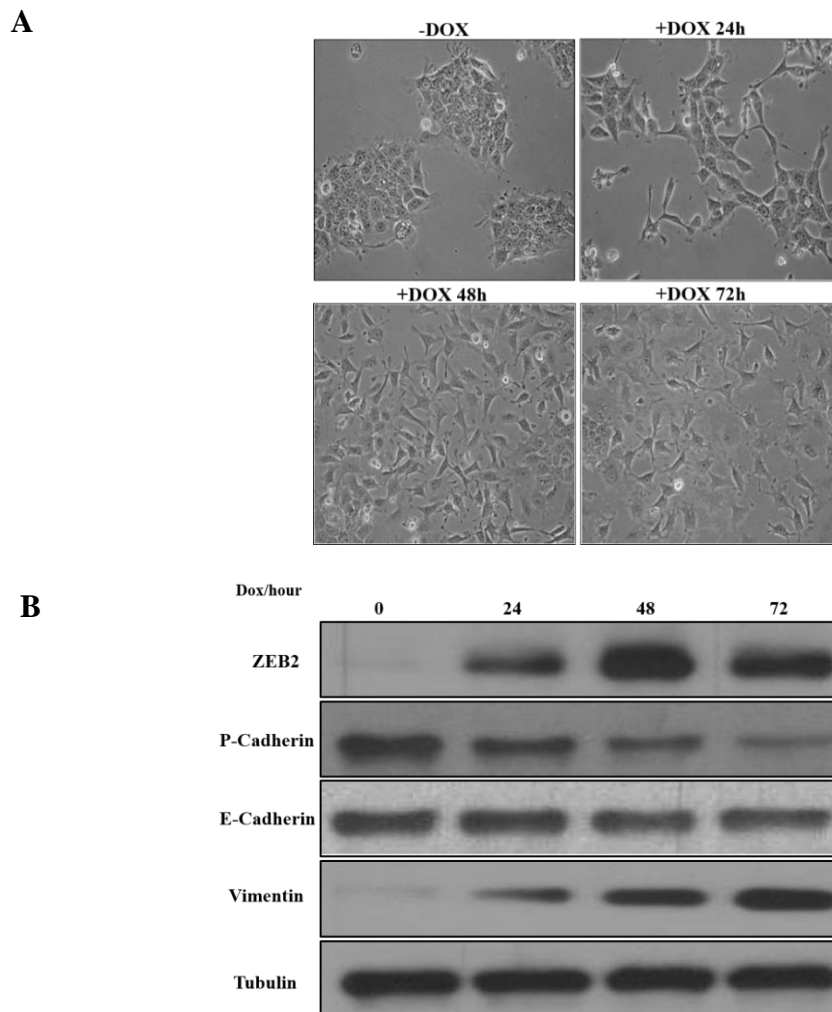
Figure 3.1 DOX-dependent activation of ZEB2 alters cell morphology and initiates expression of mesenchymal proteins in A431 cells.

(**A).** A431-ZEB2 cells were cultivated in the presence and absence of DOX at different time points (0, 24, 48 and 72h) and phase-contrast images were taken with 20x objective. (**B)**. Western blot analysis of A431-ZEB2 cell lysates collected at different time point. The lysates were resolved on polyacrylamide gel. Membranes were stained with antibodies to epithelial markers (P-Cadherin and E-Cadherin) and mesenchymal markers (ZEB2, Vimentin) as well as tubulin as loading control.

3.2.1.2 ZEB1 induced EMT alters S100 gene expression in A431 cells

Since S100 proteins are among many molecules considered to be involved in the EMT process, it was hypothesised that the expression of the family members of these proteins may be altered during EMT. For that reason, the expression profiles of multiple S100 genes were investigated in the A431-ZEB2 cell line using qPCR. The previous results showed that the expression of mesenchymal markers was highest and the expression of epithelial markers was lowest at 72h compared to any other time points (Figure 3.1B). 72h is therefore considered to be the ideal time point for the full initiation of EMT. Consequently, RNA was extracted from A431-ZEB2 cells after they had been grown for 72h both in the presence and in the absence of DOX, and then reverse transcribed.

The cDNA product was amplified using a series of primers for S100 genes, including S100A2, S100A4, S100A6, S100A7, S100A8, S100A9, S100A10, S100A11, S100A13, S100A14 and S100P. Additionally, the resulting cDNA was amplified using primer sets specific to EMT-associated genes such as ZEB2, Vimentin, E-Cadherin and P-Cadherin.

It is apparent from Figure 3.2A that there was a significant activation of S100A4 and S100A6 mRNA in A431 (+DOX) cells compared to (-DOX) cells ($P \leq 0.0001$), and upregulation of the expression of these genes corresponds to activation of the ZEB2 and Vimentin mesenchymal-associated genes ($P \leq 0.0001$) (Figure 3.2B).

Significant reductions in the mRNA expression levels of S00A2, S100A7, S100A8, S100A9, S100A10, S100A14 and S100P were observed in A431 (+DOX) compared with A431 (-DOX), which coincided with the reduced expression levels of the epithelial markers, E-Cadherin and P-Cadherin. There were no notable observations for S100A13 expression, however (Figures 3.2A and B). Next, cell lysates were collected from A431 cells maintained in the presence or absence of DOX for 72h, and Western blot analysis was perform to check the protein level. Very similar observations were detected for the protein levels with selected S100 proteins as for those with EMT-associated markers (Figure 3.2C). In general, therefore, it seems that, of all the tested S100 protein members, only S100A4 and S100A6 were activated during ZEB2 induced EMT, but their expression reflected the expression pattern of EMT-associated markers, with P-Cadherin and E-Cadherin being downregulated and ZEB2 and Vimentin upregulated.
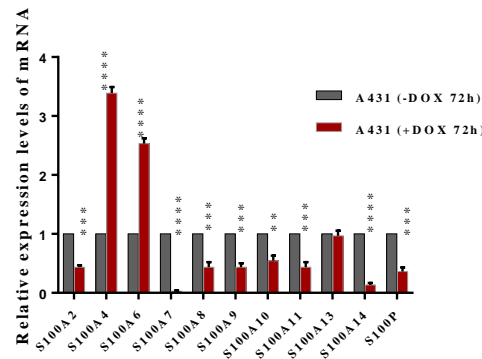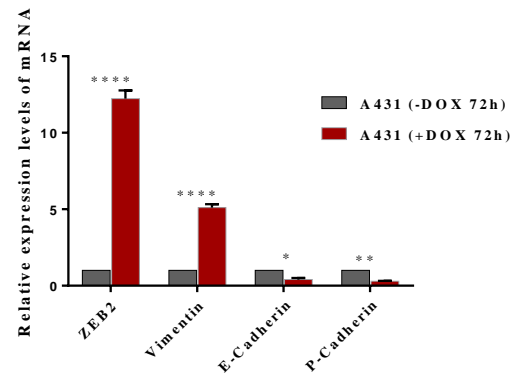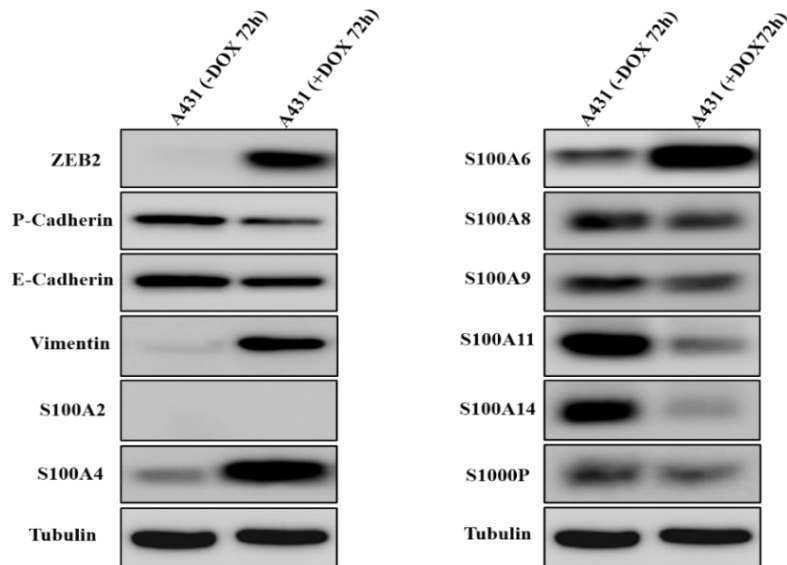
Figure 3.2 Alteration of the transcriptome of S100 genes in A431 cells during ZEB2-induced EMT.

qPCR analysis of the expression of the selected S100 genes **(A)** and EMT-associated genes **(B)** in A431-ZEB2 cells cultivated in the presence or absence of DOX for 72h. The relative mRNA expression level was quantified using the $2^{-\Delta\Delta CT}$ method, and mRNA level was normalized to housekeeping gene GAPDH. Bar charts with standard errors of the mean represent delta CT value,*P=0.03, **P=0.001 and ****P≤0.0001.The results from 3 representative experiments are shown. **(C).** Western blot analysis was carried out to further verify the alteration of S100 proteins expression and EMT-associated proteins.

3.2.2 Establishing zebrafish xenografts as a tool for *in vivo* studies of cancer cells migration

Zebrafish have emerged as a useful tool to study tumour biology *in vivo* since, due to their visual clarity, they can be exploited by the use of fluorescent dyes to label cells and visualise invasion and metastasis (Shive, 2013).

In order to first establish a zebrafish xenograft model to study the migration behaviour of DOX-induced A431-ZEB2 cells, the cells were injected into different strains of pigment-deficient zebrafish such as ''*Casper*'', "*Nacre*" and wild type "*Danio rerio*", with or without PTU treatment.

In subsequent experiments, two PC cell lines, AsPC-1 and BxPC-3, were injected into three more transgenic zebrafish strains; tg (*mpx:eGFP*) with green fluorescent neutrophil (Renshaw et al., 2006), tg (*mpeg:Cherry*) with red macrophage (Ellett et al., 2011) and tg (*fli1:eGFP*) with green vasculature (Lawson and Weinstein, 2002) (Figure 3.3).

Various experimental parameters were then optimised. For example, the length of time to keep the fish before screening for cell dissemination, and the incubator temperature at which the fish were kept after injection. The developmental stages of the embryos used, and the anatomical site at which the cells were injected into the Yolk sac or perivitelline cavity of zebrafish embryos were also optimised.

In addition to the above, several technical parameters were tested, such as the concentration and temperature of the agarose used to immobilise the fish, the number of injected cells, the method of keeping cells prior to injection, the concentration of fluorescent dye for labelling, and the appropriate size and the type of needles used for microinjection.

Injections were repeated several times for each experiment so as to increase the reliability. From the data in table 3.1 it is apparent that the best conditions for obtaining reasonable data for the A431 cell line were to use "*Casper*" or "*Danio rerio*" strains treated with PTU. While for PC, the best results were obtained using "*Danio rerio*" treated with PTU. Furthermore, the best findings were observed when cells were injected into the perivitelline cavity of 2dpf zebrafish embryo immobilised in 1% agarose gel and incubated at 33 ºC for 48h before screening for cell migration.
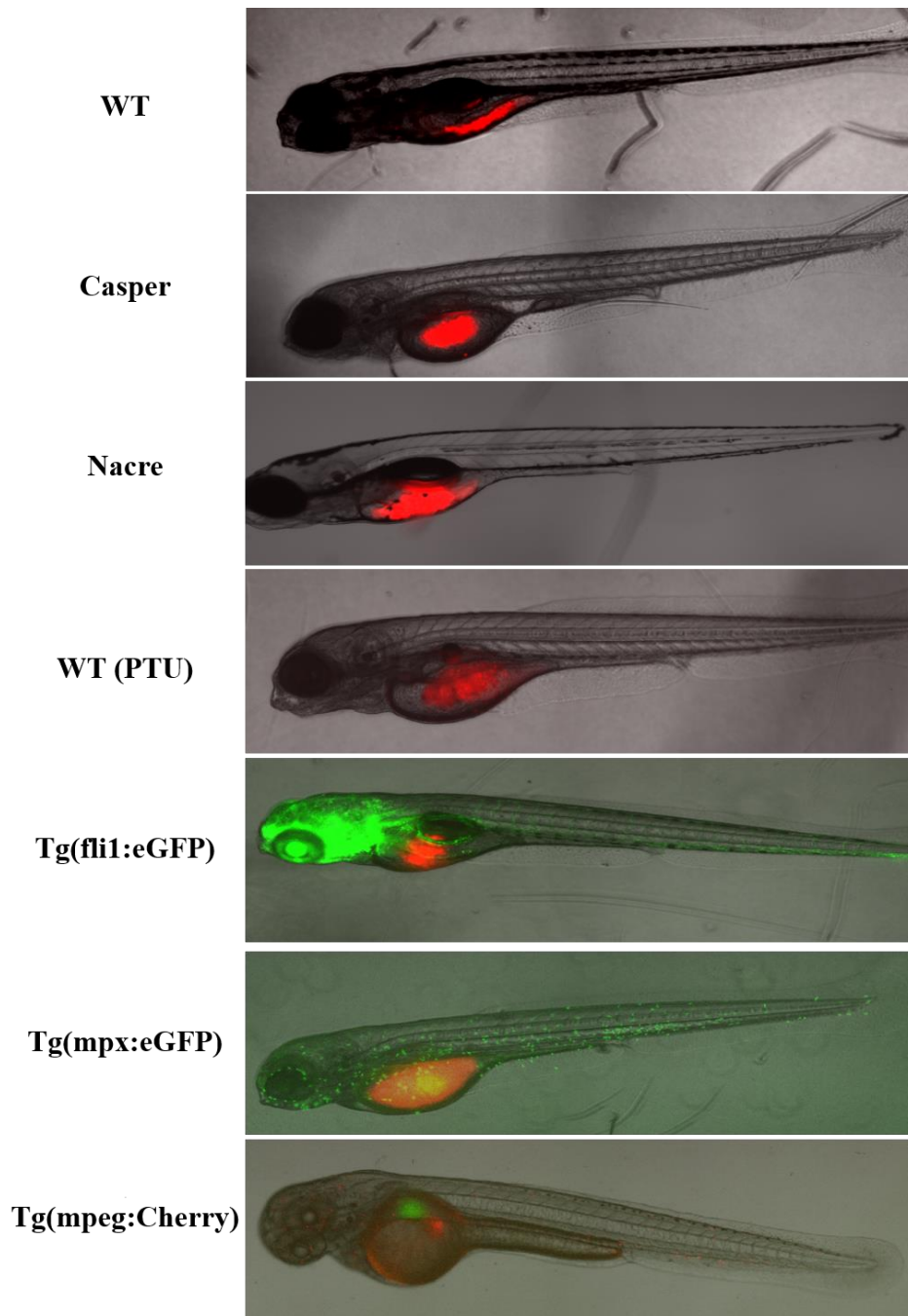
Figure 3.3 Strains of zebrafish used in this study.

DOX-induced A431-ZEB2 cells were fluorescently labelled and injected into different strains of pigment-deficient zebrafish ''*Casper*'', "*Nacre*" and wild type "*Danio rerio*", with or without PTU treatment. Furthermore, pancreatic cancer cells were injected into three more transgenic zebrafish strains; tg (*mpx:eGFP*) with green fluorescent neutrophil, tg (*mpeg:Cherry*) with red macrophage and tg (*fli1:eGFP*) with green vasculature. Fluorescence images were taken 2dpi with 4x objectives.

Table 3.1 Description of conditions used to optimize the microinjection protocol.

The best conditions are highlighted with red fonts.

Type of cells injected	Type of fish injected	Site of injection	Incubation temperature	Incubation time	Migration %
A431-ZEB2	W/T	Yolk Sac	28	48	10
A431-ZEB2	W/T	Yolk Sac	33	48	18
A431-ZEB2	W/T	Yolk Sac	33	72	0
A431-ZEB2	W/T	Perivitelline cavity	28	48	22
A431-ZEB2	W/T	Perivitelline cavity	33	48	10
A431-ZEB2	W/T	Perivitelline cavity	33	72	12
A431-ZEB2	W/T PTU	Yolk Sac	33	72	18
A431-ZEB2	W/T PTU	Perivitelline cavity	33	72	33
A431-ZEB2	**W/T PTU**	**Perivitelline cavity**	**33**	**48**	**36**
A431-ZEB2	**Casper**	**Perivitelline cavity**	**33**	**48**	**40**
A431-ZEB2	Casper	Perivitelline cavity	28	48	28
A431-ZEB2	Casper	Perivitelline cavity	28	72	10
A431-ZEB2	Nacre	Yolk Sac	33	48	0
A431-ZEB2	Nacre	Perivitelline cavity	33	48	12
AsPC-1	W/T	Perivitelline cavity	28	48	0
AsPC-1	W/T	Perivitelline cavity	33	48	9
AsPC-1	W/T PTU	Yolk Sac	33	48	16
AsPC-1	W/T PTU	Perivitelline cavity	33	72	22
AsPC-1	**W/T PTU**	**Perivitelline cavity**	**33**	**48**	**46**
AsPC-1	Casper	Perivitelline cavity	33	48	18
AsPC-1	Nacre	Perivitelline cavity	33	48	0
AsPC-1	Fli1:GFP	Perivitelline cavity	33	48	8
AsPC-1	mpeg:cherry	Perivitelline cavity	28	48	10
AsPC-1	mpeg:cherry	Perivitelline cavity	33	48	10
AsPC-1	mpeg:cherry	Yolk Sac	33	72	28
AsPC-1	mpx:GFP	Perivitelline cavity	33	48	25
AsPC-1	mpx:GFP	Youc ac	33	48	0
BxPC-3	W/T	Perivitelline cavity	28	48	0
BxPC-3	**W/T PTU**	**Perivitelline cavity**	**33**	**48**	**22**
BxPC-3	mpeg:cherry	Perivitelline cavity	33	48	0
BxPC-3	mpx:GFP	Perivitelline cavity	33	48	9
BxPC-3	mpx:GFP	Perivitelline cavity	33	72	20
BxPC-3	mpx:GFP	Yolk Sac	33	72	9

3.2.3 ZEB2 expression promotes migration of A431-ZEB2 cells in zebrafish

To determine whether the induction of EMT in A431 cells by activation of ZEB2 expression has any effect on cell migration, however, the cells were grown in the absence and presence of DOX for 48h. The cells were then fluorescently labelled (Figure 3.4) and injected into the perivitelline cavity of 2dpf zebrafish embryos. The processes of the invasion and migration of cancer cells within the living animal body were visualised at 48hpi using fluorescence microscopy.

It can be seen from the data in table 3.2 that the average migration rate for cells cultured in the presence of DOX before injection was 43.3%, while the rate for non-treated cells was only 6.3%; a result which was statistically significant ($P=0.001$) (Figure 3.5A). Untreated cells remained inside the transplantation site and did not disseminate, whereas cells treated with DOX spread through the vasculature into other parts of the body of the fish such as the head and tail (Figure 3.5B).
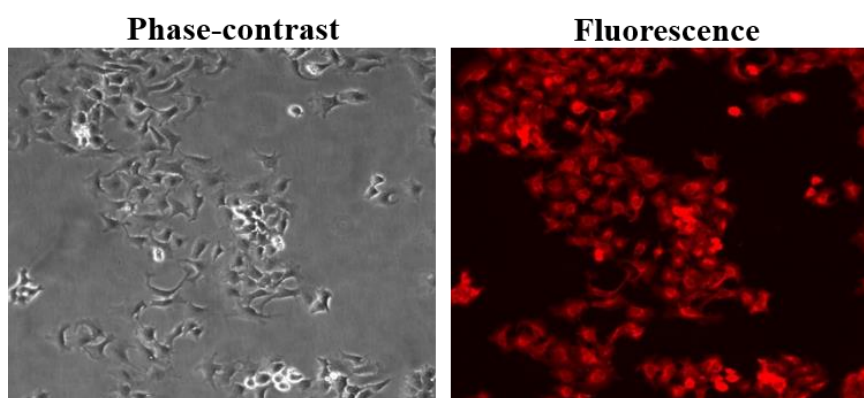
Figure 3.4 Fluorescence labelling of A431-ZEB2 cells prior to injection.

In order to check the efficiency of the labelling, fluorescence and phase-contrast images of cells were taken for Dilc12-labelled A431-ZEB2 cells using a 20x-objective.

Table 3.2 Migration of control (-DOX) and treated (+DOX) A431-ZEB2 cells.

Cell migration in zebrafish embryos was quantified in 3 independent experiments.

Type of injected cells	Migration %	Average migration %
(-DOX) A431-ZEB2	0	6.3
	9	
	10	
(+DOX) A431-ZEB2	50	43.3
	40	
	40	

A
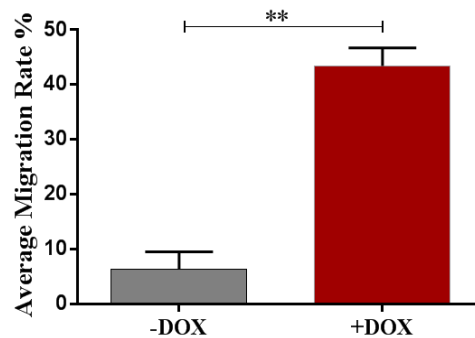
B
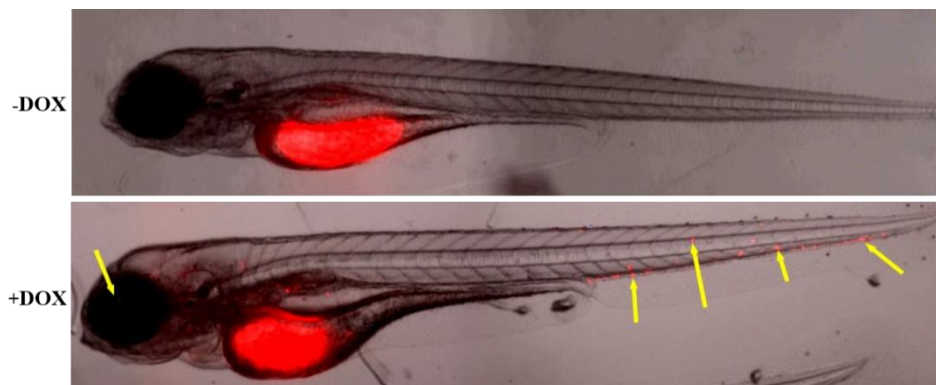
Figure 3.5 ZEB2 activation enhances A431 cell migration in zebrafish.

(A). Statistical analysis of the effect of ZEB2 on the dissemination of A431 cells. Bar charts with standard errors of the mean represent the average migration rate of control (-DOX) or treated (+DOX) A431-ZEB2 cells, ** P=0.001. The results of 3 independent experiments are shown. **(B).** Merged images of zebrafish embryos 48hpi. A431-ZEB2 cells cultured in the presence or absence of DOX were fluorescently labelled and injected into the perivitelline cavity of 2dpf zebrafish embryos. Fluorescence images were taken 2dpi with 4x objectives. Untreated cells (-DOX) remained inside the yolk sac and did not disseminate, while treated cells (+DOX) spread to other parts of the body. Arrows indicate disseminated tumour cells.

3.2.4 The effect of siRNA-mediated S100A4 and S100A6 knockdown on EMT in A431 cells

3.2.4.1 Optimisation of the transfection protocols for A431-ZEB2 cells

Since S100A4 and S100A6 have been shown to be activated during ZEB2-induced EMT, the expression of these proteins was modulated by an RNAi approach so as to study their role in the EMT process. A series of transfection protocols was performed to optimise the efficiency of the transfection. For this purpose, A431-ZEB2 cells were transfected with pmaxGFP plasmid using Ingenio® Electroporation solution and Amaxanucleofector II devices with different programs, including T-020, T-030 and A-020, as well as transfection with jetPRIME (See Materials and Methods). Fluorescence and phase-contrast images were taken 48h after transfection in order to assess the level of GFP-fluorescence as a measure of transfection efficiency.

The result showed that, among all the protocols, transfection with Ingenio® Electroporation solution and jetPRIME had the highest transfection efficiency, with a reasonable number of intact cells, compared with the other methods. Although transfection using Amaxanucleofector II devices with different programs produced higher efficiency, the majority of cells were dead, which meant viability was inadequate for the required experiments (Figure 3.6).
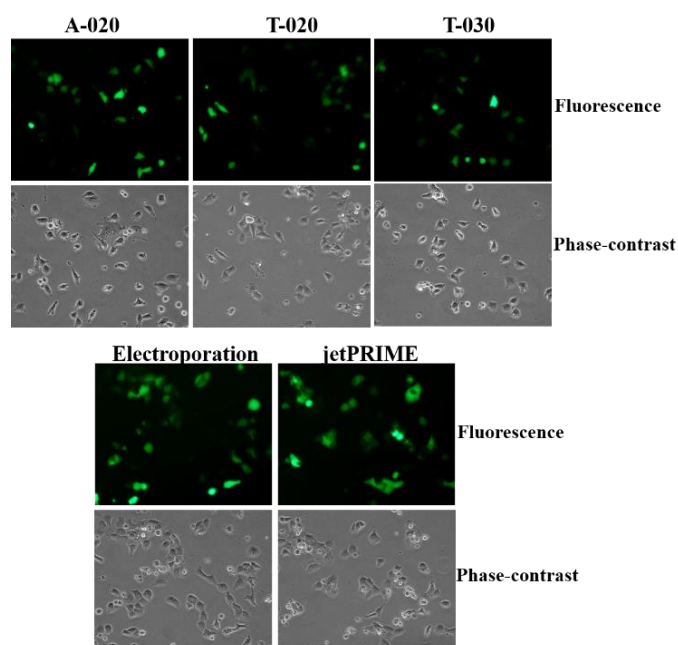
Figure 3.6 Optimization of transfection protocol for A431-ZEB2 cells.

Fluorescence and phase-contrast images of cells were taken with 20x objective after transfection with 1µg pmaxGFP plasmid using nucleofection protocols (Amaxa nucleofector) with different program, electroporation and jetPRIME.

3.2.4.2 Knockdown of S100A4 and S100A6 delay EMT development in A431 cells

In order to correlate the expression of S100 proteins with the morphological changes that occur during the EMT process, phase-contrast time lapse microscopy for A431-ZEB2 cells was performed. Cells were seeded in six well plates containing 2ml of growth media. After 24h, the cells were transfected with 2μg of siS100A4, siS100A6, a combination of both siS100A4&A6 and a siControl using the jetPRIME protocol. Cells were maintained in the presence of DOX and time lapse microscopy was started immediately after transfection. Acquisition settings and experimental conditions were set up in an environmental microscope chamber operated at ~90% humidity, 37 °C and 5% CO_2. Three positions were selected for each well and the cells were imaged every 15 mins with a total recording time of 72h.

As mentioned previously, at the 0h time point, cells in all wells displayed an epithelial phenotype and formed small clusters. Interestingly, 24h post transfection, control cells (i.e. those transfected with the siControl) tended to escape from their boundaries and appeared to be more scattered than cells in which S100A4 or S100A6 had undergone knockdown, raising the possibility that activation of S100A4 or S100A6 could be required for this phenotypical change. This effect was also observed at 72h, in that the control cells appeared to migrate more individually and became semi-fully scattered compared to S100A4&A6 repression cells (Figure 3.7). Overall, activation of S100A4 or S100A6 in DOX-induced A431-ZEB2 cells accelerated the transition of cells from an epithelial to fibroblast-like shape, indicating that the presence of both proteins is a requirement for EMT progression.
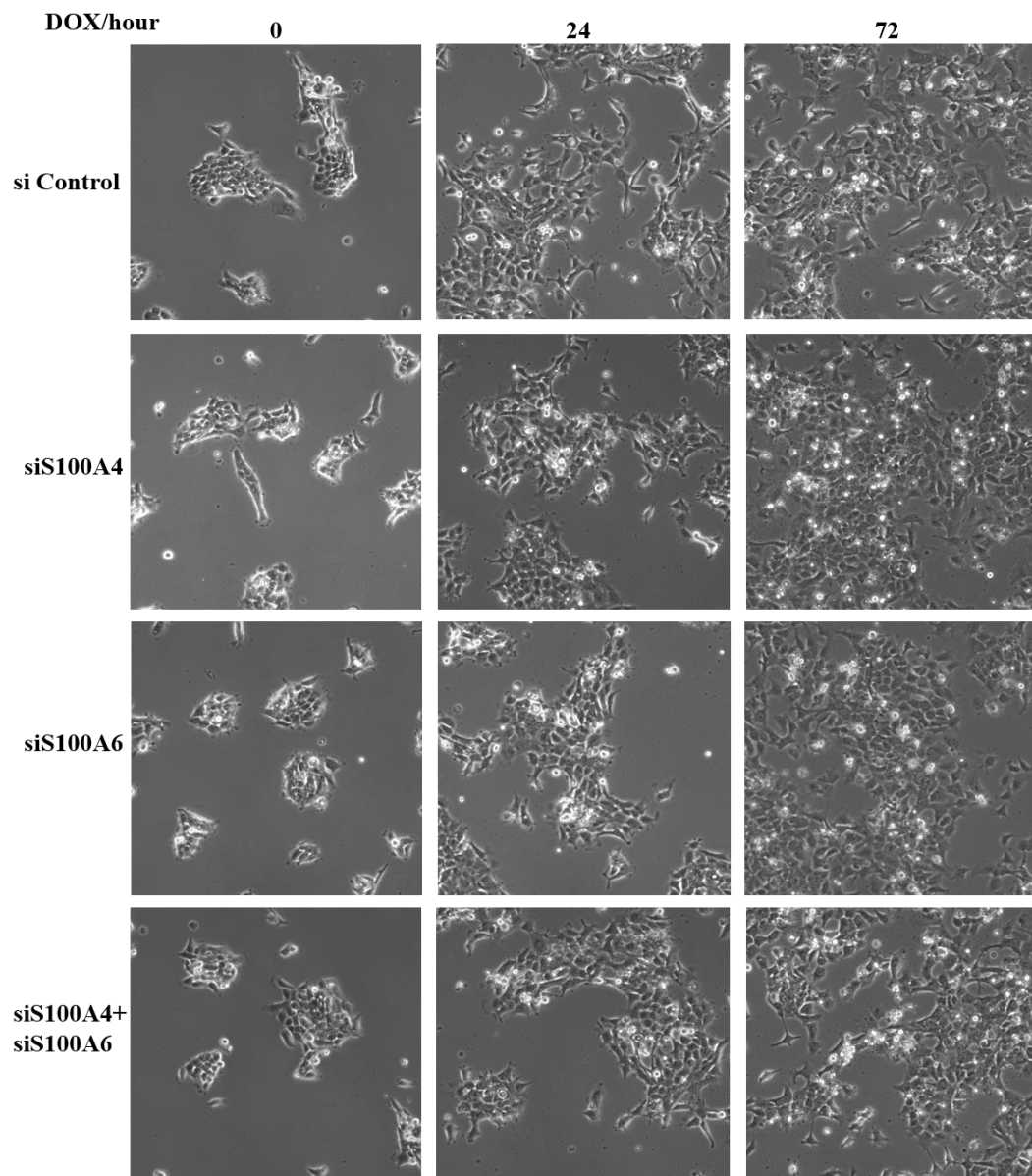
Figure 3.7 Time-lapse microscopy of the effect of S100 proteins knockdown on EMT process in A431 cells.
A431 cells were transfected with siS100A4, siS100A6, a combination of both siS100A4&A6 and siControl using jetPRIME protocol. Phase-contrast images were taken every 15 mins for 72h with a 4x objective using Nikon microscope. This is what the cells looked like when the experiment was performed.

3.2.4.3 siRNA knockdown of S100A4 and S100A6 inhibits A431-ZEB2 cell migration and invasion *in vivo*

Since S100A4 and S100A6 activation was observed during ZEB2 induced EMT, it can therefore be suggested that the molecular mechanism of ZEB2 promoting cancer cells migration may has been caused by activation of these proteins. To confirm their role during EMT, S100A4&A6 expression was modulated using an RNAi approach.

We first determined the time point at which the expression level of S100A4 and S100A6 reached peaked during ZEB2 induced EMT. To this end, cell lysates were collected from A431 cells after treatment with DOX at different time points (0, 24, 48 and 72h). Analysis of protein levels showed that the expression levels of both S100A4 and S100A6 activated at the 24h time point and increased progressively, reaching the highest level at the 48h time point (Figure 3.8A). Consequently, A431-ZEB2 cells were transfected with siS100A4, siS100A6, a combination of both siS100A4&A6 and siControl, and the cells maintained in the presence of DOX for 48h. The cells were then injected into 2dpf zebrafish embryos and fluorescent microscopy imaging acquired for 48hpi to screen for A431-ZEB2 cell dissemination and migration.

Zebrafish injected with siControl cells exhibited an average migration rate of 40.3%, which was higher than from those injected with siS100A4, siS100A6 and a combination of siS100A4&A6 cells, which displayed average migration of 13.6%, 6.7% and 6.7%, respectively (Table 3.3). This led to the following significant differences between the control group and the other groups: (siControl vs. siS100A4 $P= 0.001$) (siControl vs. siS100A6 $P= 0.0003$) (siControl vs. siS100A4+siS100A6 $P= 0.0004$) (Figure 3.8B). Cells in which S100A4 and S100A6 had undergone knockdown remained within the confines of the injection site and did not disseminate, compared to the control cells, which disseminated extensively throughout the body of the fish (Figure 3.8C).

To confirm the efficiency of siRNA knockdown, the expression of S100A4 and S100A6 were assessed at the mRNA and protein levels in S100A4&A6-knockdown cells. S100A4 or S100A6 targeted siRNA knockdown reduced the mRNA expression level of its specific target transcript (S100A4: siControl vs siS100A4 $P= 0.005$, siControl vs siS100A6 $P=ns$ and si control vs siS100A4&A6 $P=0.0006$) (S100A6: siControl vs siS100A4 $P=ns$, siControl vs siS100A6 $P=0.005$ and siControl vs siS100A4&A6 $P=0.003$).

94

Additionally, Western blot analyses validated the downregulation of S100A4 and S100A6 in respect to the protein level in cells transfected with targeting siRNA.

Together these findings provide important insights into the role of S100A4 and S100A6 proteins in EMT and tumour progression.

Table 3.3 Migration of A431-ZEB2 cells transfected with siControl, siS100A4, siS100A6 and combination of siS100A4&A6.

Cell migration was quantified in 3 independent experiments

Type of injected cells	Migration %	Average migration %
siControl	40	40.3
	36	
	45	
siS100A4	8	13.6
	15	
	18	
siS100A6	0	6.7
	10	
	10	
siS100A4+ siS100A6	9	6.7
	0	
	11	

A
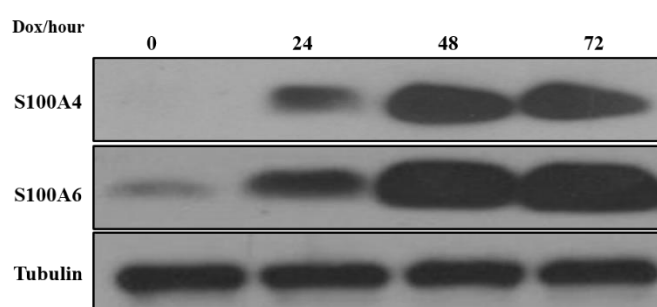
B
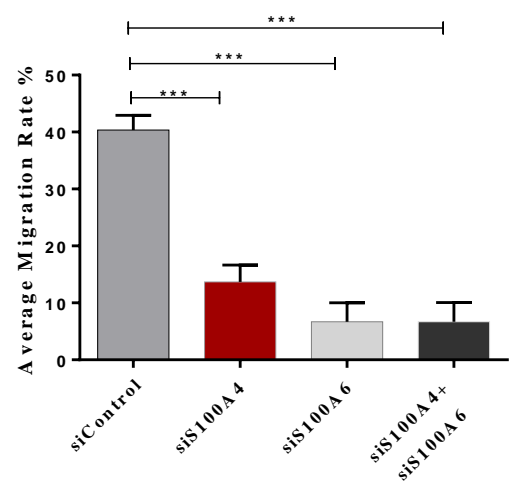
C
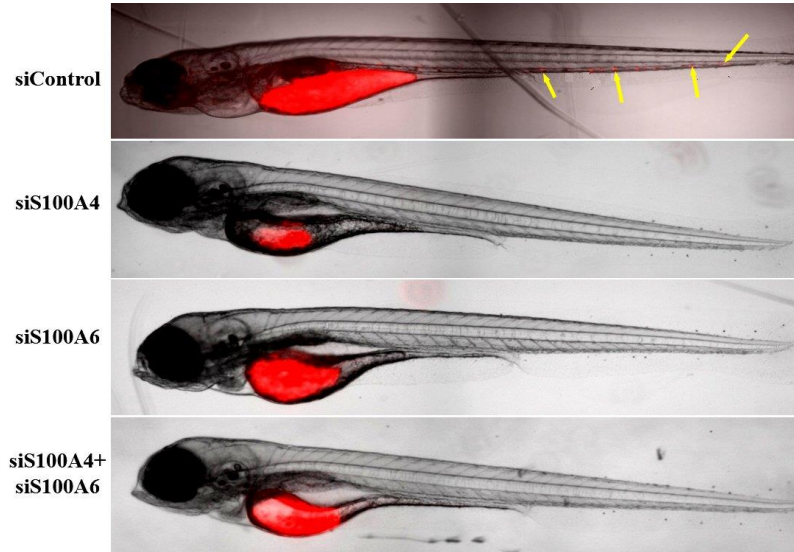
D
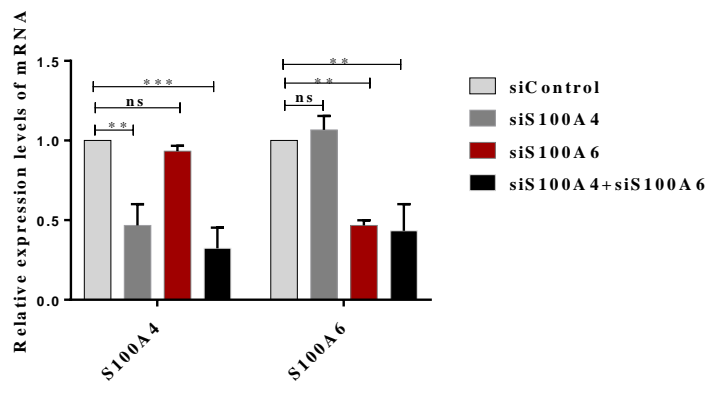
E
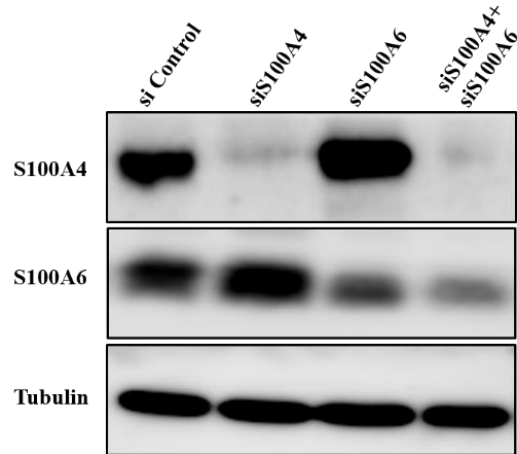
Figure 3.8 Effect of S100A4 and S100A6 silencing on A431 cells migration.

 (A). Protein analysis showed that S100A4 and S100A6 protein expression reached a peak at 48h post DOX treatment. **(B)** Statistical analysis of knockdown of S100A4 or S100A6 on the dissemination of A431-ZEB2 in zebrafish. Bar charts with standard errors of the mean represent the average migration rate of control A431-ZEB2 cells or cells with reduced expression of S100 proteins, *** $P \leq 0.001$. All experiments were performed in the presence of DOX. The results of 3 independent experiments are shown. **(C).** Merged images of zebrafish embryos at 48hpi**.** A431-ZEB2 cells were transfected with siS100A4, siS100A6, combination of both and siControl and injected into zebrafish. Fluorescence images were taken 2dpi using 4x objective. Arrows indicate disseminated tumour cell. **(D).** The relative mRNA expression level was quantified using the $2^{-\Delta\Delta CT}$ method. Bar charts with standard errors of the mean represent delta CT value, ** $P \leq 0.005$, *** $P = 0.0006$. The results from 3 representative experiments are shown. **(E).** Downregulation of S100A4 and A6 proteins levels were confirmed by Western blot.

3.3 Discussion

3.3.1 Establishing zebrafish xenografts as a tool for the *in vivo* study of cancer cell migration

Transplantation of cancer cells into transparent zebrafish embryo has provided a new insight into the processes by which tumour cells disseminate and migrate. There has been no previous use of zebrafish as an animal model to study *in vivo* migration of cancer cells here in the University of Leicester. Establishing a zebrafish model was therefore one of the priorities of this study. Protocols for zebrafish requirements included feeding and breeding, in addition to environmental factors such as incubation temperature, which differ from lab to lab. Efforts to define the optimum standards associated with handling and use of zebrafish for research purpose have been made by (Obenschain and Aldrich, 2007), nevertheless, it was necessary to make some modification to conform to new cell requirements.

In this study, certain issues were taken into consideration which may affect the behaviour of cancer cells when injected into zebrafish; for example, selection of zebrafish strains to serves as the xenograft recipient. Most published results using zebrafish as a model to study cell migration behaviour have emphasised the use of the wild type strain "*Danio rerio*" due to the restricted availability of transparent mutant and transgenic zebrafish strains. Pigmentation in the wild type usually starts at 30 hpf (Hill et al., 2005) and pigment cells become fully differentiated during a few hours from this point, reducing visualisation through the epidermis layers.

Karlsson et al. developed a new protocol to generate transparent zebrafish by treating wild type embryos with PTU during their early developmental stages (Karlsson et al., 2001). This protocol has traditionally been used in subsequent studies as a rapid and inexpensive way to get optically clear zebrafish for use as a powerful model to evaluate cancer cell migration (Teng et al., 2013, Wang et al., 2015a, Breznik et al., 2017). Recently, new strains of transgenic zebrafish which entirely lack pigmentation, such as "*Casper*" and "*Nacre*" (El-Naggar et al., 2015), as well as fluorescent reporter fish strains which display fluorescent dye within the endothelial tg(*fli1:eGFP*) (Zoni et al., 2017), neutrophil tg(*mpx:eGFP*) (Wang et al., 2015a) and macrophage cells tg(*mpeg:Cherry*) (Wertman et al., 2016) have been used in xenotransplantation experiments.

During the optimisation of the zebrafish protocol undertaken for this study, A431 and the selected PC cell lines, AsPC-1 and BxPC-3, were injected into all the zebrafish strains mentioned previously, in addition to wild type zebrafish treated with PTU. The results showed that the number of disseminated cells in "*Casper*" and WT fish treated with PTU were higher compared to other strains and could be seen more clearly, demonstrating that the optical clarity of these fish during fluorescence microscopy permitted high resolution imaging, deep into the tissue, thus enabling the migration behaviour of tumour cells to be clearly observed.

One of the most important steps for microinjection protocols is the orientation of the fish in a single direction in order to access the site of injection and facilitate imaging. This process was achieved by immobilising the fish by placing them in low melting point agarose. The fish were immobilised twice in each experiment, once at the time of injection and the other at 48hpi so as to screen for dissemination of cells (as described in Materials and Methods). The concentration and temperature of agarose therefore proved to be a very critical factor. Using agarose that is too hot can result in heat shock, resulting in the death of the fish after few hours; whereas, agarose that was not warm enough dried out quickly, affecting the orientation of the fish after a short period of time. The appropriate temperature for the agarose was tested, with 28ºC being selected as the ideal. Additionally, the concentration of agarose is important and different concentrations were tested (0.5%, 1% and 2%) to obtain the optimal concentration to facilitate cutting the embryo out of the agarose. A 1% agarose was selected as a working concentration for fish mounting.

The anatomical site of injection within embryonic zebrafish is essential for allograft transplantation experiments, and this is closely linked to the developmental stage of the zebrafish. For instance, the yolk sac completely disappears after 7dpf, preventing it be used as a site of injection (Wertman et al., 2016). Most studies which used a zebrafish as a model to study cancer cell migration have only focused on 2dpf embryos as transplant recipients (Ghotra et al., 2015), since at this stage of development fish are optically transparent and lack the functional immune system components that may cause transplanted cells to be rejected (Lam et al., 2004). Yolk sac, blood circulation, hindbrain ventricle and perivitelline spaces are considered to be the most common injection sites during transplantation experiments (Wertman et al., 2016).

Recent studies that have using zebrafish as an *in vivo* model have tended to select the yolk sac (El-Naggar et al., 2015) and perivitelline spaces (Chiavacci et al., 2015) as optimal sites for injection. Accordingly, in this study, cells were transplanted either into the yolk sac or perivitelline spaces of embryos.

Moreover, environmental factors also needed to be considered, especially the incubation temperature for injected fish. Zebrafish embryos are usually kept at 28.5°C but this temperature is not appropriate for the growth of mammalian cells. (Haldi et al., 2006) raised the incubation temperature to 35 °C without any noticeable effect on the zebrafish development and cell behaviour. Subsequent studies have also reported that incubation of injected fish at 35 ºC enabled normal growth of transplanted human cells without any noticeable effect on zebrafish embryogenesis (Zoni et al., 2017). Two different temperatures were tested here, however: 28 °C and 33 °C, with the latter selected as the ideal standard for both fish and cells in this model.

Besides the previous issues, some technical parameters were also tested, such as the proper size and the type of needles using for microinjection. Non-filamentous needles were used to transplant tumour cells, because needles with filament can result in sheering of cancer cells during injection. Furthermore, the diameter of the needle should be appropriate for the size of the tumour cells: not too small as this could lead to blockages in the needle but not so large as to risk causing damage at the site of injection thereby leading to transplanted cancer cells leaking out.

In summary, after this series of steps to optimise microinjection protocols for this study, a set of experimental parameters were adopted which were believed to be optimal for zebrafish xenotransplantation applications. In conclusion, these parameters include using 2 dpf "*Casper*" embryos or WT zebrafish treated with PTU as the host, 1% agarose for mounted fish, perivitelline spaces as the ideal injection site, 33°C as the optimal temperature at which to keep the injected fish and, finally, 48h as the appropriate incubation period before screening for cell migration.

3.3.2 ZEB2 activation initiates EMT and promotes migration of A341-ZEB2 cells in zebrafish embryos

EMT is the process whereby polarised epithelial cells convert into the motile mesenchymal cells that underpin cancer cells' invasiveness and metastasis (Bhardwaj et al., 2015). Evidence suggests that ZEB2 is among the most EMT-inducing factors, and exerts its transcriptional activity by binding to E-Cadherin promoter and downregulating the expression of this cell-cell adhesion junction (Yang et al., 2015).

In this study, activation of ZEB2 was observed in A431 cells after 24h treatment with DOX, when cells were observed to lose adhesion to their neighbouring cells and to begin to scatter. Since ZEB2 represses the expression of E-Cadherin, and stimulates the expression of genes involved with cell motility (Ouyang et al., 2010), the level of expression of epithelial markers (E-Cadherin and P-Cadherin) began to decrease, whilst expression of the mesenchymal marker, Vimentin was increased. These observations are consistent with other published results showing an inverse correlation between E-Cadherin and ZEB2 expression level in various models of epithelial cancer cells, such as MDAMB-231 and MDA-MB-435S1 (Vandewalle et al., 2005).

More recently, expression of ZEB2 has been reported to be implicated in cancer cell invasion and metastasis in a variety of cancer types (Okugawa et al., 2013, Yoshida et al., 2015). A431 cells are a human epidermoid carcinoma with epithelial features which are usually arrested on the basement membrane, and are joined tightly to neighbouring cells. Under normal conditions, epithelial cells cannot escape from the layer (Schock and Perrimon, 2002). In contrast, mesenchymal cells show strong migratory and invasive behaviour.

Activation of ZEB2 during treatment of cells with DOX repressed the expression of E-Cadherin and thus led to the bonds between cells breaking, and consequently increasing cell migration. Zebrafish injected with treated-A431-ZEB2 cells (+DOX), therefore, exhibited an average migration rate of 43.3%, which was significantly higher (P=0.001) than that of untreated cells (-DOX), which had a 6.3% average migration rate. Untreated cells remained inside the yolk sac and did not disseminate, raising the possibility that these cells have an epithelial phenotype and cannot spread or move away. Meanwhile, treated cells, which had more mesenchymal phenotypes, spread and disseminated, indicating that ZEB2 activation increases A431-ZEB2 cell migration *in vivo.*

These findings are in agreement with other research that has found that ZEB2 enhanced EMT progression, and acquisition of an invasiveness and migratory phenotype in hepatocellular carcinoma (Yang et al., 2015), in eyelid sebaceous gland carcinoma (Bhardwaj et al., 2015), acute myeloid leukaemia (Li et al., 2017) and ovarian cancer (Prislei et al., 2015). The discrepancy of -/+DOX cell behaviour could be attributed to ZEB2 expression, suggesting that ZEB2 can be a major contributor to cell migration.

3.3.3 Activation of S100A4 and S100A6 proteins during ZEB2 induced EMT

The precise mechanism underlying activation of ZEB2 promoted A431 cell migration is poorly understood. Expression levels of different members of S100 proteins have been found to be altered during ZEB2 induced EMT, leading to speculation as to their causative role in different human cancers (Sedaghat and Notopoulos, 2008, Lesniak, 2011). A well-known example for this assumption is the fact that expression of S100A4 is increased in metastatic cancer and so called metastasin (Sherbet, 2009), whereas expression of S100A2, which often acts as a tumour suppressor protein, is decreased in many malignant tissues (Wicki et al., 1997).

According to the data obtained by qPCR and Western blot (Figure 3.2), expression of S100 at mRNA and protein levels was altered during ZEB2 induced EMT in the A431 cell line, and only S100A4 and S100A6 among the S100 member proteins was activated. These results support previous studies (Elder and Zhao, 2002, Cross et al., 2005) which concluded that, although S100 protein members have a similar structure and gene cluster location, expression patterns of these proteins are altered from cell to cell or in cancer versus normal tissues.

Generally, much evidence has emerged from previous research to indicate that expression of S100A4 and S100A6 proteins could be a contributing factor to EMT progression, especially since an inverse correlation has been identified between E-Cadherin and S100A4 (Zhai et al., 2014) and S100A6 (Li et al., 2014). Moreover, Snail, the master EMT regulator transcriptional factor, has been found to increase the expression of S100A4 in cells which undergo EMT (Moody et al., 2005).

In the current study, activation of both S100A4 and S100A6 expression was related to ZEB2 induced EMT in A431 cells after treatment with DOX, which gave rise to speculation that ZEB2 can be a transcriptional regulator for S100 proteins.

ZEB2, however, has so far not been reported to be one of the factors activating transcription of S100 proteins. Another link between ZEB2 and S100 proteins expression, however, is that ZEB2 is strongly involved in the activation of TGF-β signalling, the major inducer for EMT (Xu et al., 2009). Indeed, a study by (Naz et al., 2014) revealed that expression of S100A4 was activated in a TGF-β -dependent manner.

3.3.4 Knockdown of S100A4 and S100A6 delays EMT development and inhibits A431-ZEB2 cell migration *in vivo*

EMT is defined as a multistep process which begins with loss of cell-cell adhesion, cell scattering, re-modelling of the cytoskeleton and formation of membrane protrusions (lamillopodia), and the subsequent acquisition of a mesenchymal phenotype (Moreno-Bueno et al., 2009). Activation of S100A4 and S100A6 expression in A431 cells was observed 24h post DOX treatment and its expression increased markedly, continuing to be present until at least 72hpi. This activation is consistent with loss of cell-cell contact, scattering, spreading and the formation of large lamellipodial protrusions, raising the possibility that the formation of such protrusions may have been caused by activation of S100A4&A6.

These observations are in agreement with the findings of (Okada et al., 1997) that expression of S100A4 is associated with morphological changes that occur during EMT in the proximal tubular epithelial cells (MCT). Furthermore, exposure of cells to S100A4 antisense oligomers resulted in the blocking of EMT, suggesting that S100A4 expression is required for EMT progression.

Additionally, the cells in which the expression of S100A4&A6 was downregulated by siRNA look less scattered than those which were transfected with non-targeting siRNA, supporting (Lo et al., 2011) finding that the silencing of S100A4 in two head and neck squamous cell carcinoma cell lines that exhibited mesenchymal-like features led to impaired cells stemness abilities, indicating that S100A4 does play a critical role in maintaining mesenchymal properties in these cells.

The potential role of S100A6 in phenotypic changes of cells during EMT is still unclear, but, according to earlier reports, S100A6 has the ability to interact with the tropomyosin-actin complex (Golitsina et al., 1996), which is important for cell architecture and lamellipodium formation (Small and Resch, 2005).

The proposed function of S100A4 and S100A6 has focused on their role in the regulation of cell migration, with their downregulation suppressing the ability of cell migration while their upregulation promotes it (Tarabykina et al., 2007). This is in accord with the fact that highly motile cells, such as macrophages and neutrophils, express high levels of S100A4&A6 (Cabezon et al., 2007). Although much is known about the strong correlation between S100A4/A6 and EMT, no study has analysed the effect of these proteins on cell migration during EMT. In this study, therefore, the presence of S100A4&A6 was found to promote cell migration in zebrafish approximately three times more powerfully than cells in which expression of these proteins was not activated by DOX, or was reduced by siRNA.

In agreement with this, for example, in gastric cancer, overexpression of S100A4 or S100A6 promotes cell migration, while their downregulation inhibits the rate of cell migration (Yuan et al., 2014, Li et al., 2013). In another study regarding the functional role of S100A4 in cancer, (Yuan et al., 2014) overexpressed S100A4 in two gastric cell lines, AGS and SCM-1, and found that this expression significantly increased the invasive activity of these cells. Silencing S100A4 expression in MKN-45 and TMK-1, which displayed high levels of endogenous S100A4, resulted in a decrease in the migration rate but without any effect on cell survival.

3.4 Conclusion

From the research that has been undertaken, it is possible to conclude that the expression pattern of S100 proteins is altered during ZEB2-induced EMT in the cell line A431, and among the selected S100 proteins, only S100A4 and S100A6 are activated. Additionally, S100A4 and S100A6 are required for EMT development and play a vital role in cancer cell migration in zebrafish. Finally, we could conclude that zebrafish xenografts are a useful tool for *in vivo* studies of EMT.

Chapter 4: EMT-associated S100 proteins are modulators for the progression of pancreatic cancer

4.1 Introduction

Pancreatic cancer (PC) is considered to be the fourth leading cause of cancer-related mortality and the tenth most common cancer in the UK (Cancer Research UK, 2016). Metastasis is considered the most critical factor for PC lethality and is associated strongly with poor outcomes (Le Large et al., 2017). There is much evidence to suggest that the highly metastatic behaviour of PC may be due to the ability of its cells to undergo EMT (Karamitopoulou, 2013, Castellanos et al., 2013). More than 70% of primary pancreatic tumours that display mesenchymal properties can metastasise into another organ (Rasheed et al., 2010, Dangi-Garimella et al., 2012).

The S100 family of small Ca-binding proteins are among many genes that have been found to be implicated in PC cancer progression and with poor clinical outcomes. Activation of some members of the S100 protein family, such as S100A4 and S100A6, have been postulated to be a common mediator of the EMT process and a key driver for PC cell migration and invasion (Mirza et al., 2014, Chen et al., 2015b). To our knowledge, however, there is no conclusive evidence that the presence of the S100 family is causally implicated in EMT-induced PC progression.

Recently, there is a growing body of evidence that recognises the important role of exosomes in the pathogenesis of PC, via the transfer of various oncogenic proteins and RNAs to adjacent or distant cells (Costa-Silva et al., 2015). Although many studies have shown that S100 proteins members are among the protein cargo of exosomes (He et al., 2015, Prieto et al., 2017), the role of S100 proteins containing exosomes in PC progression has not previously been described.

The aim of this chapter was to explore the role of S100 proteins in the EMT process in PC progression by investigating the expression of S100 family members and their correlation with EMT-associated proteins in PC cells. Additionally, this chapter aimed to study the effectiveness of S100 proteins in PC cell migration in zebrafish embryos.

4.2 Results

4.2.1 The expression profile of EMT-associated genes in pancreatic cell lines

A series of pancreatic cell lines with different morphological and adhesion features were selected in this study. We firstly categorised the cell lines as either epithelial or mesenchymal-like according to morphological features or clustering. The cell lines BxPC-3, SU.86.86, HPAF-II, CAPAN-1, PANC-1, and the immortalised cell line HPDE, displayed an epithelial phenotype which comprised of cells that attach tightly together by intracellular adhesion. MIA PaCa-2 cells, meanwhile, were unambiguously classified as mesenchymal cells, characterised by small protrusions and focal cell-cell adhesion. AsPC-1 cells were more difficult to classify because these cells exhibited some features of each type (epithelial or mesenchymal) (Figure 4.1A). This experiment, therefore, aimed to determine the expression of EMT-related proteins as a way of classifying and differentiating these phenotypes.

Western blot analysis was consistent with the morphological phenotyping and showed that all the epithelial cells expressed high level of the epithelial markers, E-Cadherin and P-Cadherin. MIA PaCa-2 also appeared to be strongly positive for the mesenchymal protein Vimentin. The AsPC-1 cells again had characteristics of both epithelial and mesenchymal cells, since both E-Cadherin and Vimentin were expressed in this cell line. Regarding different EMT-TFs, the expression pattern was inconclusive in PC cells.

 The expression of Snail and Slug was detected in different cell lines but could not be specifically assigned to individual phenotypes. ZEB2 was not detected in any cell line, while Twist1 was expressed only in HPDE cells (Figure 4.1B). ZEB1, however, was the factor that most obviously corresponded to morphological features and the downregulation of E-Cadherin and upregulation of Vimentin.
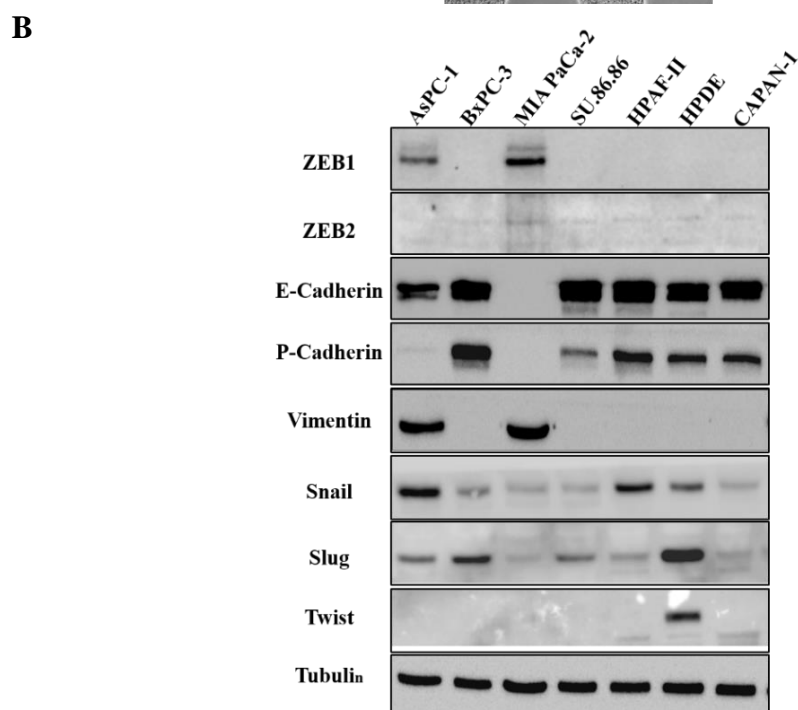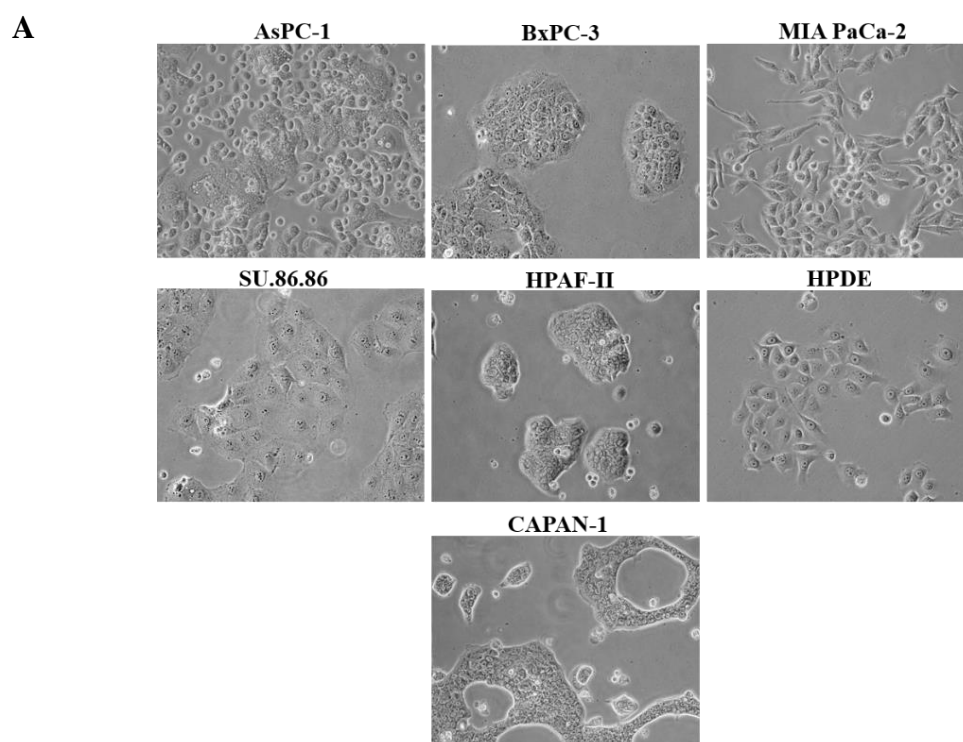
Figure 4.1 Expression of the EMT-associated proteins in the selected pancreatic cell lines.

(A). BxPC-3, SU.86.86, HPAF-II, HPDE and CAPAN-1 exhibited epithelial phenotypes. MIA PaCa-2 cells have mesenchymal futures with spindle like extension, while AsPC-1 cell line have characteristics of both epithelial and mesenchymal cells. Phase-contrast images were taken with 20x objective. **(B).** Cell lysates were collected and resolved on polyacrylamide gel. The transferred membranes were stained for EMT-related proteins including ZEB1, ZEB2, Vimentin, E-Cadherin, P-Cadherin, Snail, Slug, Twist as well as tubulin as a loading control.

4.2.2 Differential expression of S100 proteins in pancreatic cell lines

It has been reported that expression of members of the S100 gene family differs in different human malignancies. The expression of these family members varies between cells and may be specific for certain phenotypes, with some of them upregulated in epithelial cells, while others tend to be mesenchymal markers. qPCR and Western blot analysis were therefore conducted in order to analyse the expression profiles in pancreatic cell lines of eleven members of the S100 family of genes at the mRNA level (S100A2, S100A4, S100A6, S100A7, S100A8, S100A9, S100A10, S100A11, S100A13, S10014 and S100P) and eight members at protein levels (S100A2, S100A4, S100A6, S100A8, S100A9, S100A11, S10014 and S100P). Additionally, mRNA expression levels of the EMT-associated genes ZEB2, Vimentin, E-Cadherin and P-Cadherin were also analysed.

qPCR data, represented as a heat map in Figure 4.2A, showed that mRNA expression levels of S100A2, S100A7, S100A8, S100A9, S100A10, S100A13, S100A14 and S100P genes were upregulated in epithelial phenotype cells compared to mesenchymal cells, and this expression was associated positively with the epithelial related genes, E-Cadherin and P-Cadherin. Expression of S100A4, meanwhile, was found to be upregulated in cells with mesenchymal features, AsPC-1 and MIA PaCa-2, in parallel with the activation of the mesenchymal genes, ZEB1 and Vimentin. Although S100A6 was found to be expressed in all cell lines, it was especially highly expressed in mesenchymal cells and corresponded to S100A4 expression. S100A11 genes were inconsistently expressed among all cell lines and could not be specifically assigned to certain phenotypes, since high expression levels were found in both epithelial and mesenchymal cells (Figure 4.2A).

At the protein level, differential expression of S100 proteins was further verified by Western blot analysis and revealed that protein levels for selected S100 proteins were consistent with the level of mRNA (Figure 4.2B). Western blot analysis for EMT associated proteins was performed previously (Figure 4.1B). In general, therefore, it seems that expression of S100A4 and S100A6 is elevated in cells positive for ZEB1 and Vimentin, while other members of the S100 family are expressed in epithelial PC cells and immortalised HPDE cells positive for E-Cadherin and P-Cadherin.
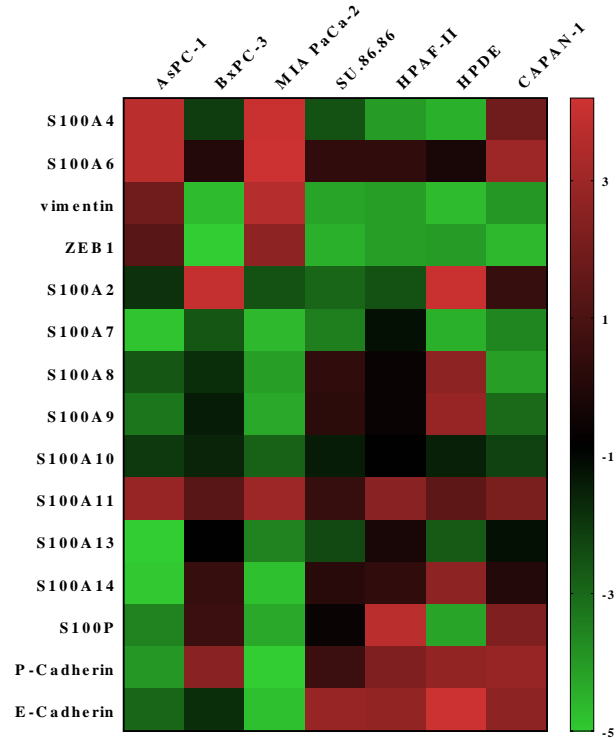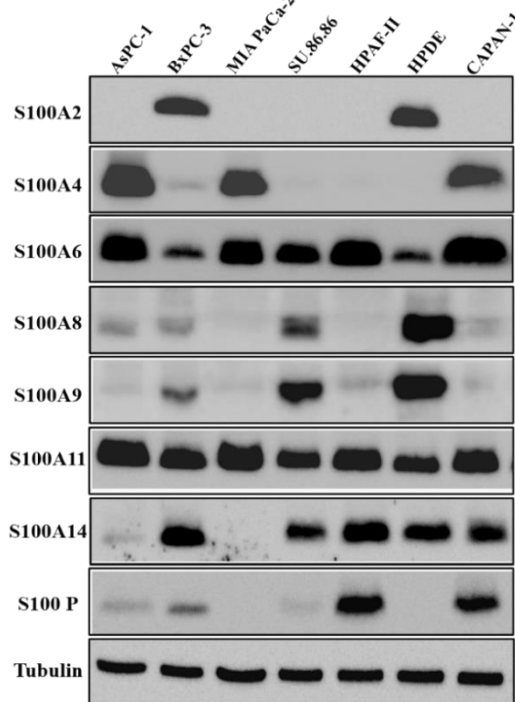
Figure 4.2 Expression profile of S100 proteins in pancreatic cell lines.

(A). mRNA expression level of different members of S100 and EMT-related genes was quantified as ΔCt, calculated by normalizing expression level of gene of interest to a reference gene (GAPDH). The heap map was drawn by blotting ΔCt-value in Prism Graph7. The color saturation scale represents the level of gene expression; green indicates a low expression, whereas red indicates a maximum of expression. (B). Cells lysate were collected and resolved into polyacrylamide gel. Expression of S100 proteins members were visualised using specific antibodies. Tubulin was used as a loading control.

4.2.3 Migratory behaviour of pancreatic cell lines in zebrafish embryos

In these experiments, a selected panel of pancreatic cell lines (epithelial, mesenchymal and those with mixed phenotypic features) were transplanted into zebrafish embryos to investigate their migration behaviour and metastatic potential. To this end, the cells were fluorescently labelled and injected into the perivitelline space of 48hpf zebrafish embryos. The process of invasion and migration of cancer cells in the living animal body were visualised 48hpi using fluorescence microscopy. The results showed that the average migration rates of MIA PaCa-2, HPDE and AsPC-1 cells were 51.6%, 51% and 42.6% respectively (Table 4.1), where these cells disseminated extensively throughout the body of the fish compared to other cell lines which showed less invasion potential (Figure 4.3).

Table 4.1 Migration of pancreatic cell lines in zebrafish.

Cell migration in zebrafish embryos was quantified in 3 independent experiments.

Type of injected cells	Migration %	Average migration %
AsPC-1	46	42.6
	42	
	40	
BxPC-3	20	15.6
	9	
	18	
MIA PaCa-2	45	51.6
	55	
	55	
SU.86.86	10	9.5
	9	
	9	
HPAF-II	9	3
	0	
	0	
HPDE	50	51
	58	
	45	
CAPAN-1	18	12
	9	
	9	
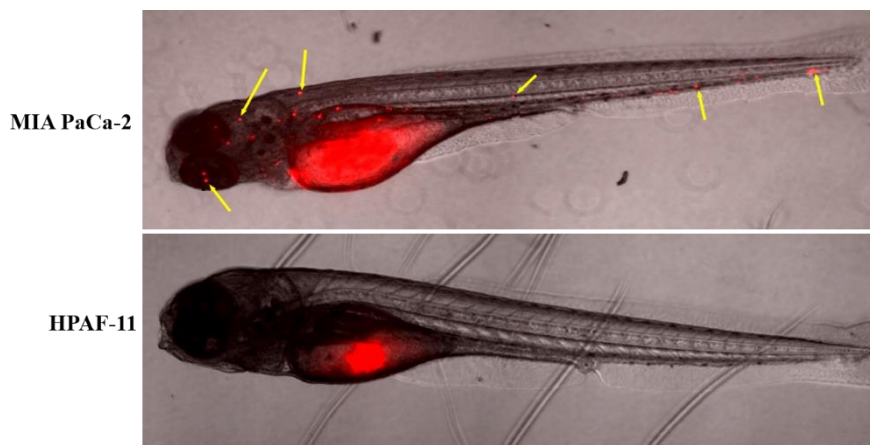
Figure 4.3 Migratory behaviour of pancreatic cell lines in zebrafish embryo.

Merged images of zebrafish embryos injected with MIA PaCa-2 and HPAF-II cells 48hpi. Cells were fluorescently labelled with Dil12 and injected into perivitelline space 48hpf zebrafish embryo. Fluorescence images were taken with 4x objectives. MIA PaCa-2 were extensively disseminated through the fish body in comparison to HPAF-II cells. (Arrows indicate disseminated tumour cells).

4.2.4 The functional role of S100 proteins in regulating PC cell migration

4.2.4.1 Silencing of S100A4 and S100A6 reduces PC cell migration in zebrafish

Much evidence has linked S100A4 and S100A6 overexpression with high metastasis potential and poor clinical outcomes in numerous malignancies. It was shown (Table 4.1) that AsPC-1 and MIA PaCa-2 displayed the highest migration rate among all selected pancreatic cell lines, and that S100A4 and S100A6 was highly expressed in both these cell lines (Figure 4.2). It is possible, therefore, that a high ability of cells to migrate could be attributed to over-expression of these proteins. To determine the functional role of S100A4 and S100A6 in promoting cancer cell migration, expression of S100A4 and S100A6, either alone or in combination, was downregulated in AsPC-1 and MIA PaCa-2 cells using specific siRNA.

The transfected cells were fluorescently labelled and injected into zebrafish embryos. Fluorescence microscopy was performed 48hpi and showed that the average migration rate of AsPC-1 cells transfected against S100A4, S100A6 and S100A4&A6 were 17.3%, 10% and 17.3% respectively, which was lower than from siControl (45.3%) (Table 4.2). Compared to siControl cells, the silencing in AsPC-1 cells of S100A4, S100A6 and both S100A4&A6 together resulted in a significant decrease in cell migration (P=0.002, P=0.001 and P=0.002, respectively) (Figure 4.4A).

Likewise, the same effect of protein silencing on cell migration was observed in MIA PaCa-2 cell lines. S100A4, S100A6 and S100A4&A6 knockdown reduced the migration rate of MIA PaCa-2 cells to 14.6%, 17% and 14% compared to the control 46.3% (Table 4.2). There were the following significant differences between the control groups compared with the others: (siControl vs. siS100A4 P= 0.0006) (siControl vs. siS100A6 P= 0.001) (siControl vs. siS100A4+siS100A6 P= 0.0007) (Figure 4.4A). Cells in which S100A4 and S100A6 had undergone knockdown remained within the injection site and did not disseminate, whereas control cells disseminated into other parts of the body. The efficiency of transfection at both mRNA and protein level was then evaluated by quantitative real-time PCR and Western blot analysis.

The mRNA and protein expression levels were significantly decreased in cells transfected with siS100A4, siS100A6, both individually and in combination, compared to control cells (Figure 4.4B and C).

 Taken together, these findings suggest that the silencing of S100A4&A6 affected the migration ability of PC cells in zebrafish embryos, thus highlighting their role in tumour progression.

Table 4.2 Migration of AsPC-1 and Mia PaCa-2 cells transfected with siControl, siS100A4, siS100A6 or combination of siS100A4&A6.

Cell migration in zebrafish embryos was quantified in 3 independent experiments.

Type of injected cells		Migration %	Average migration %
Untreated cells	AsPC-1	45	46.3
		54	
		40	
	MIA PaCa-2	58	50.6
		50	
		44	
siControl	AsPC-1	50	45.3
		43	
		43	
	MIA PaCa-2	45	46.3
		50	
		44	
siS100A4	AsPC-1	14	17.3
		13	
		25	
	MIA PaCa-2	11	14.6
		11	
		22	
siS100A6	AsPC-1	0	10
		22	
		18	
	MIA PaCa-2	20	17
		20	
		11	
siS100A+ siS100A6	AsPC-1	14	17.3
		18	
		20	
	MIA PaCa-2	0	14
		20	
		22	
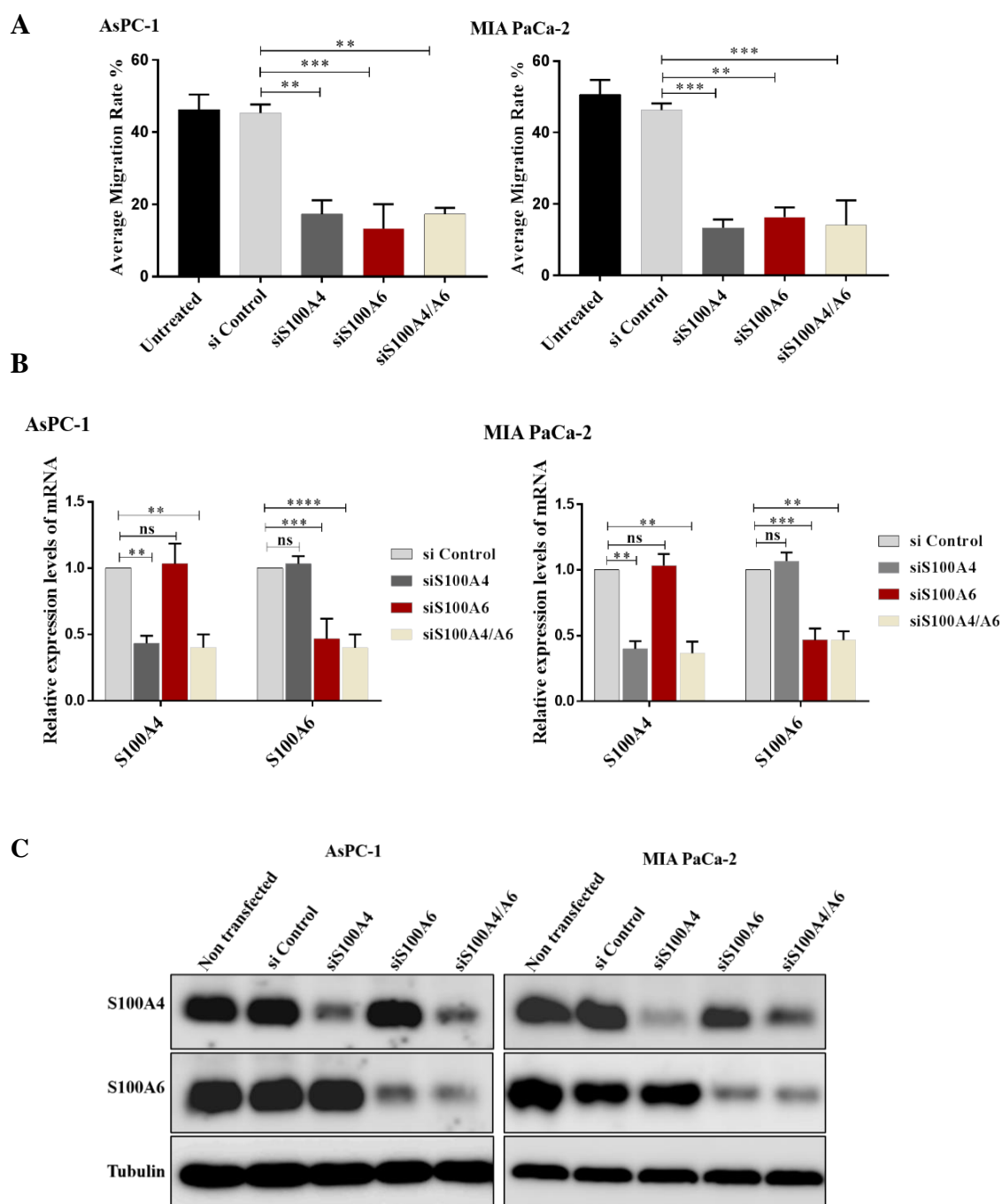
Figure 4.4 Silencing of S100A4 and S100A6 reduces PC cell migration in zebrafish.

(A). Statistical analysis of knockdown of S100A4 or S100A6 on the migration of AsPC-1 and MIA PaCa-2 cells in zebrafish. Bar charts with standard errors of the mean represent the average migration rate of control cells or cells with reduced expression of S100 proteins, ** P=0.002, *** $P \leq 0.001$. The results of 3 independent experiments are shown. **(B)** Depletion of S100A4 and S100A6 by siRNA at mRNA level were confirmed by qPCR. The relative mRNA level was evaluated by the $2^{-\Delta\Delta CT}$ method, and mRNA level was normalized to housekeeping gene GAPDH. Bar charts with standard errors of the mean represent delta CT value, ** P=0.001, *** P=0.0001, **** P<0.000. The results from 3 representative experiments are shown. **(C).** Reduced expression of S100A4 and A6 was confirmed by Western blot.

4.2.4.2 Knockdown of S100A2 and S100A11 does not affect the migration of pancreatic cells

High expression levels of S100A11 were detected in invasive PC cell lines including AsPC-1 and MIA PaCa-2, as well as the immortalised HPDE cell line (Figure 4.2). Additionally, in the HPDE cell line, S100A2 protein was also observed to be overexpressed (Figure 4.2). To investigate whether S100A2 and S100A11 are involved in the promotion of the migration of PC cells, the expression of these proteins was modulated by siRNA. All three cell lines were initially transfected with siS100A11 and siControl and injected into zebrafish embryos, as described previously. No significant difference in migration rate between the control cells and those transfected with siS100A11 could be seen, however (Table 4.3 and Figure 4.5A). Similarly, in the case of S100A2, migration of HPDE cells was not significantly changed upon S100A2 silencing (Table 4.4 and Figure 4.5A). Western blot analysis was carried out to verify the downregulation of S100A2 and S100A11 in transfected cells. The expression of these proteins was markedly reduced following transfection (Figure 4.5B). Overall, the evidence from this experiment suggests that knockdown of S100A2 and S100A11 did not influence the migration of pancreatic cells.

Table 4.3 Migration of AsPC-1 and Mia PaCa-2 cells transfected with siControl and siS100A11.

Cell migration in zebrafish embryos was quantified in 3 independent experiments.

Type of injected cells		Migration %	Average migration %
Non Transfected cells	AsPC-1	50	49.5
		55	
		43	
	MIA PaCa-2	50	50
		56	
		44	
si Control	AsPC-1	44	40.5
		40	
		37	
	MIA PaCa-2	44	50
		50	
		46	
siS100A11	AsPC-1	42	40
		37	
		40	
	MIA PaCa-2	33	42.5
		50	
		44	

Table 4.4 Migration of HPDE cells transfected with siControl and siS100A2.

Cell migration in zebrafish embryos was quantified in 3 independent experiments.

Type of injected cells	Migration %	Average migration %
Untreated	45	53
	60	
	54	
siControl	54	48
	50	
	40	
siS100A2	42	47.5
	55	
	45	

A
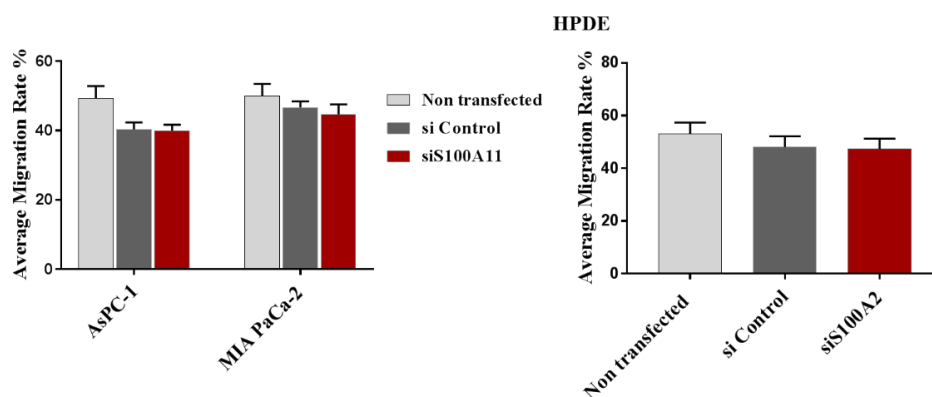
B
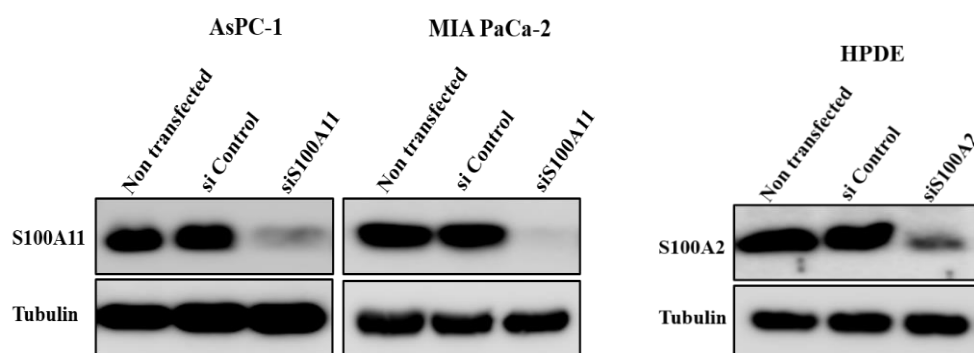
Figure 4.5 Silencing of S100A2 and S100A11 do not affect pancreatic cell migration.

(A). No significant difference was observed on migration of cells when transfected with siS100A11 or S100A2. (B). Downregulation of S100A11 and S100A2 expression was confirmed by Western blot.

4.2.4.3 The functional role of S100A14 in the migration of pancreatic cells

4.2.4.3.1The expression and subcellular localisation of S100A14 in pancreatic cells

The expression of S100A14 protein was demonstrated exclusively in cells with the epithelial phenotype, and its expression was positively associated with epithelial proteins E-Cadherin and P-Cadherin and negatively with the mesenchymal marker, Vimentin. Additionally, the expression of this protein was found to be downregulated during ZEB1 mediated EMT, considering this proteins as an epithelial marker (Figure 4.9). This experiment, however, also sought to determine the localisation of S100A14 in PC cells. Three epithelial pancreatic cell lines (BxPC-3, SU.86.86 and HPDE) which showed high expression of S100A14 by qPCR and Western blot were selected. Immunostaining using a specific S100A14 antibody was applied, and confocal microscopy was used to visualise the fluorescence signal. The results showed that S100A14 specific staining is predominantly localised to the cell membrane in all cell lines (Figure 4.6).
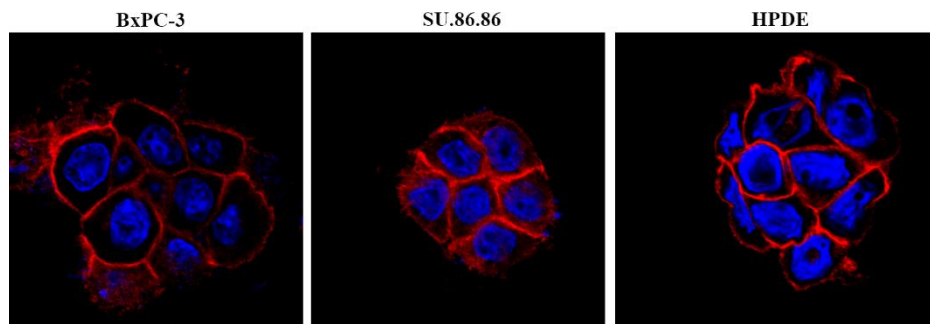
Figure 4.6 Immunofluorescence analysis of S100A14 protein localization in pancreatic cells.

Cells were grown on glass coverslips and immunostained with S100A14 antibody (green) and DAPI (blue) for nucleus staining. The fluorescence images were captured with 60x by using confocal laser scanning microscope.

4.2.4.3.2 Downregulation of S100A14 initiates activation of S100A4 and S100A6 and promotes the migration of pancreatic cells

A comprehensive investigation regarding the role of S100 protein members in regulating pancreatic cell migration is still ongoing. In this experiment the expression of S100A14 was initially modulated in higher migratory HPDE pancreatic cells because they expressed high levels of S100A14 and showed high migration rate in embryonic zebrafish (Figure 4.2 and Table 4.1). In order to investigate the potential role of S100A14 in pancreatic cell migration, therefore, HPDE cells were transfected with siControl and siS100A14 and maintained in regular media. Interestingly, phase-contrast imaging taken 72h post transfection showed that S100A14-silenced cells tend to gain a mesenchymal phenotype exhibiting spindle-like protrusions (Figure 4.7).

The transfected cells were next fluorescently labelled and injected into zebrafish embryos (Figure 4.8B). It is again somewhat surprising that the average migration rate for the fish group injected with S100A14 downregulated cells was 66%, which was higher than those injected with control cells 46%, and this result was statistically significant (P=0.03) (Table 4.4 and Figure 4.8A). Depletion of S100A14 proteins was further verified by Western bolt analysis, which revealed a significant reduction of protein expression following transfection (Figure 4.8C).

As indicated previously, it is clear that both S100A4 and S100A6 overexpression are strongly associated with cell morphological change and required for protrusion formation, as well as involved in promoting PC cell migration. Hence, it could conceivably be hypothesised that the morphological changes and increased migration capability of HPDE cells upon S100A14 knockdown may contribute to the activation of S100A4 and S100A6. Western blot analysis was performed for HPDE cells after they were transfected with siS100A14 and siControl, and the membranes were then stained with S100A4 and S100A6 specific antibodies in order to detect any activation in the expression level of S100A4 and S100A6 in S100A14 silenced cells. The results demonstrated a significant upregulation of S100A4 and S100A6 in cells transfected with siS100A14 compared to control cells, supporting the validity of the hypothesis (Figure 4.8C).

Since downregulation of S100A14 resulted in the activation of S100A4&A6 and increased the migration ability of HPDE cells, it was next investigated whether the same affect can be observed in other cell lines.

The functional role of S100A14 was therefore also investigated in the BxPC-3 and SU.86.86 cell lines using the RNAi approach. Once again, the cells in which S100A14 had been knocked out began to scatter and to form small protrusions (Figure 4.7). Additionally, Western blot analysis showed a significant decrease in S100A14 expression, while S100A4&A6 were upregulated in the silenced S100A14 cells compared to the control (Figure 4.8C). The effects of S100A14 knockdown on BxPC-3 and SU.86.86 migration in zebrafish are therefore similar to with HPDE. The average migration rate was markedly increased in BxPC-3 and SU.86.86 by 34.3% and 30.3%, respectively, compared to the control (14.3% and 15.3%, respectively) (Table 4.5). The following significant differences were obtained when comparing the control groups with the others in both cell lines (BxPC-3: siControl vs siS100A14 P=0.004) (SU.86.86: siControl vs siS100A14 P=0.007) (Figure 4.8A). These findings suggest that S100A14 can be considered to be an epithelial marker, and its expression is important for maintaining the epithelial architecture. Further work is required, however, to determine whether the increased migration of pancreatic cells due to S100A14 is via upregulation of metastasis related S100 proteins (S100A4&A6) or by another mechanism.
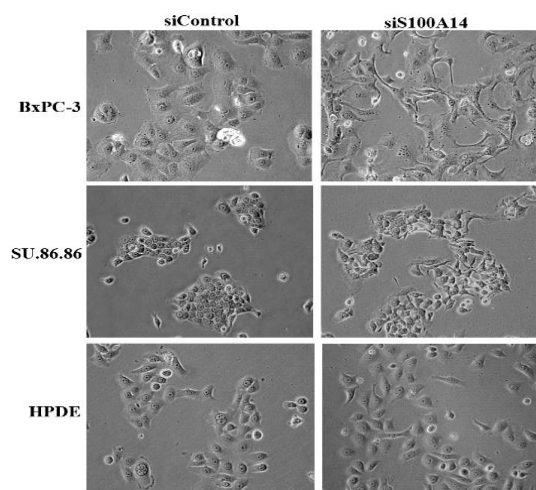
Figure 4.7 Downrugulation of S100A14 leads to cell scattering and loosing epithelial polarity in pancreatic cells.

Cells were transfected with siS100A14 and si control, and phase-contrast images were taken with 20x objective 48h post transfection. S100A14 knockdown cells obtained elongated phenotype.

Table 4.5 Migration of BxPC-3, SU.86.86 and HPDE cells transfected with siControl and siS100A14.

Cell migration in zebrafish embryos was quantified in 3 independent experiments.

Type of injected cells		Migration %	Average migration %
Non transfected cells	**BxPC-3**	18	**17**
		22	
		11	
	SU86-86	9	**6.6**
		0	
		11	
	HPDE	50	**42.3**
		44	
		33	
siControl	**BxPC-3**	11	**14.3**
		22	
		10	
	SU86-86	13	**15.3**
		22	
		11	
	HPDE	54	**46**
		44	
		40	
siS100A14	**BxPC-3**	36	**34.3**
		40	
		27	
	SU86-86	33	**30.3**
		36	
		22	
	HPDE	60	**66**
		72	
		66	

A
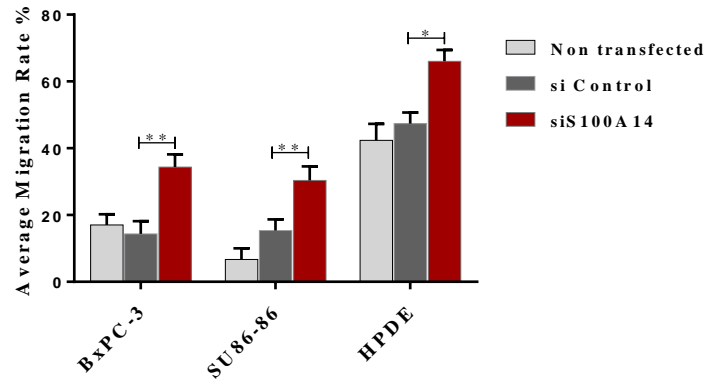
B

C
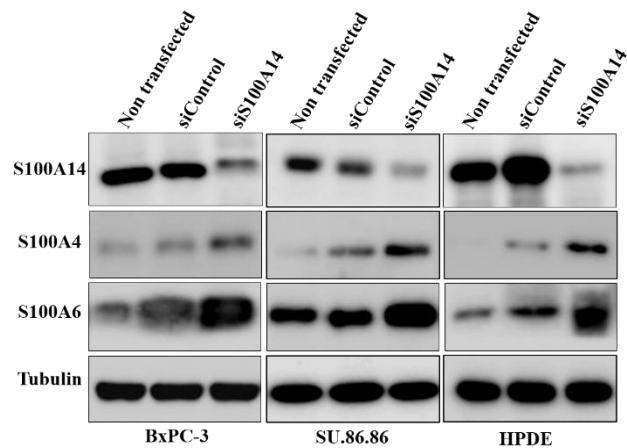
Figure 4.8 Knockdown of S100A14 induces activation of S100A4&A6 and promotes pancreatic cells migration.

(A). Statistical analysis of the effect of knockdown of S100A14 on the migration of BxPC-3, SU.86.86 and HPDE cells in zebrafish. Bar charts with standard errors of the mean represent the average migration rate of control cells or cells with reduced expression of S100 proteins, $^*P$=0.03, $^{**}P\leq$0.007. The results of 3 independent experiments are shown. (B). Merged images of zebrafish embryos 48hpi. HPDE cells were transfected with siRNAs targeting S100A14 and siControl and injected into zebrafish. Fluorescence images were taken 48hpi with 4x objective. Arrows indicate disseminated tumour cell. (C). Depletion of S100A14 by siRNA and activation of S100A4 and S100A6 in S100A14 knockdown cells were confirmed by Western blot.

4.2.5 ZEB1 expression promotes morphological and molecular changes in PC cells

4.2.5.1 ZEB1 induced EMT mediates alteration of S100 gene expression in pancreatic cell lines

It is now well established that alteration of the expression of S100 proteins and EMT induction are among many genetic events involved in PC progression. Since the expression of genes from the S100 family was altered by ZEB2 induced EMT in A431 cell lines (Figure 3.2 Chapter 3), it is possible to hypothesise that members of this family may be associated with EMT in the development of PC progression.

EMT was therefore induced in two selected PC cell lines, BxPC-3 and SU.86.86, by transfecting cells transiently with a GFP-ZEB1 overexpression construct, as well as an empty GFP vector as a control. Fluorescence and phase-contrast images were taken 48h after transfection to assess the level of GFP-fluorescence as a measure of transfection efficiency (the images are not shown). The morphological changes in the cells indicating a transition from epithelial to mesenchymal status can be clearly seen as resulting from ZEB1 induced EMT. The ZEB1 overexpressed cells tend to gain a mesenchymal-like morphology and become more elongated. In contrast, the parental cells maintained epithelial-like features and formed clusters (Figure 4.9A).

Next, RNA was extracted from transfected cells after 48h and subjected to quantitative PCR in order to investigate the expression profiles of S100 genes as well as EMT-associated genes. The mRNA alterations for these genes are shown in figure 4.9B. Overall, the cells transfected with the GFP-ZEB1 construct exhibited a significant increase in the expression level of ZEB1 mRNA compared to cells transfected with a GFP control vector. Expression profiles of several S100 genes demonstrated that only S100A4 and S100A6 transcripts were activated in ZEB1 overexpression cells in both BxPC-3 and SU.86.86 cell lines. Whereas, other genes (S100A2, S100A7, S100A8, S100A9, S100A11, S100A13, S100A14, S100P) appeared to be downregulated. For S100A10, a nearly similar gene expression was observed in ZEB1 overexpressed and control cells in both cell lines. The expression levels of a panel of S100 proteins were next confirmed by Western blot analysis (Figure 4.9C). Comparing the Western blot results with the qPCR data, a concordance of S100 expression at protein and mRNA level was found in all transfected cell lines.

These findings seem to be consistent with data obtained in chapter 3, indicating that ZEB1 overexpression resulted in a significant increase in the activation of S100A4 and S100A6. These proteins are unambiguously classified as mesenchymal markers and strongly associated with EMT in PC, therefore.

A

B
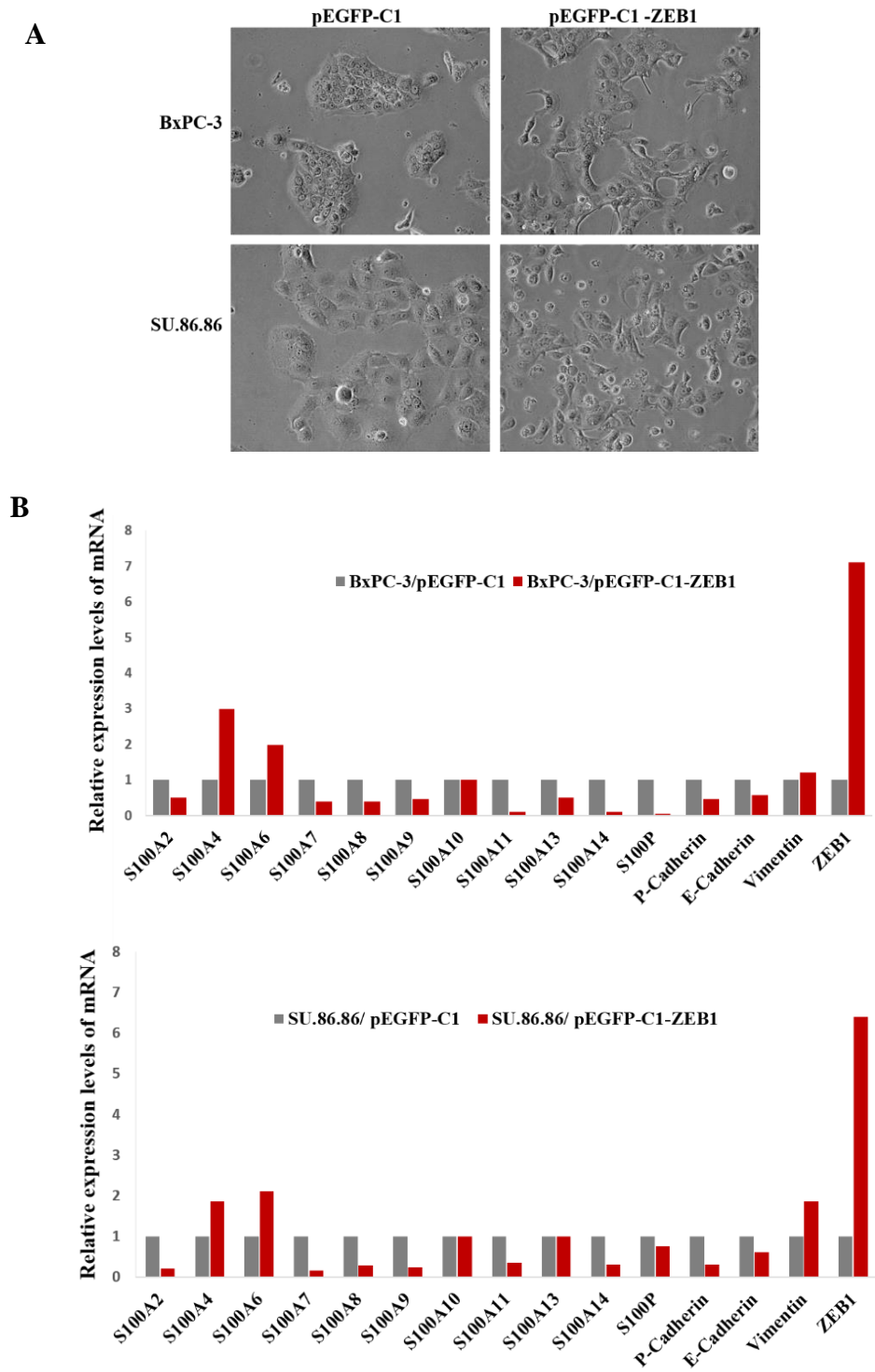
C
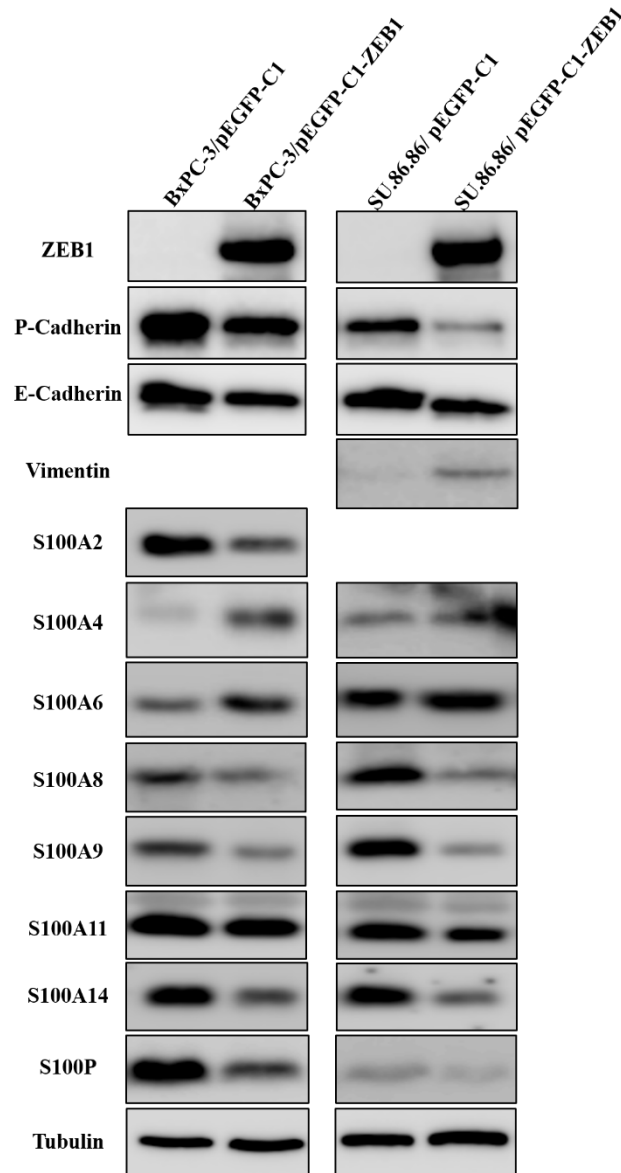
Figure 4.9 ZEB1 expression alters cell morphology and transcriptome of S100 genes in PC cell lines.

(A). Morphological changes induced by ZEB1 expression in BxPC-3 and SU.86.86 PC cell lines. Cells were transfected with GFP-ZEB1 consruct and GFP-control vector, and phase-contrast images were taken with 20x objective 48h post transfection. Under ZEB1expression, cells became more elongated and gain mesenchymal properteis compared to control cells. (B). qPCR was performed to analyse mRNA expression of selected S100 genes in BxPC-3 and SU.86.86 cell lines 48h post transfection. The relative mRNA level was estimated by the $2^{-\Delta\Delta CT}$ method, and mRNA level was normalized to housekeeping gene GAPDH. Results from one representative experiment is shown. (C). Cell lysates were collected 48h after transfection and loaded into acrylamide gel. The transferred membranes were stained with selected antibodies to confirm level of proteins expression. Vimentin in BxPC-3 and S100A2 in SU86.86 cells is not shown because Western blot analysis revealed no protein expression in both control and ZEB1 overexpressed cells.

4.2.5.2 ZEB1 overexpression promotes PC cell migration in zebrafish

To determine whether ZEB1 is involved in the regulation of PC cancer cell migration, BxPC-3 and SU.86.86 cells were transiently transfected with GFP-ZEB-1 construct and injected into zebrafish embryos. Table 4.6 shows that the average migration rate in zebrafish groups injected with ZEB1 overexpressed cells was 31.3% for BxPC-3 and 28.3% for SU.86.86, while the rate for control cells was 16.6% and 12.6% respectively. The difference between these results was statistically significant (BxPC-3: P =0.05 and SU.86.86: P=0.01) (Figure 4.10A). The blotting results confirmed the strong activation of ZEB1 in transfected cells (Figure 4.10B).

Table 4.6 Migration of BxPC-3 and SU.86.86 cells transfected with pEGFP-C1 and pEGFP-C1 -ZEB1.

Cell migration in zebrafish embryos was quantified in 3 independent experiments.

Type of injected cells		Migration %	Average migration %
BxPC-3	pEGFP-C1	22	16.6
		18	
		10	
	pEGFP-C1 -ZEB1	33	31.3
		33	
		28	
SU86-86	pEGFP-C1	8	12.6
		10	
		20	
	pEGFP-C1 -ZEB1	25	28.3
		27	
		33	
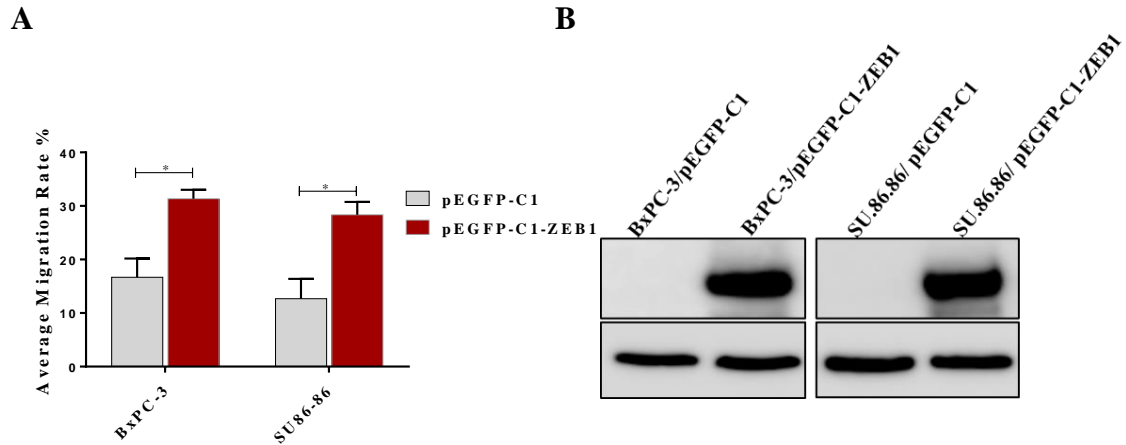
Figure 4.10 ZEB1 expression enhances PC cell migration.
(A). Statistical analysis of the effect of overexpressed ZEB1 on the migration of BxPC-3 and SU.86.86 cells in zebrafish. Bar charts with standard errors of the mean represent the average migration rate of control cells or cells with transit expression of ZEB1, * $P \leq 0.05$. The results of 3 representative experiments are shown. **(B).** Activation of ZEB1 was confirmed by Western blot.

4.2.6 The emerging roles of exosomes in PC progression

4.2.6.1 Mass spectrometry analysis of exosomes derived from PC cell lines

It is now well established from a variety of studies that S100 proteins are among many molecules that constitute protein cargos for exosomes (He et al., 2015). Basic proteomic approaches are usually used to analyse exosomal protein cargos quantitatively. To investigate the presence of S100 protein members within exosomes shed by PC cells, the exosomes were isolated from the MIA PaCa-2 with high motility ability and less invasive PC cell lines BxPC-3 and SU.86.86. The typical size (50-150nm) and morphology of exosomes were confirmed using transmission electron microscopy (Figure 4.11). The total protein concentration in exosomes was measured using a BCA protein assay kit and 200µg of exosome fraction was loaded into polyacrylamide linear gradient gels. Distinct bands were excised from the gel for mass spectrum analysis.

Nine members of the S100 protein family were identified in exosomes derived from PC cell lines, and S100A4 protein was specifically expressed in exosomes derived from highly migratory MIA PaCa-2 cells. There were two proteins shared among all exosomes from all cell lines, S100A6 and S100A11; while S100A14, S100A16 and S100P were shared among exosomes from BxPC-3 and SU.86.86 cells.

S100A2 was specifically expressed in BxPC-3 derived exosomes (Table 4.6 and Figure 4.12). These results are in accord with the results obtained by Western blot and qPCR.
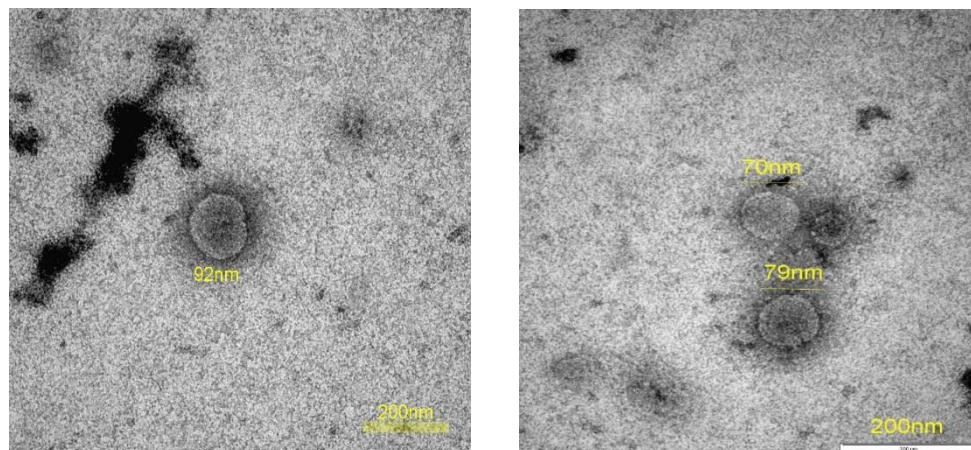
Figure 4.11MIA PaCa-2 derived exosomes.

Representative transmission electron microscope image illustrating structure and size of exosomes isolated form cells. Scale bar 200n.

Table 4.7 Mass spectrometry analysis showing presence of S100 proteins in exosomes derived from PC cells.

Results from two experiments are shown.

Proteins	Number of peptides		
	MIA PaCa-2	BxPC-3	SU86.86
S100A2	--	3	--
S100A4	4	--	--
S100A6	1	1	2
S100A10	1	2	--
S100A11	5	3	4
S100A13	1	1	--
S100A16	--	5	2
S100A14	--	4	1
S100P	--	1	1
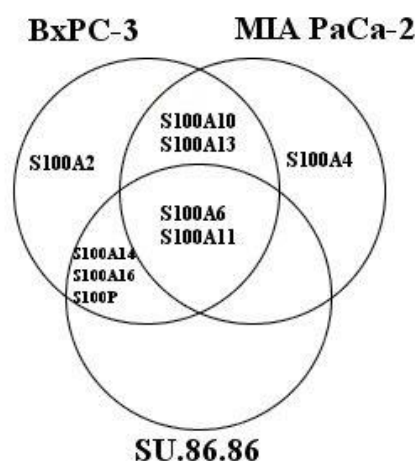
Figure 4.12 Schematic diagram representing S100 protein identified in PC cells derived exosomes.

Each circle represents one cell line and compared to the number of S100 proteins that shared among all cell lines.

4.2.6.2 MIA PaCa-2 derived exosomes enhances BxPC-3 migration in zebrafish

Because exosomes from motile MIA PaCa-2 cells showed an appreciable amount of metastasis related proteins such as S100A4, we next explored whether they could influence the migratory behaviour of non-motile cells such as BxPC-3. To this end, exosomes were isolated from two cell populations with different migratory behaviour: the more invasive MIA PaCa-2 and the less invasive SU.86.86 cell lines. Validation of exosome isolation was performed as described previously by measuring the protein concentrations and by transmission electron microscope. The BxPC-3 cells were pre-mixed with exosomes purified from MIA PaCa-2 or SU.86.86 for 24h. The cells were then labelled and injected into zebrafish. The fish group which was injected with BxPC-3 co-cultured with MIA PaCa-2 derived exosomes exhibited a high migration rate (34%) compared to the fish group injected with BxPC-3 incubated with exosomes shed by SU.86.86 cells (16%) (Figure 4.13). The mechanism underlying the role of exosomes in increasing the migration rate of BxPC-3 cells is unclear, however. Further studies will need to be undertaken that take these variables into account.
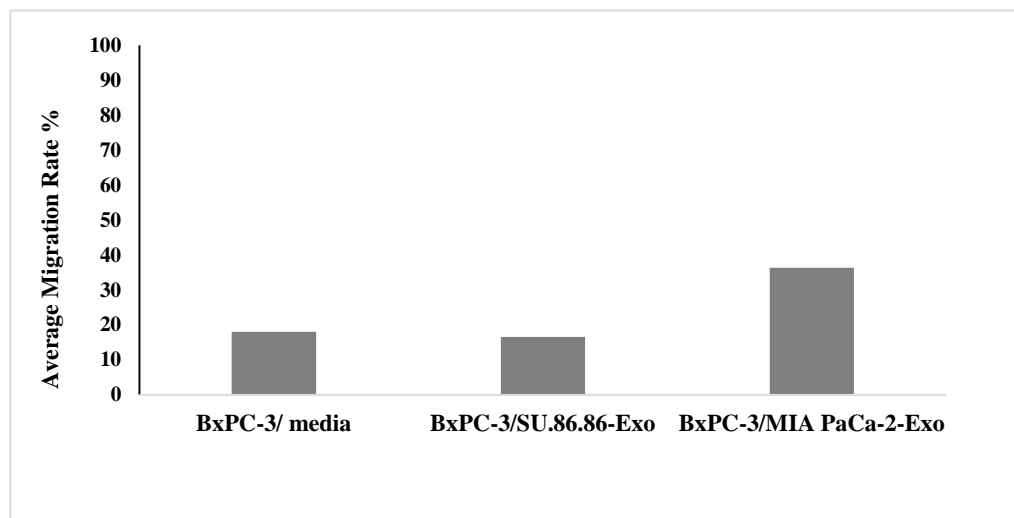
Figure 4.13 Migration rate of BxPC-3 cells premixed with exosomes derived from MIA PaCa-2 and SU.86.86 in zebrafish. A result of one experiment is shown.

4.3 Discussion

4.3.1 Expression profile of EMT and S100 proteins in pancreatic cell lines

PC is one of the most lethal and aggressive of all malignancies, and emerging evidence suggests that EMT is one of the most common factors contributing to metastatic progression and drug resistance in PC (Karamitopoulou, 2013). Recently, it has been found that the S100 family plays an active role in PC progression, and the expression pattern of S100 genes is linked to EMT (Ji et al., 2014).

Although various studies have explored either the expression of the individual S100 proteins or EMT-TFs in PC progression, up to date there are no investigations linking S100 proteins to the EMT as a mechanism of PC development. The current study provides a clear picture of the molecular and morphological evidence surrounding EMT in PC cell lines, and has also developed a new and more rigorous understanding of the role of S100 proteins in EMT in PC.

Initially, the expression of EMT-TFs (ZE1, ZEB2, Snail, Slug and Twist), two epithelial markers (E-Cadherin and P-Cadherin) and the mesenchymal marker (Vimentin) were investigated in a collection of pancreatic cell lines with different morphological features, including both epithelial and mesenchymal.

In agreement with previous studies, we found that the PC cells BxPC-3, SU.86.86, HPAF-II, CAPAN-1 and HPDE immortalised pancreatic cells exhibited high expression levels of epithelial markers such as E-Cadherin and P-Cadherin, while the AsPC-1 and MIA PaCa-2 cell lines showed a strong expression of mesenchymal markers; ZEB1 and Vimentin (Li et al., 2009, Arumugam et al., 2009, Sarkar et al., 2009).

Accumulating evidence has demonstrated that expression of the Snail family of transcription factors is correlated inversely with E-Cadherin and positively with Vimentin (Bolos et al., 2003, Medici et al., 2008, Tomono et al., 2017). Contrary to expectations, this study did not find a significant correlation between the Snail family and E-Cadherin, although Snail and Slug expression was detected in almost all selected pancreatic cells, albeit with different intensities.

Expression of Twist was only detected in HPDE immortalised cells which expressed high levels of E-Cadherin and P-Cadherin. This finding is also contrary to previous studies that have suggested that Twist correlates negatively with E-Cadherin in pancreatic cells (Chen et al., 2016, Tan et al., 2017).

ZEB1 is the only one out of all the EMT-TFs which appeared to be strongly positive in cells with a mesenchymal phenotype and its expression correlated negatively with E-Cadherin and positively with Vimentin, thus confirming previous studies (Arumugam et al., 2009, Hanrahan et al., 2017). Collectively, these data suggest that a population of different pancreatic cell lines that exists in pancreatic tumours display EMT characteristics. The presence of these EMT cells in pancreatic tumours may therefore be responsible for the aggressive behaviour of PC.

Next, we systematically evaluated the expression profile of members of the S100 family in a collection of pancreatic cell lines in order to define the S100 protein signature for PC. Additionally, expression of these proteins was determined in EMT-induced PC cells to investigate whether an S100 expression pattern is required for EMT progression.

Differential expression of mRNA levels of several members of S100 genes was observed in pancreatic cells. mRNA levels for the majority of the selected members of S100 genes, including S100A2, S100A7, S100A8, S100A9, S100A10, S100A11, S100A13, S100A14 and S100P genes, were found to be upregulated in cells with an epithelial phenotype, and associated positively with E-Cadherin and P-Cadherin. The expression of S100A4, meanwhile, was found to be upregulated in cells with mesenchymal features; AsPC-1 and MIA PaCa-2, coinciding with the activation of the ZEB1 and Vimentin. Although expression of S100A6 was detected in all cell lines, it was found to be particularly highly expressed in mesenchymal cells, consistent with S100A4 expression.

The differential expression profile for members of the S100 protein family may be attributed to the stage of disease, cellular disorder, or issues related to proteins and mRNA detection (Bresnick et al., 2015). For instance, expression of S100A11 is upregulated in non-small cell lung carcinoma, but is downregulated in small cell lung cancer (Koboldt et al., 2012). S100A7 is detected in well differentiated and early stages of oral squamous carcinoma but not in poorly differentiated and late stages of tumour (Hunter et al., 2005).

As was pointed out in chapter 3, the expression level of the S100 family was altered following ZEB2-induced EMT in A431 cells. The same finding was observed in BxPC-3 and SU.86.86 PC cells when they were transfected transiently with ZEB1. It is interesting to note that out of all the selected members of the S100 family, only S100A4 and S100A6 were found to be upregulated during EMT. These observations raise the possibility that expression of these proteins may be linked to the EMT process in PC.

Our results supports previous research and that there is a strong association between S100A4 and S100A6 proteins and EMT in PC (Xu et al., 2014, Chen et al., 2015b). The association between S100 proteins and EMT is not exclusive for PC, however. It has been found that S100A4 is a key mediator of EMT in breast cancer (Xu et al., 2016b), hepatocellular carcinoma (Zhai et al., 2014), ovarian cancer (Yan et al., 2016), oesophageal squamous cell carcinoma (Jian et al., 2015) and endometrial cancer (Hua et al., 2016). Additionally, S100A6 has also been found to be, to lesser extent, involved in EMT in hepatocellular carcinoma (Li et al., 2014) and prostate cancer (Orr et al., 2012).

4.3.2 The functional role of S100 family members in regulating PC cell migration

Several studies have thus far linked many S100 protein members with PC progression via different roles in cell proliferation, invasion, angiogenesis and metastasis (Ji et al., 2014). Experimental evidence from previous studies has demonstrated that silencing the expression of members of the S100 protein family, such as S100A4 (Che et al., 2015), S100A6 (Nedjadi et al., 2009), S100A7 (Liu et al., 2017c) and S100P (Dakhel et al., 2014) was able to reduce the invasion and migration potential of PC quite remarkably, both *in vivo* and *in vitro*. To explore the effect of S100 proteins on the migration behaviour of selected pancreatic cells, the migration ability of these cells was initially assessed using zebrafish xenotransplantation assay.

It was found that AsPC-1, MIA PaCa-2 and HPDE cells disseminated extensively throughout the bodies of the fish and showed higher migration ability. AsPC-1 and MIA PaCa-2 expressed a high level of S100A4, S100A6 and S100A11, while HPDE cells appeared to be strongly positive for S100A2, S100A11 and S100A14.

This study undertook a comprehensive analysis of the consequences for the migration behaviour of pancreatic cells of the role of expressed S100 protein members S100A2, S100A4, S100A6, S100A11 and S100A14.

In the present study, it was found that high levels of S100A4 and S100A6 expression were significantly associated with high migratory capability of PC cells, and siRNA mediated knockdown of their expression resulted in a decreased migration rate for AsPC-1 and MIA PaCa-2 cells *in vivo*.

Additionally, we found that the migration rate of BxPC-3 and SU.86.86 cells was increased when expression of S100A4&A6 was activated during ZEB1 induced EMT, suggesting that these proteins may have contributed to increase in cells migration.

Several publications have been published that support our results and document that S100A4 or S100A6 might contribute to the regulation of PC cell invasion and migration (Tsukamoto et al., 2013, Ohuchida et al., 2005). Silencing the expression of these proteins supressed PC cells migration both *in vivo* and *in vitro* (Nedjadi et al., 2009, Che et al., 2015). Similarly to our work, (Nutter et al., 2014) found that two cells lines, AsPC-1 and MIA PaCa-2, expressed high levels of S100A4, and that knocking out S100A4 expression led to reduced cell migration.

Notwithstanding the fact that S100A4 and S100A6 play a critical role in the enhancement of cell invasion and migration of different human cancers, the precise mechanism of their function has remained elusive. One mechanism by which it is suggested S100A4 and S100A6 exert their oncogenic effect is based on their ability to interact with the cytoskeleton related proteins, leading to the promotion of cancer cell migration (Golitsina et al., 1996, Kriajevska et al., 1998). Furthermore, binding of S100A4 or S100A6 to their specific receptor, RAGE promotes cancer cell migration via activation signalling pathways such as MAPK/ERK (Dahlmann et al., 2014, Leclerc et al., 2007). Additionally, it was found that the metastatic function of S100A4 correlates to its ability to induce expression of matrix metalloproteinases which degrade the extracellular matrix, thereby enhancing cancer cells' migration (Saleem et al., 2006).

Finally, we, along with other investigators, have found that both S100A4 and S100A6 may act as key mediators of EMT, which is the first step towards cancer cell migration and invasion, and the expression of these proteins was strongly activated in highly migratory cells with a mesenchymal-like phenotype (Xu et al., 2014, Chen et al., 2015b).

S100A2 is another member of the S100 proteins that has been found to be associated with the development of PC. Aberrant expression of S100A2 alters during transformation and metastasis in many types of cancer. For example, this protein was found to be under expressed in lungs (Feng et al., 2001) and gastric cancer (Liu et al., 2014b), while a high level of S100A2 proteins was reported in ovarian cancer (Santin et al., 2004). Although previous findings into S100A2 have been inconsistent and contradictory, it has been indicated that S100A2 acts as a poor prognostic marker in the pathogenesis of PC (Ji et al., 2014).

To our knowledge, this is the first study that has investigated the effect of S100A2 on the migration capability of pancreatic cells. In our study, a high expression level of S100A2 was detected in immortalised pancreatic cells HPDE with the highest migration rate. Knockdown of S100A2 did not affect HPDE cell migration and no significant difference was observed in migration rate between control cells and those with silenced S100A2. This was in contrast to some reports in the literature that indicate a significant association between S100A2 and migration capabilities of various cancer cells (Zha et al., 2015, Naz et al., 2012).

S100A11 is considered as a potential prognostic marker for patients with PC, and high expression of S100A11 in PC specimens has been associated with lymph node metastasis (Xiao et al., 2012). Expression levels of S100A11 at mRNA and protein levels were detected in all selected PC cells used in this study. Similar findings were observed in (Ohuchida et al., 2006b) study, which showed that 11 of the 15 selected PC cells expressed s high level of S100A11 mRNA.

With regard to its role in the regulation of migration and invasion properties for cancer cells, evidence from previous studies has demonstrated that induction or silencing of S100A11 expression could affect the migration ability of renal carcinoma cells (Liu et al., 2017b), cervical carcinoma cells (Shin et al., 2017), colorectal cancer (Niu et al., 2016) and ovarian cancer (Liu et al., 2015).

Unlike with these other cancer types, our study showed that knockdown of S100A11 expression in high migratory cells AsPC-1 and MIA PaCa-2 cell lines did not affect the migration capability of PC cells.

The most interesting finding to emerge from the analysis is that knockdown of S100A14 promotes PC cell migration *in vivo*. The vast majority of studies into S100A14 have focused on the mechanism of metastasis in cancer. S100A14 may contribute to controlling cancer cells' invasion and migration in cervical cancer (Wang et al., 2015b), breast cancer (Tanaka et al., 2015), hepatocellular carcinoma (Zhao et al., 2013) oesophageal squamous carcinoma (Chen et al., 2012), but its functional role in PC has not previously been investigated. Contrary to the previous studies, and our expectations, knockdown of S100A14 in high migratory HDPE cells which are positive for S100A14 resulted in an increased cell migration rate.

 Accordingly, in subsequent experiments, we knocked down the expression of S100A14 in the BxPC-3 and SU.86.86 cell lines which are characterised by low migration ability and positivity to S100A14 expression. It is again somewhat surprising that the average migration rate was markedly increased in BxPC-3 and SU.86.86 (34.3% and 30.3%, respectively) compared to the control (14.3% and 15.3%). The most likely explanation of this result comes from the observation which accompanied S100A14 knockdown in PC cells. Firstly, expression of S100A14 was only detected in epithelial cells and its expression decreased during EMT induction in all EMT cell models. Secondly, the cells in which S100A14 had been knocked down began to scatter and form small extending protrusion, as well as gaining a mesenchymal like phenotype. Furthermore, the immunofluorescence analysis showed that these proteins are predominantly localised on cell membranes in all cell lines.

It can therefore be assumed that this protein is associated with cell adhesion related proteins and its expression is important for maintaining epithelial architecture. Finally, western blot analysis showed a significant increase in the expression of metastasis related S100 proteins (S100A4 and S100A6) in silencing S100A14 cells compared to the control.

4.3.3 Exosomes initiate PC cell migration

Exosomes are an important component in the tumour microenvironment, and play a key role in cell-cell communication. Tumour derived exosomes contain various oncogenic proteins and nucleic acids that deliver biological information to the target cells, thus affecting multiple steps in cancer metastasis including promotion of EMT, invasion and migration (Robinson et al., 2016). For example, exosomes derived from KRAS mutated colon cancer cells carry various cancer promoting proteins such as KRAS, EGFR and integrin to healthy recipient cells, leading to activation of KRAS in recipient cells (Demory Beckler et al., 2013).

In this study, exosomes were purified from PC cell lines MIA PaCa-2 (higher migratory cells) and BxPC-3 and SU.8686 (lower migratory cells). A proteomic approach was utilised to explore a comprehensive protein list of exosomes derived from these cells, focusing in particular on members of the S100 protein family. Metastasis related S100 proteins S100A4 have been found in high abundance in exosomes derived only from MIA PaCa-2 cells.

We found, however, that co-culture of BxPC-3 cells with MIA PaCa-2 derived exosomes resulted in increased migration capability of BxPC-3 cells compared to control cells or cells cultured with exosomes purified from lower motile cells SU.86.86. It is possible to hypothesise that exosomal S100A4 proteins derived from MIA PaCa-2 cells may affect the migration behaviour of other cancer cells.

Our hypothesis supported data obtained by (He et al., 2015) when they found that treated non motile hepatocellular cells (HKCI-C3) with exosomes derived from highly metastatic hepatocellular cells led to significant increase in cells migration. They found that the purified exosomes enriched with S100A4 may have contributed to the increase in cell migration. The precise mechanisms underlying the role of exosomes in increasing the migration ability of cancer cells are still not well understood, however, and thus further work needs to be done to determine the precise mechanism by which exosomes affect the migration ability of PC cells.

4.4 Conclusion

Summing up the results, it can be concluded that expression of S100A4 and S100A6 is activated during ZEB1-induced EMT, and plays a vital role in the regulation of PC cell migration. Knockdown of S100A2 and S100A11 does not affect PC cell migration. In contrast, downregulation of S100A14 initiates the activation of S100A4 and S100A6 and promotes PC migration. Furthermore, we found that MIA PaCa-2 derived exosomes enhance the migration of BxPC-3 cells. As with the previous chapter, we demonstrate that zebrafish xenografts are a useful tool for the *in vivo* study of the of PC cell migration.

Chapter 5: Immunohistochemical analysis of S100 proteins expression in pancreatic cancer tissues

5.1 Introduction

Histological diagnosis of pancreatic cancer (PC) is a challenging process that is limited by the amount of available tissue collected in fine needle biopsies and is often accompanied by chronic inflammation. Various biomarkers have been found to be clinically useful for diagnosis. Characterization of the gene and protein expression profiles of the PC samples is a traditional approach to search for the new biomarkers (Hustinx et al., 2004).

Recently, experimental evidences demonstrate that EMT-related genes could be used as potential markers for PC diagnosis and their expression is associated with higher histological grades and overall survival rates (Krebs et al., 2017, Chen et al., 2016, Sakamoto et al., 2015, Lahat et al., 2014). Additionally, the differential expression of S100 proteins between PC and normal tissues was proposed to be associated with tumour progression, and can therefore be considered as important diagnosis biomarkers for patient stratification. Immunohistochemical analysis performed in different labs demonstrated that expression of some S100 protein family members such as S100A4 and S100A6 were elevated in surgically resected PC compare to the normal tissue (Huang et al., 2016a, Vimalachandran et al., 2005).

Noticeably, mutations in the P53 tumour suppressor gene are considered to play an important role in PC and it has been detected in more than 50% of cases (Redston et al., 1994). Additionally, a number of studies have been observed a convergence between P53 and EMT development (Jiang et al., 2011, Mizuno et al., 2010). It was clearly shown in cell lines and *in vitro* experiments that S100 proteins modulate P53 activity by preventing its tetramerization (Fernandez-Fernandez et al., 2008). Moreover, it has been found that different members of S100 proteins including S100A2 (Tan et al., 1999), S100A4 (Parker et al., 1994) and S100B (Lin et al., 2004) transcriptionally regulated by tumour suppressor P53.

An important role of the transcription factor, STAT3, has been reported in a variety of human cancers, including PC (Denley et al., 2013). p-STAT3 contributes to PC progression either by modulating the expression of EMT transcriptional factors (Yuan et al., 2015) or by activation of multiple pro-inflammatory genes that promote malignant transformation (Yu et al., 2009).

This study was aimed to examine a possible link between expression of S100 proteins and activation of the EMT programs using patient archive samples, and to evaluate the feasibility of S100 proteins as clinical biomarkers. The study was also aimed to analyse S100A4 and S100A6 expression in chronic inflammation and PC development using tissue microarrays. A further aim was to assess the correlation between S100 proteins and P53 or STAT3 expression.

5.1.1 Study design

A total of 41 human pancreatic tissue samples were included in this study, consisting of 31 cancer and 11 normal cases. Out of 31 cancer samples, 17 (54.8%) cases were classified as operable and 14 (45.8%) as inoperable. Nineteen (61.2%) out of 31 cancer samples has both cancer and adjust normal tissue. All blocks were obtained from Leicester General Hospital. Ethics committee approval for the study was obtained (LREC 7176).

5.1.2 Clinicopathological data, histopathological characteristics and long-term survival

Out of the 17 operable patients, 8 (47%) were male and 9 (53%) were female, with the median age of 64 years (range 45-80 years) at time of surgery. Fourteen (82.3%) patients underwent Whipple's procedure, 2 (11.7%) patients underwent distal pancreatectomy and only one patient (5.8%) underwent total pancreatectomy. Out of the 14 inoperable patients, 7 (50%) were male and 7 (50%) were female, with ages ranging between 55-80.9 years. The medium tumour size for resected tumours from operable patients was 27mm (range 10-50mm). Seven (41.1%) tumours were poorly differentiated, 9 (52.9%) moderately differentiated and 1 (6%) was well differentiated. Node status was positive in 9 (52.9%) and negative in 8 (47.1%) patients. Vascular invasion was found in 9 (52.9%) tumours and neural invasion in 12 (70.5%). Positive resection margin (R1 ie. Cancer at margin) was achieved in 5 (29.4%) patients. The overall survival was 42.1 months in operable and 8.5 months in inoperable patients. The disease-free survival in operable patients was 36.6 months, while it could not be calculated in inoperable patients.

5.1.3 Immunohistochemical analysis of pancreatic cancer tissue samples

Immunohistochemical staining of two epithelial S100 proteins (S100A2 and S100A14) and two mesenchymal proteins (S100A4 and S100A6), EMT-associated proteins (ZEB1, E-Cadherin, P-Cadherin, Vimentin, Slug and Twist1), p-STAT3 and P53 was performed on human PC specimens. The selection of S100 protein members for analysis was based on the data collected from the cell lines. *Evaluation* of pancreatic *pathology* specimens was performed by two independent pathologists; Dr Peter Greaves and Catherine Moreman as described in Materials and Methods (section 2.2.5.2.1). All statistical analysis of the data was performed by Dr Christopher Paul Neal.

5.2 Results

5.2.1 The expression profile of EMT-associated proteins in human pancreatic tissues

Expression of the majority of EMT-associated proteins, including ZEB1, E-Cadherin, P-Cadherin, Vimentin, Slug1 and Twist1, were identified in PC tissue samples. Immunohistochemical staining of 31 PC tissues showed moderate expression of nuclear and cytoplasmic ZEB1 in 8 (26%) cases. Expression of Vimentin was detected in 19% of PC cases. Stromal cells that were ZEB1-positive and Vimentin-positive were considered as an internal positive control. The majority of the analysed tumours were E-Cadherin (30/31, 97%) and P-Cadherin (29/31, 93%) positive, reflecting either an epithelial or a mixed epithelial and mesenchymal status, and their expression was mainly detected on the cell membrane of cancerous cells. Of note, strong cytoplasmic and nuclear expression of Twist1 was detected in the majority of the analysed tumours (29/31, 93%), independent of their epithelial or mesenchymal characteristics. Similarly, Slug expression was not correlated with E-Cadherin or P-Cadherin expression and was detected in half of the analysed specimens (15/31, 48%) with cytoplasmic and nuclear expression (Figure 5.1).
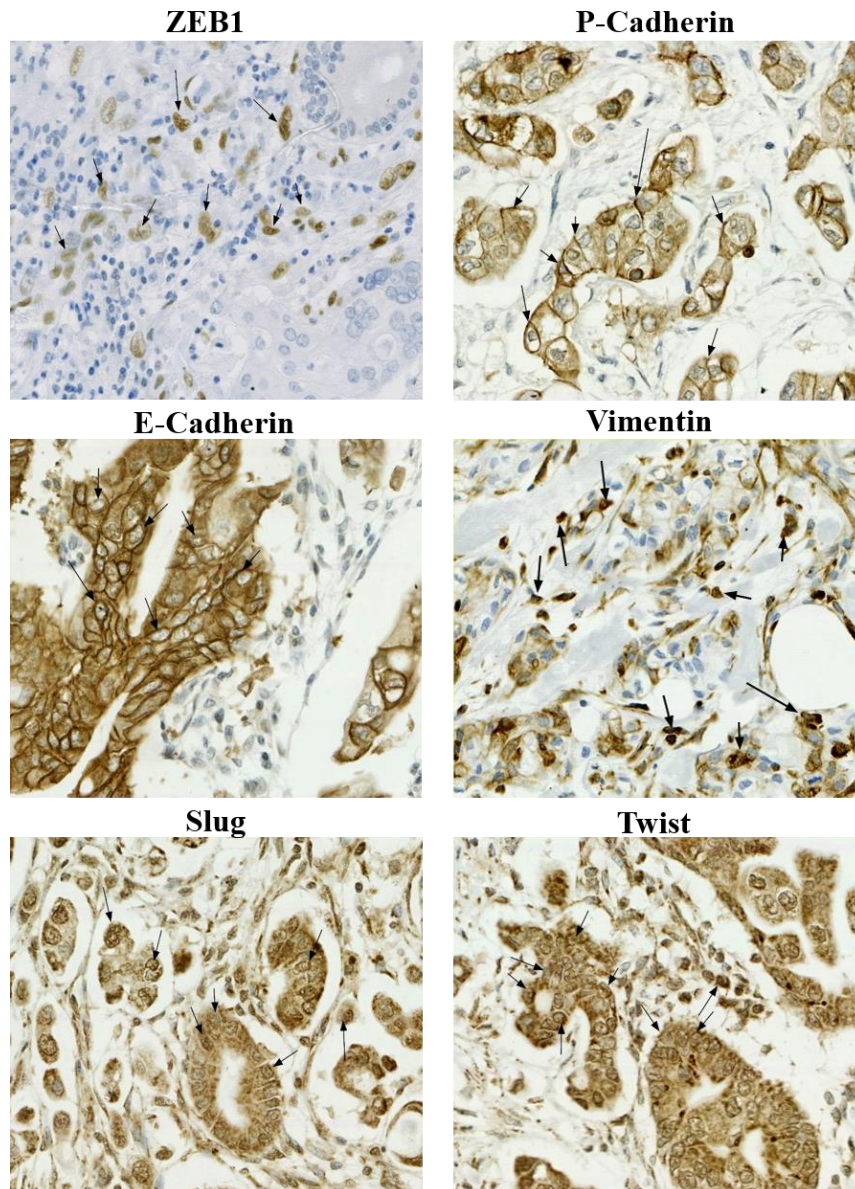
Figure 5.1 Expression of EMT-associated proteins in representative pancreatic cancer tissues.

E-Cadherin and P-Cadherin showed high dense cell membrane staining. Vimentin showed cytoplasmic staining. ZEB1, Slug1 and Twist1 showed cytoplasmic and nuclear staining. Images were captured by using Hamamatsu Slide Scanner microscopy (Magnification 40x). Black arrows indicate stained tumour cells.

5.2.2 Correlation of S100 and EMT-associated proteins in pancreatic cancer tissues

Differential expression of S100 proteins and their correlation with EMT markers was assessed in 31 PC samples. The results demonstrated that 22%, 61%, 83% and 83% of tumours were noted to show moderate to strong staining for S100A2, S100A4, S100A6 and S100A14, respectively. The expression of S100A2, S100A4 and S100A6 was observed in the nucleus and/or cytoplasm, while S100A14 was detected mainly on the cell membrane (Figure 5.2).

There was no notable correlation observed between expression of S100A2 and any other S100 family members or EMT proteins. However, a positive correlation between S100A4 and ZEB1 was detected (P=0.01), and was inversely correlated with E-Cadherin expression (P=0.02). Conversely, high expression of S100A14 was associated with increased expression of E-Cadherin (P=0.0001), and decreased expression of S100A4 (P=0.04) and Vimentin (P=0.0001). There was also a significant positive correlation between expression of S100A4 and S100A6 (P=0.01) (Appendix 1). Expression of S100A14 and E-Cadherin was detected in tumour cells, which were lacking expression of mesenchymal markers ZEB1, S100A4 and Vimentin. Conversely, expression of mesenchymal markers was observed in mesenchymal stromal cells, which were negative for S10014 and E-Cadherin (Figure 5.3A and B).
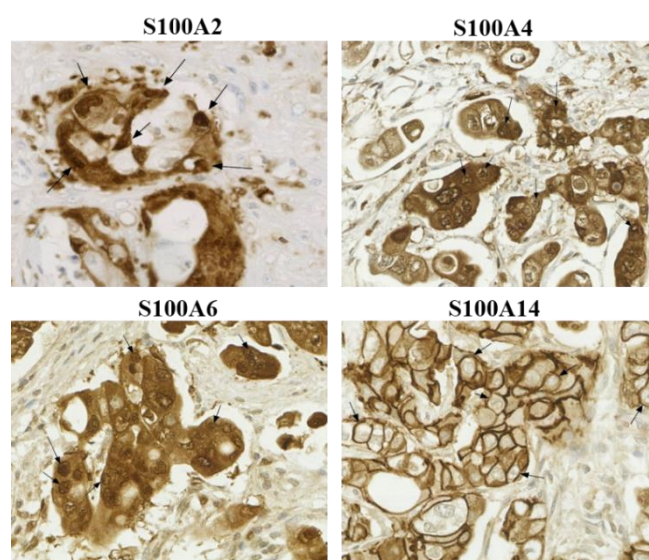
Figure 5.2 Expression of S100 proteins in representative pancreatic cancer tissues.

Intensive cytoplasmic and nuclear staining of S100A2, S100A4 and S100A6 was detected in PC cells. Immunohistochemical labelling of S100A14 was seen predominately on the cell membrane of cancer cells. Images were captured by using Hamamatsu Slide Scanner microscopy (Magnification 40x). Black arrows indicate stained tumour cells

A

ZEB1   S100A4   Vimentin

E-Cadherin   S100A14

B

ZEB1   S100A4   Vimentin
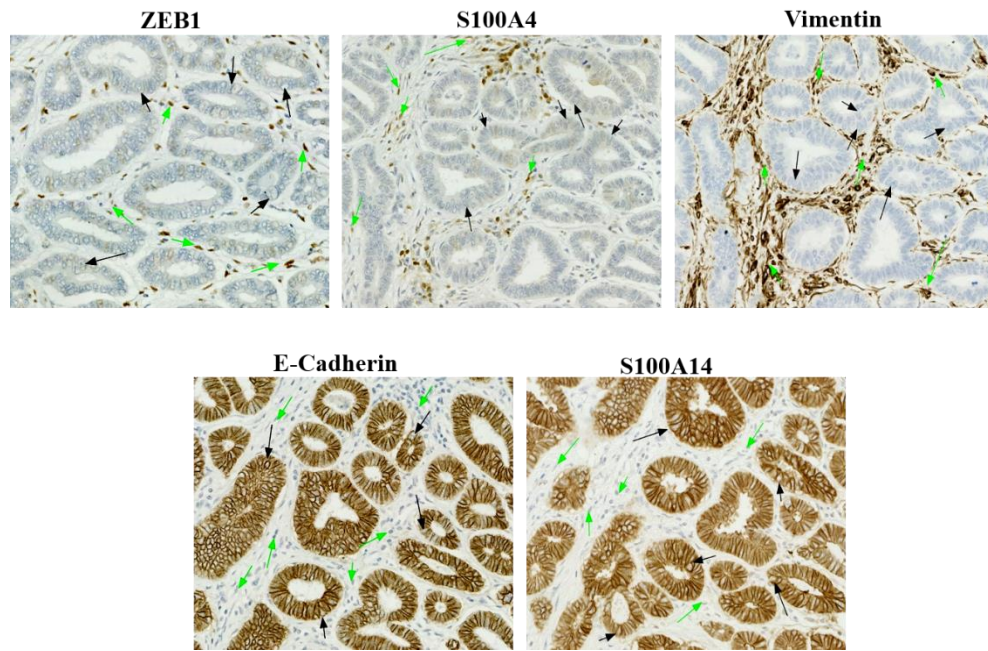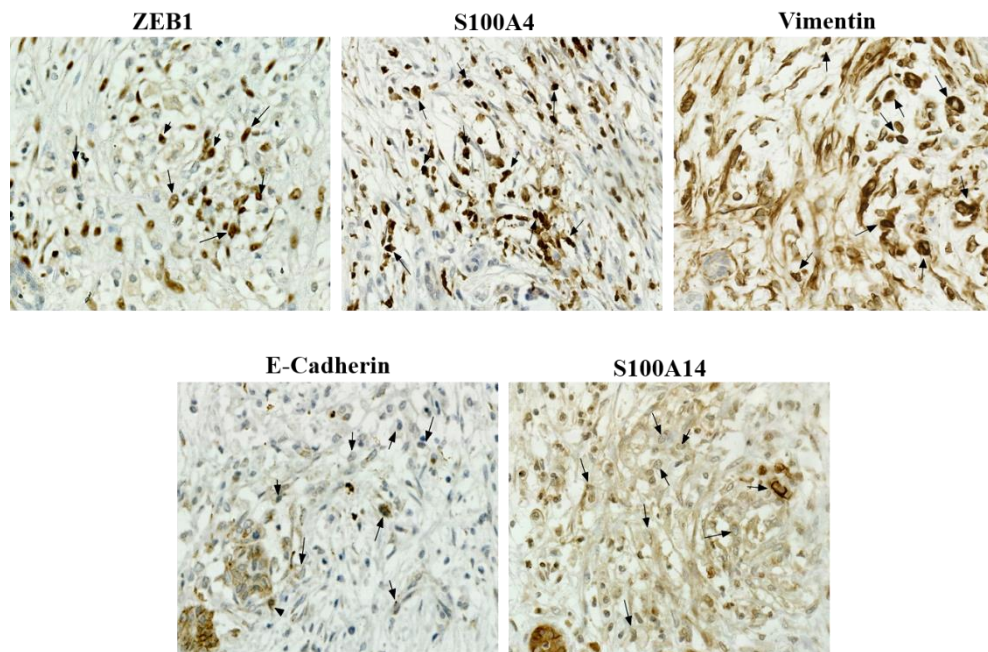
E-Cadherin   S100A14

Figure 5.3 Immunohistochemical analysis shows a correlation between S100 and EMT-associated proteins.

(A). Cancer cells which expressed epithelial markers (E-Cadherin and S100A14) (black arrows) appeared to be negative for mesenchymal markers (ZEB1, S100A4 and Vimentin). In contrast, expression of mesenchymal markers was detected in stromal cells, mostly fibroblasts (green arrows), which were negative for epithelial markers. **(B).** Black arrows indicate positive staining of mesenchymal markers and negative staining of epithelial markers (Proteins expression is the reverse of what is presented in the first image). Images of the parallel sections are shown. Images were captured by using Hamamatsu Slide Scanner microscopy (Magnification is 20x for A and 40x for B).

145

5.2.3 S100 proteins expression positively correlates with p-STAT3 in PC tissues

High nuclear and moderate cytoplasmic staining of p-STAT3 was identified in 19 (61.2%) out of 31 cases. Interestingly, in many cases, expression of p-STAT3 was detected in cells positive for S100A4 or S100A6. Furthermore, there was a significant positive correlation between expression of p-STAT3 and S100A4 (P=0.008) and S100A6 (P=0.03) (Appendix 1 and Figure 5.4). These data suggest a possible link between expression of STAT3 and S100A4&A6; STAT3 activation may regulate expression of the S100 proteins.
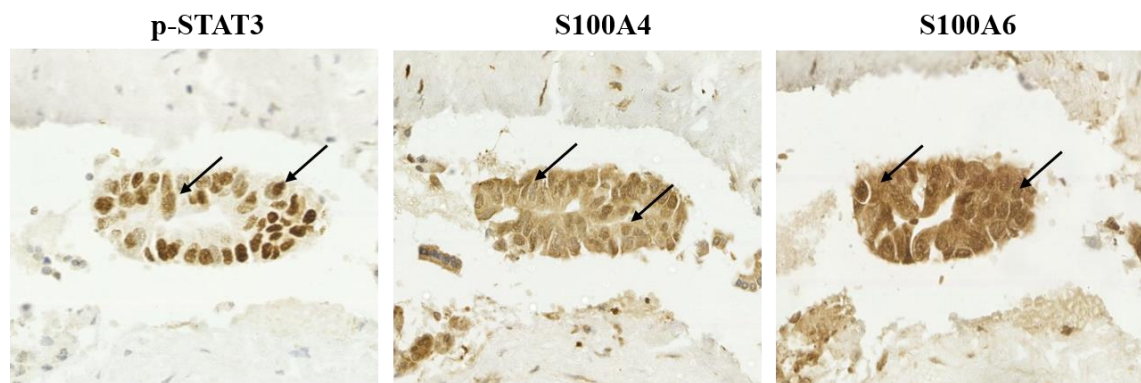
Figure 5.4 Immunohistochemical analysis of p-STAT3, S100A4 and S100A6 in representative pancreatic cancer tissues.

Co-expression of S100A4&A6 and p-STAT3 was detected in parallel sections (black arrows). p-STAT3 showed dense nuclear and moderate cytoplasmic staining. S100A4 and S100A6 showed dense nuclear and cytoplasmic staining. Images were captured by using Hamamatsu Slide Scanner microscopy (Magnification 20x).

5.2.4 ZEB1 expression inversely correlates with P53 in PC

Strong ZEB1 expression was detected in stromal spindle cells but the majority of tumour cells were ZEB1-negative, although it was difficult to clearly define differences in staining intensity due to strongly stained adjacent connective tissue cells. 24 cases out of 31 (77%) of PC tissues were positive for P53 expression; the majority of P53 staining was localised to the nucleus, with some cytoplasmic staining in cancer cells. Interestingly, there was a negative correlation between ZEB1 and P53 expression in PC tissues ($P=$ 0.01) (Appendix 1 and Figure 5.5). No significant correlation was observed between P53 expression and other EMT markers. Further work is needed to examine a close link between P53 and ZEB1 in PC.
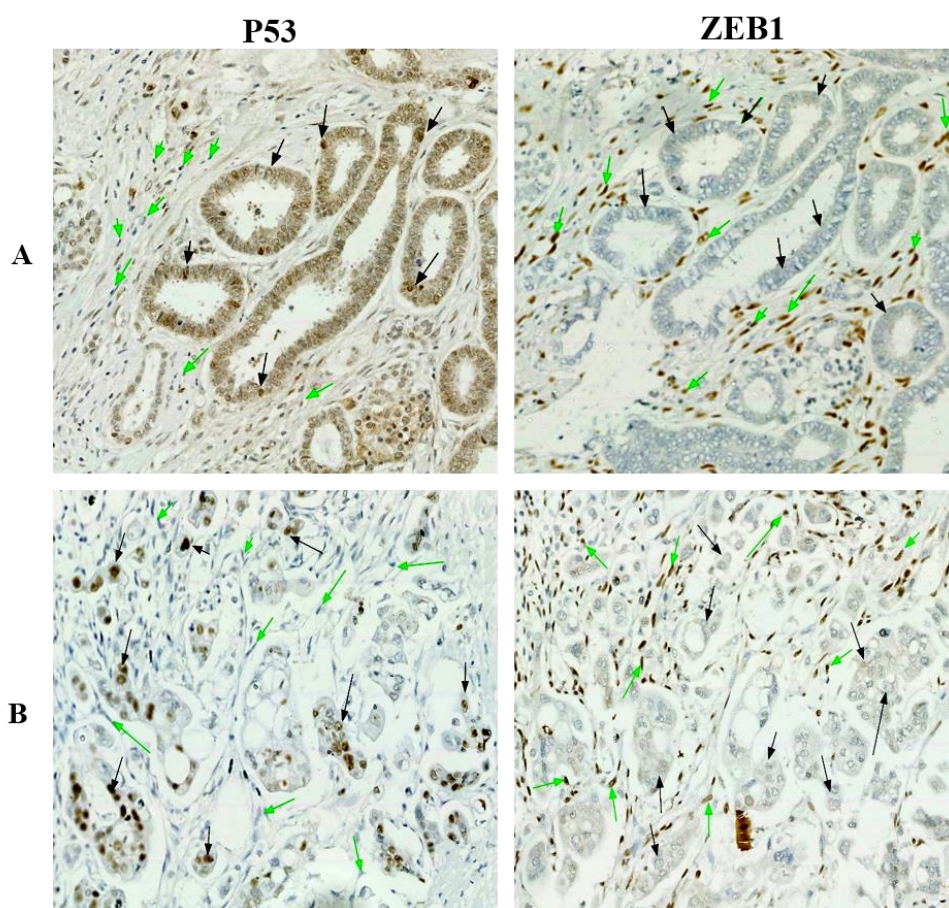
Figure 5.5 Immunohistochemical analysis shows a negative correlation between P53 and ZEB1 in pancreatic cancer tissues.

Immunohistochemical expression of P53 and ZEB1 in parallel sections (A and B) showed P53 staining in cancer cells (black arrows), and no staining in stromal cells (green arrows). In contrast, ZEB1 expression was detected in stromal cells, which were negative for P53. Images were captured by using Hamamatsu Slide Scanner microscopy (Magnification 20x).

5.2.5 Expression of S100 proteins is significantly higher in PC tissues compared to normal tissues

A comparison of protein expression between cancer and matching adjacent normal tissues was performed only in tissue blocks containing both normal and cancerous tissue (19 cases out of 31). Although expression of the majority of selected members of S100 proteins was detected in normal tissues, level of expression was increased in tumours compared to adjacent normal tissues (Figure 5.6). Expression of S100A4, S100A6 and S100A14 was significantly higher in tumour tissue compared to normal (P=0.004, P=0.01 and P=0.0001 respectively), whilst no statistical significant correlation was found between S100A2 in cancerous and normal tissue (P=0.1).
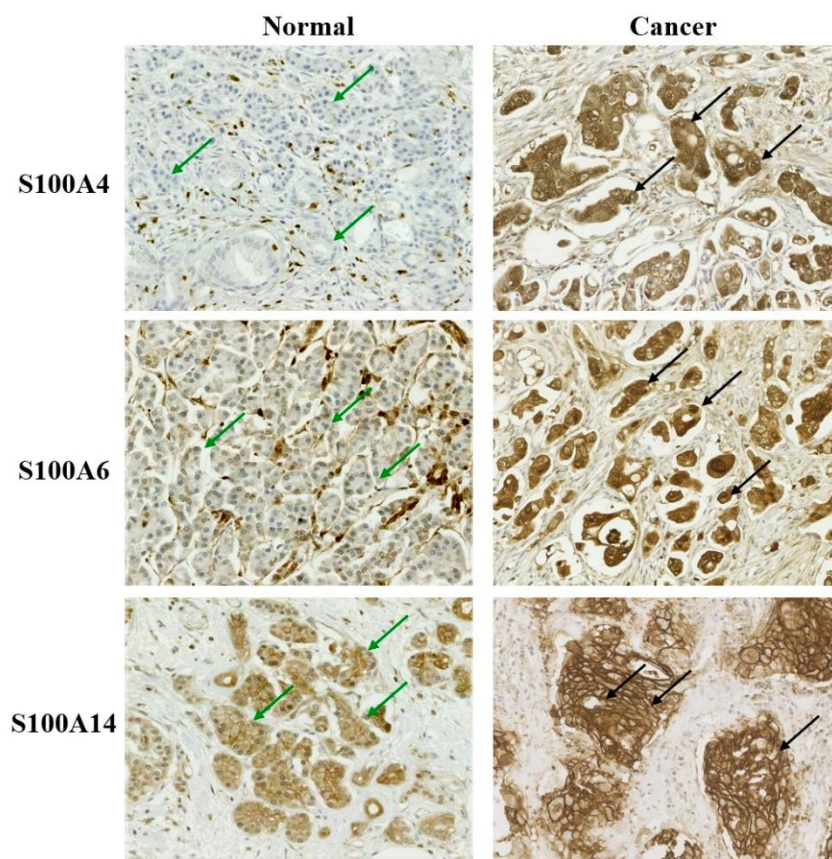
Figure 5.6 Differential S100 proteins expression between pancreatic cancer and normal tissues.

Expression of S100A4, S100A6 and S100A14 was observed in both cancer and normal tissue, but their expression was significantly higher in cancerous tissue. Cancer cells appeared to be densely stained (black arrows) and there was some positive staining in some normal cells but with less densely (green arrows).

5.2.6 Study of S100A4 and S100A6 expression in chronic inflammation and PC stages

To investigate whether expression of S100A4 or S100A6 is specific for certain stages of tumour progression, tissue microarray analysis was performed to identify differential expression of these proteins during chronic inflammation and different stages of PC development, including intraepithelial neoplasia and ductal adenocarcinoma. Very low expression of S100A4 was detected in the majority of the patients' specimens diagnosed with chronic inflammation (21/22, 95.4%) but moderate staining was detected in (5/17, 71%) cases during intraepithelial neoplasia, early stage of the PC. Majority of the ductal adenocarcinomas were strongly positive on the S100A4 expression (8/9, 87.5%) (Figure 5.7 and Table 5.1). It is in line with published data that S100A4 can be used as a useful prognostic marker for the advanced stage of PC. However, expression of S100A6 was detected in all chronic pancreatitis cases and both stages of the PC.
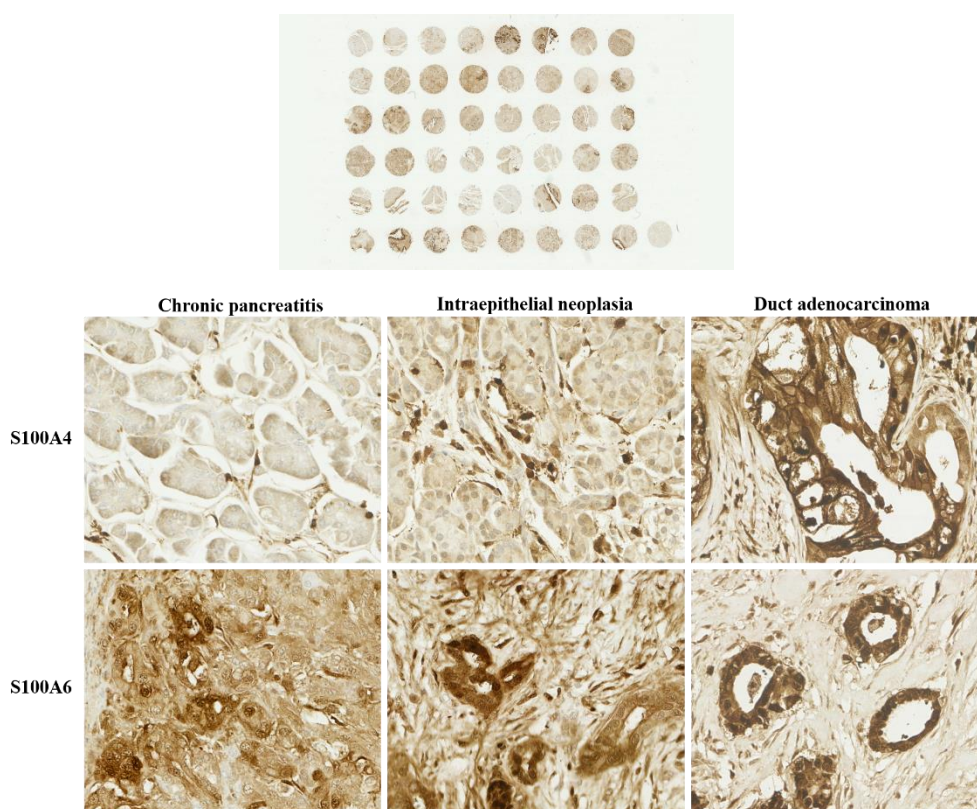
Figure 5.7 Immunohistochemical analysis of S100A4 and S100A6 in tissue microarray.

Tissue microarrays containing various histological categories of the pancreatic tissues were analysed for S100A4/A6 expression. The expression of S100A4 increased with PC development from intraepithelial neoplasia to ductal adenocarcinoma. S100A4 showed high and dense staining in cells corresponding to ductal adenocarcinoma cores compared to inflammation and intraepithelial neoplasia. High expression level of S100A6 was observed nearly at the same level through all stages. Images were captured by using Hamamatsu Slide Scanner microscopy.

Table 5.1 Immunohistochemical staining of S100A4 and S100A6 in inflammation and pancreatic cancer tissue microarray.

(Evaluation of section was performed by pathologist Peter Greaves).

Nº	Sex	Diagnosis	S100A4	S100A6	Comments
E8	F	Chronic pancreatitis	++	+++	A4 in acinar cells, A6 Ducts strongly stained
A1	M	Chronic pancreatitis	+	+++	A4 in acinar cells, A6 Ducts strongly stained
A2	M	Chronic pancreatitis	+	+++	A4 in acinar cells, A6 Ducts strongly stained
A3	F	Chronic pancreatitis	+	+++	A4 in acinar cells, A6 Ducts strongly stained
A4	F	Chronic pancreatitis	+	+++	A4 in acinar cells, A6 Ducts strongly stained
A7	F	Chronic pancreatitis	+	+++	A4 cytoplasmic, A6 Ducts strongly stained
A8	F	Chronic pancreatitis	+	+++	A4 in acinar cells, A6 Ducts strongly stained
B1	M	Chronic pancreatitis	+	+++	A4 in acinar cells but +++ in connective tissue and fibrosis A6 Ducts strongly stained
B2	M	Chronic pancreatitis	+	+++	A6 Ducts strongly stained
B3	M	Chronic pancreatitis	+	+++	A4 in acinar cells but +++ in connective tissue and fibrosis A6 Ducts strongly stained
B4	M	Chronic pancreatitis	+	+++	A4 in acinar cells but +++ in connective tissue and fibrosis A6 Ducts strongly stained
C5	M	Chronic pancreatitis	+	+++	A4 in acinar cells, A6 Ducts strongly stained
C6	M	Chronic pancreatitis	+	+++	A4 in acinar cells, A6 Ducts strongly stained
C7	F	Chronic pancreatitis	+	+++	A4 in acinar cells, A6 Ducts strongly stained
C8	F	Chronic pancreatitis	+	+++	A4 in acinar cells, A6 Ducts strongly stained
D1	M	Chronic pancreatitis	+	+++	A4 in acinar cells, A6 Ducts strongly stained
D2	M	Chronic pancreatitis	+	+++	A4 in acinar cells, A6 Ducts strongly stained
D3	M	Chronic pancreatitis	+	+++	A4 in acinar cells, A6 Ducts strongly stained
D4	M	Chronic pancreatitis	+	+++	A4 in acinar cells, A6 Ducts strongly stained
D6	F	Chronic pancreatitis	+	+++	A4 in acinar cells
E3	M	Chronic pancreatitis	+	+++	A4 in acinar cells, A6 Ducts strongly stained
E5	F	Chronic pancreatitis	+	+++	A4 in acinar cells, A6 Ducts strongly stained

Nº	Sex	Diagnosis	S100A4	S100A6	Comments
A5	F	Intraepithelial neoplasia	+++	+++	A4 cytoplasmic , A6 Neoplastic cells strongly stained
A6	F	Intraepithelial neoplasia	+	+++	A4 cytoplasmic, A6 Neoplastic cells strongly stained
D8	M	Intraepithelial neoplasia	+	+++	A6 Neoplastic cells strongly stained
E7	F	Intraepithelial neoplasia	+	+++	A6 Neoplastic cells strongly stained
D5	F	Intraepithelial neoplasia	++	+++	One or two neoplastic glands +++, some + A6 Neoplastic cells strongly stained
D7	M	Intraepithelial neoplasia	+++	+++	Small fragment staining strongly for A4 A6 Neoplastic cells strongly stained
E1	M	Intraepithelial neoplasia	++	+++	A6 Neoplastic cells strongly stained
E4	M	Intraepithelial neoplasia	++	+++	Scanty tissue, A6 Neoplastic cells strongly stained
B5	F	Intraepithelial neoplasia	+	+++	A4 pale cytoplasmic stain in neoplastic cells. A6 Neoplastic cells strongly stained
B6	F	Intraepithelial neoplasia	+	+++	A6 Neoplastic cells strongly stained
B7	M	Intraepithelial neoplasia	+	+++	A6 Neoplastic cells strongly stained
B8	M	Intraepithelial neoplasia	+	+++	A6 Neoplastic cells strongly stained
C1	M	Intraepithelial neoplasia	+	+++	A6 Neoplastic cells strongly stained
C2	M	Intraepithelial neoplasia	+	+++	A6 Neoplastic cells strongly stained
C3	F	Intraepithelial neoplasia	+	+++	A6 Neoplastic cells strongly stained
C4	F	Intraepithelial neoplasia	+	+++	A6 Neoplastic cells strongly stained
E2	M	Intraepithelial neoplasia	+	+++	A6 Neoplastic cells strongly stained
E6	F	Intraepithelial neoplasia	+	+++	A6 Neoplastic cells strongly stained

Nº	Sex	Diagnosis	S100A4	S100A6	Comments
F2	F	Duct adenocarcinoma	+++	+++	A6 Neoplastic cells strongly stained
F8	F	Duct adenocarcinoma	++	+++	A6 Neoplastic cells strongly stained
F1	F	Duct adenocarcinoma	+++	+++	A6 Neoplastic cells strongly stained
F3	M	Duct adenocarcinoma	+	+++	A6 Neoplastic cells strongly stained
F4	M	Duct adenocarcinoma	+++	+++	A6 Neoplastic cells strongly stained
F5	F	Duct adenocarcinoma	+++	+++	A6 Neoplastic cells strongly stained
F6	F	Duct adenocarcinoma	+++	+++	A6 Neoplastic cells strongly stained
F7	F	Duct adenocarcinoma	+++	+++	A6 Neoplastic cells strongly stained

5.3 Discussion

5.3.1 Expression profile of the EMT-related proteins in pancreatic cancer tissues

Alterations in the expression of the EMT-associated proteins have been used as potential biomarkers in diagnosis, overall survival prediction and disease monitoring. Overall, poor prognosis and the undifferentiated phenotype of PC have been linked to the presence of EMT (Masugi et al., 2010).

In our study, we found that the majority of cancer samples were positive for P-Cadherin (97%), E-Cadherin (93%), Twist (93%) and Slug (48%). These findings are expected and have confirmed previous research, which links high expression level of EMT-related proteins with PC tissue. One such study (Hotz et al., 2007) found that 50% of resected PDAC specimens displayed positive to Slug. Immunostaining of Twist in PC tissues showed that more than 70% of tissues were positive for Twist and its expression was correlated with the advanced stages of the disease (Li et al., 2016a). Membranous E-Cadherin expression was found in more than 85% of developmental stages of PC (Pignatelli et al., 1994). Immunohistochemical analysis of the PC tissues showed high expression level of P-Cadherin with cell membrane localization in 50% of cases and its expression contributes to the aggressive behaviour and clinicopathological features of PC (Sakamoto et al., 2015).

The correlation between expression of EMT-TFs and E-Cadherin in PC tissues has not been found. Our data do not match those observed in earlier studies, which found negative correlation between expression of Snail, Slug and Twist, relative to E-Cadherin expression (Hotz et al., 2007, Chen et al., 2016, Zhao et al., 2017). One exception is the expression of E-Cadherin, which was associated negatively with ZEB1 and mesenchymal protein Vimentin in cancer tissue; this data consistent with other studies (Yamada et al., 2013, Liu et al., 2014a, Galvan et al., 2015).

Due to the lack of an adequate number of samples and relative clinicopathological information, which was used in this study, expression of selected EMT-associated proteins did not show correlation with any clinical-pathological features. This finding is contrary to previous studies which have suggested that expression of ZEB1 (Krebs et al., 2017), Twist (Wang et al., 2017a), Slug (Hotz et al., 2007), Vimentin (Handra-Luca et al., 2011) and P-Cadherin (Sakamoto et al., 2015) are associated with advanced tumour grade and worse outcomes for patients with PC.

However, based on the results obtained in this study, further investigation in a larger cohort is warranted.

5.3.2 Correlation expression of S100 proteins and EMT related proteins in pancreatic cancer tissues

Differential expression of S100 proteins in cancer progression is used as a prognostic marker (Huang et al., 2016a, Vimalachandran et al., 2005). Some S100 proteins, such as S100P, are suggested to be a novel biomarker for PC diagnosis, and its expression has been detected in 100% PC of fine needle aspiration samples. In contrast, none of the non-cancerous pancreatic tissue displayed immunoreactivity for S100P (Lin et al., 2008).

In the current study, we evaluated expression of several members of S100 proteins, including S100A2, S100A4, S100A6 and S100A14 in PC specimens in connection to the EMT. We found that 61% and 83% of tumours were noted to show strong staining for S100A4 and S100A6, respectively. Moreover, we demonstrated that expression of S100A4 and S100A6 was significantly higher in cancer tissues compared to normal, which was consistent with data from other investigators (Ohuchida et al., 2005, Huang et al., 2016a).

High expression level of S100A14 was detected in 83% of tumours and its expression was higher in malignant than in benign tumours. However, to date, there are no studies that have investigated the expression of S100A14 and its clinical value in PC tissues.

No positive association between expression of any of the selected members of S100 proteins with clinical pathological characteristics such as disease-free survival, operability or node status was observed in this study, which is contrary to previous research (Huang et al., 2016a, Vimalachandran et al., 2005, Tsukamoto et al., 2013).

Because of the small sample size used in this study, and to identify whether expression of S100A4 and S100A6 are specific for certain developmental stages, immunohistochemical labelling of S100A4 and S100A6 was analysed on tissue microarray containing chronic pancreatitis and two stages of PC tissues including intraepithelial neoplasia and ductal adenocarcinoma.

We, along with other investigators, have found that S100A6 is expressed at high level in early and late stages of PC development including intraepithelial neoplasia and duct adenocarcinoma (Shekouh et al., 2003, Ohuchida et al., 2005). It is interesting to note that all chronic pancreatitis sections were positive for S100A6. However, this result has not previously been described. Therefore, expression of S100A6 may be a promising modality not only to characterise PC but also to detect chronic pancreatitis.

Low expression level of S100A4 was found in chronic pancreatitis and its expression increased during cancer development from intraepithelial neoplasia to duct adenocarcinoma, suggesting that expression of S100A4 can be used as a differential marker in PC.

On the other hand, low or moderate expression of S100A2 was detected in only 22% of the PC cases. Although previous research findings into S100A2 have been inconsistent and contradictory, it has been suggested that S100A2 serves as a negative prognostic marker in PC. Protein status by immunohistochemical staining of 462 samples from PC patients showed low expression of S100A2 in 59% of cases (Bachet et al., 2013). Low expression level of S100A2 was not only observed in PC but also in other human cancers including esophageal squamous cell carcinoma (Zhang et al., 2012) and gastric cancer (Liu et al., 2014b).

In reviewing the literature, no data was found on the association between expression of S100 proteins and EMT-related proteins in PC tissue specimens. Current research has investigated the correlation between some members of S100 proteins and EMT-related proteins. From these studies, it was found that expression of S100A4 was inversely correlated with E-Cadherin and positively correlated with ZEB1 expression. The same results were observed in cell lines when ZEB1 or ZEB2 expression induced EMT in A431 cells, and two PC cell lines (BxBC-3 and SU.86.86) resulted in increased expression of S100A4 and decreased E-Cadherin expression (See Chapter 3 and 4). This is a proven fact where it is well known that both S100A4 and ZEB1 usually considered as markers for mesenchymal cells and their expression is inversely correlated with E-Cadherin expression (Zhai et al., 2014, Xu et al., 2012, Techasen et al., 2014).

Immunohistochemical analysis of S100A14 expression detected S100A14 only in cells with an epithelial phenotype and its expression distributed mainly on the cell membrane. Additionally, in the analysed cell lines S100A14 mRNA and protein expression was positively correlated with expression of the epithelial markers, E-Cadherin and P-Cadherin, and inversely with the mesenchymal marker, Vimentin (See chapter 4).

The same finding was observed in human tissues, where membranous S100A14 was detected in tumour cells and its expression was positively correlated with E-Cadherin (P=0.0001), and inversely correlated with Vimentin (P=0.001).

Additionally, a negative correlation between expression of S100A14 and mesenchymal S100 proteins including S100A4 and S100A6 was reported in PC tissues. This result is in line with data described in the chapters 3 and 4, which was conducted on cell lines. We found that induced EMT in A431, BxPC-3 and SU.86.86 cells resulted in upregulation of S100A4 and S100A6 and downregulation of S100A14 expression. Moreover, knockdown of S100A14 in PC cell lines led to increased expression of both S100A4/A6, indicating that S100A14 expression is inversely associated with S100A4&A6 expression.

Only one other study, to our knowledge, has examined the correlation between expression of these proteins in cells and tumour tissues. They found that upregulation of S100A14 was observed with the concurrent downregulation of S100A4 in colorectal tissue specimens, and expression status of both proteins was associated with clinical outcome (Wang et al., 2010).

5.3.3 ZEB1 expression inversely correlates with P53 expression in PC tissues

It has been previously reported that P53 mutations occur in more than 50% of PC cases, and immunohistochemical staining for P53 has been used as a valuable marker to investigate duct lesions for P53 mutations (Redston et al., 1994). For instance, (DiGiuseppe et al., 1994) found that 12 % of high grade lesions appeared to be positive for P53 mutations. Conversely, all other histological samples with lower grade duct lesions were labelled normally, indicating that mutations in P53 genes represent the most genetic event occur during the late stage of PC development.

Additionally, there is clear evidence regarding a direct interaction between many members of S100 proteins and P53 such as S100A2 (Mueller et al., 2005), S100A4 (Grigorian et al., 2001), S100A14 (Chen et al., 2012). Furthermore, increasing evidences shows that P53 regulates the expression of EMT-inducing TFs such as ZEB1, Twist and Slug, suggesting that such links exist between P53 and EMT program in different cancers (Kogan-Sakin et al., 2011, Wang et al., 2009, Dong et al., 2013).

Because of these observations, immunohistochemical labelling of mutant P53 in PC tissues was tested. In our study, twenty four samples (77%) of PC tissue stained positive for P53 and its expression was not correlated with any clinicopathological features.

In our study, with regard to its correlation with members of the S100 protein family and EMT proteins, expression of P53 has only been found to be associated with ZEB1. This result is consistent with the Kim et al study who found that such association exists between P53 and the ZEB family in cancer cells. They showed that P53 regulated the expression of miR-200 and miR-192 family members in hepatocellular carcinomas cell lines, which, in turn, repressed ZEB1 and ZEB2 activation, which are critical mediators of EMT (Kim et al., 2011). Similarly, P53 regulates the expression of miR-200 and miR-34 at the transcriptional level, generating reciprocal feedback loops to suppress the EMT-TFs ZEB1 and Snail (Chang et al., 2011, Kim et al., 2011). This data regarding the correlation between *P53* and ZEB1 has been further validated by using PC cell lines (Chapter seven) to investigate the precise mechanism of this correlation.

5.3.4 Expression of S100 proteins positively correlates with p-STAT3 in PC tissues

It is well known that STAT3 is constitutively activated in different human cancers. Increasing evidences suggests that STAT3 activation is important for the initiation and development of PC (Toyonaga et al., 2003, Scholz et al., 2003). In a KRAS-driven mouse model of pancreatic ductal adenocarcinoma (Hingorani et al., 2003), STAT3 was found to be involved in the initiation and progression of PanINs to PDAC, and its depletion resulted in smaller lesions, lower tumour grade and fewer metastasis, suggesting that STAT3 activation is important for pancreatic tumour formation. (Fukuda et al., 2011, Lesina et al., 2011).

In the current study, high level of STAT3 phosphorylation was detected in nuclei of 80% of tumour tissues. This result is in agreement with (Toyonaga et al., 2003, Scholz et al., 2003) findings which showed that 30-100% of human cancer tissue exhibited high expression levels of p-STAT3, while normal tissue appeared to be negative for p-STAT3 expression. Similarly, (Corcoran et al., 2011) study found that almost 40 % PDAC cell lines was positive for P-STAT3 expression.

In our analysis significant positive correlation was found between S100A4&A6 and p-STAT3. These data suggest that there is a link between STAT3 activation and S100A4/A6 expression in PC. Immunohistochemical investigations of STAT3 phosphorylation in different human cancer revealed that co expression of p-STAT3 with other proteins may be an indicator that STAT3 involved in regulation of protein transcription.

For example, (Wei et al., 2003) study found that high expression level of vascular endothelial growth factor (VEGF) coincided with the elevated p-STAT3 level in PC tissues, indicating that VEGF is regulated directly by STAT3. Immunohistochemical analysis of gastric cancer specimens demonstrated that STAT3 directly regulates EZH2 expression, which was confirmed by luciferase reporter analyses and chromatin immunoprecipitation (ChIP) assays (Pan et al., 2016).

To determine whether STAT3 is implicated in the transcriptional regulation of S100 proteins, the correlation between STAT3 and S100A4&A6 expression has been validated in cell lines (Chapter six).

As pointed out in the introduction to this chapter, the oncogenic effect of STAT3 in PC occurrs through transcriptional regulation of cancer associated inflammation or EMT-related genes (Jie et al., 2015). Experiments performed in PC cell lines showed that there is a strong correlation between p-STAT expression and other EMT markers (Wu et al., 2017, Hamada et al., 2016, Zhou et al., 2015). However, the findings of the current study do not support the previous research.

5.4 Conclusions

Based on the obtained results, the following conclusions can be drawn: Firstly, expression of the four analysed S100 proteins is significantly higher in PC tumour tissues in comparison to normal tissues. Secondly, S100A4 can be a useful prognostic marker of the advanced stages of PC, whilst S100A6 may be used as a prominent inflammatory marker (tissue microarray). Thirdly, expression of S100A4, ZEB1 and Vimentin, is inversely correlated with S100A14 and E-Cadherin expression in PC specimens. Fourthly, expression of S100 proteins is positively correlated with p-STAT3 level. Finally, ZEB1 expression is inversely correlated with P53 expression in PC tissues.

Chapter 6: IL-6 family cytokines control the expression of S100 proteins and promote invasion of pancreatic cancer cells

6.1 Introduction

It is well known that inflammatory processes could be a contributing factor to an increased risk of PDAC, and the link between inflammation and the progression of PC has been long recognised (Holmer et al., 2014).

Recently, members of the S100 family have been found to be strongly associated with the inflammation process, playing a critical role in cancer metastasis through modulation of the tumour microenvironment (Nasser et al., 2015a). High expression levels of some S100 proteins, such as S100A8 and S100A9, have been detected in inflammation lesions, with this expression apparently induced in response to different cytokines (Goyette and Geczy, 2011).

There are extensive existing studies on tumour-associated inflammation, focusing particularly on some cytokinesis such as IL-6 family members as major factors linking inflammation to tumour progression (Ernst and Putoczki, 2014). It has been demonstrated that the binding of cytokines to their receptors results in the activation of many inflammation-associated pathways, such as NF-kB and STAT3, and consequent control of the transcriptional regulation of many downstream genes (Jiang et al., 2017a).

This tumour-associated inflammation represented by the IL-6 family of cytokines and by STAT3 activation has a key role in PDAC progression (Corcoran et al., 2011), but so far there is no clear evidence indicating that IL-6/STAT3 signalling is implicated in the regulation of the expression of S100 proteins. In addition, it may be that the IL-6/STAT3 signalling pathway is linked to PC progression through initiation and resolution of the EMT program (Sullivan et al., 2009, Yadav et al., 2011, Xiong et al., 2012).

It has been reported in chapter five of the present study that STAT3 activation was positively associated with the overexpression of S100A4 and S100A6 proteins in PC tissue, suggesting that STAT3 may mediate the regulation of S100 proteins. This chapter, however, first aimed to investigate the effect of cytokine-induced STAT3 activation on the expression of S100 proteins *in vitro*. Additionally, it seeks to assess the effect on PC cell migration of using IL-6/STAT3 inhibition by siRNA and Stattic inhibitors to modulate the expression of metastasis associated S100 proteins (S100A4 and S100A6) *in vivo*.

6.2 Results

6.2.1 Treatment of cells with cytokines regulates the expression of S100 proteins

6.2.1.1 The IL-6 cytokine family initiates activation of S100A4 and S100A6 proteins

Activation of STAT3 in response to cytokine family members has been shown to be a key regulator for the transcription of a variety of genes (Yu et al., 2009). This experiment was designed to investigate whether the expression of S100 is regulated in response to STAT3 activation in cells treated with different cytokines. For that purpose, two cell lines, BxPC-3 and SU.86.86, were stimulated for 48h with a series of selected recombinant human cytokines and chemokines including IL-1 alpha, IL-6, IL-8, IL-10, IL-11, IL-15, CCL-2, CCL-3, CLL-5 and M-CSF. Cell lysates were collected and analysed by Western blot for total STAT3, STAT3pY705, and two selected S100 proteins, S100A4 and S100A6.

Western blot analysis showed that the band intensity of STAT3 expression appeared similar in both the BxPC-3 and SU.86.86 cell lines and was not affected by the presence or absence of cytokines or chemokines. STAT3 phosphorylation was, however, entirely dependent on the presence of the IL-6 family of cytokines: IL-6, IL-11, IL-8 and IL-10. Expression of S100A4 and S100A6 was found to be markedly upregulated in parallel with activation of STAT3 in cells treated with IL-6 and IL-11, in particular IL-11. Although expression of p-STAT3 was detected in cells treated with IL-8 and IL-10, expression of S100A4 and S100A6 was changeable (Figure 6.1A).

We next investigated the time point at which the expression level of p-STAT3 reached a peak during IL-11 treatment. To this end, cell lysates were collected from BxPC-3 and SU.86.86 cells after treatment with IL-11 at different time points (0, 24, 48 and 72h). Analysis of protein levels showed that expression of p-STAT3 activated after 24h and became stable at 48h in SU.86.86 and 72h in BxPC-3 cells (Figure 6.1B). Further verification of the effect of IL-11 stimulation on the expression of S100A4 and S100A6 was performed using immunofluorescent staining. Staining revealed a similar trend in which cells treated with IL-11 resulted in significant activation of S100A4 and S100A6 (Figure 6.1C). In general, therefore, it clearly seems that S100A4 and S100A6 was activated in response to activation of STAT3 mediated by the IL-6 cytokine family.

A

BxPC3

SU86-86

B
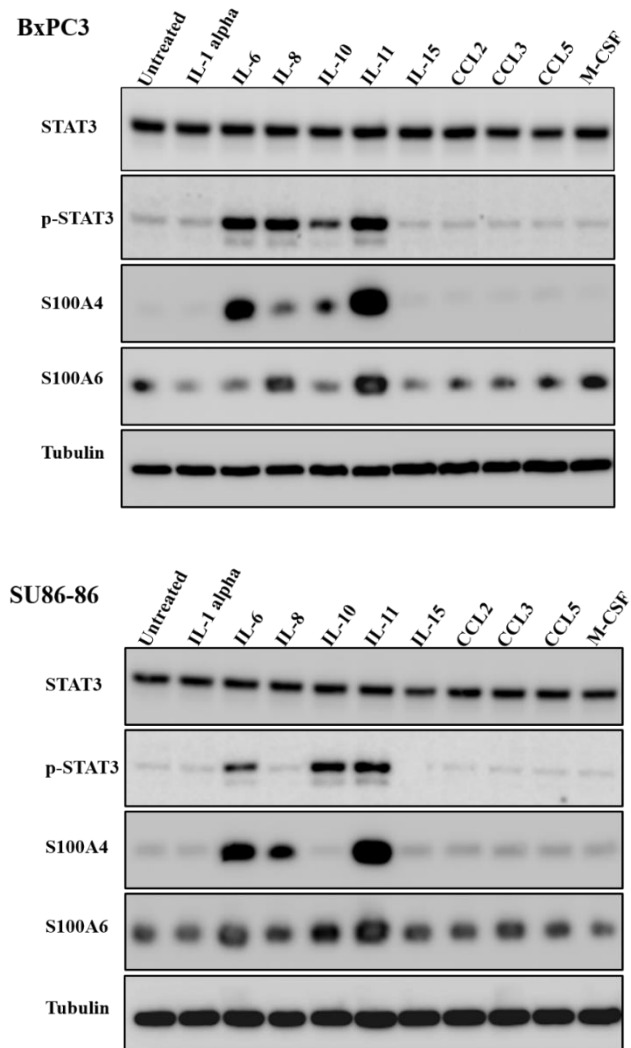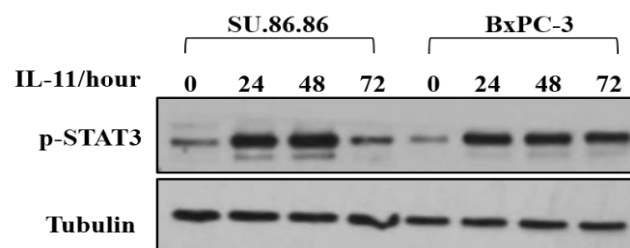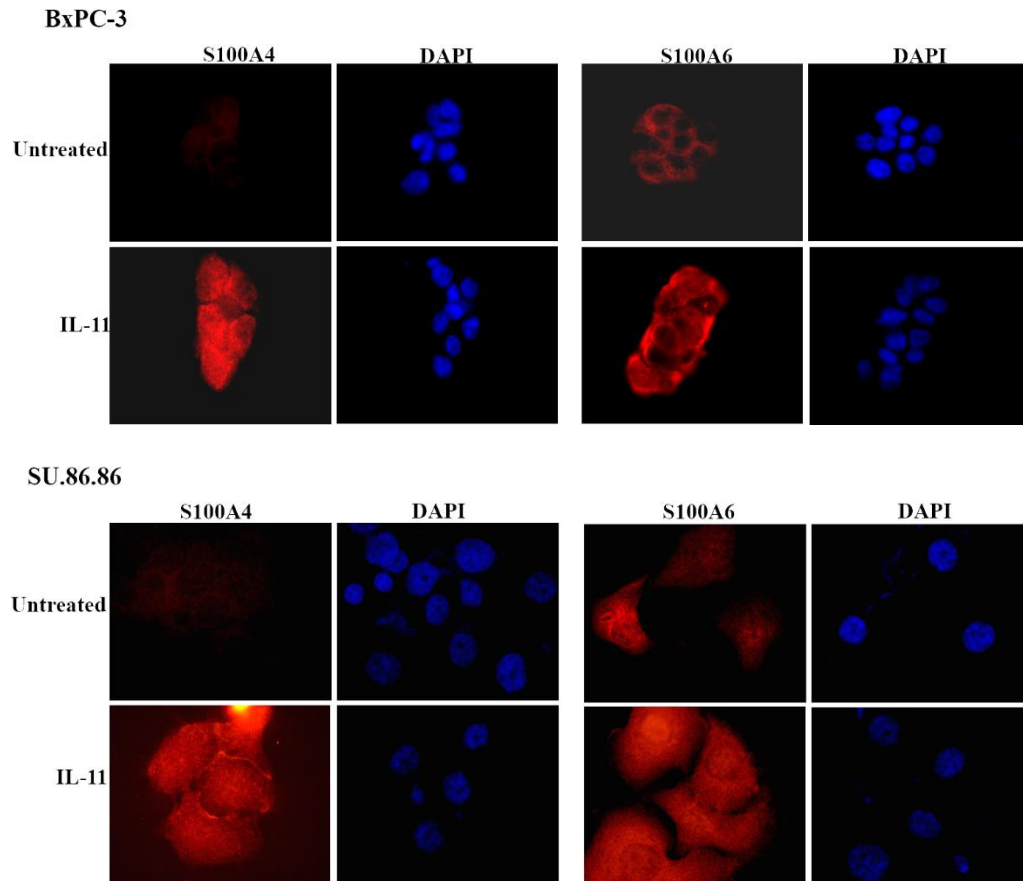
Figure 6.1 IL-6 cytokines family activates S100A4 and S100A6 expression.

(A). Phosphorylation of STAT3 and expression of S100A4 and S100A6 were examined by Western blot. BxPC-3 and SU.86.86 cells were stimulated with a series of cytokines and chemokines at concertation according to manufacturer's recommendations for 48h. Cells lysates were collected and resolved in polyacrylamide gel, and the transferred membranes were probed with total STAT3, STAT3 pY705, S100A4 and S100A6 antibodies. (B). Western blot analysis showed that p-STAT3 expression reached a peak at 48h post IL-11 treatment. (C). Immunofluorescence staining of S100A4/A6 in stimulated BxPC-3 and SU.86.86 cells. Cells were seeded on glass coverslips and immunostained with S100A4 and S100A6 antibodies (red) and DAPI (blue) for nuclear staining. Fluorescence images were captured using Nikon fluorescence microscope.

6.2.1.2 Effect of IL-11 on the expression of S100 proteins

As stated previously, the expression of S100A4 and S100A6 proteins was significantly elevated in cells stimulated by IL-11 (Figure 6.1A). Next, to investigate whether expression of other S100 protein members may be regulated by IL-11/STAT3, BxPC-3 and SU.86.86 cells were stimulated by IL-11 for 48h. Lysates were collected and Western blotting was performed to analyse the expression profile of S100 protein members including S100A2, S100A4, S100A6, S100A8, S100A9, S100A11, S100A14 and S100P, as well as total STAT3 and p-STAT3. It was demonstrated that the expression level of the majority of the selected S100 proteins was upregulated in both cell lines, consistent with STAT3 activation (Figure 6.2A).

To further investigate whether STAT3 activation regulates expression of S100 proteins transcriptionally, the quantification of S100 gene expression was assessed using qPCR. After 48h of growth in the presence and absence of 1L-11, cDNA from BxPC-3 and SU.86.86 cells was amplified using a series of primers for four selected S100 proteins: S100A4, S100A6, S100A9 and S100A14. It is apparent from (Figure 6.2B) that there was a significant activation of the mRNA level of all these proteins in cells treated with IL-11 compared to untreated cells (For BxPC-3: $P=0.004$, $P=0.001$, $P=0.0001$ and $P=0.02$, while for SU86.86: $P=0.0007$, $P=0.01$, $P=0.001$ and $P=0.001$ respectively).

According to these data, it can be inferred that treatment with IL-11 drives the transcription regulation of the expression of S100 proteins in PC cells.
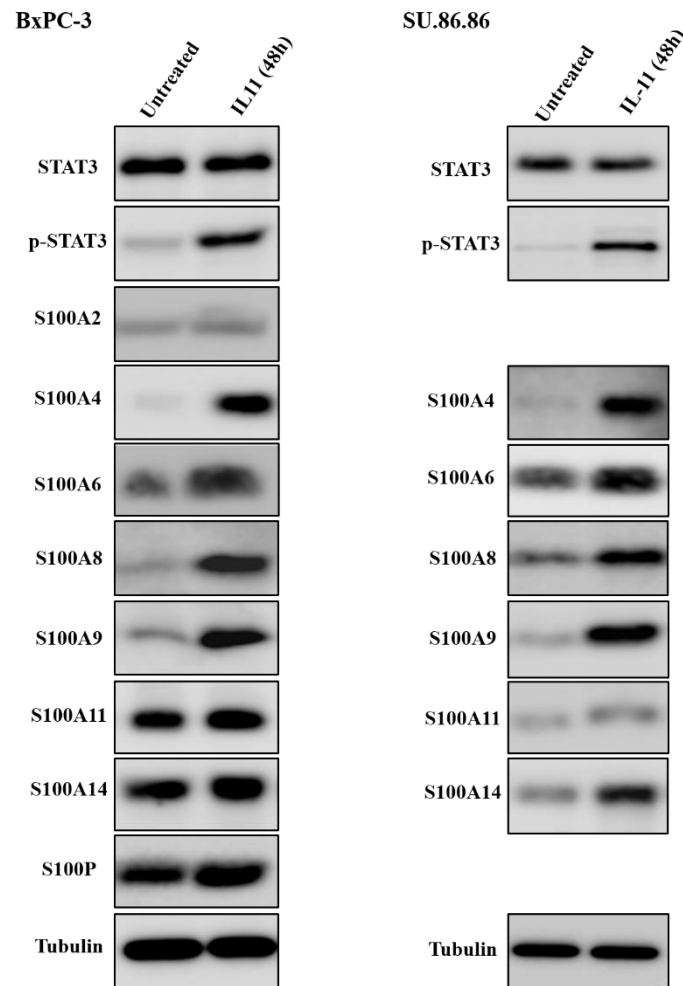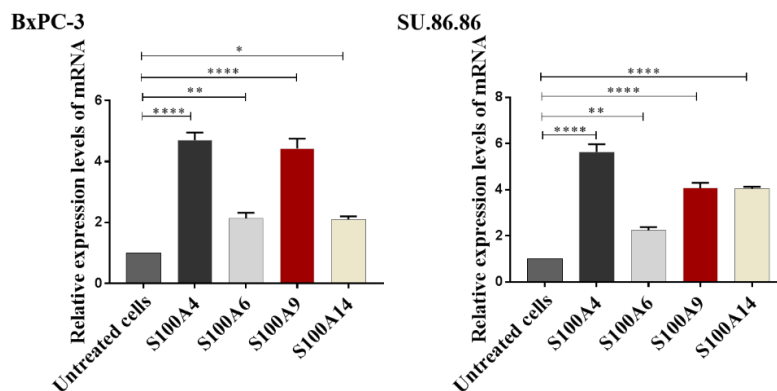
Figure 6.2 IL-11 regulates expression of S100 proteins in PC cells.

 (A). Expression level of S100 proteins was examined by Western blot. BxPC-3 and SU.86.86 cells were treated with 200ng/ml of recombinant human IL-11 for 48h. Lysates were collected and resolved on polyacrylamide gel. Membranes were stained with total STAT3, STAT3 pY705, and different members of S100 proteins antibodies. **.** S100A2 and S100A6 are not shown in SU86.86 cell line because Western blot analysis revealed no protein expression in both treated and untreated cells. **(B).** The relative mRNA level of S100A4, S100A6, S100A9 and S100A14 in BxPC-3 and SU.86.86 in the presence of absence of IL-11 for 48h was evaluated by the $2^{-\Delta\Delta CT}$ method. The mRNA level of target genes was normalized to mRNA level of GAPDH, and bar charts with standard errors of the mean represent delta CT value* $P \leq 0.02$, ** $P=0.001$, ***$P=0.0001$, ****$P<0.000$. The results from 3 experiments are shown. 0.004

6.2.2 Expression of S100 proteins is downregulated via siRNA mediated STAT3 silencing

As was shown above, inducing STAT3 activation by IL-11 resulted in increased expression of S100 proteins (Figure 6.2). To validate the dependency of S100 protein expression on STAT3 activity, siRNA-mediated STAT3 silencing was performed. To this end, BxPC-3 and SU.86.86 cell lines were transfected with siControl and cultivated in the presence or absence of IL-11 or siSTAT3 stimulated with IL-11 for 48h. After transfection, the cell extracts were prepared and the expression level of many of the S100 proteins, including S100A4, S100A6, S100A8, S100A9 and S100A14, as well as p-STAT3, was assessed by Western blot.

Cells which had been transfected with siControl and stimulated by IL-11 did result in both STAT3 phosphorylation and increased S100 protein expression compared with cells transfected only with the siControl without stimulation. Meanwhile, the protein expression level of S100 protein members was significantly decreased, consistent with attenuation of STAT3 phosphorylation in cells transfected with siSTAT3 even with the presence of IL-11 (Figure 6.3).

These results provide further support for the hypothesis that expression of S100 proteins is controlled by IL-11 and is intimately linked to aberrant STAT3 activation.
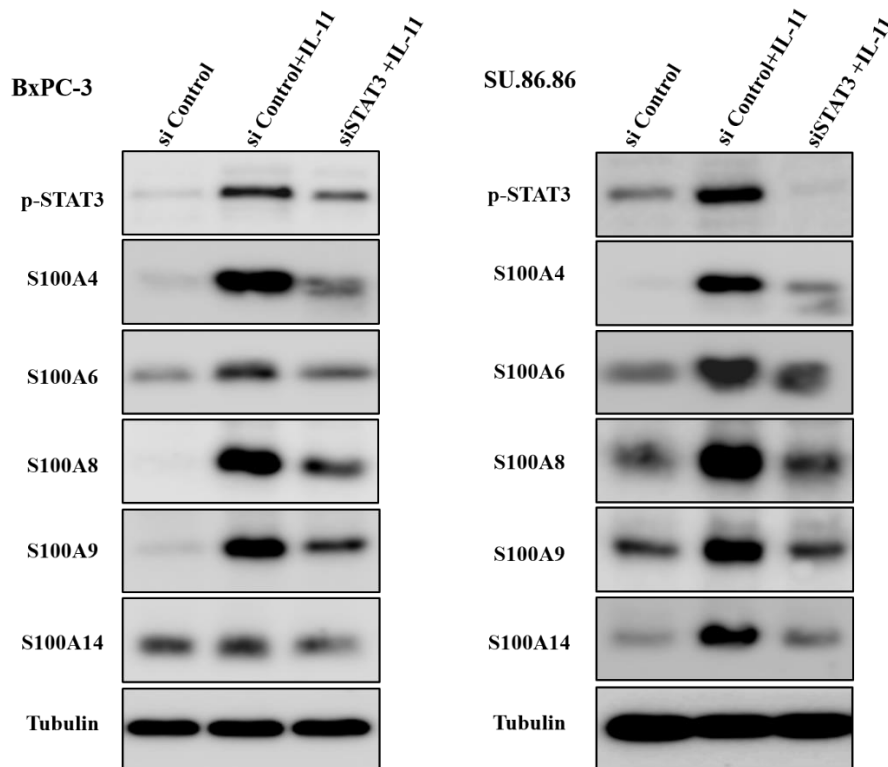
Figure 6.3 Effect of STAT3 knockdown on the expression of S100 proteins in PC cells.

Expression level of S100 proteins and p-STAT3 in transfected cells was analysed by Western blot. BxPC-3 and SU.86.86 cells were transfected with siControl (without stimulation), siControl (stimulated by 200ng/ml IL-11) and siSTAT3 stimulated for 48h. The lysates were collected and resolved on polyacrylamide gel. Membranes were probed for p-STAT3, S100A4, S100A6, S100A8, S100A9 and S100A14 as well as tubulin as a loading control.

6.2.3 Inhibitory effect of Stattic on the regulation of the expression of S100 proteins

6.2.3.1 Calculation of IC50 concentration of Stattic in PC cells

To determine the IC50 dose of Stattic in MIA PaCa-2, BxPC-3 and SU.86.86 cells, cells were treated with different concentrations of Stattic (0, 1.2, 2.5, 5, and 10 µM) for 48h. The IC50 values determined in MTT assay were 4, 5.3 and 5 µM for BxPC-3, MIA PaCa-2 and SU.86.86, respectively. 5µM of inhibitor was applied in the subsequent experiments as it was proved to be the most effective concentration in all cell lines (Figure 6.4).
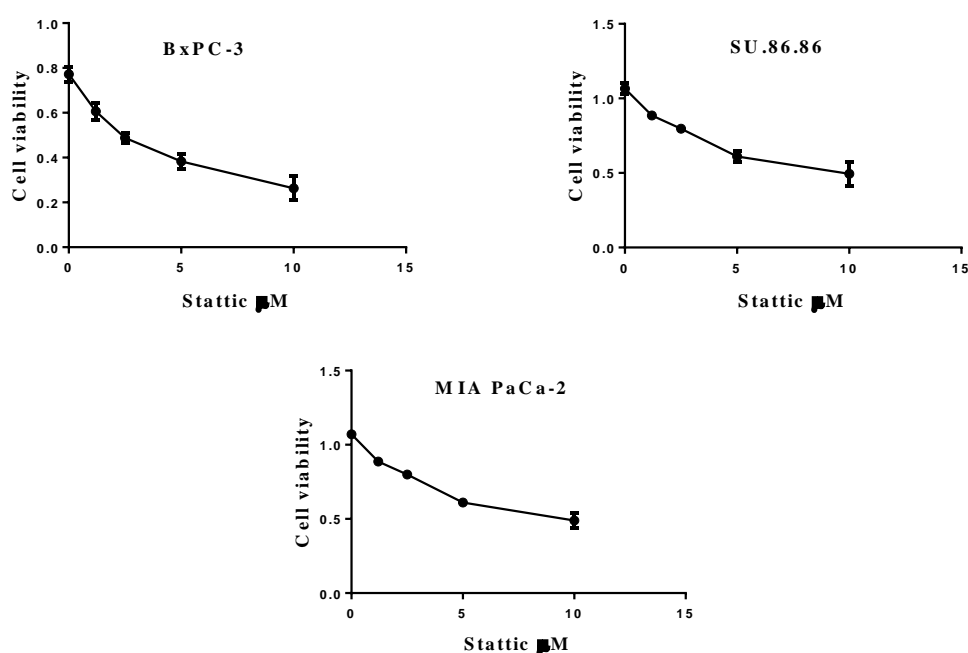
Figure 6.4 MTT analysis of PC cells viability following the treatment with various concentrations of Stattic inhibitor.

MIA PaCa-2 (1000 cells/well), BxPC-3 and SU.86.86 (2000 cells/well) were seeded in 96 well plates in growth media (10%FBS) for 24h. 24h later, the media was replaced with serum-free medium and various doses of Stattic were applied. MTT assay was performed 48h post treatment. The results from three representative assays are shown.

6.2.3.2 Stattic blocks STAT3-mediated expression of S100 proteins

To investigate the direct effect of Stattic inhibitor on STAT3 activation mediated regulation of S100 proteins, both BxPC-3 and SU.86.86 cell lines were treated either with DMSO, as a control, or Stattic at indicated concentration and cultured in the presence or absence of IL-11 for 48h. The lysates were collected and Western blot analysis was performed for p-STAT3, S100A4, S100A6, S100A8, S100A9 and S100A14.

The results revealed that IL-11 induced STAT3 activation in cells treated with DMSO+IL-11, and that STAT3 activation was inhibited by Stattic in a dose-dependent manner (Figure 6.5). Consistent with activation of STAT3, the expression of all selected S100 proteins was upregulated in cells treated with DMSO+IL-11 but downregulated in the presence of Stattic inhibitor. Depending on this finding, it can be stated that Stattic had an effective role similar to the RNAi approach to the downregulation of S100 protein expression.
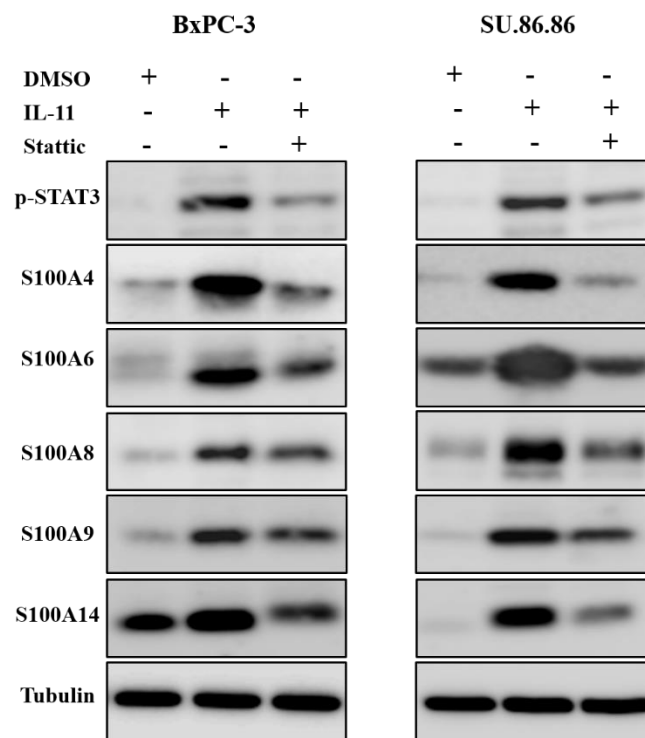
Figure 6.5 Western blot analysis of the effect of Stattic on STAT3 activation mediated S100 proteins expression.

BxPC-3 and SU.86.86 cells were treated with 0.1% DMSO as a control, 0.1%DMSO+200ng/ml IL-11, and 5μM Stattic+200ng/ml IL-11 for 48h. Cells lysates were collected and resolved in polyacrylamide gel, and the transferred membranes were probed with p-STAT3, S100A4, S100A6, S100A8, S100A9 and S100A14 antibodies.

6.2.4 IL-11 promotes the migration of PC cells in zebrafish embryos

To investigate whether IL-11 affected the invasion and migration of PC cells, the cells were stimulated by IL-11 and injected into zebrafish. The average migration rate for zebrafish groups injected with BxPC-3 cells and stimulated with IL-11 was 40.5% while the rate for untreated cells was only 15%; a result that was statistically significant (P=0.003) (Table 6.1 and Figure 6.6A).

Untreated cells remained inside the transplantation site and did not disseminate, whereas cells treated with IL-11 spread and disseminated through the vasculature into other parts of the fish body, such as the head and tail (Figure 6.6 B). The same effect was observed in SU.86.86 cells. Stimulation with IL-11 increased the migration rate of cells to 35% compared to just 7% for the control (P=0.001) (Table 6.1 and Figure 6.6 A).

Table 6.1 Migration of BxPC-3 and SU.86.86 cells untreated or treated with IL-11 in zebrafish. Cell migration in zebrafish embryos was quantified in 3 independent experiments.

Type of injected cells		Migration %	Average migration %
BxPC-3	Untreated cells	12	15
		11	
		22	
	Cells+IL11 48h	37	40.5
		44	
		40	
SU86-86	Untreated cells	11	7
		10	
		0	
	Cells+IL11 48h	33	35
		36	
		36	

A

B
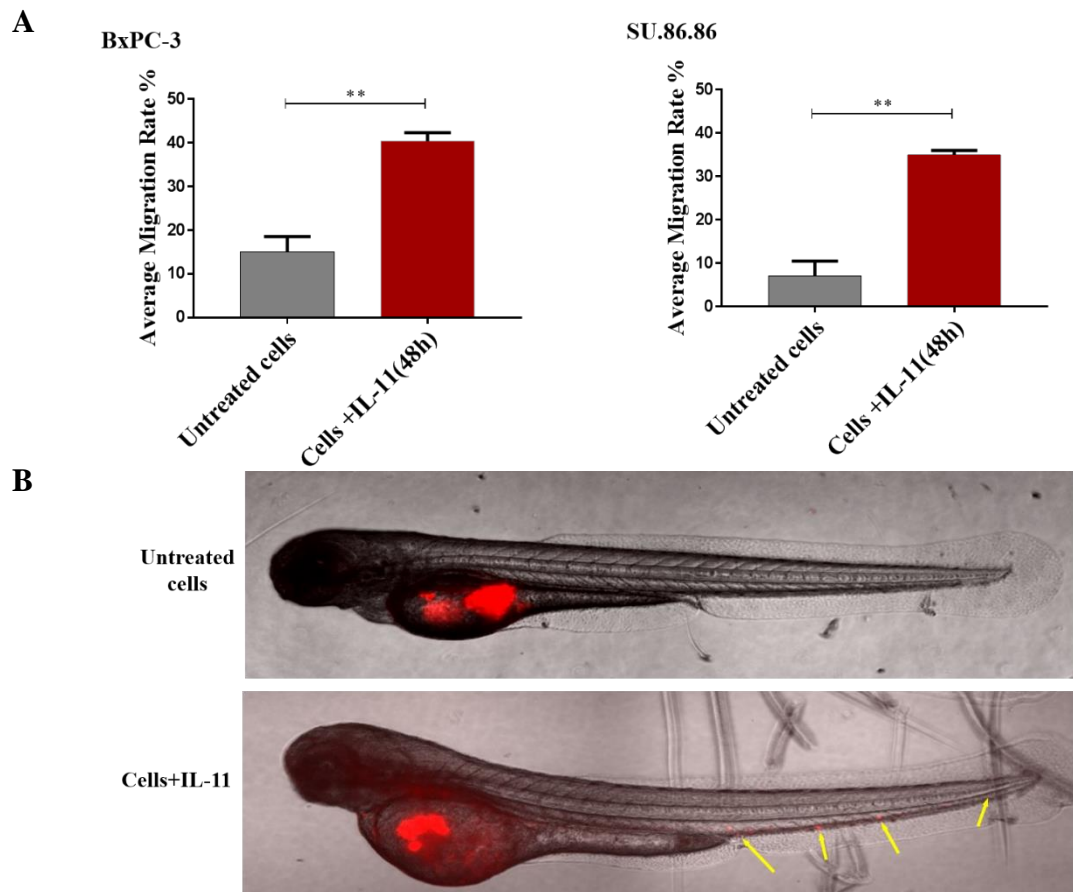
Figure 6.6 IL-11 promotes PC cells migration.

(**A**). Statistical analysis of IL-11 treatment on migration of BxPC-3 and SU.86.86 cells in zebrafish. Bar charts with standard errors of the mean represent the average migration rate of untreated or treated cells with IL-11. The results of 3 independent experiments are shown, ** $P \leq 0.003$ (**B**). Merged images of zebrafish embryos 48hpi. BxPC-3 cells were cultured in the presence or absence of IL-11 and injected into zebrafish. Fluorescence images were taken 2dpi with 4x objective. Arrows indicate disseminated tumour cells.

6.2.5 Targeting STAT3 supresses PC migration via downregulation of S100 proteins

6.2.5.1 siRNA-mediated silencing of STAT3 decreases PC migration via downregulation of S100A4 and S100A6 expression.

It has been previously reported that IL-11 activated expression of S100A4 and S100A6 in a STAT3 dependent manner (Figure 6.1). Additionally, cells treated with IL-11 resulted in increased PC cell migration *in vivo* (Figure 6.6). Hence, it could conceivably be hypothesised that IL-11/STAT3 may promote PC migration through activation of S100A4 and S100A6. In order to validate this hypothesis, a series of transfections were performed in BxPC-3 and SU.86.86 cells.

The cells were transfected and stimulated by IL-11 as follows: si Control, siControl+IL-11, siS100A4+IL-11, siS100A6+IL-11, siS100A4&A6+IL-11 and siSTAT3+IL-11. The transfected cells were fluorescence labelled and injected into zebrafish embryos. The cell migration rates within fish injected with stimulated BxPC-3 cells transfected with S100A4, S100A6, S100A4&A6 were 15.6%, 14.3% and 14%, respectively, which was lower than from those injected with stimulated cells transfected with siControl cells, 32% (Table 6.2 and Figure 6.7 A).

Compared to the control cells, however, when S100A4, S100A6 and S100A4&A6 silenced BxPC-3 cells were stimulated by IL-11 there was a significant decrease in cell migration (P=0.006, P=0.003 and P=0.002, respectively). It is interesting to note that the same effect was observed in BxPC-3 cells transfected with siSTAT3 when injected into zebrafish. Impaired STAT3 activation in cells reduced the migration rate of BxPC-3 cells to 16.6% compared to 32% for the control (P=0.01), even in the presence of IL-11. Likewise, the effects of protein knockout on SU.86.86 migration in zebrafish were similar to that for BxPC-3: the average migration rate was markedly decreased in stimulated SU.86.86 cells transfected with siS100A4, siS100A6, siS100A4&A6 and siSTAT3 by 12.6%, 16.6%, 10.3% and 17.3%, respectively,, compared to 27.6% for the control. This led to the significant differences of P=0.004, P=0.01, P=0.01 and P=0.02 between the control group (siControl+IL-11) and siS100A4, siS100A6, siS100A4&A6 and siSTAT3, respectively (Table 6.2 and Figure 6.7A).

Next, the expression level of S100A4 and S100A6 proteins was analysed by Western blot. No expression of S100A4 and S100A6 was detected in cells transfected with siControl without stimulation, whereas a high expression level of S100A4 and S100A6 was observed in cells transfected with siControl and cultivated in the presence of IL-11. On the other hand, the expression of these proteins was markedly reduced following transfection with siS100A4, siS100A6, siS100A4&A6 and siSTAT3, despite the presence of IL-11 (Figure 6.7B). In summary, these results showed that inducing the activation of STAT3 by IL-11 led to increased S100A4 and S100A6 expression, and thereby increased cancer cell migration. On the contrary, impairing the activity of STAT3 using siRNA resulted in downregulation of both proteins and a decreased migration rate.

Table 6.2 Migration of BxPC-3 and SU.86.86 cells transfected with siControl, siS100A4, siS100A6, siS100A4&A6 and siSTAT3.

Cell migration in zebrafish embryos was quantified in 3 independent experiments.

Type of injected cells		Migration %	Average migration %
siControl	BxPC-3	10	6.3
		0	
		0	
	SU.86.86	0	6.6
		9	
		13	
siControl+IL-11	BxPC-3	36	32
		33	
		27	
	SU.86.86	25	27.6
		22	
		36	
siS100A4+IL-11	BxPC-3	18	15.6
		18	
		11	
	SU.86.86	9	12.6
		9	
		11	
siS100A6+IL-11	BxPC-3	20	14.3
		10	
		13	
	SU.86.86	11	16.6
		10	
		18	
siS100A+siS100A6 +IL-11	BxPC-3	18	14
		13	
		11	
	SU.86.86	9	10.3
		13	
		18	
siSTAT3+IL-11	BxPC-3	18	16.6
		10	
		22	
	SU.86.86	10	17.3
		13	
		18	
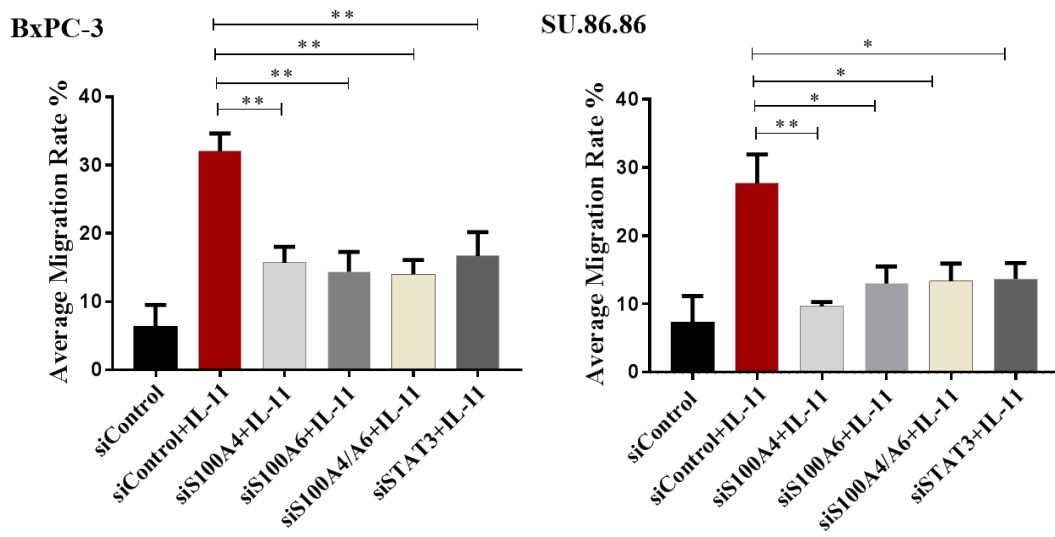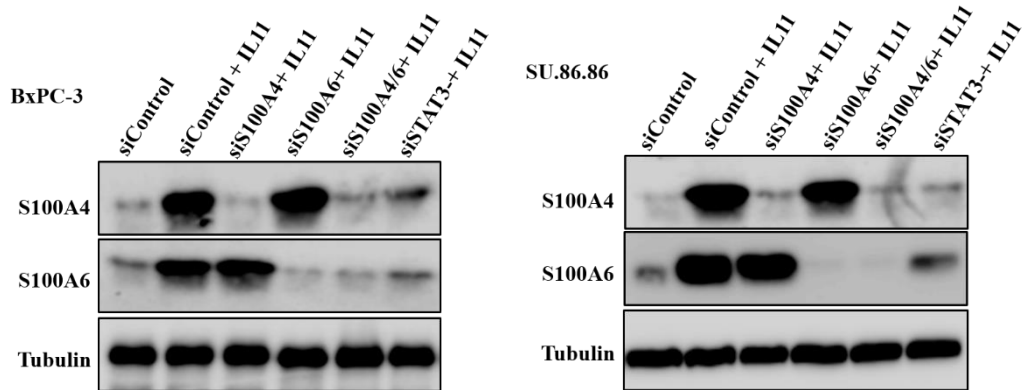
Figure 6.7 Effect of S100A4 and S100A6 downregulation on PC cells migration.

 (A). Statistical analysis of the effect of knockdown of S100A4 or S100A6 and STAT3 on the migration of BxPC-3 and SU.86.86 cells in zebrafish. Bar chart**s** with standard errors of the mean represent the average migration rate of control cells or cells with reduced expression of S100 proteins, * P=0.01, ** $P{\leq}0.006$. The results of 3 independent experiments are shown. (B). Expression of S100A4 and S100A6 in transfected cells was assessed by Western blot.

6.2.5.2 Stattic reduces the migration of PC cells in a zebrafish model

After determining the efficacy of Stattic as a potent inhibitor for STAT3-mediated S100 proteins expression, its effect on PC cell migration was tested next using a zebrafish *in vivo* assay. As was reported in the previous chapter, knockdown of S100A4 and S100A6 in high migratory MIA PaCa-2 cells resulted in a decrease in cell migration in zebrafish (Chapter 4, Figure 4.5).

Additionally, these cells expressed a high level of p-STAT3 and S100A4&A6 without any stimulation with cytokines. It is therefore likely that similar connections may exist between p-STAT3 activation and S100A4&A6 expression in this cells line.

Initially, however, to investigate whether Stattic can reduce MIA PaCa-2 cells through inhibition of STAT3 mediated activation of S100A4&A6 expression, the cells were treated with Stattic and injected into zebrafish embryos. Treatment with Stattic reduced the migration rate of MIA PaCa-2 cells to 17.3% compared to 46% for control cells (treated with DMSO) and the result was statistically significant (P=0.006) (Table 6.3 and Figure 6.8A). The depletion of STAT3 phosphorylation, S100A4 and S100A6 following Stattic treatment was confirmed by Western blot analysis (Figure 6.8B)

For further analysis, the inhibitory effect of Stattic on cell migration was confirmed in other PC cell lines. The expression level of S100A4 and S100A6 was modulated in BxPC-3 and SU.86.86 by stimulating cells by IL-11 and treatment with Stattic. The cells then were injected into zebrafish embryo. The cells which had been treated only with DMSO exhibited a low migration rate (BxPC-3: 6.6%, SU.86.86: 7.3%), but this increased significantly following treatment with IL-11: to 36.6% and 33% for BxPC-3 and SU.86.86, respectively. The migration rate was reduced significantly again when cells were stimulated by IL-11 and treated with Stattic (BxPC-3: 19.3%, SU.86.86: 9.6%). There were the following significant differences between the control groups (DMSO+IL-11) compared with the others: for BxPC-3 (control vs. DMSO P= 0.002, control vs. IL-11+Stattic P = 0.004) while, for SU.86.86 (control vs. DMSO P = 0.007, control vs. IL-11+Stattic P = 0.01) (Table 6.4 and Figure 6.8A). Western blot analysis was performed to assess the upregulation and downregulation of S100A4&A6 following stimulation or treatment with IL-11 and Stattic. These proteins were found to be overexpressed in IL-11+DMSO cells, but their expression was substantially reduced following treatment with Stattic (Figure 6.8B).

It can be clearly seen from these data, therefore, that the migration capability of cells increased consistent with S100A4 and S100A6 activation, and that the Stattic inhibitor effectively suppressed PC cell migration through inhibition of the IL-11/STAT3/S100A4/A6 axis.

Table 6.3 Migration of MIA PaCa-2 cells treated with DMSO (control) and Stattic in zebrafish.

Data are representative of three independent experiments.

Type of injected cells	Migration %	Average migration %
DMSO	44	46
	54	
	40	
Stattic	25	17.3
	22	
	18	

Table 6.4 Migration of BxPC-3 and SU.86.86 cells treated with DMSO, IL-11+DMSO and IL-11+Stattic in zebrafish.

Data are representative of three independent experiments.

Type of injected cells		Migration %	Average migration %
DMSO	BxPC-3	11	6.6
		0	
		9	
	SU86-86	0	7.3
		9	
		13	
IL-11+DMSO	BxPC-3	37	36.6
		40	
		33	
	SU86-86	27	33
		36	
		36	
IL-11+Stattic	BxPC-3	18	19.3
		22	
		18	
	SU86-86	0	9.6
		18	
		11	
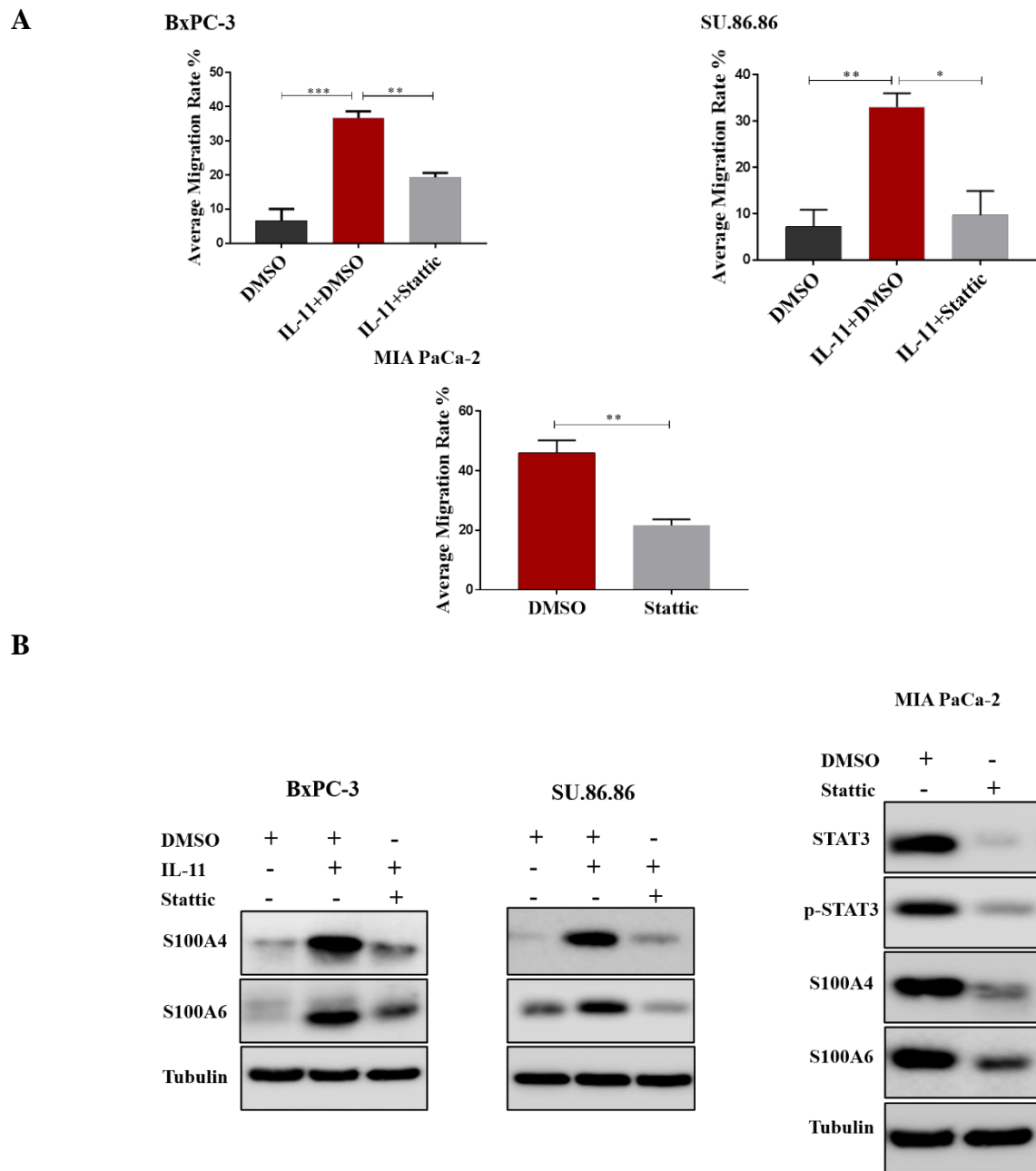
Figure 6.8 Effect of Stattic on PC migration.

(A). Statistical analysis of the effect of Stattic on the migration of BxPC-3, SU.86.86 and MIA PaCa-2 cells in zebrafish. Bar charts with standard errors of the mean represent the average migration rate of DMSO, IL-11+DMSO and Stattic treatment cells, , $^*P{=}0.01$, $^{**}P{=}0.001$, $^{***}P{=}0.0001$. The results of 3 independent experiments are shown. **(B).** Expression of total STAT3, p-STAT3, S100A4 and S100A6 in treated cells was assessed by Western blot.

6.2.6 Activation of STAT3 does not initiate EMT.

It has been proven from the previous experiments that expression of S100A4 and S100A6 is modulated during the EMT process, and also that their expression is activated in response to STAT3 activation induced by IL-11. It is possible, therefore, that IL-11/STAT3 could induce specific molecular changes related to EMT. To this end, BxPC-3 and SU.86.86 cells were cultured in the presence or absence of IL-11 for 48h. The cell lysates were collected and Western blot analysis was performed for EMT-associated proteins including ZEB1, E-Cadherin, P-Cadherin, Vimentin, Slug and Twist. It can clearly be seen from the blot (Figure 6.9) that the expression level of EMT-associated proteins was not affected by the presence of IL-11. (ZEB1, Vimentin and Twist are not shown because Western blot analysis revealed no protein expression in both treated and untreated cells)
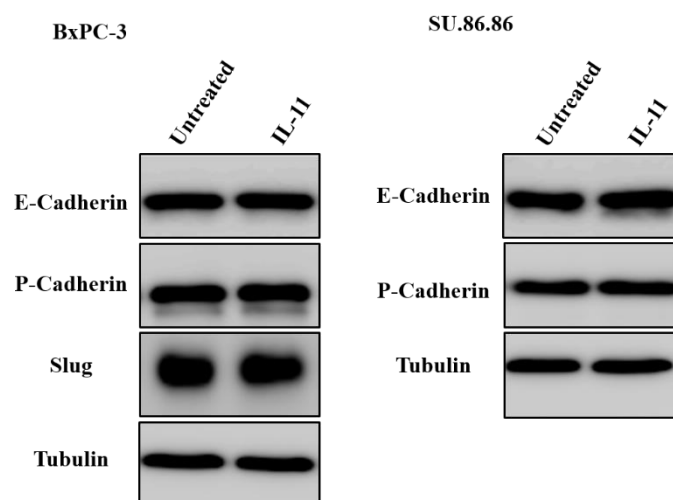
Figure 6.9 Western blot analysis of the effect of IL-11treatment on EMT-associated proteins.

 BxPC-3 and SU.86.86 cells were cultured in the presence or absence of IL-11 for 48h. Cells lysates were collected and resolved in polyacrylamide gel, and the transferred membranes were probed with specific antibodies to EMT-associated proteins.

6.3 Discussion

6.3.1 IL-6 cytokines family regulates expression of S100 proteins

Inflammation is implicated in nearly every step of cancer development, and its role in the recurrence and metastasis of tumours has been investigated (Cohen et al., 2015). Recently, the S100 family of small Ca-binding proteins have received increased attention because of a growing body of evidence linking them to inflammation-induced cancer. For example, in a transgenic melanoma mouse model, S100A4 activates malignant cells to produce inflammatory chemokines (CCL2 and CCL18) which participate in promoting tumour metastasis (Bettum et al., 2014).

As described previously, the expression of S100 proteins is regulated either by epigenetic mechanisms or by transcriptional activity resulting from activation of many signal pathways. For example, S100A4 is regulated by activation of Wnt–β-catenin pathways (Sack and Stein, 2009), whilst S1008 and S100A9 expression is activated as a consequence of activation of NF kb signalling (Nemeth et al., 2009).

Additionally, it has been found that the expression of these proteins may be regulated during inflammation in response to different pro-inflammatory cytokines. For instance, expression of S100A9 is induced by IL-27 in endothelial cells (Susann et al., 2015), while S100A7 is expressed in skin in response to IL-17 and IL-22 (Glaser et al., 2005). Despite the fact that it is known that cytokines induce the expression of S100 proteins, the detailed mechanism for this is still not well understood.

In the current study, the expression of two specific S100 proteins (S100A4 and 100A6) was activated in both BxPC-3 and SU.86.86 PC cell lines by stimulation with the IL-6 family of cytokines. Interestingly, we found that both S100A4 and S100A6 were upregulated consistent with the activation of p-STAT3, raising the possibility that STAT3 may contribute to the regulation of S100 protein expression.

STAT3 is the most inflammatory signal, and is activated by tyrosine phosphorylation in response to various extracellular stimuli such as cytokines and growth factors (Rebe et al., 2013).

Once STAT3 is activated, STAT3 protein translocates to the nucleus in order to regulate the expression of various genes such as c-Fos, c-Myc, ZEB1, Cyclin D1, MMP3, Rho, FGF, AKT, IL-6, TNF-alpha and STAT1, which are involved in regulating multiple steps of cancer progression including cell cycle, proliferation, EMT, migration, invasion, metastasis and tumour-associated inflammation (Carpenter and Lo, 2014). STAT3 exert its effect in gene regulation either by direct interaction with promoter of target gene or indirectly by mediating expression of the other transcriptional factors, leading to supress or enhance their functional role in regulation of target genes (Carpenter and Lo, 2014)

Our data demonstrates that STAT3 was activated in BxPC-3 and SU.86.86 PC cells when the cells were stimulated by IL-6, IL-8, IL-10 and IL-11. The level of STAT3 phosphorylation was almost the same in cells stimulated by IL-6 and IL-11. It seems possible that these results are due to the fact that both IL-6 and IL-11 belong to the same family of cytokines which share the same receptor subunit gp130 and have similar, or even identical, biological functions (Xu et al., 2016a). These findings seem to be consistent with other research which has found that STAT3 activated significantly in PC in the presence of IL-6 and IL-11 (Fukuda et al., 2011). Recently, there has been increasing evidence to demonstrate that both IL-6 and IL-11 are key drivers for STAT3 activation (Furtek et al., 2016, Zheng et al., 2016). Additionally, a high expression level of STAT3 phosphorylation was also observed in cells stimulated with IL-8 or IL-10, supporting previous research into the brain area which links STAT3 activation with IL-8 (Qu et al., 2015) and IL-10 (Goswami et al., 2016).

Although STAT3 activation is involved in modulating a large number of genes, there have been few studies on its causal implication in modulating the expression of S100 protein family members. Such studies have focused only on S100A4 and S100A8/A9 members, and have found that cytokines mediate STAT3 activation in response to the regulation of the expression of S100A4 in rhomboid-phenotype pulmonary arterial smooth muscle cells (Liu et al., 2012) and S100A8 and S100A9 in Colonic Epithelial Cells (Lee et al., 2012) and breast cancer cells (Rodriguez-Barrueco et al., 2015).

This work, however, is the first study to investigate whether the expression profile of S100 proteins can result from STAT3 activation induced by IL-11. The experiments reported here have revealed that the expression of selected S100 family members at mRNA and protein levels was upregulated in both BxPC-3 and SU.86.86 PC cell lines when STAT3 was activated by IL-11.

In contrast, targeting STAT3 activation either by siRNA or Stattic inhibitor led to the downregulation of S100 protein expression. These findings suggest that persistent STAT3 activation mediated by IL-11 may have contributed to programming the S100 gene expression.

Further experimental investigations should be undertaken to explore how STAT3 activation contributes to the regulation of S100 proteins. For example, activating STAT3 constitutively by active STAT3-C plasmid instead of treatment cells with cytokines and then studying its role in the regulation of the expression of S100 proteins. Additionally, further work needs to be done to establish whether STAT3 regulates the transcription of S100 proteins directly.

6.3.2 Targeting STAT3 activation supresses PC migration via downregulation of S100A4 and S100A6 expression

Conclusive evidence supports the idea that persistent STAT3 activation plays a vital role in every step of cancer metastasis. The detailed mechanism of how STAT3 affects the steps of metastasis comes from the observation that STAT3 is involved in regulating the expression of genes associated with apoptosis (Bcl2 and BclxL) (Bhattacharya et al., 2005), tumour growth (Cyclin D1 and cMyc) (Kamran et al., 2013), invasion (MMP1, MMP9) (Itoh et al., 2006, Sano et al., 1999) , migration (Rho GTPase) (Debidda et al., 2005) and angiogenesis (VEGF) (Chen and Han, 2008) . Targeting the activation of these signalling pathways can be therefore be considered as an excellent therapeutic target in cancer therapy (Taniguchi and Karin, 2014).

Different approaches have been used to suppress STAT3 activation, either using RNAi approaches or specific inhibitors (Mali, 2015). Our study provides new insights into the role of STAT3 mediated PC cell migration and invasion through upregulation of the expression of S100 associated metastasis proteins (S100A4, S100A6). We found that the activation of STAT3 in BxPC-3 and SU.86.86 cells led to upregulation of the expression of S100A4 and S100A6, and that this upregulation was consistent with increase migratory ability of cells *in vivo*.

In contrast, targeting STAT3 activation by siRNA or Stattic inhibitors resulted in a significant decrease in the expression level of S100A4 and S100A6 and, subsequently, suppression of the migration rate of PC cells when injected into zebrafish.

The effect of siRNA-mediated knockdown of STAT3 on PC cell metastasis through modulating the expression of migration- and invasion-associated genes has been investigated previously. For example, (Huang et al., 2011) found that inhibiting the expression of total STAT3 and p-STAT3 using interference RNA supressed PC cell migration via downregulation of VEGF and MMP-2 expression.

Also, knockdown of STAT3 using siRNA reduced cancer cell migration and invasion by modulating the expression of the EMT-associated proteins, ZEB1 and E-Cadherin (Xiong et al., 2012). Although the Stattic inhibitor has been widely used as a potent STAT3 inhibitor in different human malignancies, its use in respect to PC has not previously been described.

A large body of experimental evidence demonstrates that Stattic-mediated inhibition of STAT3 activation can lead to impaired development of multiple steps in cancer metastasis in endometrial cancer cells (Subramaniam et al., 2016), gastric cancer stem cells (Jiang et al., 2017c), prostate cancer (Han et al., 2014), colorectal cancer (Nguyen et al., 2017) and breast cancer (Hung et al., 2016). Collectively, the results of this study indicate that inhibition of STAT3 activation mediated the regulation of S100A4&A6 expression, and that this may provide a rational strategy for targeting PC.

6.3.3 STAT3 activation does not affect EMT in PC cells

It is well known that STAT3 activation has been reported in various cancers. In addition to its traditional role in cancer cell metastasis, tumour growth and cancer association-inflammation, STAT3 can promote tumour development by modulating EMT-related gene expression and promoting cancer stemness (Jie et al., 2015). For example, in head and neck and breast cancer cells, STAT3 was found to bind to the promoter of Snail and Twist, mediate their transcriptional activity and induce the EMT process (Sullivan et al., 2009); (Yadav et al., 2011). More recently, it has been found that IL-6 in combination with CCL2 is capable of inducing EMT in small lung carcinoma via activation of STAT3 pathways(Chen et al., 2015a).

A similar effect of STAT3 activation in inducing the EMT process has been reported in PC cells when they are treated with IL-6; specifically, such treatment resulted in the activation of STAT3, the modulation of EMT-associated gene expression, with upregulation of Snail and Twist and downregulation of E-Cadherin, thereby promoting cancer cell migration and invasion (Huang et al., 2011). In contrast to earlier findings about the role of STAT3 in the EMT process, however, our study revealed that STAT3 activation did not affect the expression of EMT-associated proteins in PC cells.

6.4 Conclusion

From the outcome of our investigation we conclude the following: Firstly, IL-11 regulates the expression of S100 proteins in a STAT3-dependent manner. Secondly, targeting STAT3 suppresses the migration ability of PC cells via downregulation of S100A4/A6. Finally, the activation of STAT3 does not affect the expression of EMT-associated factors.

Chapter 7: EMT master regulator transcriptional factor ZEB1 targets P53 Tumour suppressor protein stability

7.1 Introduction

Tumour suppressor protein P53 is a transcriptional factor that is activated in response to DNA damage and stress. Following activation, P53 induces either cell cycle arrest or apoptosis depending on the extent of the stress (Makohon-Moore and Iacobuzio-Donahue, 2016). Mutations in the P53 gene are the most frequent molecular change identified in more than 50% of human cancers. In particular, P53 mutation has been detected in up to 75% of PC and is considered to be one of the most frequent genetic events in developmental stage PC (Yachida et al., 2012).

Under normal conditions, P53 is expressed at low level with s very short half-life and is regulated by Murine double minute 2 (Mdm2) E3 ubiquitin ligase. The transcriptional activity of P53 can be regulated via protein-protein interaction, posttranslational modifications and protein stabilization (Ryan et al., 2001). Serine 15 phosphorylation in response to DNA damage is a crucial step in regulating both the stability and functional activity of P53 (Dumaz and Meek, 1999). P53 expression levels and activity are regulated via multiple signalling pathways (Melnikova et al., 2003, Baresova et al., 2014, Tibbetts et al., 1999), but evidence exists for the involvement of some EMT-TFs in the regulation of P53 such as Snail (Ni et al., 2016) and Twist (Piccinin et al., 2012). P53, in turn, counteracts EMT by upregulating transcription of miR-200 family members, leading to the repression of ZEB1 and ZEB2 (Kim et al., 2011). The effect of ZEB proteins on P53 has not been investigated, however.

This chapter, therefore, aims to elucidate whether P53 expression and function is modulated by activation of ZEB1 in cell lines harbouring w/t or mutant P53.

7.2 Results

7.2.1 ZEB1 expression negatively regulates P53 protein stability

Since a negative correlation was observed in human PC tissues between the expression of ZEB1 and P53 (chapter 5), it is hypothesised that this correlation is due to a direct effect of ZEB1 on P53 expression levels. To test this hypothesis, BxPC-3 and SU.86.86 PC cell lines were used since they carry mutant P53, and also a stable clone MCF-7-ZEB1 of a breast cancer cell line (Doxycycline-inducible expression of ZEB1 protein) harbouring w/t P53. The reason for selecting MCF-7-ZEB1 cells was because no w/t P53 PC cell lines were available for this study. ZEB1 expression was induced in BxPC-3 and SU.86.86 by transiently transfecting PC cells with a ZEB1 overexpression construct or an empty vector (GFP) as a control. In MCF-7-ZEB1 cells, ZEB1 was induced by maintaining cells in a DOX-containing growth medium for 72h. It was found that the expression of w/t or mutant P53 tended to be downregulated in ZEB1-expressing cells as compared to the controls (Figure 7.1A, B).

To further investigate whether ZEB1 regulates the expression of P53 proteins at the transcriptional level, the levels of P53 mRNA were assessed using qPCR. Total RNA was extracted from BxPC-3 and SU.86.86 cells, transfected with ZEB1-expressing or a control vector and reverse transcribed. cDNA was analysed using SYBR Green reagents and the primers specific for P53. This failed to detect any significant effect of ZEB1 on P53 mRNA levels in either of the cell lines, however (Figure 7.1C).

A

B

C
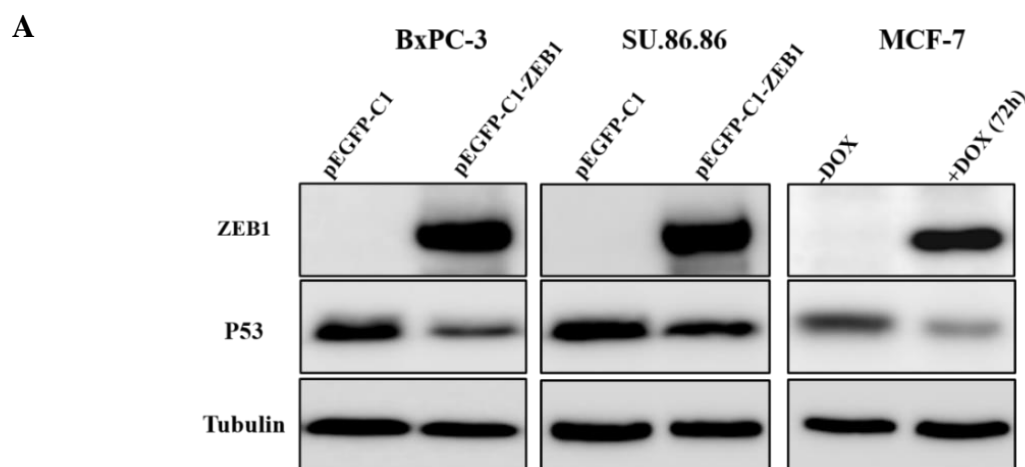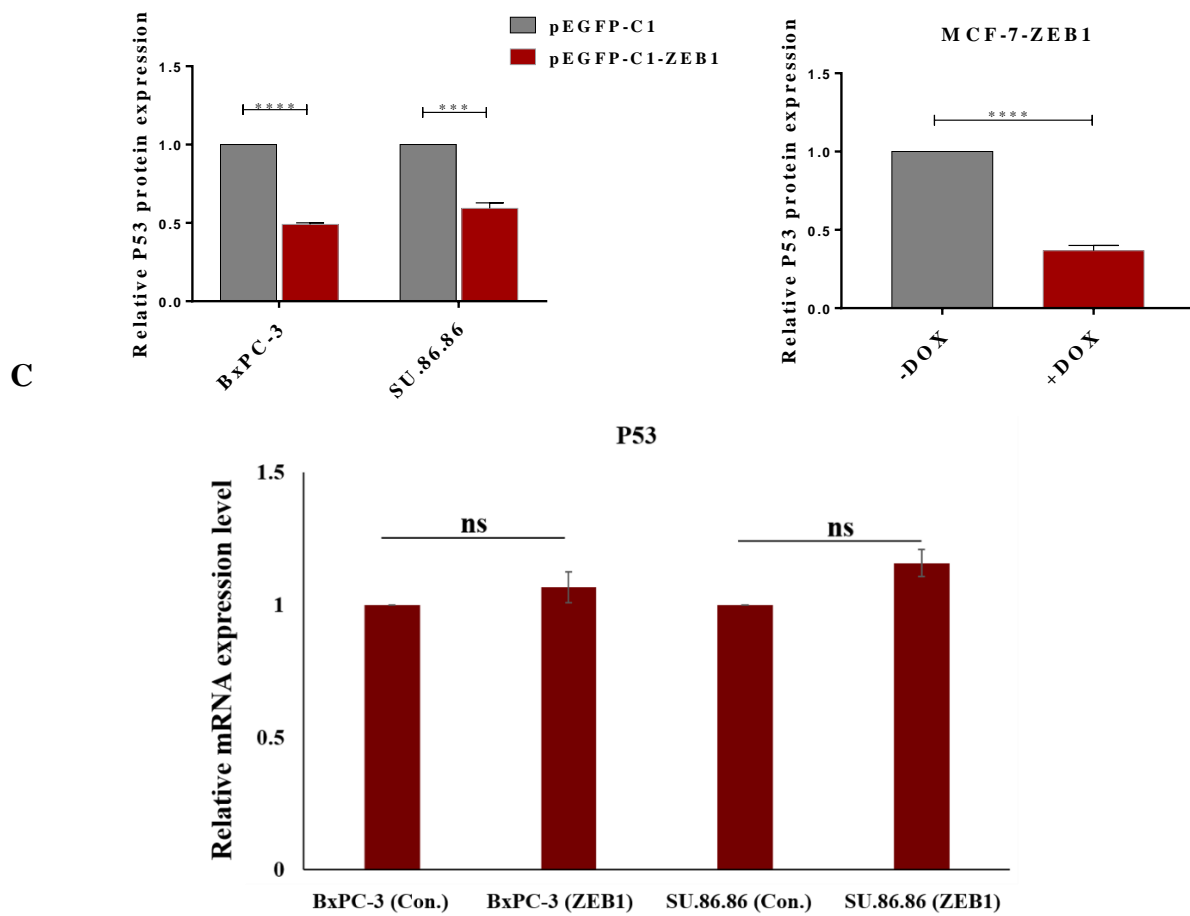
Figure 7.1 Activation of ZEB1 reduces the expression of P53.

 (A). BxPC-3 and SU86.86 cells were transfected with a ZEB1-expressing consruct or a control vector, and maintained for 48h. MCF-7-ZEB1 cells were cultivated in the presence or absence of DOX for 72h. Cell lysates then were collected and analysed by immunoblotting with the indicated antibodies **(B).** The relative intensity of protein bands was quantified using Image J software by normalization the intensity of each band to tubulin. Bar charts represent standard errors of the mean of three experiments (****P =0.001 and****$P < 0.0001$). **(C).** The relative mRNA level of P53 in transfected BxPC-3 and SU.86.86 was evaluated by the $2^{-\Delta\Delta CT}$ method. The mRNA level was normalized to housekeeping gene GAPDH. Non-significant different was observed between control and ZEB1 expressing cells at P53 mRNA level.

7.2.2 ZEB1 expression decreases P53 protein half-life

Since ZEB1 did not downregulate P53 at the transcriptional level, it was investigated whether ZEB1 expression decreased P53 protein stability. To this end, the half-life of P53 in MCF-7-ZEB1 cells was determined following inhibition of protein synthesis by treatment cells with cycloheximide (CHX). Cells were initially cultured in the presence or absence of DOX for 72h and were then treated with 50μg/ml (CHX) for different time periods: 0, 15, 30, 60 and 120 mins. The expression levels of P53 protein in cell lysates were determined by Western blot.

 In cells which did not express ZEB1, CHX induced a gradual decrease in the P53 level. In contrast, a 15 mins treatment with CHX was sufficient to reduce P53 expression to the steady-state level (Figure 7.2). These data clearly show that ZEB1 destabilises w/t P53 in MCF-7 cells, probably by inducing its degradation via the ubiquitin-proteasome pathway.
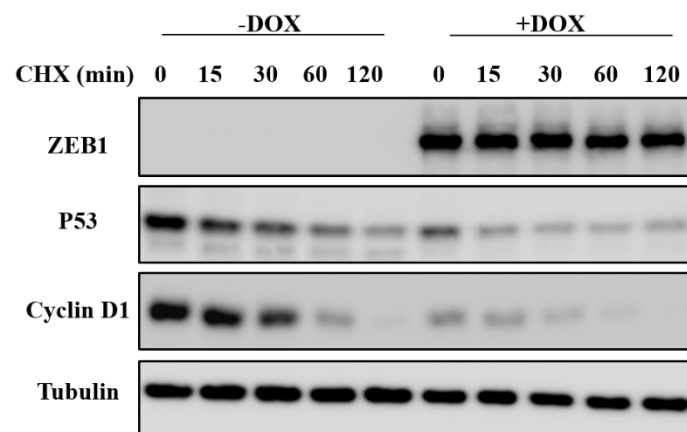
Figure 7.2 ZEB1 expression leads to a decrease in P53 protein half-life.

 MCF-7 cells were seeded in 6cm dishes and treated with or without DOX for 72h to induce ZEB1 expression. CHX was added and cells lysates were collected at the indicated time points. The lysates then were loaded into acrylamide gel. The transferred members were stained for ZEB1 and P53 antibodies which detected both w/t and mutant as well as Cyclin D1 as a control for sensitivity of treatment and short half-life.

7.2.3 ZEB1 expression reduces P53 phosphorylation in DNA damaged cells

Phosphorylation at Ser15 promotes the functional activation of P53 in response to the DNA damage induced by UV (Siliciano et al., 1997). Since ZEB1 acts as an upstream regulator of P53 expression levels, it was intended to investigate whether ZEB1 prevents P53 activation by DNA damage. To this end, we treated ZEB1-expressing or non-expressing cells with UV at 50 mJ/cm2 and incubated them for 2 or 4h prior to harvesting. To assess the extent of DNA damage, we analysed the accumulation of the DNA damage biomarker, the phosphorylated form of histone 2A (γ-H2AX). Expression of ZEB1 resulted in reduced levels of γ-H2AX in both PC cell lines and also in MCF7 (Figure 7.3A). The analysis of P53 activation has shown that ZEB1 completely blocked phosphorylation of P53 at Ser15 in BxPC3 cells. In SU86.86 and MCF7 cells, although P53 activation was not fully blocked by ZEB1, it was markedly reduced (Figure 7.3B).

Taken together, these data indicate that ZEB1 destabilises P53 and prevents its phosphorylation at Ser15 induced by DNA damage.

A
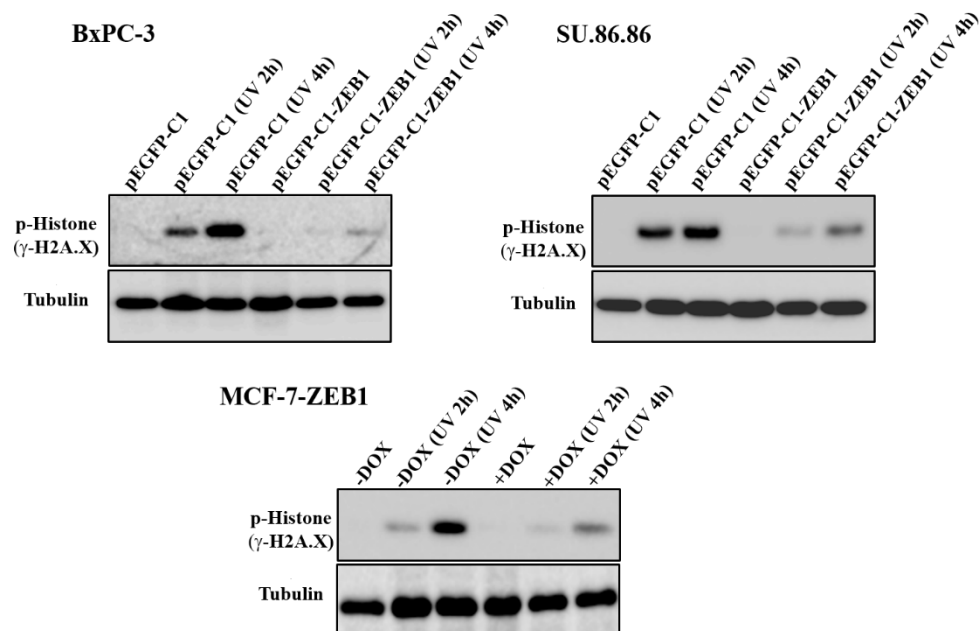
B
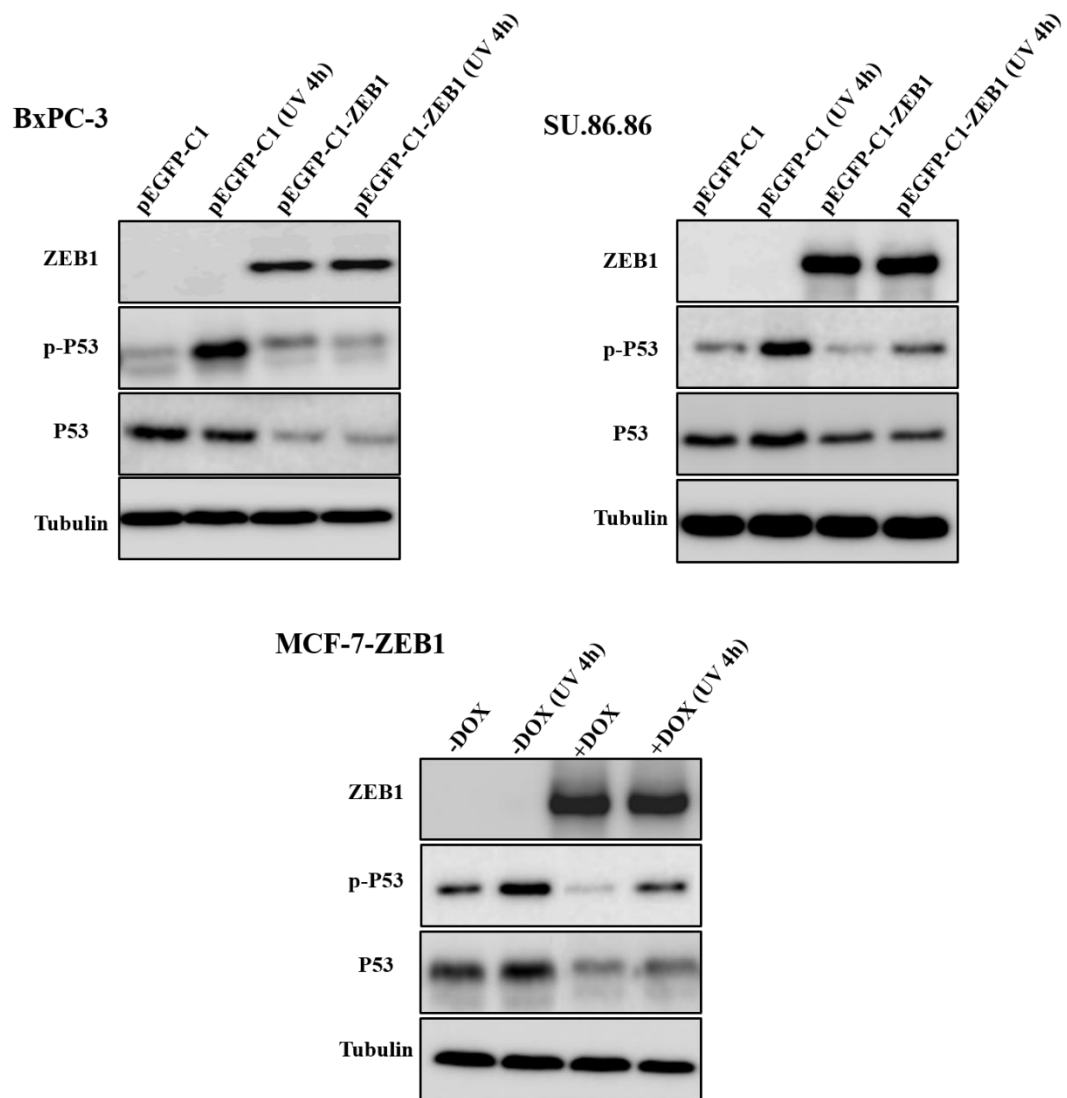
Figure 7.3 Expression of ZEB1 inhibits DNA damage-induced P53 phosphorylation.

ZEB1 expression was induced in BxPC-3, SU.86.86 and MCF-7-ZEB1 either by transfected cells transiently with ZEB1 overexpression construct or treated them with DOX. The cells then were irradiated with UV at 50 mJ/cm^2. Cell lysates were collected 4h post irradiation and subjected to Western blot using antibodies for ZEB1, P53 (detect both w t and mutant), p-P53 at Ser-15, and p-Histone H2A.X as well as tubulin as a loading control.

7.3 Discussion

The stability and activation of P53 is regulated by a variety of molecular events, such as phosphorylation and protein-protein interaction (Chernov et al., 1998). Very low levels of P53 are typically found in cells since it degrades rapidly through the ubiquitin-dependent proteasome pathway. This degradation of P53 through the proteasome pathway is regulated by Mdm2, functioning as an ubiquitin E3 ligase (Honda et al., 1997, Haupt et al., 1997). Indeed, other E3 ligases, such as Pirh2 and Cop1, may also play a role in regulating the turnover of P53 (Leng et al., 2003, Dornan et al., 2004).

In PC, different proteins are implicated in regulating w/t or mutant P53 protein expression at transcriptional or posttranscriptional levels (Jiang et al., 2016, Zheng et al., 2012). We demonstrated previously that ZEB1 reduced the expression of both w/t and mutant P53 protein in cancer cell lines, and the immuhistochemical staining for ZEB1 and P53 in formalin-fixed paraffin-embedded pancreatic tissue carried out in Chapter five supports this observation that expression of P53 protein is negatively correlated with ZEB1.

This decrease in P53 expression was not reflected by a decrease in mRNA level, however. In fact, the level of mRNA remained stable, suggesting that ZEB1 expression stimulated a decrease in P53 protein independent of P53 mRNA accumulation. Similar results were reported by (Chernov et al., 1998), who found that treatment of human or mouse cells with protein kinase C (PKC) inhibitor H7 resulted in the accumulation of P53 independently of transcriptional activation. Additionally, (McVean et al., 2000) found that accumulation of P53 could occur in keratinocytes even in the absence of an increase mRNA transcription.

The specific targeting of P53 for degradation depends crucially on the binding between P53 and Mdm2 and has therefore been extensively studied as a potential target of regulation by DNA damage signalling (Cheng et al., 2011). DNA damage in response to radiation initiates P53 phosphorylation leading to stabilization and an increase in transcriptional activity (Xu, 2003, Appella and Anderson, 2001). Studies in mouse models have shown that if mouse P53 phosphorylation is blocked at serine 18 or serine 23 (which correspond to human S15 and S20) this only partly reduces P53 stabilization after DNA damage (Chao et al., 2006, MacPherson et al., 2004). We observed that ZEB1 expression reduced P53 phosphorylation at serine 15 in response to DNA damage, suggesting that inhibition of the phosphorylation of P53 in the presence of ZEB1 may have contributed to reduced stability.

Although there is a large volume of published studies that have linked the EMT program with onco-suppressive proteins, including P53, the molecular mechanism of P53 regulation by ZEB1 has not previously been established. In our study, we found that induction of ZEB1 expression significantly reduced the P53 half-life but currently, the exact underlying mechanism remains unclear. We propose that ZEB1 enhances expression or activity of an ubiquitin E3 ligase that targets P53 for proteasomal degradation (Figure 7.4).

It has been shown previously that w/t P53 regulates expression of certain microRNAs implicated in EMT, such as miR-200 family members (Chang et al., 2011, Kim et al., 2011) . In turn, miR-200 supresses the expression of ZEB1 resulting in mesenchymal epithelial transition (Brabletz et al., 2011). We hypothesise that mutation in the TP53 gene may dysregulate miR-200 expression, leading in turn to the increased expression of ZEB1. Subsequently, ZEB1 expression destabilises P53, generating P53-negative cells maintaining high levels of ZEB1 expression (Figure 7.4). In the w/t P53 background, activation of ZEB1 by TGF-β or other EMT-inducing pathways may contribute to cell survival/drug resistance through destabilisation of P53.

Additionally, there is growing body of studies linking other EMT transcriptional factors with P53 regulation. For example, Twist inhibits P53 post-translational modification and induces Mdm2-mediated P53 degradation through direct interaction with P53 (Piccinin et al., 2012). The Snail family of EMT transcription factors reduces the expression and tumour-suppressing function of P53 by direct interaction with the DNA binding domain of P53 and by antagonizing its transcriptional activity (Wu et al., 2005, Lee et al., 2009). These data indicate that there is a complex interaction between P53-dependent pathways and molecular networks regulating EMT in cancer cells. (Brabletz et al., 2011)
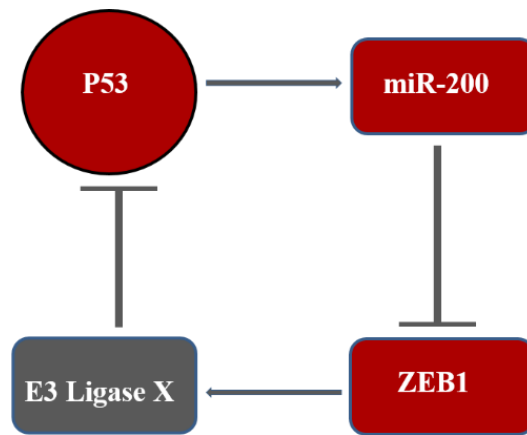
Figure 7.4 Hypothetical scheme setting out the interaction between the P53 and ZEB1/miR-200 axis.

7.4 Conclusion

From the outcome of our investigations it is possible to conclude that the expression of the EMT master regulator ZEB1 regulates P53 protein stability.

Chapter 8: General discussion

8.1 Discussion

Pancreatic cancer is one of the major causes of cancer-related mortality in the world and is characterized by its aggressive behaviour (Lin and Lin, 2017). Better understanding of the molecular mechanisms responsible for the enhanced PC aggressiveness is required.

To this end, several studies thus far have linked many S100 protein members with PC progression (Ji et al., 2014). Expression analysis of the S100 family members in a collection of PC cell lines allowed categorization of the S100 genes into two groups, mesenchymal-associated and epithelial-associated. This study focused on the molecular mechanisms responsible for the up-regulation of mesenchymal S100 genes in the pathogenesis of PC, highlighting that EMT pathways and inflammatory factors including IL6/STAT3 coordinate the expression of these genes.

Overexpression of ZEB1 and ZEB2 during EMT induction resulted in altered expression of certain S100 protein family members. Of note, only S100A4 and S100A6 were activated, and their expression correlated with expression of EMT-associated proteins, with P-Cadherin and E-Cadherin being down-regulated whilst ZEB1 or ZEB2 and Vimentin were up-regulated. Additionally, expression of S100A4 with associated with EMT was observed in PC tissues, and its expression was detected at high level in developmental stages of PC using tissue microarray. These proteins are unambiguously classified as mesenchymal markers and strongly associated with EMT, and the levels observed here confirm previous studies (Chen et al., 2015b, Xu et al., 2016b).

Expression of S100A6 was significantly higher in PC tissues compared to normal tissues. Additionally, tissue microarray analysis revealed that all chronic pancreatitis sections were positive for S100A6, suggesting that expression of S100A6 may be a promising modality not only to characterise PC but also to detect chronic pancreatitis.

In addition, it is possible that some cytokines may contribute to the regulation of S100 protein family expression in PC. Firstly, it is well known that the inflammatory process could be a contributing factor to an increased risk of PC, and the link between inflammation and the progression of PC has been long recognized (Holmer et al., 2014). Secondly, members of the S100 family have been found to be strongly associated with inflammation processes and play a critical role in tumour-associated inflammation (Nasser et al., 2015a). Thirdly, tumour-associated inflammation regulated by the IL-6 family of cytokines and STAT3 activation play a key role in PC progression (Corcoran et al., 2011).

Furthermore, the IL-6/STAT3 signalling pathway has been linked to PC progression through initiation and regulation of EMT (Xiong et al., 2012). Finally, based on the immunohistochemical analysis in this study, p-STAT3 was detected in cells positive for S100A4 or S100A6. Collectivelyy, these observations gave us inducement to hypothesis that cytokines/STAT3 may play a critical role in connecting expression of S100 proteins with pathogenesis of PC.

A limited number of studies have analysed causally implicated STAT3 activation induction by cytokines in modulating the expression of S100 proteins family members, which focused only on S100A4 and S100A8/A9 members (Liu et al., 2012);(Rodriguez-Barrueco et al., 2015). However, the treatment of selected PC cell lines with IL-11 cytokines in this study resulted in upregulation the majority of tested members of S100 proteins through IL-11/STAT3 signalling. These observations indicated that a link may exist between expression of STAT3 and S100 proteins, and STAT3 activation may affect the regulation of members of the S100 protein family.

Mesenchymal S100 proteins including S100A4 and A6 has been found to play a critical role in enhancement of cell invasion and migration in PC (Nutter et al., 2014);(Nedjadi et al., 2009). In the current study, depletion of S100A4/A6 significantly reduced A431-ZEB1 and PC cell motility in zebrafish embryo xenograft cell motility assays. Furthermore, co-culture of the non-migratory PC cell line BxPC-3 with exosomes derived from MIA PaCa-2 cells, which are enriched with S100A4 protein, resulted in increased cell migration compared to cells cultured with exosomes purified from lower motile cells SU.86.86, which are negative for S100A4. Therefore, it is possible to hypothesise that exosomal S100A4 proteins derived from MIA PaCa-2 cells may affect the migration behaviour of other cancers cells.

In this study, all experiments to study the migration and invasion ability of cells were performed *in vivo*. Traditionally, studies on metastatic potential of human tumour cells are performed in mice, but, in this study, we establish zebrafish xenografts as a tool for *in vivo* studies of cancer cell migration.

During comprehensive investigation of the role of S100 protein members in regulating PC migration, silencing of epithelial S100 proteins including S100A2 and S100A11 did not influence PC migration. The most interesting finding to emerge from the analysis is that knockdown of S100A14 promoted PC cell migration *in vivo*. A possible explanation for this might be that expression of S100A14 was only detected in epithelial cells and its expression was positively correlated with E-Cadherin and inversely with ZEB1 and S100A4 in both pancreatic cells and tissues. Another possible explanation for this is the extension protrusion, mesenchymal-like phenotype and an upregulation of mesenchymal S100A4/A6 proteins, with concomitant silencing of S100A14 in cells compared to controls.

Moreover, expression of S100 proteins in connection to EMT-associated genes was investigated in PC specimens. Although the expression of the majority of selected members of S100 proteins family was higher in cancer tissue compared to adjacent normal tissue, no positive association of proteins with clinical pathological characteristics was observed in this study, which is contrary to previous research (Vimalachandran et al., 2005, Huang et al., 2016a), likely as a result of the small size of the study cohort. However, based on the results obtained in this study, further investigation in a larger cohort is warranted. .

Mutations in TP53 mutation is considered to be one of the critical hallmarks for PC (Redston et al., 1994) and it is an interaction target for different members of S100 proteins (Grigorian et al., 2001, Berge and Maelandsmo, 2011, Chen et al., 2012). Hence, expression of P53 was examined in PC tissues.

No correlation between P53 expression and members of the S100 family was detected in PC samples using tissue microarray. One unexpected finding was that expression of P53 was only found to be associated positively with ZEB1 in PC tissues. Accordingly, the correlation between P53 and ZEB1 has been further validated by using PC cell lines to determine the precise mechanism of this correlation. This study showed that ZEB1 expression downregulated mutant P53 activation in PC and destabilised w/t P53 in MCF-7 cells likely by inducing its degradation via the ubiquitin- proteasome pathway.

8.2 Conclusion and future directions

I performed the analysis of the expression, regulation and function of S100 proteins in PC.

I observed that expression of S100 proteins is rapidly activated in the course of ZEB1-induced EMT programs or in response to the inflammatory cytokines, such as IL-6, 8 and 11. Activation of two members of the S100 family, S100A4&6, was associated with inflammation and metastatic dissemination in PC samples. Analysis of the signalling pathways, involved in their activation, highlighted a role for STAT3.

These data propose that the development of the specific S100A4/A6 inhibitors, which are less toxic than currently available STAT3 inhibitors, may have a better therapeutic effect in PC patients.

Potentially interesting data demonstrate a role for exosomes secreted by highly migratory PC cells in inducing cell migration of slowly-migrating cells. Further investigation of a role for S100A4 & S100A6 in this phenomenon may represent a new line of research.

Targeting S100A4&A6 proteins by RNAi significantly reduced PC cell motility in zebrafish xenograft cell motility assays. Contrary, silencing of epithelial S100A14 protein promoted PC cells migration. I observed that the depletion of S100A14 resulted in enhanced expression of "mesenchymal" S100 proteins. I hypothesise that their activation is the determinant of migratory phenotype of PC cells with depleted S100A14. Further works need to be carried out in order to validate this hypothesis.

Data obtained from the analysis of the S100 proteins in PC specimens were in line with the results obtained in cell line models: S100A4 protein expression correlated with the levels of ZEB1 and p-STAT3. However, no statistically significant correlations with clinicopathological characteristics were observed. The cohort size of analysed tumours was limited, and further investigation in a larger cohort is warranted.

One of the interesting findings to emerge from this study is my data showing an inverse correlation between ZEB1 and P53 expression in tumours and cell lines. My data demonstrated that ZEB1 has a potential to down-regulate both wild-type and mutant P53 by decreasing protein stability. These data may indicate a novel mechanism of senescence escape imposed by ZEB1 at early PC stages.

Appendixes

Appendix 1: Person correlation coefficient between S100 and EMT-associated markers. Significant positive associations are highlighted in yellow, while negative correlation trends are highlighted in red.

Correlations

		S100A2	S100A4	S100A6	S100A14	Vimentin	P-Cadherin	E-Cadherin	Slug	Twist	ZEB1	P53	p-STAT3
S100A2	Pearson Correlation	1	.246	.047	.121	-.001	.173	.170	.030	.057	.301	-.028	-.091
	Sig. (2-tailed)		.181	.801	.517	.994	.351	.362	.872	.760	.100	.882	.627
	N	31	31	31	31	31	31	31	31	31	31	31	31
S100A4	Pearson Correlation	.246	1	.444*	-.371*	.042	.074	-.409*	.207	.310	.428*	-.286	.470**
	Sig. (2-tailed)	.181		.012	.040	.821	.692	.022	.263	.090	.016	.118	.008
	N	31	31	31	31	31	31	31	31	31	31	31	31
S100A6	Pearson Correlation	.047	.444*	1	.096	-.007	-.030	.012	.156	.189	.083	-.177	.387*
	Sig. (2-tailed)	.801	.012		.607	.970	.873	.948	.403	.310	.657	.340	.032
	N	31	31	31	31	31	31	31	31	31	31	31	31
S100A14	Pearson Correlation	.121	-.371*	.096	1	-.589**	.338	.828**	-.088	-.221	-.264	.251	-.261
	Sig. (2-tailed)	.517	.040	.607		.000	.063	.000	.636	.232	.152	.172	.155
	N	31	31	31	31	31	31	31	31	31	31	31	31
Vimentin	Pearson Correlation	-.001	.042	-.007	-.589**	1	-.180	-.422*	.069	.237	-.035	.071	.283
	Sig. (2-tailed)	.994	.821	.970	.000		.332	.018	.712	.199	.854	.704	.124

198

	N	31	31	31	31	31	31	31	31	31	31	31	31
P-Cadherin	Pearson Correlation	.173	.074	-.030	.338	-.180	1	.426*	.210	.042	.369*	-.209	-.077
	Sig. (2-tailed)	.351	.692	.873	.063	.332		.017	.257	.823	.041	.260	.680
	N	31	31	31	31	31	31	31	31	31	31	31	31
E-Cadherin	Pearson Correlation	.170	-.409*	.012	.828**	-.422*	.426*	1	-.203	-.318	-.176	.050	-.296
	Sig. (2-tailed)	.362	.022	.948	.000	.018	.017		.273	.081	.345	.789	.106
	N	31	31	31	31	31	31	31	31	31	31	31	31
Slug	Pearson Correlation	.030	.207	.156	-.088	.069	.210	-.203	1	.233	.310	.044	.056
	Sig. (2-tailed)	.872	.263	.403	.636	.712	.257	.273		.206	.090	.816	.765
	N	31	31	31	31	31	31	31	31	31	31	31	31
Twist	Pearson Correlation	.057	.310	.189	-.221	.237	.042	-.318	.233	1	.125	.012	.419*
	Sig. (2-tailed)	.760	.090	.310	.232	.199	.823	.081	.206		.505	.948	.019
	N	31	31	31	31	31	31	31	31	31	31	31	31
ZEB1	Pearson Correlation	.301	.428*	.083	-.264	-.035	.369*	-.176	.310	.125	1	-.436*	.122
	Sig. (2-tailed)	.100	.016	.657	.152	.854	.041	.345	.090	.505		.014	.512
	N	31	31	31	31	31	31	31	31	31	31	31	31
P53	Pearson Correlation	-.028	-.286	-.177	.251	.071	-.209	.050	.044	.012	-.436*	1	-.095
	Sig. (2-tailed)	.882	.118	.340	.172	.704	.260	.789	.816	.948	.014		.611
	N	31	31	31	31	31	31	31	31	31	31	31	31

p-STAT3	Pearson Correlation	-.091	.470**	.387*	-.261	.283	-.077	-.296	.056	.419*	.122	-.095	1
	Sig. (2-tailed)	.627	.008	.032	.155	.124	.680	.106	.765	.019	.512	.611	
	N	31	31	31	31	31	31	31	31	31	31	31	31

*. Correlation is significant at the 0.05 level (2-tailed).

**. Correlation is significant at the 0.01 level (2-tailed).

200

Participating conferences

Zebrafish as a model organism to study *in vivo* invasion and Epithelial Mesenchymal Transition in cancer

Qais AL Ismaeel[1-2], Elvira Diamantopoulou[1-2], Andrew F. Irvine[1], Kees. R. Straatman[3], Jonathan McDearmid[2] and Marina Kriajevska[1]

[1] Department of Cancer Studies and Molecular Medicine, University of Leicester; [2]Department of Biology, University of Leicester; [3] Advanced Imaging Facility, University of Leicester

Intrinsic invasive abilities of cancer cells are important in the process of metastatic dissemination. Traditionally, studies on metastatic potential of human tumour cells are performed in mice, but, recently, transparent zebrafish became popular as a model system in cancer research.

Epithelial mesenchymal transition (EMT) is implicated in tumour progression and is characterised by alterations in cell morphology and formation of highly motile cells.

During EMT, cytoskeleton undergoes global reorganisation; dynamic actin-myosin stress fibres are formed and modify cellular polarity. Assembly/disassembly of myosin filaments is primarily controlled by myosin light chain phosphorylation, which is activated during EMT. However, emerging evidence suggests that small calcium-binding proteins of the S100 family also play an active role in the dynamics of actin-myosin filaments.

In the present study, we analysed dissemination of squamous carcinoma A431 cells in zebrafish embryos 48 hours after injection. Expression of the *ZEB2* gene, a master regulator of EMT, dramatically activated invasion of A431 cells. Significant changes were observed in the expression pattern of S100 genes with majority of them being down-regulated. In contrast, S100A4 and S100A6 were strongly activated during ZEB2-induced EMT. Silencing of S100A4/A6 affected dissemination A431 cells in Zebrafish embryos highlighting their role in EMT and tumour progression.

This abstract submitted to M5 Biomedical Imaging Conference. University of Nottingham/UK, 09 September 2014

S100A4 binds to the extended and compact forms of nonmuscle myosin in A431 cells undergoing Epithelial Mesenchymal Transition and modulates tumour cell dissemination in Zebrafish embryos

Ban H.K. Alwash[1], Qais I.I. Al Ismael[1], Andrew F. Irvine[1, 2], Natalie S. Allcock[3], Jonathan McDearmid[4], Mohammed El-Mezgueldi[2], Clive R. Bagshaw[2, 5], and Marina Kriajevska[1]

[1]Department of Cancer StudiesUniversity of Leicester, UK
[2]Department of Biochemistry, University of Leicester, UK
[3]Electron Microscopy Facilities, University of Leicester, UK
[4]Department of Biology, University of Leicester, UK
[5]Current address: Department of Chemistry & Biochemistry, University of California at Santa Cruz, USA

Background

S100A4 protein is a mesenchymal marker that is expressed in several forms of human cancer and implicated in regulation of cell motility and Epithelial Mesenchymal Transition (EMT) when cells lose epithelial polarity, scatter and gain mesenchymal phenotype.*In vitro*, S100A4 interacts with several molecular targets including nonmuscle myosin IIA, a major actin-associated motor protein, which is involved in cell motility and cytokinesis.

Observations

We studied expression and function of S100A4 in A431 cells, in which EMT was induced by a transcription factor ZEB2. We show that induction of S100A4 expression in this cell system promoted increased cell motility and dissemination in Zebrafish embryos.

During EMT, cytoskeleton undergoes global reorganisation when the dynamic actin-myosin stress fibres are formed. No muscle myosin II is a chemo-mechanical protein that converts chemical energy into mechanical work. We detected a decrease in ATPase activity of no muscle myosin IIA in cells undergoing EMT, a phenomenon that was largely S100A4-dependent. Using transmission electron microscopy, we demonstrated that S100A4 and no muscle myosin IIA directly interact *in vivo*. Importantly, our approach allowed us to discriminate between different conformations of no muscle myosin within cells. The presence of two major monomeric myosin forms in a solution, compact 10S and extended 6S has been known for many years. However, the *in vivo* relevance of these conformations remains debated. Here we show that cytosol contains 10S and 6S forms of no muscle myosin IIA, and both these forms interact with S100A4.

In conclusion, our work highlights the role of S100A4 in EMT. Our data show that S100A4 is up-regulated by ZEB2 and is implicated in the dynamic regulation myosin filaments by switching the balance towards monomeric myosin.

This abstract submitted to The 6ᵗʰ EMBO meeting advancing the life science Conference. Birmingham/UK, 5-8 September 2015

The Role of S100 Proteins in Epithelial Mesenchymal Transition Pathways in Pancreatic Cancer

Qais I. Al Ismaeel[1], Kees Straatman[2], Jonathan McDearmid[3], and Marina Kriajevska[1]

[1]Department of Cancer Studies, University of Leicester, UK
[2]Centre for Core Biotechnology Sevices, University of Leicester, UK
[3]Department of Neuroscience, Psychology and Behaviour, University of Leicester, UK

Pancreatic cancer (PC) is one of the major causes of cancer-related mortality in the Western world and is characterized by the overall 5-year survival rate around 4%(Hidalgo, 2010). Better understanding of molecular mechanisms responsible for the enhanced PC aggressiveness is required.
S100 family of small Ca-binding proteins has been implicated in the progression of different cancer types. Lineage-tracking study in a mouse model of p53-/-/KRas-induced PC has shown that activation of one of the S100 family members, S100A4, is an initial event in the pathogenesis of PC which is associated with early metastatic dissemination (Rhim et al., 2012).

We analyzed expression of all S100 family members in a collection of PC cell lines. The data obtained and the analyses of publically available databases allowed us to categorize S100 genes in three groups, mesenchymal, epithelial and transitional. Depletion of "mesenchymal" S100 proteins significantly reduced PC cell motility in zebrafish embryo xenograft cell motility assays. We focused on the molecular mechanisms responsible for the up-regulation of mesenchymal S100 genes in the pathogenesis of PC. We have shown that epithelial-mesenchymal transition (EMT) pathways and inflammatory factors such as IL6 coordinate the expression of these genes. Uncoupling inflammatory signaling from EMT and S100 gene activation may have a perspective in PC treatment in the future.

This abstract submitted to Cell signalling and Cancer Therapy. Dubrovnik/ Croatia, 27-31 May 2016 and Athena Swan Conference, University of Leicester/UK, 5 September 2016

References

ABDELMAKSOUD-DAMMAK, R., CHAMTOURI, N., TRIKI, M., SAADALLAH-KALLEL, A., AYADI, W., CHARFI, S., KHABIR, A., AYADI, L., SALLEMI-BOUDAWARA, T. & MOKDAD-GARGOURI, R. 2017. Overexpression of miR-10b in colorectal cancer patients: Correlation with TWIST-1 and E-cadherin expression. *Tumour Biol,* 39**,** 1010428317695916.

ABDELRAHMAN, A. E., ARAFA, S. A. & AHMED, R. A. 2017. Prognostic Value of Twist-1, E-cadherin and EZH2 in Prostate Cancer: An Immunohistochemical Study. *Turk Patoloji Derg*.

AGHAZADEH, S. & YAZDANPARAST, R. 2017. Activation of STAT3/HIF-1alpha/Hes-1 axis promotes Trastuzumab resistance in HER2- overexpressing Breast cancer cells via down-regulation of PTEN. *Biochim Biophys Acta*.

AKIRA, S., NISHIO, Y., INOUE, M., WANG, X. J., WEI, S., MATSUSAKA, T., YOSHIDA, K., SUDO, T., NARUTO, M. & KISHIMOTO, T. 1994. Molecular cloning of APRF, a novel IFN-stimulated gene factor 3 p91-related transcription factor involved in the gp130-mediated signaling pathway. *Cell,* 77**,** 63-71.

ALEXAKIS, N., HALLORAN, C., RARATY, M., GHANEH, P., SUTTON, R. & NEOPTOLEMOS, J. P. 2004. Current standards of surgery for pancreatic cancer. *Br J Surg,* 91**,** 1410-27.

AMBARTSUMIAN, N. & GRIGORIAN, M. 2016. [S100A4, a link between metastasis and inflammation]. *Mol Biol (Mosk),* 50**,** 577-588.

ANELLI, V., VILLEFRANC, J. A., CHHANGAWALA, S., MARTINEZ-MCFALINE, R., RIVA, E., NGUYEN, A., VERMA, A., BAREJA, R., CHEN, Z., SCOGNAMIGLIO, T., ELEMENTO, O. & HOUVRAS, Y. 2017. Oncogenic BRAF disrupts thyroid morphogenesis and function via twist expression. *Elife,* 6.

ANSIEAU, S., BASTID, J., DOREAU, A., MOREL, A. P., BOUCHET, B. P., THOMAS, C., FAUVET, F., PUISIEUX, I., DOGLIONI, C., PICCININ, S., MAESTRO, R., VOELTZEL, T., SELMI, A., VALSESIA-WITTMANN, S., CARON DE FROMENTEL, C. & PUISIEUX, A. 2008. Induction of EMT by twist proteins as a collateral effect of tumor-promoting inactivation of premature senescence. *Cancer Cell,* 14**,** 79-89.

ANTINUCCI, P. & HINDGES, R. 2016. A crystal-clear zebrafish for in vivo imaging. *Sci Rep,* 6**,** 29490.

APARICIO, L. A., BLANCO, M., CASTOSA, R., CONCHA, A., VALLADARES, M., CALVO, L. & FIGUEROA, A. 2015. Clinical implications of epithelial cell plasticity in cancer progression. *Cancer Lett,* 366**,** 1-10.

APPELLA, E. & ANDERSON, C. W. 2001. Post-translational modifications and activation of p53 by genotoxic stresses. *Eur J Biochem,* 268**,** 2764-72.

ARUMUGAM, T., RAMACHANDRAN, V., FOURNIER, K. F., WANG, H., MARQUIS, L., ABBRUZZESE, J. L., GALLICK, G. E., LOGSDON, C. D., MCCONKEY, D. J. & CHOI, W. 2009. Epithelial to mesenchymal transition contributes to drug resistance in pancreatic cancer. *Cancer Res,* 69**,** 5820-8.

AZMI, A. S., BAO, B. & SARKAR, F. H. 2013. Exosomes in cancer development, metastasis, and drug resistance: a comprehensive review. *Cancer Metastasis Rev,* 32**,** 623-42.

BACHET, J. B., MARECHAL, R., DEMETTER, P., BONNETAIN, F., CROS, J., SVRCEK, M., BARDIER-DUPAS, A., HAMMEL, P., SAUVANET, A., LOUVET, C., PAYE, F., VAILLANT, J. C., ANDRE, T., CLOSSET, J., SALMON, I., EMILE, J. F. & VAN LAETHEM, J. L. 2013. S100A2 is a predictive biomarker of adjuvant therapy benefit in pancreatic adenocarcinoma. *Eur J Cancer,* 49**,** 2643-53.

BALIC, J. J., GARBERS, C., ROSE-JOHN, S., YU, L. & JENKINS, B. J. 2017. Interleukin-11-driven gastric tumourigenesis is independent of trans-signalling. *Cytokine,* 92**,** 118-123.

BARAJAS-GOMEZ, B. A., ROSAS-CARRASCO, O., MORALES-ROSALES, S. L., PEDRAZA VAZQUEZ, G., GONZALEZ-PUERTOS, V. Y., JUAREZ-CEDILLO, T., GARCIA-ALVAREZ, J. A., LOPEZ-DIAZGUERRERO, N. E., DAMIAN-MATSUMURA, P., KONIGSBERG, M. & LUNA-LOPEZ, A. 2017. Relationship of inflammatory profile of elderly patients serum and senescence-associated secretory phenotype with human breast cancer cells proliferation: Role of IL6/IL8 ratio. *Cytokine,* 91**,** 13-29.

BARAK, Y., JUVEN, T., HAFFNER, R. & OREN, M. 1993. mdm2 expression is induced by wild type p53 activity. *EMBO J,* 12**,** 461-8.

BARESOVA, P., MUSILOVA, J., PITHA, P. M. & LUBYOVA, B. 2014. p53 tumor suppressor protein stability and transcriptional activity are targeted by Kaposi's sarcoma-associated herpesvirus-encoded viral interferon regulatory factor 3. *Mol Cell Biol,* 34**,** 386-99.

BARRIUSO, J., NAGARAJU, R. & HURLSTONE, A. 2015. Zebrafish: a new companion for translational research in oncology. *Clin Cancer Res,* 21**,** 969-75.

BERGE, G. & MAELANDSMO, G. M. 2011. Evaluation of potential interactions between the metastasis-associated protein S100A4 and the tumor suppressor protein p53. *Amino Acids,* 41**,** 863-73.

BETTUM, I. J., VASILIAUSKAITE, K., NYGAARD, V., CLANCY, T., PETTERSEN, S. J., TENSTAD, E., MAELANDSMO, G. M. & PRASMICKAITE, L. 2014. Metastasis-associated protein S100A4 induces a network of inflammatory cytokines that activate stromal cells to acquire pro-tumorigenic properties. *Cancer Lett,* 344**,** 28-39.

BHARDWAJ, M., SEN, S., SHARMA, A., KASHYAP, S., CHOSDOL, K., PUSHKER, N., BAJAJ, M. S. & BAKHSHI, S. 2015. ZEB2/SIP1 as novel prognostic indicator in eyelid sebaceous gland carcinoma. *Hum Pathol,* 46**,** 1437-42.

BHARTI, R., DEY, G. & MANDAL, M. 2016. Cancer development, chemoresistance, epithelial to mesenchymal transition and stem cells: A snapshot of IL-6 mediated involvement. *Cancer Lett,* 375**,** 51-61.

BHATTACHARYA, S., RAY, R. M. & JOHNSON, L. R. 2005. STAT3-mediated transcription of Bcl-2, Mcl-1 and c-IAP2 prevents apoptosis in polyamine-depleted cells. *Biochem J,* 392**,** 335-44.

BILIMORIA, K. Y., BENTREM, D. J., KO, C. Y., RITCHEY, J., STEWART, A. K., WINCHESTER, D. P. & TALAMONTI, M. S. 2007. Validation of the 6th edition AJCC Pancreatic Cancer Staging System: report from the National Cancer Database. *Cancer,* 110**,** 738-44.

BLACKBURN, J. S. & LANGENAU, D. M. 2014. Zebrafish as a model to assess cancer heterogeneity, progression and relapse. *Dis Model Mech,* 7**,** 755-62.

BOLOS, V., PEINADO, H., PEREZ-MORENO, M. A., FRAGA, M. F., ESTELLER, M. & CANO, A. 2003. The transcription factor Slug represses E-cadherin expression and induces epithelial to mesenchymal transitions: a comparison with Snail and E47 repressors. *J Cell Sci,* 116**,** 499-511.

BOYE, K. & MAELANDSMO, G. M. 2010. S100A4 and metastasis: a small actor playing many roles. *Am J Pathol,* 176**,** 528-35.

BRABLETZ, S., BAJDAK, K., MEIDHOF, S., BURK, U., NIEDERMANN, G., FIRAT, E., WELLNER, U., DIMMLER, A., FALLER, G., SCHUBERT, J. & BRABLETZ, T. 2011. The ZEB1/miR-200 feedback loop controls Notch signalling in cancer cells. *EMBO J,* 30**,** 770-82.

BRESNICK, A. R., WEBER, D. J. & ZIMMER, D. B. 2015. S100 proteins in cancer. *Nat Rev Cancer,* 15**,** 96-109.

BREZNIK, B., MOTALN, H., VITTORI, M., ROTTER, A. & LAH TURNSEK, T. 2017. Mesenchymal stem cells differentially affect the invasion of distinct glioblastoma cell lines. *Oncotarget,* 8**,** 25482-25499.

BRUENDERMAN, E. & MARTIN, R. C., 2ND 2015. A cost analysis of a pancreatic cancer screening protocol in high-risk populations. *Am J Surg,* 210**,** 409-16.

BUNGER, S., LAUBERT, T., ROBLICK, U. J. & HABERMANN, J. K. 2011. Serum biomarkers for improved diagnostic of pancreatic cancer: a current overview. *J Cancer Res Clin Oncol,* 137**,** 375-89.

BUTLER, M. S., ROSHAN-MONIRI, M., HSING, M., LAU, D., KIM, A., YEN, P., MROCZEK, M., NOURI, M., LIEN, S., AXERIO-CILIES, P., DALAL, K., YAU, C., GHAIDI, F., GUO, Y., YAMAZAKI, T., LAWN, S., GLEAVE, M. E., GREGORY-EVANS, C. Y., MCINTOSH, L. P., COX, M. E., RENNIE, P. S. & CHERKASOV, A. 2017. Discovery and characterization of small molecules targeting the DNA-binding ETS domain of ERG in prostate cancer. *Oncotarget.*

CABEZON, T., CELIS, J. E., SKIBSHOJ, I., KLINGELHOFER, J., GRIGORIAN, M., GROMOV, P., RANK, F., MYKLEBUST, J. H., MAELANDSMO, G. M., LUKANIDIN, E. & AMBARTSUMIAN, N. 2007. Expression of S100A4 by a variety of cell types present in the tumor microenvironment of human breast cancer. *Int J Cancer,* 121**,** 1433-44.

CAI, M. Y., LUO, R. Z., CHEN, J. W., PEI, X. Q., LU, J. B., HOU, J. H. & YUN, J. P. 2012a. Overexpression of ZEB2 in peritumoral liver tissue correlates with favorable survival after curative resection of hepatocellular carcinoma. *PLoS One,* 7**,** e32838.

CAI, Z., YANG, F., YU, L., YU, Z., JIANG, L., WANG, Q., YANG, Y., WANG, L., CAO, X. & WANG, J. 2012b. Activated T cell exosomes promote tumor invasion via Fas signaling pathway. *J Immunol,* 188**,** 5954-61.

CAPELLA, C., ALBARELLO, L., CAPELLI, P., SESSA, F. & ZAMBONI, G. 2011. Carcinoma of the exocrine pancreas: the histology report. *Dig Liver Dis,* 43 Suppl 4**,** S282-92.

CARPENTER, R. L. & LO, H. W. 2014. STAT3 Target Genes Relevant to Human Cancers. *Cancers (Basel),* 6**,** 897-925.

CARRIERE, C., YOUNG, A. L., GUNN, J. R., LONGNECKER, D. S. & KORC, M. 2009. Acute pancreatitis markedly accelerates pancreatic cancer progression in mice expressing oncogenic Kras. *Biochem Biophys Res Commun,* 382**,** 561-5.

CASTELLANOS, J. A., MERCHANT, N. B. & NAGATHIHALLI, N. S. 2013. Emerging targets in pancreatic cancer: epithelial-mesenchymal transition and cancer stem cells. *Onco Targets Ther,* 6**,** 1261-1267.

CERVANTES-ARIAS, A., PANG, L. Y. & ARGYLE, D. J. 2013. Epithelial-mesenchymal transition as a fundamental mechanism underlying the cancer phenotype. *Vet Comp Oncol,* 11**,** 169-84.

CHANDRAMOULI, A., MERCADO-PIMENTEL, M. E., HUTCHINSON, A., GIBADULINOVA, A., OLSON, E. R., DICKINSON, S., SHANAS, R., DAVENPORT, J., OWENS, J., BHATTACHARYYA, A. K., REGAN, J. W., PASTOREKOVA, S., ARUMUGAM, T., LOGSDON, C. D. & NELSON, M. A. 2010. The induction of S100p expression by the Prostaglandin E(2) (PGE(2))/EP4 receptor signaling pathway in colon cancer cells. *Cancer Biol Ther,* 10**,** 1056-66.

CHANG, C. J., CHAO, C. H., XIA, W., YANG, J. Y., XIONG, Y., LI, C. W., YU, W. H., REHMAN, S. K., HSU, J. L., LEE, H. H., LIU, M., CHEN, C. T., YU, D. & HUNG, M. C. 2011. p53 regulates epithelial-mesenchymal transition and stem cell properties through modulating miRNAs. *Nat Cell Biol,* 13**,** 317-23.

CHAO, C., HERR, D., CHUN, J. & XU, Y. 2006. Ser18 and 23 phosphorylation is required for p53-dependent apoptosis and tumor suppression. *EMBO J,* 25**,** 2615-22.

CHE, P., YANG, Y., HAN, X., HU, M., SELLERS, J. C., LONDONO-JOSHI, A. I., CAI, G. Q., BUCHSBAUM, D. J., CHRISTEIN, J. D., TANG, Q., CHEN, D., LI, Q., GRIZZLE, W. E., LU, Y. Y. & DING, Q. 2015. S100A4 promotes pancreatic cancer progression through a dual signaling pathway mediated by Src and focal adhesion kinase. *Sci Rep,* 5**,** 8453.

CHEN, H., XU, C., JIN, Q. & LIU, Z. 2014. S100 protein family in human cancer. *Am J Cancer Res,* 4**,** 89-115.

CHEN, H., YUAN, Y., ZHANG, C., LUO, A., DING, F., MA, J., YANG, S., TIAN, Y., TONG, T., ZHAN, Q. & LIU, Z. 2012. Involvement of S100A14 protein in cell invasion by affecting expression and function of matrix metalloproteinase (MMP)-2 via p53-dependent transcriptional regulation. *J Biol Chem,* 287**,** 17109-19.

CHEN, L., GROENEWOUD, A., TULOTTA, C., ZONI, E., KRUITHOF-DE JULIO, M., VAN DER HORST, G., VAN DER PLUIJM, G. & EWA SNAAR-JAGALSKA, B. 2017. A zebrafish xenograft model for studying human cancer stem cells in distant metastasis and therapy response. *Methods Cell Biol,* 138**,** 471-496.

CHEN, S., CHEN, J. Z., ZHANG, J. Q., CHEN, H. X., YAN, M. L., HUANG, L., TIAN, Y. F., CHEN, Y. L. & WANG, Y. D. 2016. Hypoxia induces TWIST-activated epithelial-mesenchymal transition and proliferation of pancreatic cancer cells in vitro and in nude mice. *Cancer Lett,* 383**,** 73-84.

CHEN, W., GAO, Q., HAN, S., PAN, F. & FAN, W. 2015a. The CCL2/CCR2 axis enhances IL-6-induced epithelial-mesenchymal transition by cooperatively activating STAT3-Twist signaling. *Tumour Biol,* 36**,** 973-81.

CHEN, W. H., HOROSZEWICZ, J. S., LEONG, S. S., SHIMANO, T., PENETRANTE, R., SANDERS, W. H., BERJIAN, R., DOUGLASS, H. O., MARTIN, E. W. & CHU, T. M. 1982. Human pancreatic adenocarcinoma: in vitro and in vivo morphology of a new tumor line established from ascites. *In Vitro,* 18**,** 24-34.

CHEN, X., LIU, X., LANG, H., ZHANG, S., LUO, Y. & ZHANG, J. 2015b. S100 calcium-binding protein A6 promotes epithelial-mesenchymal transition through beta-catenin in pancreatic cancer cell line. *PLoS One,* 10**,** e0121319.

CHEN, Z. & HAN, Z. C. 2008. STAT3: a critical transcription activator in angiogenesis. *Med Res Rev,* 28**,** 185-200.

CHENG, Q., CROSS, B., LI, B., CHEN, L., LI, Z. & CHEN, J. 2011. Regulation of MDM2 E3 ligase activity by phosphorylation after DNA damage. *Mol Cell Biol,* 31**,** 4951-63.

CHERNOV, M. V., RAMANA, C. V., ADLER, V. V. & STARK, G. R. 1998. Stabilization and activation of p53 are regulated independently by different phosphorylation events. *Proc Natl Acad Sci U S A,* 95**,** 2284-9.

CHIAVACCI, E., RIZZO, M., PITTO, L., PATELLA, F., EVANGELISTA, M., MARIANI, L. & RAINALDI, G. 2015. The zebrafish/tumor xenograft angiogenesis assay as a tool for screening anti-angiogenic miRNAs. *Cytotechnology,* 67**,** 969-75.

CHIKINA, A. S. & ALEKSANDROVA, A. 2014. [The cellular mechanisms and regulation of metastasis formation]. *Mol Biol (Mosk),* 48**,** 195-213.

CHOMCZYNSKI, P. & SACCHI, N. 2006. The single-step method of RNA isolation by acid guanidinium thiocyanate-phenol-chloroform extraction: twenty-something years on. *Nat Protoc,* 1**,** 581-5.

COHEN, E. N., GAO, H., ANFOSSI, S., MEGO, M., REDDY, N. G., DEBEB, B., GIORDANO, A., TIN, S., WU, Q., GARZA, R. J., CRISTOFANILLI, M., MANI, S. A., CROIX, D. A., UENO, N. T., WOODWARD, W. A., LUTHRA, R., KRISHNAMURTHY, S. & REUBEN, J. M. 2015. Inflammation Mediated Metastasis: Immune Induced Epithelial-To-Mesenchymal Transition in Inflammatory Breast Cancer Cells. *PLoS One,* 10**,** e0132710.

CORCORAN, R. B., CONTINO, G., DESHPANDE, V., TZATSOS, A., CONRAD, C., BENES, C. H., LEVY, D. E., SETTLEMAN, J., ENGELMAN, J. A. & BARDEESY, N. 2011. STAT3 plays a critical role in KRAS-induced pancreatic tumorigenesis. *Cancer Res,* 71**,** 5020-9.

COSTA-SILVA, B., AIELLO, N. M., OCEAN, A. J., SINGH, S., ZHANG, H., THAKUR, B. K., BECKER, A., HOSHINO, A., MARK, M. T., MOLINA, H., XIANG, J., ZHANG, T., THEILEN, T. M., GARCIA-SANTOS, G., WILLIAMS, C., ARARSO, Y., HUANG, Y., RODRIGUES, G., SHEN, T. L., LABORI, K. J., LOTHE, I. M., KURE, E. H., HERNANDEZ, J., DOUSSOT, A., EBBESEN, S. H., GRANDGENETT, P. M., HOLLINGSWORTH, M. A., JAIN, M., MALLYA, K., BATRA, S. K., JARNAGIN, W. R., SCHWARTZ, R. E., MATEI, I., PEINADO, H., STANGER, B. Z., BROMBERG, J. & LYDEN, D. 2015. Pancreatic cancer exosomes initiate pre-metastatic niche formation in the liver. *Nat Cell Biol,* 17**,** 816-26.

COWLEY, M. J., CHANG, D. K., PAJIC, M., JOHNS, A. L., WADDELL, N., GRIMMOND, S. M. & BIANKIN, A. V. 2013. Understanding pancreatic cancer genomes. *J Hepatobiliary Pancreat Sci.*

CRNOGORAC-JURCEVIC, T., MISSIAGLIA, E., BLAVERI, E., GANGESWARAN, R., JONES, M., TERRIS, B., COSTELLO, E., NEOPTOLEMOS, J. P. & LEMOINE, N. R. 2003. Molecular alterations in pancreatic carcinoma: expression profiling shows that dysregulated expression of S100 genes is highly prevalent. *J Pathol,* 201**,** 63-74.

CROSS, S. S., HAMDY, F. C., DELOULME, J. C. & REHMAN, I. 2005. Expression of S100 proteins in normal human tissues and common cancers using tissue microarrays: S100A6, S100A8, S100A9 and S100A11 are all overexpressed in common cancers. *Histopathology,* 46**,** 256-69.

DAHLMANN, M., OKHRIMENKO, A., MARCINKOWSKI, P., OSTERLAND, M., HERRMANN, P., SMITH, J., HEIZMANN, C. W., SCHLAG, P. M. & STEIN, U. 2014. RAGE mediates S100A4-induced cell motility via MAPK/ERK and hypoxia signaling and is a prognostic biomarker for human colorectal cancer metastasis. *Oncotarget,* 5**,** 3220-33.

DAKHEL, S., PADILLA, L., ADAN, J., MASA, M., MARTINEZ, J. M., ROQUE, L., COLL, T., HERVAS, R., CALVIS, C., MESSEGUER, R., MITJANS, F. & HERNANDEZ, J. L. 2014. S100P antibody-mediated therapy as a new promising strategy for the treatment of pancreatic cancer. *Oncogenesis,* 3**,** e92.

DANGI-GARIMELLA, S., KRANTZ, S. B., SHIELDS, M. A., GRIPPO, P. J. & MUNSHI, H. G. 2012. Epithelial-mesenchymal transition and pancreatic cancer progression. *In:* GRIPPO, P. J. & MUNSHI, H. G. (eds.) *Pancreatic Cancer and Tumor Microenvironment.* Trivandrum (India): Transworld Research Network

Transworld Research Network.

DEBIDDA, M., WANG, L., ZANG, H., POLI, V. & ZHENG, Y. 2005. A role of STAT3 in Rho GTPase-regulated cell migration and proliferation. *J Biol Chem,* 280**,** 17275-85.

DEMORY BECKLER, M., HIGGINBOTHAM, J. N., FRANKLIN, J. L., HAM, A. J., HALVEY, P. J., IMASUEN, I. E., WHITWELL, C., LI, M., LIEBLER, D. C. & COFFEY, R. J. 2013. Proteomic analysis of exosomes from mutant KRAS colon cancer cells identifies intercellular transfer of mutant KRAS. *Mol Cell Proteomics,* 12**,** 343-55.

DENLEY, S. M., JAMIESON, N. B., MCCALL, P., OIEN, K. A., MORTON, J. P., CARTER, C. R., EDWARDS, J. & MCKAY, C. J. 2013. Activation of the IL-6R/Jak/stat pathway is associated with a poor outcome in resected pancreatic ductal adenocarcinoma. *J Gastrointest Surg,* 17**,** 887-98.

DENZER, K., KLEIJMEER, M. J., HEIJNEN, H. F., STOORVOGEL, W. & GEUZE, H. J. 2000. Exosome: from internal vesicle of the multivesicular body to intercellular signaling device. *J Cell Sci,* 113 Pt 19**,** 3365-74.

DIEPENBRUCK, M. & CHRISTOFORI, G. 2016. Epithelial-mesenchymal transition (EMT) and metastasis: yes, no, maybe? *Curr Opin Cell Biol,* 43**,** 7-13.

DIGIUSEPPE, J. A., HRUBAN, R. H., GOODMAN, S. N., POLAK, M., VAN DEN BERG, F. M., ALLISON, D. C., CAMERON, J. L. & OFFERHAUS, G. J. 1994. Overexpression of p53 protein in adenocarcinoma of the pancreas. *Am J Clin Pathol,* 101**,** 684-8.

DMYTRIYEVA, O., PANKRATOVA, S., OWCZAREK, S., SONN, K., SOROKA, V., RIDLEY, C. M., MARSOLAIS, A., LOPEZ-HOYOS, M., AMBARTSUMIAN, N., LUKANIDIN, E., BOCK, E., BEREZIN, V. & KIRYUSHKO, D. 2012. The metastasis-promoting S100A4 protein confers neuroprotection in brain injury. *Nat Commun,* 3**,** 1197.

DONG, P., KARAAYVAZ, M., JIA, N., KANEUCHI, M., HAMADA, J., WATARI, H., SUDO, S., JU, J. & SAKURAGI, N. 2013. Mutant p53 gain-of-function induces epithelial-mesenchymal transition through modulation of the miR-130b-ZEB1 axis. *Oncogene,* 32**,** 3286-95.

DORNAN, D., WERTZ, I., SHIMIZU, H., ARNOTT, D., FRANTZ, G. D., DOWD, P., O'ROURKE, K., KOEPPEN, H. & DIXIT, V. M. 2004. The ubiquitin ligase COP1 is a critical negative regulator of p53. *Nature,* 429**,** 86-92.

DOWEN, S. E., CRNOGORAC-JURCEVIC, T., GANGESWARAN, R., HANSEN, M., ELORANTA, J. J., BHAKTA, V., BRENTNALL, T. A., LUTTGES, J., KLOPPEL, G. & LEMOINE, N. R. 2005. Expression of S100P and its novel binding partner S100PBPR in early pancreatic cancer. *Am J Pathol,* 166**,** 81-92.

DRUCKER, B. J., MARINCOLA, F. M., SIAO, D. Y., DONLON, T. A., BANGS, C. D. & HOLDER, W. D., JR. 1988. A new human pancreatic carcinoma cell line developed for adoptive immunotherapy studies with lymphokine-activated killer cells in nude mice. *In Vitro Cell Dev Biol,* 24**,** 1179-87.

DU, M., WANG, G., ISMAIL, T. M., GROSS, S., FERNIG, D. G., BARRACLOUGH, R. & RUDLAND, P. S. 2012. S100P dissociates myosin IIA filaments and focal adhesion sites to reduce cell adhesion and enhance cell migration. *J Biol Chem,* 287**,** 15330-44.

DUFFY, M. J., STURGEON, C., LAMERZ, R., HAGLUND, C., HOLUBEC, V. L., KLAPDOR, R., NICOLINI, A., TOPOLCAN, O. & HEINEMANN, V. 2010.

Tumor markers in pancreatic cancer: a European Group on Tumor Markers (EGTM) status report. *Ann Oncol,* 21**,** 441-7.

DUMAZ, N. & MEEK, D. W. 1999. Serine15 phosphorylation stimulates p53 transactivation but does not directly influence interaction with HDM2. *EMBO J,* 18**,** 7002-10.

EDME, N., DOWNWARD, J., THIERY, J. P. & BOYER, B. 2002. Ras induces NBT-II epithelial cell scattering through the coordinate activities of Rac and MAPK pathways. *J Cell Sci,* 115**,** 2591-601.

EHRCHEN, J. M., SUNDERKOTTER, C., FOELL, D., VOGL, T. & ROTH, J. 2009. The endogenous Toll-like receptor 4 agonist S100A8/S100A9 (calprotectin) as innate amplifier of infection, autoimmunity, and cancer. *J Leukoc Biol,* 86**,** 557-66.

EL-NAGGAR, A. M., VEINOTTE, C. J., CHENG, H., GRUNEWALD, T. G., NEGRI, G. L., SOMASEKHARAN, S. P., CORKERY, D. P., TIRODE, F., MATHERS, J., KHAN, D., KYLE, A. H., BAKER, J. H., LEPARD, N. E., MCKINNEY, S., HAJEE, S., BOSILJCIC, M., LEPRIVIER, G., TOGNON, C. E., MINCHINTON, A. I., BENNEWITH, K. L., DELATTRE, O., WANG, Y., DELLAIRE, G., BERMAN, J. N. & SORENSEN, P. H. 2015. Translational Activation of HIF1alpha by YB-1 Promotes Sarcoma Metastasis. *Cancer Cell,* 27**,** 682-97.

ELDER, J. T. & ZHAO, X. 2002. Evidence for local control of gene expression in the epidermal differentiation complex. *Exp Dermatol,* 11**,** 406-12.

ELLETT, F., PASE, L., HAYMAN, J. W., ANDRIANOPOULOS, A. & LIESCHKE, G. J. 2011. mpeg1 promoter transgenes direct macrophage-lineage expression in zebrafish. *Blood,* 117**,** e49-56.

ERNST, M. & PUTOCZKI, T. L. 2014. Molecular pathways: IL11 as a tumor-promoting cytokine-translational implications for cancers. *Clin Cancer Res,* 20**,** 5579-88.

FELIX, K. & GAIDA, M. M. 2016. Neutrophil-Derived Proteases in the Microenvironment of Pancreatic Cancer -Active Players in Tumor Progression. *Int J Biol Sci,* 12**,** 302-13.

FENG, G., XU, X., YOUSSEF, E. M. & LOTAN, R. 2001. Diminished expression of S100A2, a putative tumor suppressor, at early stage of human lung carcinogenesis. *Cancer Res,* 61**,** 7999-8004.

FERNANDEZ-FERNANDEZ, M. R., RUTHERFORD, T. J. & FERSHT, A. R. 2008. Members of the S100 family bind p53 in two distinct ways. *Protein Sci,* 17**,** 1663-70.

FOELL, D., WITTKOWSKI, H., VOGL, T. & ROTH, J. 2007. S100 proteins expressed in phagocytes: a novel group of damage-associated molecular pattern molecules. *J Leukoc Biol,* 81**,** 28-37.

FORD, H. L., SILVER, D. L., KACHAR, B., SELLERS, J. R. & ZAIN, S. B. 1997. Effect of Mts1 on the structure and activity of nonmuscle myosin II. *Biochemistry,* 36**,** 16321-7.

FRANCO-BARRAZA, J., VALDIVIA-SILVA, J. E., ZAMUDIO-MEZA, H., CASTILLO, A., GARCIA-ZEPEDA, E. A., BENITEZ-BRIBIESCA, L. &

MEZA, I. 2010. Actin cytoskeleton participation in the onset of IL-1beta induction of an invasive mesenchymal-like phenotype in epithelial MCF-7 cells. *Arch Med Res,* 41**,** 170-81.

FRIXEN, U. H., BEHRENS, J., SACHS, M., EBERLE, G., VOSS, B., WARDA, A., LOCHNER, D. & BIRCHMEIER, W. 1991. E-cadherin-mediated cell-cell adhesion prevents invasiveness of human carcinoma cells. *J Cell Biol,* 113**,** 173-85.

FU, H., YANG, H., ZHANG, X. & XU, W. 2016. The emerging roles of exosomes in tumor-stroma interaction. *J Cancer Res Clin Oncol,* 142**,** 1897-907.

FUKUDA, A., WANG, S. C., MORRIS, J. P. T., FOLIAS, A. E., LIOU, A., KIM, G. E., AKIRA, S., BOUCHER, K. M., FIRPO, M. A., MULVIHILL, S. J. & HEBROK, M. 2011. Stat3 and MMP7 contribute to pancreatic ductal adenocarcinoma initiation and progression. *Cancer Cell,* 19**,** 441-55.

FURTEK, S. L., BACKOS, D. S., MATHESON, C. J. & REIGAN, P. 2016. Strategies and Approaches of Targeting STAT3 for Cancer Treatment. *ACS Chem Biol,* 11**,** 308-18.

FURUKAWA, T., DUGUID, W. P., ROSENBERG, L., VIALLET, J., GALLOWAY, D. A. & TSAO, M. S. 1996. Long-term culture and immortalization of epithelial cells from normal adult human pancreatic ducts transfected by the E6E7 gene of human papilloma virus 16. *Am J Pathol,* 148**,** 1763-70.

GALVAN, J. A., ZLOBEC, I., WARTENBERG, M., LUGLI, A., GLOOR, B., PERREN, A. & KARAMITOPOULOU, E. 2015. Expression of E-cadherin repressors SNAIL, ZEB1 and ZEB2 by tumour and stromal cells influences tumour-budding phenotype and suggests heterogeneity of stromal cells in pancreatic cancer. *Br J Cancer,* 112**,** 1944-50.

GARBERS, C., HERMANNS, H. M., SCHAPER, F., MULLER-NEWEN, G., GROTZINGER, J., ROSE-JOHN, S. & SCHELLER, J. 2012. Plasticity and cross-talk of interleukin 6-type cytokines. *Cytokine Growth Factor Rev,* 23**,** 85-97.

GARRETT, S. C., VARNEY, K. M., WEBER, D. J. & BRESNICK, A. R. 2006. S100A4, a mediator of metastasis. *J Biol Chem,* 281**,** 677-80.

GEBHARDT, C., RIEHL, A., DURCHDEWALD, M., NEMETH, J., FURSTENBERGER, G., MULLER-DECKER, K., ENK, A., ARNOLD, B., BIERHAUS, A., NAWROTH, P. P., HESS, J. & ANGEL, P. 2008. RAGE signaling sustains inflammation and promotes tumor development. *J Exp Med,* 205**,** 275-85.

GHOTRA, V. P., HE, S., VAN DER HORST, G., NIJHOFF, S., DE BONT, H., LEKKERKERKER, A., JANSSEN, R., JENSTER, G., VAN LEENDERS, G. J., HOOGLAND, A. M., VERHOEF, E. I., BARANSKI, Z., XIONG, J., VAN DE WATER, B., VAN DER PLUIJM, G., SNAAR-JAGALSKA, B. E. & DANEN, E. H. 2015. SYK is a candidate kinase target for the treatment of advanced prostate cancer. *Cancer Res,* 75**,** 230-40.

GILLILAND, T. M., VILLAFANE-FERRIOL, N., SHAH, K. P., SHAH, R. M., TRAN CAO, H. S., MASSARWEH, N. N., SILBERFEIN, E. J., CHOI, E. A., HSU, C.,

MCELHANY, A. L., BARAKAT, O., FISHER, W. & VAN BUREN, G. 2017. Nutritional and Metabolic Derangements in Pancreatic Cancer and Pancreatic Resection. *Nutrients,* 9.

GIOVANNETTI, E., VAN DER BORDEN, C. L., FRAMPTON, A. E., ALI, A., FIRUZI, O. & PETERS, G. J. 2017. Never let it go: Stopping key mechanisms underlying metastasis to fight pancreatic cancer. *Semin Cancer Biol.*

GLASER, R., HARDER, J., LANGE, H., BARTELS, J., CHRISTOPHERS, E. & SCHRODER, J. M. 2005. Antimicrobial psoriasin (S100A7) protects human skin from Escherichia coli infection. *Nat Immunol,* 6**,** 57-64.

GNOSA, S., CAPODANNO, A., MURTHY, R. V., JENSEN, L. D. & SUN, X. F. 2016. AEG-1 knockdown in colon cancer cell lines inhibits radiation-enhanced migration and invasion in vitro and in a novel in vivo zebrafish model. *Oncotarget,* 7**,** 81634-81644.

GOLITSINA, N. L., KORDOWSKA, J., WANG, C. L. & LEHRER, S. S. 1996. Ca2+-dependent binding of calcyclin to muscle tropomyosin. *Biochem Biophys Res Commun,* 220**,** 360-5.

GOSWAMI, K. K., SARKAR, M., GHOSH, S., SAHA, A., GHOSH, T., GUHA, I., BARIK, S., BANERJEE, S., ROY, S., BOSE, A., DASGUPTA, P. & BARAL, R. 2016. Neem leaf glycoprotein regulates function of tumor associated M2 macrophages in hypoxic tumor core: Critical role of IL-10/STAT3 signaling. *Mol Immunol,* 80**,** 1-10.

GOYETTE, J. & GECZY, C. L. 2011. Inflammation-associated S100 proteins: new mechanisms that regulate function. *Amino Acids,* 41**,** 821-42.

GRANDIS, J. R., DRENNING, S. D., CHAKRABORTY, A., ZHOU, M. Y., ZENG, Q., PITT, A. S. & TWEARDY, D. J. 1998. Requirement of Stat3 but not Stat1 activation for epidermal growth factor receptor- mediated cell growth In vitro. *J Clin Invest,* 102**,** 1385-92.

GRIGORIAN, M., ANDRESEN, S., TULCHINSKY, E., KRIAJEVSKA, M., CARLBERG, C., KRUSE, C., COHN, M., AMBARTSUMIAN, N., CHRISTENSEN, A., SELIVANOVA, G. & LUKANIDIN, E. 2001. Tumor suppressor p53 protein is a new target for the metastasis-associated Mts1/S100A4 protein: functional consequences of their interaction. *J Biol Chem,* 276**,** 22699-708.

GROSS, J. C., CHAUDHARY, V., BARTSCHERER, K. & BOUTROS, M. 2012. Active Wnt proteins are secreted on exosomes. *Nat Cell Biol,* 14**,** 1036-45.

GROSS, S. R., SIN, C. G., BARRACLOUGH, R. & RUDLAND, P. S. 2014. Joining S100 proteins and migration: for better or for worse, in sickness and in health. *Cell Mol Life Sci,* 71**,** 1551-79.

GUERRA, C., SCHUHMACHER, A. J., CANAMERO, M., GRIPPO, P. J., VERDAGUER, L., PEREZ-GALLEGO, L., DUBUS, P., SANDGREN, E. P. & BARBACID, M. 2007. Chronic pancreatitis is essential for induction of pancreatic ductal adenocarcinoma by K-Ras oncogenes in adult mice. *Cancer Cell,* 11**,** 291-302.

GUO, M., WEI, H., HU, J., SUN, S., LONG, J. & WANG, X. 2015. U0126 inhibits pancreatic cancer progression via the KRAS signaling pathway in a zebrafish xenotransplantation model. *Oncol Rep,* 34**,** 699-706.

GUPTA, G. P. & MASSAGUE, J. 2006. Cancer metastasis: building a framework. *Cell,* 127**,** 679-95.

HAHN, S. A., GREENHALF, B., ELLIS, I., SINA-FREY, M., RIEDER, H., KORTE, B., GERDES, B., KRESS, R., ZIEGLER, A., RAEBURN, J. A., CAMPRA, D., GRUTZMANN, R., REHDER, H., ROTHMUND, M., SCHMIEGEL, W., NEOPTOLEMOS, J. P. & BARTSCH, D. K. 2003. BRCA2 germline mutations in familial pancreatic carcinoma. *J Natl Cancer Inst,* 95**,** 214-21.

HALDI, M., TON, C., SENG, W. L. & MCGRATH, P. 2006. Human melanoma cells transplanted into zebrafish proliferate, migrate, produce melanin, form masses and stimulate angiogenesis in zebrafish. *Angiogenesis,* 9**,** 139-51.

HAMADA, S., MASAMUNE, A., YOSHIDA, N., TAKIKAWA, T. & SHIMOSEGAWA, T. 2016. IL-6/STAT3 Plays a Regulatory Role in the Interaction Between Pancreatic Stellate Cells and Cancer Cells. *Dig Dis Sci,* 61**,** 1561-71.

HAN, Z., WANG, X., MA, L., CHEN, L., XIAO, M., HUANG, L., CAO, Y., BAI, J., MA, D., ZHOU, J. & HONG, Z. 2014. Inhibition of STAT3 signaling targets both tumor-initiating and differentiated cell populations in prostate cancer. *Oncotarget,* 5**,** 8416-28.

HANAHAN, D. & WEINBERG, R. A. 2011. Hallmarks of cancer: the next generation. *Cell,* 144**,** 646-74.

HANDRA-LUCA, A., HONG, S. M., WALTER, K., WOLFGANG, C., HRUBAN, R. & GOGGINS, M. 2011. Tumour epithelial Vimentin expression and outcome of pancreatic ductal adenocarcinomas. *Br J Cancer,* 104**,** 1296-302.

HANRAHAN, K., O'NEILL, A., PRENCIPE, M., BUGLER, J., MURPHY, L., FABRE, A., PUHR, M., CULIG, Z., MURPHY, K. & WATSON, R. W. 2017. The role of epithelial-mesenchymal transition drivers ZEB1 and ZEB2 in mediating docetaxel-resistant prostate cancer. *Mol Oncol,* 11**,** 251-265.

HARRIS, S. L. & LEVINE, A. J. 2005. The p53 pathway: positive and negative feedback loops. *Oncogene,* 24**,** 2899-908.

HAUPT, Y., MAYA, R., KAZAZ, A. & OREN, M. 1997. Mdm2 promotes the rapid degradation of p53. *Nature,* 387**,** 296-9.

HE, M., QIN, H., POON, T. C., SZE, S. C., DING, X., CO, N. N., NGAI, S. M., CHAN, T. F. & WONG, N. 2015. Hepatocellular carcinoma-derived exosomes promote motility of immortalized hepatocyte through transfer of oncogenic proteins and RNAs. *Carcinogenesis,* 36**,** 1008-18.

HEIZMANN, C. W., FRITZ, G. & SCHAFER, B. W. 2002. S100 proteins: structure, functions and pathology. *Front Biosci,* 7**,** d1356-68.

HERWIG, N., BELTER, B., WOLF, S., HAASE-KOHN, C. & PIETZSCH, J. 2016. Interaction of extracellular S100A4 with RAGE prompts prometastatic activation of A375 melanoma cells. *J Cell Mol Med,* 20**,** 825-35.

HEZEL, A. F., KIMMELMAN, A. C., STANGER, B. Z., BARDEESY, N. & DEPINHO, R. A. 2006. Genetics and biology of pancreatic ductal adenocarcinoma. *Genes Dev,* 20**,** 1218-49.

HIDALGO, M. 2010. Pancreatic cancer. *N Engl J Med,* 362**,** 1605-17.

HIDESHIMA, T., NAKAMURA, N., CHAUHAN, D. & ANDERSON, K. C. 2001. Biologic sequelae of interleukin-6 induced PI3-K/Akt signaling in multiple myeloma. *Oncogene,* 20**,** 5991-6000.

HIGASHIKAWA, K., YONEDA, S., TOBIUME, K., TAKI, M., SHIGEISHI, H. & KAMATA, N. 2007. Snail-induced down-regulation of DeltaNp63alpha acquires invasive phenotype of human squamous cell carcinoma. *Cancer Res,* 67**,** 9207-13.

HILL, A. J., TERAOKA, H., HEIDEMAN, W. & PETERSON, R. E. 2005. Zebrafish as a model vertebrate for investigating chemical toxicity. *Toxicol Sci,* 86**,** 6-19.

HINGORANI, S. R., PETRICOIN, E. F., MAITRA, A., RAJAPAKSE, V., KING, C., JACOBETZ, M. A., ROSS, S., CONRADS, T. P., VEENSTRA, T. D., HITT, B. A., KAWAGUCHI, Y., JOHANN, D., LIOTTA, L. A., CRAWFORD, H. C., PUTT, M. E., JACKS, T., WRIGHT, C. V., HRUBAN, R. H., LOWY, A. M. & TUVESON, D. A. 2003. Preinvasive and invasive ductal pancreatic cancer and its early detection in the mouse. *Cancer Cell,* 4**,** 437-50.

HIRATSUKA, S., WATANABE, A., ABURATANI, H. & MARU, Y. 2006. Tumour-mediated upregulation of chemoattractants and recruitment of myeloid cells predetermines lung metastasis. *Nat Cell Biol,* 8**,** 1369-75.

HOLLSTEIN, M., RICE, K., GREENBLATT, M. S., SOUSSI, T., FUCHS, R., SORLIE, T., HOVIG, E., SMITH-SORENSEN, B., MONTESANO, R. & HARRIS, C. C. 1994. Database of p53 gene somatic mutations in human tumors and cell lines. *Nucleic Acids Res,* 22**,** 3551-5.

HOLMER, R., GOUMAS, F. A., WAETZIG, G. H., ROSE-JOHN, S. & KALTHOFF, H. 2014. Interleukin-6: a villain in the drama of pancreatic cancer development and progression. *Hepatobiliary Pancreat Dis Int,* 13**,** 371-80.

HONDA, R., TANAKA, H. & YASUDA, H. 1997. Oncoprotein MDM2 is a ubiquitin ligase E3 for tumor suppressor p53. *FEBS Lett,* 420**,** 25-7.

HONG, S. M., PARK, J. Y., HRUBAN, R. H. & GOGGINS, M. 2011. Molecular signatures of pancreatic cancer. *Arch Pathol Lab Med,* 135**,** 716-27.

HOTARY, K., LI, X. Y., ALLEN, E., STEVENS, S. L. & WEISS, S. J. 2006. A cancer cell metalloprotease triad regulates the basement membrane transmigration program. *Genes Dev,* 20**,** 2673-86.

HOTZ, B., ARNDT, M., DULLAT, S., BHARGAVA, S., BUHR, H. J. & HOTZ, H. G. 2007. Epithelial to mesenchymal transition: expression of the regulators snail, slug, and twist in pancreatic cancer. *Clin Cancer Res,* 13**,** 4769-76.

HOWE, K., CLARK, M. D., TORROJA, C. F., TORRANCE, J., BERTHELOT, C., MUFFATO, M., COLLINS, J. E., HUMPHRAY, S., MCLAREN, K., MATTHEWS, L., MCLAREN, S., SEALY, I., CACCAMO, M., CHURCHER, C., SCOTT, C., BARRETT, J. C., KOCH, R., RAUCH, G. J., WHITE, S.,

CHOW, W., KILIAN, B., QUINTAIS, L. T., GUERRA-ASSUNCAO, J. A., ZHOU, Y., GU, Y., YEN, J., VOGEL, J. H., EYRE, T., REDMOND, S., BANERJEE, R., CHI, J., FU, B., LANGLEY, E., MAGUIRE, S. F., LAIRD, G. K., LLOYD, D., KENYON, E., DONALDSON, S., SEHRA, H., ALMEIDA-KING, J., LOVELAND, J., TREVANION, S., JONES, M., QUAIL, M., WILLEY, D., HUNT, A., BURTON, J., SIMS, S., MCLAY, K., PLUMB, B., DAVIS, J., CLEE, C., OLIVER, K., CLARK, R., RIDDLE, C., ELLIOT, D., THREADGOLD, G., HARDEN, G., WARE, D., BEGUM, S., MORTIMORE, B., KERRY, G., HEATH, P., PHILLIMORE, B., TRACEY, A., CORBY, N., DUNN, M., JOHNSON, C., WOOD, J., CLARK, S., PELAN, S., GRIFFITHS, G., SMITH, M., GLITHERO, R., HOWDEN, P., BARKER, N., LLOYD, C., STEVENS, C., HARLEY, J., HOLT, K., PANAGIOTIDIS, G., LOVELL, J., BEASLEY, H., HENDERSON, C., GORDON, D., AUGER, K., WRIGHT, D., COLLINS, J., RAISEN, C., DYER, L., LEUNG, K., ROBERTSON, L., AMBRIDGE, K., LEONGAMORNLERT, D., MCGUIRE, S., GILDERTHORP, R., GRIFFITHS, C., MANTHRAVADI, D., NICHOL, S., BARKER, G., et al. 2013. The zebrafish reference genome sequence and its relationship to the human genome. *Nature,* 496**,** 498-503.

HOWLETT, M., MENHENIOTT, T. R., JUDD, L. M. & GIRAUD, A. S. 2009. Cytokine signalling via gp130 in gastric cancer. *Biochim Biophys Acta,* 1793**,** 1623-33.

HRUBAN, R. H., GOGGINS, M., PARSONS, J. & KERN, S. E. 2000. Progression model for pancreatic cancer. *Clin Cancer Res,* 6**,** 2969-72.

HUA, T., LIU, S., XIN, X., CAI, L., SHI, R., CHI, S., FENG, D. & WANG, H. 2016. S100A4 promotes endometrial cancer progress through epithelial-mesenchymal transition regulation. *Oncol Rep,* 35**,** 3419-26.

HUANG, C., JIANG, T., ZHU, L., LIU, J., CAO, J., HUANG, K. J. & QIU, Z. J. 2011. STAT3-targeting RNA interference inhibits pancreatic cancer angiogenesis in vitro and in vivo. *Int J Oncol,* 38**,** 1637-44.

HUANG, S., ZHENG, J., HUANG, Y., SONG, L., YIN, Y., OU, D., HE, S., CHEN, X. & OUYANG, X. 2016a. Impact of S100A4 Expression on Clinicopathological Characteristics and Prognosis in Pancreatic Cancer: A Meta-Analysis. *Dis Markers,* 2016**,** 8137378.

HUANG, W. J., WU, L. J., MIN, Z. C., XU, L. T., GUO, C. M., CHEN, Z. P., LOU, X. J., XU, B. & LV, B. D. 2016b. Interleukin-6 -572G/C polymorphism and prostate cancer susceptibility. *Genet Mol Res,* 15.

HUGO, H., ACKLAND, M. L., BLICK, T., LAWRENCE, M. G., CLEMENTS, J. A., WILLIAMS, E. D. & THOMPSON, E. W. 2007. Epithelial--mesenchymal and mesenchymal--epithelial transitions in carcinoma progression. *J Cell Physiol,* 213**,** 374-83.

HUNG, A. C., LO, S., HOU, M. F., LEE, Y. C., TSAI, C. H., CHEN, Y. Y., LIU, W., SU, Y. H., LO, Y. H., WANG, C. H., WU, S. C., HSIEH, Y. C., HU, S. C., TAI, M. H., WANG, Y. M. & YUAN, S. S. 2016. Extracellular Visfatin-Promoted Malignant Behavior in Breast Cancer Is Mediated Through c-Abl and STAT3 Activation. *Clin Cancer Res,* 22**,** 4478-90.

HUNTER, K. D., PARKINSON, E. K. & HARRISON, P. R. 2005. Profiling early head and neck cancer. *Nat Rev Cancer,* 5**,** 127-35.

HURD, M. W., DEBRUYNE, J., STRAUME, M. & CAHILL, G. M. 1998. Circadian rhythms of locomotor activity in zebrafish. *Physiol Behav,* 65**,** 465-72.

HUSTINX, S. R., CAO, D., MAITRA, A., SATO, N., MARTIN, S. T., SUDHIR, D., IACOBUZIO-DONAHUE, C., CAMERON, J. L., YEO, C. J., KERN, S. E., GOGGINS, M., MOLLENHAUER, J., PANDEY, A. & HRUBAN, R. H. 2004. Differentially expressed genes in pancreatic ductal adenocarcinomas identified through serial analysis of gene expression. *Cancer Biol Ther,* 3**,** 1254-61.

ICHIKAWA, M., WILLIAMS, R., WANG, L., VOGL, T. & SRIKRISHNA, G. 2011. S100A8/A9 activate key genes and pathways in colon tumor progression. *Mol Cancer Res,* 9**,** 133-48.

ILIC, M. & ILIC, I. 2016. Epidemiology of pancreatic cancer. *World J Gastroenterol,* 22**,** 9694-9705.

ITOH, M., MURATA, T., SUZUKI, T., SHINDOH, M., NAKAJIMA, K., IMAI, K. & YOSHIDA, K. 2006. Requirement of STAT3 activation for maximal collagenase-1 (MMP-1) induction by epidermal growth factor and malignant characteristics in T24 bladder cancer cells. *Oncogene,* 25**,** 1195-204.

ITOU, J., TANAKA, S., LI, W., IIDA, A., SEHARA-FUJISAWA, A., SATO, F. & TOI, M. 2017. The Sal-like 4 - integrin alpha6beta1 network promotes cell migration for metastasis via activation of focal adhesion dynamics in basal-like breast cancer cells. *Biochim Biophys Acta,* 1864**,** 76-88.

JAISWAL, J. K., LAURITZEN, S. P., SCHEFFER, L., SAKAGUCHI, M., BUNKENBORG, J., SIMON, S. M., KALLUNKI, T., JAATTELA, M. & NYLANDSTED, J. 2014. S100A11 is required for efficient plasma membrane repair and survival of invasive cancer cells. *Nat Commun,* 5**,** 3795.

JENNDAHL, L. E., ISAKSON, P. & BAECKSTROM, D. 2005. c-erbB2-induced epithelial-mesenchymal transition in mammary epithelial cells is suppressed by cell-cell contact and initiated prior to E-cadherin downregulation. *Int J Oncol,* 27**,** 439-48.

JI, Y. F., HUANG, H., JIANG, F., NI, R. Z. & XIAO, M. B. 2014. S100 family signaling network and related proteins in pancreatic cancer (Review). *Int J Mol Med,* 33**,** 769-76.

JIAN, L., ZHIHONG, W., LIUXING, W. & QINGXIA, F. 2015. [Role of S100A4 in the epithelial-mesenchymal transition of esophageal squamous cell carcinoma and its molecular mechanism]. *Zhonghua Zhong Liu Za Zhi,* 37**,** 258-65.

JIANG, C., MASOOD, M., RASUL, A., WEI, W., WANG, Y., ALI, M., MUSTAQEEM, M., LI, J. & LI, X. 2017a. Altholactone Inhibits NF-kappaB and STAT3 Activation and Induces Reactive Oxygen Species-Mediated Apoptosis in Prostate Cancer DU145 Cells. *Molecules,* 22.

JIANG, W., ZHAO, S., JIANG, X., ZHANG, E., HU, G., HU, B., ZHENG, P., XIAO, J., LU, Z., LU, Y., NI, J., CHEN, C., WANG, X., YANG, L. & WAN, R. 2016. The

circadian clock gene Bmal1 acts as a potential anti-oncogene in pancreatic cancer by activating the p53 tumor suppressor pathway. *Cancer Lett,* 371**,** 314-25.

JIANG, X., GUO, D., LI, W., YU, T., ZHOU, J. & GONG, J. 2017b. Combination Twist1 and CA15-3 in axillary lymph nodes for breast cancer prognosis. *Mol Med Rep,* 15**,** 1123-1134.

JIANG, Y. X., YANG, S. W., LI, P. A., LUO, X., LI, Z. Y., HAO, Y. X. & YU, P. W. 2017c. The promotion of the transformation of quiescent gastric cancer stem cells by IL-17 and the underlying mechanisms. *Oncogene,* 36**,** 1256-1264.

JIANG, Z., JONES, R., LIU, J. C., DENG, T., ROBINSON, T., CHUNG, P. E., WANG, S., HERSCHKOWITZ, J. I., EGAN, S. E., PEROU, C. M. & ZACKSENHAUS, E. 2011. RB1 and p53 at the crossroad of EMT and triple-negative breast cancer. *Cell Cycle,* 10**,** 1563-70.

JIANWEI, Z., QI, L., QUANQUAN, X., TIANEN, W. & QINGWEI, W. 2017. TMPRSS4 Upregulates TWIST1 Expression through STAT3 Activation to Induce Prostate Cancer Cell Migration. *Pathol Oncol Res*.

JOHNSTONE, C. N., CHAND, A., PUTOCZKI, T. L. & ERNST, M. 2015. Emerging roles for IL-11 signaling in cancer development and progression: Focus on breast cancer. *Cytokine Growth Factor Rev,* 26**,** 489-98.

JUNG, M. J., MURZIK, U., WEHDER, L., HEMMERICH, P. & MELLE, C. 2010. Regulation of cellular actin architecture by S100A10. *Exp Cell Res,* 316**,** 1234-40.

JUNG, T., CASTELLANA, D., KLINGBEIL, P., CUESTA HERNANDEZ, I., VITACOLONNA, M., ORLICKY, D. J., ROFFLER, S. R., BRODT, P. & ZOLLER, M. 2009. CD44v6 dependence of premetastatic niche preparation by exosomes. *Neoplasia,* 11**,** 1093-105.

KAHLERT, C., LAHES, S., RADHAKRISHNAN, P., DUTTA, S., MOGLER, C., HERPEL, E., BRAND, K., STEINERT, G., SCHNEIDER, M., MOLLENHAUER, M., REISSFELDER, C., KLUPP, F., FRITZMANN, J., WUNDER, C., BENNER, A., KLOOR, M., HUTH, C., CONTIN, P., ULRICH, A., KOCH, M. & WEITZ, J. 2011. Overexpression of ZEB2 at the invasion front of colorectal cancer is an independent prognostic marker and regulates tumor invasion in vitro. *Clin Cancer Res,* 17**,** 7654-63.

KALLURI, R. & WEINBERG, R. A. 2009. The basics of epithelial-mesenchymal transition. *J Clin Invest,* 119**,** 1420-8.

KAMRAN, M. Z., PATIL, P. & GUDE, R. P. 2013. Role of STAT3 in cancer metastasis and translational advances. *Biomed Res Int,* 2013**,** 421821.

KARAMITOPOULOU, E. 2013. Role of epithelial-mesenchymal transition in pancreatic ductal adenocarcinoma: is tumor budding the missing link? *Front Oncol,* 3**,** 221.

KARLSSON, J., VON HOFSTEN, J. & OLSSON, P. E. 2001. Generating transparent zebrafish: a refined method to improve detection of gene expression during embryonic development. *Mar Biotechnol (NY),* 3**,** 522-7.

KIM, H., LEE, Y. D., KIM, M. K., KWON, J. O., SONG, M. K., LEE, Z. H. & KIM, H. H. 2017. Extracellular S100A4 negatively regulates osteoblast function by activating the NF-kappaB pathway. *BMB Rep,* 50**,** 97-102.

KIM, T., VERONESE, A., PICHIORRI, F., LEE, T. J., JEON, Y. J., VOLINIA, S., PINEAU, P., MARCHIO, A., PALATINI, J., SUH, S. S., ALDER, H., LIU, C. G., DEJEAN, A. & CROCE, C. M. 2011. p53 regulates epithelial-mesenchymal transition through microRNAs targeting ZEB1 and ZEB2. *J Exp Med,* 208**,** 875-83.

KLIMSTRA, D. S., MODLIN, I. R., COPPOLA, D., LLOYD, R. V. & SUSTER, S. 2010. The pathologic classification of neuroendocrine tumors: a review of nomenclature, grading, and staging systems. *Pancreas,* 39**,** 707-12.

KO, L. J. & PRIVES, C. 1996. p53: puzzle and paradigm. *Genes Dev,* 10**,** 1054-72.

KOGAN-SAKIN, I., TABACH, Y., BUGANIM, Y., MOLCHADSKY, A., SOLOMON, H., MADAR, S., KAMER, I., STAMBOLSKY, P., SHELLY, A., GOLDFINGER, N., VALSESIA-WITTMANN, S., PUISIEUX, A., ZUNDELEVICH, A., GAL-YAM, E. N., AVIVI, C., BARSHACK, I., BRAIT, M., SIDRANSKY, D., DOMANY, E. & ROTTER, V. 2011. Mutant p53(R175H) upregulates Twist1 expression and promotes epithelial-mesenchymal transition in immortalized prostate cells. *Cell Death Differ,* 18**,** 271-81.

KORC, M. 1998. Role of growth factors in pancreatic cancer. *Surg Oncol Clin N Am,* 7**,** 25-41.

KRASKOUSKAYA, D., DUODU, E., ARPIN, C. C. & GUNNING, P. T. 2013. Progress towards the development of SH2 domain inhibitors. *Chem Soc Rev,* 42**,** 3337-70.

KREBS, A. M., MITSCHKE, J., LASIERRA LOSADA, M., SCHMALHOFER, O., BOERRIES, M., BUSCH, H., BOETTCHER, M., MOUGIAKAKOS, D., REICHARDT, W., BRONSERT, P., BRUNTON, V. G., PILARSKY, C., WINKLER, T. H., BRABLETZ, S., STEMMLER, M. P. & BRABLETZ, T. 2017. The EMT-activator Zeb1 is a key factor for cell plasticity and promotes metastasis in pancreatic cancer. *Nat Cell Biol,* 19**,** 518-529.

KRIAJEVSKA, M., BRONSTEIN, I. B., SCOTT, D. J., TARABYKINA, S., FISCHER-LARSEN, M., ISSINGER, O. & LUKANIDIN, E. 2000. Metastasis-associated protein Mts1 (S100A4) inhibits CK2-mediated phosphorylation and self-assembly of the heavy chain of nonmuscle myosin. *Biochim Biophys Acta,* 20**,** 2-3.

KRIAJEVSKA, M., TARABYKINA, S., BRONSTEIN, I., MAITLAND, N., LOMONOSOV, M., HANSEN, K., GEORGIEV, G. & LUKANIDIN, E. 1998. Metastasis-associated Mts1 (S100A4) protein modulates protein kinase C phosphorylation of the heavy chain of nonmuscle myosin. *J Biol Chem,* 273**,** 9852-6.

KURAHARA, H., TAKAO, S., MAEMURA, K., MATAKI, Y., KUWAHATA, T., MAEDA, K., DING, Q., SAKODA, M., IINO, S., ISHIGAMI, S., UENO, S., SHINCHI, H. & NATSUGOE, S. 2012. Epithelial-mesenchymal transition and mesenchymal-epithelial transition via regulation of ZEB-1 and ZEB-2 expression in pancreatic cancer. *J Surg Oncol,* 105**,** 655-61.

KYRIAZIS, A. P., KYRIAZIS, A. A., SCARPELLI, D. G., FOGH, J., RAO, M. S. & LEPERA, R. 1982. Human pancreatic adenocarcinoma line Capan-1 in tissue culture and the nude mouse: morphologic, biologic, and biochemical characteristics. *Am J Pathol,* 106**,** 250-60.

LABELLE, M., SCHNITTLER, H. J., AUST, D. E., FRIEDRICH, K., BARETTON, G., VESTWEBER, D. & BREIER, G. 2008. Vascular endothelial cadherin promotes breast cancer progression via transforming growth factor beta signaling. *Cancer Res,* 68**,** 1388-97.

LAHAT, G., LUBEZKY, N., LOEWENSTEIN, S., NIZRI, E., GAN, S., PASMANIK-CHOR, M., HAYMAN, L., BARAZOWSKY, E., BEN-HAIM, M. & KLAUSNER, J. M. 2014. Epithelial-to-mesenchymal transition (EMT) in intraductal papillary mucinous neoplasm (IPMN) is associated with high tumor grade and adverse outcomes. *Ann Surg Oncol,* 21 Suppl 4**,** S750-7.

LAM, S. H., CHUA, H. L., GONG, Z., LAM, T. J. & SIN, Y. M. 2004. Development and maturation of the immune system in zebrafish, Danio rerio: a gene expression profiling, in situ hybridization and immunological study. *Dev Comp Immunol,* 28**,** 9-28.

LANDSKRON, G., DE LA FUENTE, M., THUWAJIT, P., THUWAJIT, C. & HERMOSO, M. A. 2014. Chronic inflammation and cytokines in the tumor microenvironment. *J Immunol Res,* 2014**,** 149185.

LANTON, T., SHRIKI, A., NECHEMIA-ARBELY, Y., ABRAMOVITCH, R., LEVKOVITCH, O., ADAR, R., ROSENBERG, N., PALDOR, M., GOLDENBERG, D., SONNENBLICK, A., PELED, A., ROSE-JOHN, S., GALUN, E. & AXELROD, J. H. 2017. Interleukin 6-dependent genomic instability heralds accelerated carcinogenesis following liver regeneration on a background of chronic hepatitis. *Hepatology,* 65**,** 1600-1611.

LAWSON, N. D. & WEINSTEIN, B. M. 2002. In vivo imaging of embryonic vascular development using transgenic zebrafish. *Dev Biol,* 248**,** 307-18.

LE LARGE, T. Y. S., BIJLSMA, M. F., KAZEMIER, G., VAN LAARHOVEN, H. W. M., GIOVANNETTI, E. & JIMENEZ, C. R. 2017. Key biological processes driving metastatic spread of pancreatic cancer as identified by multi-omics studies. *Semin Cancer Biol*.

LECLERC, E., FRITZ, G., WEIBEL, M., HEIZMANN, C. W. & GALICHET, A. 2007. S100B and S100A6 differentially modulate cell survival by interacting with distinct RAGE (receptor for advanced glycation end products) immunoglobulin domains. *J Biol Chem,* 282**,** 31317-31.

LEE, L. M., SEFTOR, E. A., BONDE, G., CORNELL, R. A. & HENDRIX, M. J. 2005. The fate of human malignant melanoma cells transplanted into zebrafish embryos: assessment of migration and cell division in the absence of tumor formation. *Dev Dyn,* 233**,** 1560-70.

LEE, M. J., LEE, J. K., CHOI, J. W., LEE, C. S., SIM, J. H., CHO, C. H., LEE, K. H., CHO, I. H., CHUNG, M. H., KIM, H. R. & YE, S. K. 2012. Interleukin-6 induces S100A9 expression in colonic epithelial cells through STAT3 activation in experimental ulcerative colitis. *PLoS One,* 7**,** e38801.

LEE, S. H., LEE, S. J., JUNG, Y. S., XU, Y., KANG, H. S., HA, N. C. & PARK, B. J. 2009. Blocking of p53-Snail binding, promoted by oncogenic K-Ras, recovers p53 expression and function. *Neoplasia,* 11**,** 22-31, 6p following 31.

LEE, S. W., TOMASETTO, C., SWISSHELM, K., KEYOMARSI, K. & SAGER, R. 1992. Down-regulation of a member of the S100 gene family in mammary carcinoma cells and reexpression by azadeoxycytidine treatment. *Proc Natl Acad Sci U S A,* 89**,** 2504-8.

LENG, R. P., LIN, Y., MA, W., WU, H., LEMMERS, B., CHUNG, S., PARANT, J. M., LOZANO, G., HAKEM, R. & BENCHIMOL, S. 2003. Pirh2, a p53-induced ubiquitin-protein ligase, promotes p53 degradation. *Cell,* 112**,** 779-91.

LENTINI, A., ABBRUZZESE, A., PROVENZANO, B., TABOLACCI, C. & BENINATI, S. 2013. Transglutaminases: key regulators of cancer metastasis. *Amino Acids,* 44**,** 25-32.

LESINA, M., KURKOWSKI, M. U., LUDES, K., ROSE-JOHN, S., TREIBER, M., KLOPPEL, G., YOSHIMURA, A., REINDL, W., SIPOS, B., AKIRA, S., SCHMID, R. M. & ALGUL, H. 2011. Stat3/Socs3 activation by IL-6 transsignaling promotes progression of pancreatic intraepithelial neoplasia and development of pancreatic cancer. *Cancer Cell,* 19**,** 456-69.

LESNIAK, W. 2011. Epigenetic regulation of S100 protein expression. *Clin Epigenetics,* 2**,** 77-83.

LESNIAK, W., SWART, G. W., BLOEMERS, H. P. & KUZNICKI, J. 2000. Regulation of cell specific expression of calcyclin (S100A6) in nerve cells and other tissues. *Acta Neurobiol Exp (Wars),* 60**,** 569-75.

LI, H., MAR, B. G., ZHANG, H., PURAM, R. V., VAZQUEZ, F., WEIR, B. A., HAHN, W. C., EBERT, B. & PELLMAN, D. 2017. The EMT regulator ZEB2 is a novel dependency of human and murine acute myeloid leukemia. *Blood,* 129**,** 497-508.

LI, J., WANG, X. H., LI, Z. Y., BU, Z. D., WU, A. W., ZHANG, L. H., WU, X. J., ZONG, X. L. & JI, J. F. 2013. [Regulation mechanism study of S100A6 on invasion and metastasis in gastric cancer]. *Zhonghua Wei Chang Wai Ke Za Zhi,* 16**,** 1096-101.

LI, K., XU, B., XU, G. & LIU, R. 2016a. CCR7 regulates Twist to induce the epithelial-mesenchymal transition in pancreatic ductal adenocarcinoma. *Tumour Biol,* 37**,** 419-24.

LI, N., SONG, M. M., CHEN, X. H., LIU, L. H. & LI, F. S. 2012. S100A4 siRNA inhibits human pancreatic cancer cell invasion in vitro. *Biomed Environ Sci,* 25**,** 465-70.

LI, W., ZHANG, L., CHEN, X., JIANG, Z., ZONG, L. & MA, Q. 2016b. Hyperglycemia Promotes the Epithelial-Mesenchymal Transition of Pancreatic Cancer via Hydrogen Peroxide. *Oxid Med Cell Longev,* 2016**,** 5190314.

LI, Y., DRABSCH, Y., PUJUGUET, P., REN, J., VAN LAAR, T., ZHANG, L., VAN DAM, H., CLEMENT-LACROIX, P. & TEN DIJKE, P. 2015. Genetic depletion and pharmacological targeting of alphav integrin in breast cancer cells impairs metastasis in zebrafish and mouse xenograft models. *Breast Cancer Res,* 17**,** 28.

LI, Y., VANDENBOOM, T. G., 2ND, KONG, D., WANG, Z., ALI, S., PHILIP, P. A. & SARKAR, F. H. 2009. Up-regulation of miR-200 and let-7 by natural agents leads to the reversal of epithelial-to-mesenchymal transition in gemcitabine-resistant pancreatic cancer cells. *Cancer Res,* 69**,** 6704-12.

LI, Z., TANG, M., LING, B., LIU, S., ZHENG, Y., NIE, C., YUAN, Z., ZHOU, L., GUO, G., TONG, A. & WEI, Y. 2014. Increased expression of S100A6 promotes cell proliferation and migration in human hepatocellular carcinoma. *J Mol Med (Berl),* 92**,** 291-303.

LIN, F., SHI, J., LIU, H., HULL, M. E., DUPREE, W., PRICHARD, J. W., BROWN, R. E., ZHANG, J., WANG, H. L. & SCHUERCH, C. 2008. Diagnostic utility of S100P and von Hippel-Lindau gene product (pVHL) in pancreatic adenocarcinoma-with implication of their roles in early tumorigenesis. *Am J Surg Pathol,* 32**,** 78-91.

LIN, H. J. & LIN, J. 2017. Seed-in-Soil: Pancreatic Cancer Influenced by Tumor Microenvironment. *Cancers (Basel),* 9.

LIN, J., YANG, Q., YAN, Z., MARKOWITZ, J., WILDER, P. T., CARRIER, F. & WEBER, D. J. 2004. Inhibiting S100B restores p53 levels in primary malignant melanoma cancer cells. *J Biol Chem,* 279**,** 34071-7.

LINDSEY, J. C., LUSHER, M. E., ANDERTON, J. A., GILBERTSON, R. J., ELLISON, D. W. & CLIFFORD, S. C. 2007. Epigenetic deregulation of multiple S100 gene family members by differential hypomethylation and hypermethylation events in medulloblastoma. *Br J Cancer,* 97**,** 267-74.

LIRIANO, M. A., VARNEY, K. M., WRIGHT, N. T., HOFFMAN, C. L., TOTH, E. A., ISHIMA, R. & WEBER, D. J. 2012. Target binding to S100B reduces dynamic properties and increases Ca(2+)-binding affinity for wild type and EF-hand mutant proteins. *J Mol Biol,* 423**,** 365-85.

LIU, C. F., ZHANG, Y., LIM, S., HOSAKA, K., YANG, Y., PAVLOVA, T., ALKASALIAS, T., HARTMAN, J., JENSEN, L., XING, X. M., WANG, X., LU, Y. T., NIE, G. H. & CAO, Y. 2017a. A zebrafish model discovers a novel mechanism of stromal fibroblast-mediated cancer metastasis. *Clin Cancer Res*.

LIU, L., MIAO, L., LIU, Y., QI, A., XIE, P., CHEN, J. & ZHU, H. 2017b. S100A11 regulates renal carcinoma cell proliferation, invasion, and migration via the EGFR/Akt signaling pathway and E-cadherin. *Tumour Biol,* 39**,** 1010428317705337.

LIU, T., LI, Y., LIN, K., YIN, H., HE, B., ZHENG, M. & WANG, G. 2012. Regulation of S100A4 expression via the JAK2-STAT3 pathway in rhomboid-phenotype pulmonary arterial smooth muscle cells exposure to hypoxia. *Int J Biochem Cell Biol,* 44**,** 1337-45.

LIU, X., HUANG, H., REMMERS, N. & HOLLINGSWORTH, M. A. 2014a. Loss of E-cadherin and epithelial to mesenchymal transition is not required for cell motility in tissues or for metastasis. *Tissue Barriers,* 2**,** e969112.

LIU, Y., BUNSTON, C., HODSON, N., RESAUL, J., SUN, P. H., CAI, S., CHEN, G., GU, Y., SATHERLEY, L. K., BOSANQUET, D. C., AL-SARIREH, B., TIAN, X., HAO, C., JIANG, W. G. & YE, L. 2017c. Psoriasin promotes invasion,

aggregation and survival of pancreatic cancer cells; association with disease progression. *Int J Oncol,* 50**,** 1491-1500.

LIU, Y., HAN, X. & GAO, B. 2015. Knockdown of S100A11 expression suppresses ovarian cancer cell growth and invasion. *Exp Ther Med,* 9**,** 1460-1464.

LIU, Y. F., LIU, Q. Q., WANG, X. & LUO, C. H. 2014b. Clinical significance of S100A2 expression in gastric cancer. *Tumour Biol,* 35**,** 3731-41.

LO, J. F., YU, C. C., CHIOU, S. H., HUANG, C. Y., JAN, C. I., LIN, S. C., LIU, C. J., HU, W. Y. & YU, Y. H. 2011. The epithelial-mesenchymal transition mediator S100A4 maintains cancer-initiating cells in head and neck cancers. *Cancer Res,* 71**,** 1912-23.

LUKANIDIN, E. & SLEEMAN, J. P. 2012. Building the niche: the role of the S100 proteins in metastatic growth. *Semin Cancer Biol,* 22**,** 216-25.

LUO, X., CHENG, C., TAN, Z., LI, N., TANG, M., YANG, L. & CAO, Y. 2017. Emerging roles of lipid metabolism in cancer metastasis. *Mol Cancer,* 16**,** 76.

LUO, X., SHARFF, K. A., CHEN, J., HE, T. C. & LUU, H. H. 2008. S100A6 expression and function in human osteosarcoma. *Clin Orthop Relat Res,* 466**,** 2060-70.

LUU, H. H., ZHOU, L., HAYDON, R. C., DEYRUP, A. T., MONTAG, A. G., HUO, D., HECK, R., HEIZMANN, C. W., PEABODY, T. D., SIMON, M. A. & HE, T. C. 2005. Increased expression of S100A6 is associated with decreased metastasis and inhibition of cell migration and anchorage independent growth in human osteosarcoma. *Cancer Lett,* 229**,** 135-48.

LYU, P., ZHANG, S. D., YUEN, H. F., MCCRUDDEN, C. M., WEN, Q., CHAN, K. W. & KWOK, H. F. 2017. Identification of TWIST-interacting genes in prostate cancer. *Sci China Life Sci,* 60**,** 386-396.

MACPHERSON, D., KIM, J., KIM, T., RHEE, B. K., VAN OOSTROM, C. T., DITULLIO, R. A., VENERE, M., HALAZONETIS, T. D., BRONSON, R., DE VRIES, A., FLEMING, M. & JACKS, T. 2004. Defective apoptosis and B-cell lymphomas in mice with p53 point mutation at Ser 23. *EMBO J,* 23**,** 3689-99.

MAEDA, G., CHIBA, T., OKAZAKI, M., SATOH, T., TAYA, Y., AOBA, T., KATO, K., KAWASHIRI, S. & IMAI, K. 2005. Expression of SIP1 in oral squamous cell carcinomas: implications for E-cadherin expression and tumor progression. *Int J Oncol,* 27**,** 1535-41.

MAESTRO, R., DEI TOS, A. P., HAMAMORI, Y., KRASNOKUTSKY, S., SARTORELLI, V., KEDES, L., DOGLIONI, C., BEACH, D. H. & HANNON, G. J. 1999. Twist is a potential oncogene that inhibits apoptosis. *Genes Dev,* 13**,** 2207-17.

MAHDAVINEZHAD, A., YADEGARAZARI, R., MOUSAVI-BAHAR, S. H., POOROLAJAL, J., JAFARI, M., AMIRZARGAR, M. A., EFFATPANAH, H. & SAIDIJAM, M. 2017. Evaluation of zinc finger E-box binding homeobox 1 and transforming growth factor-beta2 expression in bladder cancer tissue in comparison with healthy adjacent tissue. *Investig Clin Urol,* 58**,** 140-145.

MAIER, H. J., WIRTH, T. & BEUG, H. 2010. Epithelial-mesenchymal transition in pancreatic carcinoma. *Cancers (Basel),* 2**,** 2058-83.

MAIERTHALER, M., KRIEGSMANN, M., PENG, C., JAUCH, S., SZABO, A., WALLWIENER, M., ROM, J., SOHN, C., SCHNEEWEISS, A., SINN, H. P., YANG, R. & BURWINKEL, B. 2015. S100P and HYAL2 as prognostic markers for patients with triple-negative breast cancer. *Exp Mol Pathol,* 99**,** 180-7.

MAKOHON-MOORE, A. & IACOBUZIO-DONAHUE, C. A. 2016. Pancreatic cancer biology and genetics from an evolutionary perspective. *Nat Rev Cancer,* 16**,** 553-65.

MALETZKI, C., BODAMMER, P., BREITRUCK, A. & KERKHOFF, C. 2012. S100 proteins as diagnostic and prognostic markers in colorectal and hepatocellular carcinoma. *Hepat Mon,* 12**,** e7240.

MALI, S. B. 2015. Review of STAT3 (Signal Transducers and Activators of Transcription) in head and neck cancer. *Oral Oncol,* 51**,** 565-9.

MARENHOLZ, I., HEIZMANN, C. W. & FRITZ, G. 2004. S100 proteins in mouse and man: from evolution to function and pathology (including an update of the nomenclature). *Biochem Biophys Res Commun,* 322**,** 1111-22.

MARQUES, I. J., WEISS, F. U., VLECKEN, D. H., NITSCHE, C., BAKKERS, J., LAGENDIJK, A. K., PARTECKE, L. I., HEIDECKE, C. D., LERCH, M. M. & BAGOWSKI, C. P. 2009. Metastatic behaviour of primary human tumours in a zebrafish xenotransplantation model. *BMC Cancer,* 9**,** 128.

MASSAGUE, J. & OBENAUF, A. C. 2016. Metastatic colonization by circulating tumour cells. *Nature,* 529**,** 298-306.

MASUGI, Y., YAMAZAKI, K., HIBI, T., AIURA, K., KITAGAWA, Y. & SAKAMOTO, M. 2010. Solitary cell infiltration is a novel indicator of poor prognosis and epithelial-mesenchymal transition in pancreatic cancer. *Hum Pathol,* 41**,** 1061-8.

MAZUR, P. K. & SIVEKE, J. T. 2012. Genetically engineered mouse models of pancreatic cancer: unravelling tumour biology and progressing translational oncology. *Gut,* 61**,** 1488-500.

MCVEAN, M., XIAO, H., ISOBE, K. & PELLING, J. C. 2000. Increase in wild-type p53 stability and transactivational activity by the chemopreventive agent apigenin in keratinocytes. *Carcinogenesis,* 21**,** 633-9.

MEDICI, D., HAY, E. D. & OLSEN, B. R. 2008. Snail and Slug promote epithelial-mesenchymal transition through beta-catenin-T-cell factor-4-dependent expression of transforming growth factor-beta3. *Mol Biol Cell,* 19**,** 4875-87.

MEJLVANG, J., KRIAJEVSKA, M., VANDEWALLE, C., CHERNOVA, T., SAYAN, A. E., BERX, G., MELLON, J. K. & TULCHINSKY, E. 2007. Direct repression of cyclin D1 by SIP1 attenuates cell cycle progression in cells undergoing an epithelial mesenchymal transition. *Mol Biol Cell,* 18**,** 4615-24.

MELNIKOVA, V. O., SANTAMARIA, A. B., BOLSHAKOV, S. V. & ANANTHASWAMY, H. N. 2003. Mutant p53 is constitutively phosphorylated at Serine 15 in UV-induced mouse skin tumors: involvement of ERK1/2 MAP kinase. *Oncogene,* 22**,** 5958-66.

METZGAR, R. S., GAILLARD, M. T., LEVINE, S. J., TUCK, F. L., BOSSEN, E. H. & BOROWITZ, M. J. 1982. Antigens of human pancreatic adenocarcinoma cells defined by murine monoclonal antibodies. *Cancer Res,* 42**,** 601-8.

MIN, H., SUN, X., YANG, X., ZHU, H., LIU, J., WANG, Y., CHEN, G. & SUN, X. 2017. Exosomes Derived from Irradiated Esophageal Carcinoma-Infiltrating T Cells Promote Metastasis by Inducing the Epithelial-Mesenchymal Transition in Esophageal Cancer Cells. *Pathol Oncol Res*.

MIRZA, A., FOSTER, L., VALENTINE, H., WELCH, I., WEST, C. M. & PRITCHARD, S. 2014. Investigation of the epithelial to mesenchymal transition markers S100A4, Vimentin and Snail1 in gastroesophageal junction tumors. *Dis Esophagus,* 27**,** 485-92.

MISE, B. P., TELESMANIC, V. D., TOMIC, S., SUNDOV, D., CAPKUN, V. & VRDOLJAK, E. 2015. Correlation Between E-cadherin Immunoexpression and Efficacy of First Line Platinum-Based Chemotherapy in Advanced High Grade Serous Ovarian Cancer. *Pathol Oncol Res,* 21**,** 347-56.

MIURA, N., YANO, T., SHOJI, F., KAWANO, D., TAKENAKA, T., ITO, K., MORODOMI, Y., YOSHINO, I. & MAEHARA, Y. 2009. Clinicopathological significance of Sip1-associated epithelial mesenchymal transition in non-small cell lung cancer progression. *Anticancer Res,* 29**,** 4099-106.

MIZUNO, H., SPIKE, B. T., WAHL, G. M. & LEVINE, A. J. 2010. Inactivation of p53 in breast cancers correlates with stem cell transcriptional signatures. *Proc Natl Acad Sci U S A,* 107**,** 22745-50.

MOLL, U. M. & SLADE, N. 2004. p63 and p73: roles in development and tumor formation. *Mol Cancer Res,* 2**,** 371-86.

MOODY, S. E., PEREZ, D., PAN, T. C., SARKISIAN, C. J., PORTOCARRERO, C. P., STERNER, C. J., NOTORFRANCESCO, K. L., CARDIFF, R. D. & CHODOSH, L. A. 2005. The transcriptional repressor Snail promotes mammary tumor recurrence. *Cancer Cell,* 8**,** 197-209.

MOORE, B. W. 1965. A soluble protein characteristic of the nervous system. *Biochem Biophys Res Commun,* 19**,** 739-44.

MORENO-BUENO, G., PEINADO, H., MOLINA, P., OLMEDA, D., CUBILLO, E., SANTOS, V., PALACIOS, J., PORTILLO, F. & CANO, A. 2009. The morphological and molecular features of the epithelial-to-mesenchymal transition. *Nat Protoc,* 4**,** 1591-613.

MUELLER, A., SCHAFER, B. W., FERRARI, S., WEIBEL, M., MAKEK, M., HOCHLI, M. & HEIZMANN, C. W. 2005. The calcium-binding protein S100A2 interacts with p53 and modulates its transcriptional activity. *J Biol Chem,* 280**,** 29186-93.

NAGATHIHALLI, N. S., CASTELLANOS, J. A., SHI, C., BEESETTY, Y., REYZER, M. L., CAPRIOLI, R., CHEN, X., WALSH, A. J., SKALA, M. C., MOSES, H. L. & MERCHANT, N. B. 2015. Signal Transducer and Activator of Transcription 3, Mediated Remodeling of the Tumor Microenvironment Results in Enhanced Tumor Drug Delivery in a Mouse Model of Pancreatic Cancer. *Gastroenterology,* 149**,** 1932-1943 e9.

NAGATHIHALLI, N. S., CASTELLANOS, J. A., VANSAUN, M. N., DAI, X., AMBROSE, M., GUO, Q., XIONG, Y. & MERCHANT, N. B. 2016. Pancreatic stellate cell secreted IL-6 stimulates STAT3 dependent invasiveness of pancreatic intraepithelial neoplasia and cancer cells. *Oncotarget,* 7**,** 65982-65992.

NASSER, M. W., ELBAZ, M., AHIRWAR, D. K. & GANJU, R. K. 2015a. Conditioning solid tumor microenvironment through inflammatory chemokines and S100 family proteins. *Cancer Lett,* 365**,** 11-22.

NASSER, M. W., WANI, N. A., AHIRWAR, D. K., POWELL, C. A., RAVI, J., ELBAZ, M., ZHAO, H., PADILLA, L., ZHANG, X., SHILO, K., OSTROWSKI, M., SHAPIRO, C., CARSON, W. E., 3RD & GANJU, R. K. 2015b. RAGE mediates S100A7-induced breast cancer growth and metastasis by modulating the tumor microenvironment. *Cancer Res,* 75**,** 974-85.

NATARAJAN, J., HUNTER, K., MUTALIK, V. S. & RADHAKRISHNAN, R. 2014. Overexpression of S100A4 as a biomarker of metastasis and recurrence in oral squamous cell carcinoma. *J Appl Oral Sci,* 22**,** 426-33.

NAZ, S., BASHIR, M., RANGANATHAN, P., BODAPATI, P., SANTOSH, V. & KONDAIAH, P. 2014. Protumorigenic actions of S100A2 involve regulation of PI3/Akt signaling and functional interaction with Smad3. *Carcinogenesis,* 35**,** 14-23.

NAZ, S., RANGANATHAN, P., BODAPATI, P., SHASTRY, A. H., MISHRA, L. N. & KONDAIAH, P. 2012. Regulation of S100A2 expression by TGF-beta-induced MEK/ERK signalling and its role in cell migration/invasion. *Biochem J,* 447**,** 81-91.

NEDJADI, T., KITTERINGHAM, N., CAMPBELL, F., JENKINS, R. E., PARK, B. K., NAVARRO, P., ASHCROFT, F., TEPIKIN, A., NEOPTOLEMOS, J. P. & COSTELLO, E. 2009. S100A6 binds to annexin 2 in pancreatic cancer cells and promotes pancreatic cancer cell motility. *Br J Cancer,* 101**,** 1145-54.

NEMETH, J., STEIN, I., HAAG, D., RIEHL, A., LONGERICH, T., HORWITZ, E., BREUHAHN, K., GEBHARDT, C., SCHIRMACHER, P., HAHN, M., BEN-NERIAH, Y., PIKARSKY, E., ANGEL, P. & HESS, J. 2009. S100A8 and S100A9 are novel nuclear factor kappa B target genes during malignant progression of murine and human liver carcinogenesis. *Hepatology,* 50**,** 1251-62.

NGUYEN, T. T., LIAN, S., UNG, T. T., XIA, Y., HAN, J. Y. & JUNG, Y. D. 2017. Lithocholic Acid Stimulates IL-8 Expression in Human Colorectal Cancer Cells Via Activation of Erk1/2 MAPK and Suppression of STAT3 Activity. *J Cell Biochem*.

NI, T., LI, X. Y., LU, N., AN, T., LIU, Z. P., FU, R., LV, W. C., ZHANG, Y. W., XU, X. J., GRANT ROWE, R., LIN, Y. S., SCHERER, A., FEINBERG, T., ZHENG, X. Q., CHEN, B. A., LIU, X. S., GUO, Q. L., WU, Z. Q. & WEISS, S. J. 2016. Snail1-dependent p53 repression regulates expansion and activity of tumour-initiating cells in breast cancer. *Nat Cell Biol,* 18**,** 1221-1232.

NING, X., SUN, S., ZHANG, K., LIANG, J., CHUAI, Y., LI, Y. & WANG, X. 2012. S100A6 protein negatively regulates CacyBP/SIP-mediated inhibition of gastric cancer cell proliferation and tumorigenesis. *PLoS One,* 7**,** e30185.

NIU, Y., SHAO, Z., WANG, H., YANG, J., ZHANG, F., LUO, Y., XU, L., DING, Y. & ZHAO, L. 2016. LASP1-S100A11 axis promotes colorectal cancer aggressiveness by modulating TGFbeta/Smad signaling. *Sci Rep,* 6**,** 26112.

NUTTER, F., HOLEN, I., BROWN, H. K., CROSS, S. S., EVANS, C. A., WALKER, M., COLEMAN, R. E., WESTBROOK, J. A., SELBY, P. J., BROWN, J. E. & OTTEWELL, P. D. 2014. Different molecular profiles are associated with breast cancer cell homing compared with colonisation of bone: evidence using a novel bone-seeking cell line. *Endocr Relat Cancer,* 21**,** 327-41.

OHUCHIDA, K., MIZUMOTO, K., EGAMI, T., YAMAGUCHI, H., FUJII, K., KONOMI, H., NAGAI, E., YAMAGUCHI, K., TSUNEYOSHI, M. & TANAKA, M. 2006a. S100P is an early developmental marker of pancreatic carcinogenesis. *Clin Cancer Res,* 12**,** 5411-6.

OHUCHIDA, K., MIZUMOTO, K., ISHIKAWA, N., FUJII, K., KONOMI, H., NAGAI, E., YAMAGUCHI, K., TSUNEYOSHI, M. & TANAKA, M. 2005. The role of S100A6 in pancreatic cancer development and its clinical implication as a diagnostic marker and therapeutic target. *Clin Cancer Res,* 11**,** 7785-93.

OHUCHIDA, K., MIZUMOTO, K., MIYASAKA, Y., YU, J., CUI, L., YAMAGUCHI, H., TOMA, H., TAKAHATA, S., SATO, N., NAGAI, E., YAMAGUCHI, K., TSUNEYOSHI, M. & TANAKA, M. 2007. Over-expression of S100A2 in pancreatic cancer correlates with progression and poor prognosis. *J Pathol,* 213**,** 275-82.

OHUCHIDA, K., MIZUMOTO, K., OHHASHI, S., YAMAGUCHI, H., KONOMI, H., NAGAI, E., YAMAGUCHI, K., TSUNEYOSHI, M. & TANAKA, M. 2006b. S100A11, a putative tumor suppressor gene, is overexpressed in pancreatic carcinogenesis. *Clin Cancer Res,* 12**,** 5417-22.

OIDA, Y., YAMAZAKI, H., TOBITA, K., MUKAI, M., OHTANI, Y., MIYAZAKI, N., ABE, Y., IMAIZUMI, T., MAKUUCHI, H., UEYAMA, Y. & NAKAMURA, M. 2006. Increased S100A4 expression combined with decreased E-cadherin expression predicts a poor outcome of patients with pancreatic cancer. *Oncol Rep,* 16**,** 457-63.

OKADA, H., DANOFF, T. M., KALLURI, R. & NEILSON, E. G. 1997. Early role of Fsp1 in epithelial-mesenchymal transformation. *Am J Physiol,* 273**,** F563-74.

OKUGAWA, Y., INOUE, Y., TANAKA, K., KAWAMURA, M., SAIGUSA, S., TOIYAMA, Y., OHI, M., UCHIDA, K., MOHRI, Y. & KUSUNOKI, M. 2013. Smad interacting protein 1 (SIP1) is associated with peritoneal carcinomatosis in intestinal type gastric cancer. *Clin Exp Metastasis,* 30**,** 417-29.

OLIVOS, D. J. & MAYO, L. D. 2016. Emerging Non-Canonical Functions and Regulation by p53: p53 and Stemness. *Int J Mol Sci,* 17.

ORR, B., RIDDICK, A. C., STEWART, G. D., ANDERSON, R. A., FRANCO, O. E., HAYWARD, S. W. & THOMSON, A. A. 2012. Identification of stromally expressed molecules in the prostate by tag-profiling of cancer-associated fibroblasts, normal fibroblasts and fetal prostate. *Oncogene,* 31**,** 1130-42.

OUYANG, G., WANG, Z., FANG, X., LIU, J. & YANG, C. J. 2010. Molecular signaling of the epithelial to mesenchymal transition in generating and maintaining cancer stem cells. *Cell Mol Life Sci,* 67**,** 2605-18.

PAN, Y. M., WANG, C. G., ZHU, M., XING, R., CUI, J. T., LI, W. M., YU, D. D., WANG, S. B., ZHU, W., YE, Y. J., WU, Y., WANG, S. & LU, Y. Y. 2016. STAT3 signaling drives EZH2 transcriptional activation and mediates poor prognosis in gastric cancer. *Mol Cancer,* 15**,** 79.

PANG, W., SU, J., WANG, Y., FENG, H., DAI, X., YUAN, Y., CHEN, X. & YAO, W. 2015. Pancreatic cancer-secreted miR-155 implicates in the conversion from normal fibroblasts to cancer-associated fibroblasts. *Cancer Sci,* 106**,** 1362-9.

PARKER, C., LAKSHMI, M. S., PIURA, B. & SHERBET, G. V. 1994. Metastasis-associated mts1 gene expression correlates with increased p53 detection in the B16 murine melanoma. *DNA Cell Biol,* 13**,** 343-51.

PEELA, N., TRUONG, D., SAINI, H., CHU, H., MASHAGHI, S., HAM, S. L., SINGH, S., TAVANA, H., MOSADEGH, B. & NIKKHAH, M. 2017. Advanced biomaterials and microengineering technologies to recapitulate the stepwise process of cancer metastasis. *Biomaterials,* 133**,** 176-207.

PEINADO, H., OLMEDA, D. & CANO, A. 2007. Snail, Zeb and bHLH factors in tumour progression: an alliance against the epithelial phenotype? *Nat Rev Cancer,* 7**,** 415-28.

PELLEGATA, N. S., SESSA, F., RENAULT, B., BONATO, M., LEONE, B. E., SOLCIA, E. & RANZANI, G. N. 1994. K-ras and p53 gene mutations in pancreatic cancer: ductal and nonductal tumors progress through different genetic lesions. *Cancer Res,* 54**,** 1556-60.

PICCININ, S., TONIN, E., SESSA, S., DEMONTIS, S., ROSSI, S., PECCIARINI, L., ZANATTA, L., PIVETTA, F., GRIZZO, A., SONEGO, M., ROSANO, C., DEI TOS, A. P., DOGLIONI, C. & MAESTRO, R. 2012. A "twist box" code of p53 inactivation: twist box: p53 interaction promotes p53 degradation. *Cancer Cell,* 22**,** 404-15.

PIGNATELLI, M., ANSARI, T. W., GUNTER, P., LIU, D., HIRANO, S., TAKEICHI, M., KLOPPEL, G. & LEMOINE, N. R. 1994. Loss of membranous E-cadherin expression in pancreatic cancer: correlation with lymph node metastasis, high grade, and advanced stage. *J Pathol,* 174**,** 243-8.

POETER, M., RADKE, S., KOESE, M., HESSNER, F., HEGEMANN, A., MUSIOL, A., GERKE, V., GREWAL, T. & RESCHER, U. 2013. Disruption of the annexin A1/S100A11 complex increases the migration and clonogenic growth by dysregulating epithelial growth factor (EGF) signaling. *Biochim Biophys Acta,* 1833**,** 1700-11.

PRICE, P. & MCMILLAN, T. J. 1990. Use of the tetrazolium assay in measuring the response of human tumor cells to ionizing radiation. *Cancer Res,* 50**,** 1392-6.

PRIETO, D., SOTELO, N., SEIJA, N., SERNBO, S., ABREU, C., DURAN, R., GIL, M., SICCO, E., IRIGOIN, V., OLIVER, C., LANDONI, A. I., GABUS, R., DIGHIERO, G. & OPPEZZO, P. 2017. S100-A9 protein in exosomes from

chronic lymphocytic leukemia cells promotes NF-kappaB activity during disease progression. *Blood*.

PRISLEI, S., MARTINELLI, E., ZANNONI, G. F., PETRILLO, M., FILIPPETTI, F., MARIANI, M., MOZZETTI, S., RASPAGLIO, G., SCAMBIA, G. & FERLINI, C. 2015. Role and prognostic significance of the epithelial-mesenchymal transition factor ZEB2 in ovarian cancer. *Oncotarget,* 6**,** 18966-79.

QU, J. Q., YI, H. M., YE, X., LI, L. N., ZHU, J. F., XIAO, T., YUAN, L., LI, J. Y., WANG, Y. Y., FENG, J., HE, Q. Y., LU, S. S., YI, H. & XIAO, Z. Q. 2015. MiR-23a sensitizes nasopharyngeal carcinoma to irradiation by targeting IL-8/Stat3 pathway. *Oncotarget,* 6**,** 28341-56.

RAHIB, L., SMITH, B. D., AIZENBERG, R., ROSENZWEIG, A. B., FLESHMAN, J. M. & MATRISIAN, L. M. 2014. Projecting cancer incidence and deaths to 2030: the unexpected burden of thyroid, liver, and pancreas cancers in the United States. *Cancer Res,* 74**,** 2913-21.

RAMTEKE, A., TING, H., AGARWAL, C., MATEEN, S., SOMASAGARA, R., HUSSAIN, A., GRANER, M., FREDERICK, B., AGARWAL, R. & DEEP, G. 2015. Exosomes secreted under hypoxia enhance invasiveness and stemness of prostate cancer cells by targeting adherens junction molecules. *Mol Carcinog,* 54**,** 554-65.

RASHEED, Z. A., YANG, J., WANG, Q., KOWALSKI, J., FREED, I., MURTER, C., HONG, S. M., KOORSTRA, J. B., RAJESHKUMAR, N. V., HE, X., GOGGINS, M., IACOBUZIO-DONAHUE, C., BERMAN, D. M., LAHERU, D., JIMENO, A., HIDALGO, M., MAITRA, A. & MATSUI, W. 2010. Prognostic significance of tumorigenic cells with mesenchymal features in pancreatic adenocarcinoma. *J Natl Cancer Inst,* 102**,** 340-51.

RAWLS, J. F., MELLGREN, E. M. & JOHNSON, S. L. 2001. How the zebrafish gets its stripes. *Dev Biol,* 240**,** 301-14.

REBE, C., VEGRAN, F., BERGER, H. & GHIRINGHELLI, F. 2013. STAT3 activation: A key factor in tumor immunoescape. *JAKSTAT,* 2**,** e23010.

REDSTON, M. S., CALDAS, C., SEYMOUR, A. B., HRUBAN, R. H., DA COSTA, L., YEO, C. J. & KERN, S. E. 1994. p53 mutations in pancreatic carcinoma and evidence of common involvement of homocopolymer tracts in DNA microdeletions. *Cancer Res,* 54**,** 3025-33.

RENSHAW, S. A., LOYNES, C. A., TRUSHELL, D. M., ELWORTHY, S., INGHAM, P. W. & WHYTE, M. K. 2006. A transgenic zebrafish model of neutrophilic inflammation. *Blood,* 108**,** 3976-8.

REZVANPOUR, A. & SHAW, G. S. 2009. Unique S100 target protein interactions. *Gen Physiol Biophys,* 28 Spec No Focus**,** F39-46.

RIBATTI, D. 2017. Epithelial-mesenchymal transition in morphogenesis, cancer progression and angiogenesis. *Exp Cell Res,* 353**,** 1-5.

RICHARDS, K. E., ZELENIAK, A. E., FISHEL, M. L., WU, J., LITTLEPAGE, L. E. & HILL, R. 2017. Cancer-associated fibroblast exosomes regulate survival and proliferation of pancreatic cancer cells. *Oncogene,* 36**,** 1770-1778.

ROBINSON, S. M., FAN, L., WHITE, S. A., CHARNLEY, R. M. & MANN, J. 2016. The role of exosomes in the pathogenesis of pancreatic ductal adenocarcinoma. *Int J Biochem Cell Biol,* 75, 131-9.

RODRIGUEZ-BARRUECO, R., YU, J., SAUCEDO-CUEVAS, L. P., OLIVAN, M., LLOBET-NAVAS, D., PUTCHA, P., CASTRO, V., MURGA-PENAS, E. M., COLLAZO-LORDUY, A., CASTILLO-MARTIN, M., ALVAREZ, M., CORDON-CARDO, C., KALINSKY, K., MAURER, M., CALIFANO, A. & SILVA, J. M. 2015. Inhibition of the autocrine IL-6-JAK2-STAT3-calprotectin axis as targeted therapy for HR-/HER2+ breast cancers. *Genes Dev,* 29, 1631-48.

ROHDE, D., RITTERHOFF, J., VOELKERS, M., KATUS, H. A., PARKER, T. G. & MOST, P. 2010. S100A1: a multifaceted therapeutic target in cardiovascular disease. *J Cardiovasc Transl Res,* 3, 525-37.

ROSE, C. S. & MALCOLM, S. 1997. A TWIST in development. *Trends Genet,* 13, 384-7.

ROSTY, C., UEKI, T., ARGANI, P., JANSEN, M., YEO, C. J., CAMERON, J. L., HRUBAN, R. H. & GOGGINS, M. 2002. Overexpression of S100A4 in pancreatic ductal adenocarcinomas is associated with poor differentiation and DNA hypomethylation. *Am J Pathol,* 160, 45-50.

ROZENBLUM, E., SCHUTTE, M., GOGGINS, M., HAHN, S. A., PANZER, S., ZAHURAK, M., GOODMAN, S. N., SOHN, T. A., HRUBAN, R. H., YEO, C. J. & KERN, S. E. 1997. Tumor-suppressive pathways in pancreatic carcinoma. *Cancer Res,* 57, 1731-4.

RUCKI, A. A. & ZHENG, L. 2014. Pancreatic cancer stroma: understanding biology leads to new therapeutic strategies. *World J Gastroenterol,* 20, 2237-46.

RUIJTER, J. M., RAMAKERS, C., HOOGAARS, W. M., KARLEN, Y., BAKKER, O., VAN DEN HOFF, M. J. & MOORMAN, A. F. 2009. Amplification efficiency: linking baseline and bias in the analysis of quantitative PCR data. *Nucleic Acids Res,* 37, e45.

RUSTANDI, R. R., BALDISSERI, D. M. & WEBER, D. J. 2000. Structure of the negative regulatory domain of p53 bound to S100B(betabeta). *Nat Struct Biol,* 7, 570-4.

RYAN, D. G., TALIANA, L., SUN, L., WEI, Z. G., MASUR, S. K. & LAVKER, R. M. 2003. Involvement of S100A4 in stromal fibroblasts of the regenerating cornea. *Invest Ophthalmol Vis Sci,* 44, 4255-62.

RYAN, K. M., PHILLIPS, A. C. & VOUSDEN, K. H. 2001. Regulation and function of the p53 tumor suppressor protein. *Curr Opin Cell Biol,* 13, 332-7.

SACCO, A., ROCCARO, A. M., MA, D., SHI, J., MISHIMA, Y., MOSCHETTA, M., CHIARINI, M., MUNSHI, N., HANDIN, R. I. & GHOBRIAL, I. M. 2016. Cancer Cell Dissemination and Homing to the Bone Marrow in a Zebrafish Model. *Cancer Res,* 76, 463-71.

SACK, U. & STEIN, U. 2009. Wnt up your mind - intervention strategies for S100A4-induced metastasis in colon cancer. *Gen Physiol Biophys,* 28 Spec No Focus, F55-64.

SAKAMOTO, K., IMAI, K., HIGASHI, T., TAKI, K., NAKAGAWA, S., OKABE, H., NITTA, H., HAYASHI, H., CHIKAMOTO, A., ISHIKO, T., BEPPU, T. & BABA, H. 2015. Significance of P-cadherin overexpression and possible mechanism of its regulation in intrahepatic cholangiocarcinoma and pancreatic cancer. *Cancer Sci,* 106**,** 1153-62.

SALAMA, I., MALONE, P. S., MIHAIMEED, F. & JONES, J. L. 2008. A review of the S100 proteins in cancer. *Eur J Surg Oncol,* 34**,** 357-64.

SALEEM, M., KWEON, M. H., JOHNSON, J. J., ADHAMI, V. M., ELCHEVA, I., KHAN, N., BIN HAFEEZ, B., BHAT, K. M., SARFARAZ, S., REAGAN-SHAW, S., SPIEGELMAN, V. S., SETALURI, V. & MUKHTAR, H. 2006. S100A4 accelerates tumorigenesis and invasion of human prostate cancer through the transcriptional regulation of matrix metalloproteinase 9. *Proc Natl Acad Sci U S A,* 103**,** 14825-30.

SAMATOV, T. R., TONEVITSKY, A. G. & SCHUMACHER, U. 2013. Epithelial-mesenchymal transition: focus on metastatic cascade, alternative splicing, non-coding RNAs and modulating compounds. *Mol Cancer,* 12**,** 107.

SANO, S., ITAMI, S., TAKEDA, K., TARUTANI, M., YAMAGUCHI, Y., MIURA, H., YOSHIKAWA, K., AKIRA, S. & TAKEDA, J. 1999. Keratinocyte-specific ablation of Stat3 exhibits impaired skin remodeling, but does not affect skin morphogenesis. *EMBO J,* 18**,** 4657-68.

SANTIN, A. D., ZHAN, F., BELLONE, S., PALMIERI, M., CANE, S., BIGNOTTI, E., ANFOSSI, S., GOKDEN, M., DUNN, D., ROMAN, J. J., O'BRIEN, T. J., TIAN, E., CANNON, M. J., SHAUGHNESSY, J., JR. & PECORELLI, S. 2004. Gene expression profiles in primary ovarian serous papillary tumors and normal ovarian epithelium: identification of candidate molecular markers for ovarian cancer diagnosis and therapy. *Int J Cancer,* 112**,** 14-25.

SARKAR, F. H., LI, Y., WANG, Z. & KONG, D. 2009. Pancreatic cancer stem cells and EMT in drug resistance and metastasis. *Minerva Chir,* 64**,** 489-500.

SAVAGNER, P., YAMADA, K. M. & THIERY, J. P. 1997. The zinc-finger protein slug causes desmosome dissociation, an initial and necessary step for growth factor-induced epithelial-mesenchymal transition. *J Cell Biol,* 137**,** 1403-19.

SCHAFER, B. W., WICKI, R., ENGELKAMP, D., MATTEI, M. G. & HEIZMANN, C. W. 1995. Isolation of a YAC clone covering a cluster of nine S100 genes on human chromosome 1q21: rationale for a new nomenclature of the S100 calcium-binding protein family. *Genomics,* 25**,** 638-43.

SCHMITTGEN, T. D. & LIVAK, K. J. 2008. Analyzing real-time PCR data by the comparative C(T) method. *Nat Protoc,* 3**,** 1101-8.

SCHNEIDER, M., HANSEN, J. L. & SHEIKH, S. P. 2008. S100A4: a common mediator of epithelial-mesenchymal transition, fibrosis and regeneration in diseases? *J Mol Med,* 86**,** 507-22.

SCHOBER, M., JAVED, M. A., BEYER, G., LE, N., VINCI, A., SUND, M., NEESSE, A. & KRUG, S. 2015. New Advances in the Treatment of Metastatic Pancreatic Cancer. *Digestion,* 92**,** 175-84.

SCHOCK, F. & PERRIMON, N. 2002. Molecular mechanisms of epithelial morphogenesis. *Annu Rev Cell Dev Biol,* 18**,** 463-93.

SCHOLZ, A., HEINZE, S., DETJEN, K. M., PETERS, M., WELZEL, M., HAUFF, P., SCHIRNER, M., WIEDENMANN, B. & ROSEWICZ, S. 2003. Activated signal transducer and activator of transcription 3 (STAT3) supports the malignant phenotype of human pancreatic cancer. *Gastroenterology,* 125**,** 891-905.

SCHUST, J., SPERL, B., HOLLIS, A., MAYER, T. U. & BERG, T. 2006. Stattic: a small-molecule inhibitor of STAT3 activation and dimerization. *Chem Biol,* 13**,** 1235-42.

SEDAGHAT, F. & NOTOPOULOS, A. 2008. S100 protein family and its application in clinical practice. *Hippokratia,* 12**,** 198-204.

SEMOV, A., MORENO, M. J., ONICHTCHENKO, A., ABULROB, A., BALL, M., EKIEL, I., PIETRZYNSKI, G., STANIMIROVIC, D. & ALAKHOV, V. 2005. Metastasis-associated protein S100A4 induces angiogenesis through interaction with Annexin II and accelerated plasmin formation. *J Biol Chem,* 280**,** 20833-41.

SHEKOUH, A. R., THOMPSON, C. C., PRIME, W., CAMPBELL, F., HAMLETT, J., HERRINGTON, C. S., LEMOINE, N. R., CRNOGORAC-JURCEVIC, T., BUECHLER, M. W., FRIESS, H., NEOPTOLEMOS, J. P., PENNINGTON, S. R. & COSTELLO, E. 2003. Application of laser capture microdissection combined with two-dimensional electrophoresis for the discovery of differentially regulated proteins in pancreatic ductal adenocarcinoma. *Proteomics,* 3**,** 1988-2001.

SHELDON, H., HEIKAMP, E., TURLEY, H., DRAGOVIC, R., THOMAS, P., OON, C. E., LEEK, R., EDELMANN, M., KESSLER, B., SAINSON, R. C., SARGENT, I., LI, J. L. & HARRIS, A. L. 2010. New mechanism for Notch signaling to endothelium at a distance by Delta-like 4 incorporation into exosomes. *Blood,* 116**,** 2385-94.

SHERBET, G. V. 2009. Metastasis promoter S100A4 is a potentially valuable molecular target for cancer therapy. *Cancer Lett,* 280**,** 15-30.

SHIH, J. Y. & YANG, P. C. 2011. The EMT regulator slug and lung carcinogenesis. *Carcinogenesis,* 32**,** 1299-304.

SHIN, H., LEE, J., KIM, Y., JANG, S., LEE, Y., KIM, S. & LEE, Y. 2017. Knockdown of BC200 RNA expression reduces cell migration and invasion by destabilizing mRNA for calcium-binding protein S100A11. *RNA Biol***,** 1-13.

SILICIANO, J. D., CANMAN, C. E., TAYA, Y., SAKAGUCHI, K., APPELLA, E. & KASTAN, M. B. 1997. DNA damage induces phosphorylation of the amino terminus of p53. *Genes Dev,* 11**,** 3471-81.

SIVEEN, K. S., SIKKA, S., SURANA, R., DAI, X., ZHANG, J., KUMAR, A. P., TAN, B. K., SETHI, G. & BISHAYEE, A. 2014. Targeting the STAT3 signaling pathway in cancer: role of synthetic and natural inhibitors. *Biochim Biophys Acta,* 1845**,** 136-54.

SMALL, J. V. & RESCH, G. P. 2005. The comings and goings of actin: coupling protrusion and retraction in cell motility. *Curr Opin Cell Biol,* 17**,** 517-23.

SMIT, M. A. & PEEPER, D. S. 2010. Epithelial-mesenchymal transition and senescence: two cancer-related processes are crossing paths. *Aging (Albany NY),* 2**,** 735-41.

SOHN, T. A., YEO, C. J., CAMERON, J. L., KONIARIS, L., KAUSHAL, S., ABRAMS, R. A., SAUTER, P. K., COLEMAN, J., HRUBAN, R. H. & LILLEMOE, K. D. 2000. Resected adenocarcinoma of the pancreas-616 patients: results, outcomes, and prognostic indicators. *J Gastrointest Surg,* 4**,** 567-79.

SONG, Z., LIN, Y., YE, X., FENG, C., LU, Y., YANG, G. & DONG, C. 2016. Expression of IL-1alpha and IL-6 is Associated with Progression and Prognosis of Human Cervical Cancer. *Med Sci Monit,* 22**,** 4475-4481.

SPANO, D., HECK, C., DE ANTONELLIS, P., CHRISTOFORI, G. & ZOLLO, M. 2012. Molecular networks that regulate cancer metastasis. *Semin Cancer Biol,* 22**,** 234-49.

SPIKE, B. T. & WAHL, G. M. 2011. p53, Stem Cells, and Reprogramming: Tumor Suppression beyond Guarding the Genome. *Genes Cancer,* 2**,** 404-19.

STARK, A. P., CHANG, H. H., JUNG, X., MORO, A., HERTZER, K., XU, M., SCHMIDT, A., HINES, O. J. & EIBL, G. 2015. E-cadherin expression in obesity-associated, Kras-initiated pancreatic ductal adenocarcinoma in mice. *Surgery,* 158**,** 1564-72.

STRUTZ, F., OKADA, H., LO, C. W., DANOFF, T., CARONE, R. L., TOMASZEWSKI, J. E. & NEILSON, E. G. 1995. Identification and characterization of a fibroblast marker: FSP1. *J Cell Biol,* 130**,** 393-405.

SUBRAMANIAM, K. S., OMAR, I. S., KWONG, S. C., MOHAMED, Z., WOO, Y. L., MAT ADENAN, N. A. & CHUNG, I. 2016. Cancer-associated fibroblasts promote endometrial cancer growth via activation of interleukin-6/STAT-3/c-Myc pathway. *Am J Cancer Res,* 6**,** 200-13.

SULLIVAN, N. J., SASSER, A. K., AXEL, A. E., VESUNA, F., RAMAN, V., RAMIREZ, N., OBERYSZYN, T. M. & HALL, B. M. 2009. Interleukin-6 induces an epithelial-mesenchymal transition phenotype in human breast cancer cells. *Oncogene,* 28**,** 2940-7.

SYN, N., WANG, L., SETHI, G., THIERY, J. P. & GOH, B. C. 2016. Exosome-Mediated Metastasis: From Epithelial-Mesenchymal Transition to Escape from Immunosurveillance. *Trends Pharmacol Sci,* 37**,** 606-17.

TAN, M., HEIZMANN, C. W., GUAN, K., SCHAFER, B. W. & SUN, Y. 1999. Transcriptional activation of the human S100A2 promoter by wild-type p53. *FEBS Lett,* 445**,** 265-8.

TAN, M. H., NOWAK, N. J., LOOR, R., OCHI, H., SANDBERG, A. A., LOPEZ, C., PICKREN, J. W., BERJIAN, R., DOUGLASS, H. O., JR. & CHU, T. M. 1986. Characterization of a new primary human pancreatic tumor line. *Cancer Invest,* 4**,** 15-23.

TAN, R., WANG, L., SONG, J., LI, J. & HE, T. 2017. Expression and significance of Twist, estrogen receptor, and E-cadherin in human breast cancer cells and tissues. *J Cancer Res Ther,* 13**,** 707-714.

TANAKA, M., ICHIKAWA-TOMIKAWA, N., SHISHITO, N., NISHIURA, K., MIURA, T., HOZUMI, A., CHIBA, H., YOSHIDA, S., OHTAKE, T. & SUGINO, T. 2015. Co-expression of S100A14 and S100A16 correlates with a poor prognosis in human breast cancer and promotes cancer cell invasion. *BMC Cancer,* 15**,** 53.

TANIGUCHI, K. & KARIN, M. 2014. IL-6 and related cytokines as the critical lynchpins between inflammation and cancer. *Semin Immunol,* 26**,** 54-74.

TANIUCHI, K., NAKAGAWA, H., HOSOKAWA, M., NAKAMURA, T., EGUCHI, H., OHIGASHI, H., ISHIKAWA, O., KATAGIRI, T. & NAKAMURA, Y. 2005. Overexpressed P-cadherin/CDH3 promotes motility of pancreatic cancer cells by interacting with p120ctn and activating rho-family GTPases. *Cancer Res,* 65**,** 3092-9.

TAO, L., HUANG, G., WANG, R., PAN, Y., HE, Z., CHU, X., SONG, H. & CHEN, L. 2016. Cancer-associated fibroblasts treated with cisplatin facilitates chemoresistance of lung adenocarcinoma through IL-11/IL-11R/STAT3 signaling pathway. *Sci Rep,* 6**,** 38408.

TARABYKINA, S., GRIFFITHS, T. R., TULCHINSKY, E., MELLON, J. K., BRONSTEIN, I. B. & KRIAJEVSKA, M. 2007. Metastasis-associated protein S100A4: spotlight on its role in cell migration. *Curr Cancer Drug Targets,* 7**,** 217-28.

TECHASEN, A., NAMWAT, N., LOILOME, W., DUANGKUMPHA, K., PUAPAIROJ, A., SAYA, H. & YONGVANIT, P. 2014. Tumor necrosis factor-alpha modulates epithelial mesenchymal transition mediators ZEB2 and S100A4 to promote cholangiocarcinoma progression. *J Hepatobiliary Pancreat Sci,* 21**,** 703-11.

TENG, Y. & LI, X. 2014. The roles of HLH transcription factors in epithelial mesenchymal transition and multiple molecular mechanisms. *Clin Exp Metastasis,* 31**,** 367-77.

TENG, Y., XIE, X., WALKER, S., WHITE, D. T., MUMM, J. S. & COWELL, J. K. 2013. Evaluating human cancer cell metastasis in zebrafish. *BMC Cancer,* 13**,** 453.

THERY, C., AMIGORENA, S., RAPOSO, G. & CLAYTON, A. 2006. Isolation and characterization of exosomes from cell culture supernatants and biological fluids. *Curr Protoc Cell Biol,* Chapter 3**,** Unit 3 22.

THIERY, J. P., ACLOQUE, H., HUANG, R. Y. & NIETO, M. A. 2009. Epithelial-mesenchymal transitions in development and disease. *Cell,* 139**,** 871-90.

THOMPSON, E. W., NEWGREEN, D. F. & TARIN, D. 2005. Carcinoma invasion and metastasis: a role for epithelial-mesenchymal transition? *Cancer Res,* 65**,** 5991-5; discussion 5995.

TIBBETTS, R. S., BRUMBAUGH, K. M., WILLIAMS, J. M., SARKARIA, J. N., CLIBY, W. A., SHIEH, S. Y., TAYA, Y., PRIVES, C. & ABRAHAM, R. T. 1999. A role for ATR in the DNA damage-induced phosphorylation of p53. *Genes Dev,* 13**,** 152-7.

TOBIA, C., GARIANO, G., DE SENA, G. & PRESTA, M. 2013. Zebrafish embryo as a tool to study tumor/endothelial cell cross-talk. *Biochim Biophys Acta,* 1832**,** 1371-7.

TOMONO, T., YANO, K. & OGIHARA, T. 2017. Snail-Induced Epithelial-to-Mesenchymal Transition Enhances P-gp-Mediated Multidrug Resistance in HCC827 Cells. *J Pharm Sci,* 106**,** 2642-2649.

TOYONAGA, T., NAKANO, K., NAGANO, M., ZHAO, G., YAMAGUCHI, K., KUROKI, S., EGUCHI, T., CHIJIIWA, K., TSUNEYOSHI, M. & TANAKA, M. 2003. Blockade of constitutively activated Janus kinase/signal transducer and activator of transcription-3 pathway inhibits growth of human pancreatic cancer. *Cancer Lett,* 201**,** 107-16.

TRAMS, E. G., LAUTER, C. J., SALEM, N., JR. & HEINE, U. 1981. Exfoliation of membrane ecto-enzymes in the form of micro-vesicles. *Biochim Biophys Acta,* 645**,** 63-70.

TSUKAMOTO, N., EGAWA, S., AKADA, M., ABE, K., SAIKI, Y., KANEKO, N., YOKOYAMA, S., SHIMA, K., YAMAMURA, A., MOTOI, F., ABE, H., HAYASHI, H., ISHIDA, K., MORIYA, T., TABATA, T., KONDO, E., KANAI, N., GU, Z., SUNAMURA, M., UNNO, M. & HORII, A. 2013. The expression of S100A4 in human pancreatic cancer is associated with invasion. *Pancreas,* 42**,** 1027-33.

TUROVSKAYA, O., FOELL, D., SINHA, P., VOGL, T., NEWLIN, R., NAYAK, J., NGUYEN, M., OLSSON, A., NAWROTH, P. P., BIERHAUS, A., VARKI, N., KRONENBERG, M., FREEZE, H. H. & SRIKRISHNA, G. 2008. RAGE, carboxylated glycans and S100A8/A9 play essential roles in colitis-associated carcinogenesis. *Carcinogenesis,* 29**,** 2035-43.

VANDEWALLE, C., COMIJN, J., DE CRAENE, B., VERMASSEN, P., BRUYNEEL, E., ANDERSEN, H., TULCHINSKY, E., VAN ROY, F. & BERX, G. 2005. SIP1/ZEB2 induces EMT by repressing genes of different epithelial cell-cell junctions. *Nucleic Acids Res,* 33**,** 6566-78.

VAZQUEZ RODRIGUEZ, G., ABRAHAMSSON, A., JENSEN, L. D. & DABROSIN, C. 2017. Estradiol Promotes Breast Cancer Cell Migration via Recruitment and Activation of Neutrophils. *Cancer Immunol Res,* 5**,** 234-247.

VELLA, L. J. 2014. The emerging role of exosomes in epithelial-mesenchymal-transition in cancer. *Front Oncol,* 4**,** 361.

VIEIRA, A. F. & PAREDES, J. 2015. P-cadherin and the journey to cancer metastasis. *Mol Cancer,* 14**,** 178.

VIMALACHANDRAN, D., GREENHALF, W., THOMPSON, C., LUTTGES, J., PRIME, W., CAMPBELL, F., DODSON, A., WATSON, R., CRNOGORAC-JURCEVIC, T., LEMOINE, N., NEOPTOLEMOS, J. & COSTELLO, E. 2005. High nuclear S100A6 (Calcyclin) is significantly associated with poor survival in pancreatic cancer patients. *Cancer Res,* 65**,** 3218-25.

VINCENT, A., HERMAN, J., SCHULICK, R., HRUBAN, R. H. & GOGGINS, M. 2011. Pancreatic cancer. *Lancet,* 378**,** 607-20.

WANG, H. Y., ZHANG, J. Y., CUI, J. T., TAN, X. H., LI, W. M., GU, J. & LU, Y. Y. 2010. Expression status of S100A14 and S100A4 correlates with metastatic potential and clinical outcome in colorectal cancer after surgery. *Oncol Rep,* 23**,** 45-52.

WANG, J., CAO, Z., ZHANG, X. M., NAKAMURA, M., SUN, M., HARTMAN, J., HARRIS, R. A., SUN, Y. & CAO, Y. 2015a. Novel mechanism of macrophage-mediated metastasis revealed in a zebrafish model of tumor development. *Cancer Res,* 75**,** 306-15.

WANG, J., NIKHIL, K., VICCARO, K., CHANG, L., JACOBSEN, M., SANDUSKY, G. & SHAH, K. 2017a. The Aurora-A-Twist1 axis promotes highly aggressive phenotypes in pancreatic carcinoma. *J Cell Sci,* 130**,** 1078-1093.

WANG, S. P., WANG, W. L., CHANG, Y. L., WU, C. T., CHAO, Y. C., KAO, S. H., YUAN, A., LIN, C. W., YANG, S. C., CHAN, W. K., LI, K. C., HONG, T. M. & YANG, P. C. 2009. p53 controls cancer cell invasion by inducing the MDM2-mediated degradation of Slug. *Nat Cell Biol,* 11**,** 694-704.

WANG, T., LIANG, Y., THAKUR, A., ZHANG, S., LIU, F., KHAN, H., SHI, P., WANG, N., CHEN, M. & REN, H. 2017b. Expression and clinicopathological significance of S100 calcium binding protein A2 in lung cancer patients of Chinese Han ethnicity. *Clin Chim Acta,* 464**,** 118-122.

WANG, X., YANG, J., QIAN, J., LIU, Z., CHEN, H. & CUI, Z. 2015b. S100A14, a mediator of epithelial-mesenchymal transition, regulates proliferation, migration and invasion of human cervical cancer cells. *Am J Cancer Res,* 5**,** 1484-95.

WANG, X. G., MENG, Q., QI, F. M. & YANG, Q. F. 2014. Blocking TGF-beta inhibits breast cancer cell invasiveness via ERK/S100A4 signal. *Eur Rev Med Pharmacol Sci,* 18**,** 3844-53.

WANG, Y., CHU, Y., YUE, B., MA, X., ZHANG, G., XIANG, H., LIU, Y., WANG, T., WU, X. & CHEN, B. 2017c. Adipose-derived mesenchymal stem cells promote osteosarcoma proliferation and metastasis by activating the STAT3 pathway. *Oncotarget,* 8**,** 23803-23816.

WEI, D., LE, X., ZHENG, L., WANG, L., FREY, J. A., GAO, A. C., PENG, Z., HUANG, S., XIONG, H. Q., ABBRUZZESE, J. L. & XIE, K. 2003. Stat3 activation regulates the expression of vascular endothelial growth factor and human pancreatic cancer angiogenesis and metastasis. *Oncogene,* 22**,** 319-29.

WEINSTEIN, B. 2002. Vascular cell biology in vivo: a new piscine paradigm? *Trends Cell Biol,* 12**,** 439-45.

WERTMAN, J., VEINOTTE, C. J., DELLAIRE, G. & BERMAN, J. N. 2016. The Zebrafish Xenograft Platform: Evolution of a Novel Cancer Model and Preclinical Screening Tool. *Adv Exp Med Biol,* 916**,** 289-314.

WHITE, R. M., SESSA, A., BURKE, C., BOWMAN, T., LEBLANC, J., CEOL, C., BOURQUE, C., DOVEY, M., GOESSLING, W., BURNS, C. E. & ZON, L. I. 2008. Transparent adult zebrafish as a tool for in vivo transplantation analysis. *Cell Stem Cell,* 2**,** 183-9.

WHITESIDE, T. L. 2016. Tumor-Derived Exosomes and Their Role in Cancer Progression. *Adv Clin Chem,* 74**,** 103-41.

WICKI, R., FRANZ, C., SCHOLL, F. A., HEIZMANN, C. W. & SCHAFER, B. W. 1997. Repression of the candidate tumor suppressor gene S100A2 in breast cancer is mediated by site-specific hypermethylation. *Cell Calcium,* 22**,** 243-54.

WILDER, P. T., CHARPENTIER, T. H., LIRIANO, M. A., GIANNI, K., VARNEY, K. M., POZHARSKI, E., COOP, A., TOTH, E. A., MACKERELL, A. D. & WEBER, D. J. 2010. In vitro screening and structural characterization of inhibitors of the S100B-p53 interaction. *Int J High Throughput Screen,* 2010**,** 109-126.

WINTER, J. M., MAITRA, A. & YEO, C. J. 2006. Genetics and pathology of pancreatic cancer. *HPB (Oxford),* 8**,** 324-36.

WU, W. S., HEINRICHS, S., XU, D., GARRISON, S. P., ZAMBETTI, G. P., ADAMS, J. M. & LOOK, A. T. 2005. Slug antagonizes p53-mediated apoptosis of hematopoietic progenitors by repressing puma. *Cell,* 123**,** 641-53.

WU, Y. S., CHUNG, I., WONG, W. F., MASAMUNE, A., SIM, M. S. & LOOI, C. Y. 2017. Paracrine IL-6 signaling mediates the effects of pancreatic stellate cells on epithelial-mesenchymal transition via Stat3/Nrf2 pathway in pancreatic cancer cells. *Biochim Biophys Acta,* 1861**,** 296-306.

XIA, X. H., XIAO, C. J. & SHAN, H. 2017. Facilitation of liver cancer SMCC7721 cell aging by sirtuin 4 via inhibiting JAK2/STAT3 signal pathway. *Eur Rev Med Pharmacol Sci,* 21**,** 1248-1253.

XIAO, M. B., JIANG, F., NI, W. K., CHEN, B. Y., LU, C. H., LI, X. Y. & NI, R. Z. 2012. High expression of S100A11 in pancreatic adenocarcinoma is an unfavorable prognostic marker. *Med Oncol,* 29**,** 1886-91.

XIE, J., MENDEZ, J. D., MENDEZ-VALENZUELA, V. & AGUILAR-HERNANDEZ, M. M. 2013. Cellular signalling of the receptor for advanced glycation end products (RAGE). *Cell Signal,* 25**,** 2185-97.

XIONG, H., HONG, J., DU, W., LIN, Y. W., REN, L. L., WANG, Y. C., SU, W. Y., WANG, J. L., CUI, Y., WANG, Z. H. & FANG, J. Y. 2012. Roles of STAT3 and ZEB1 proteins in E-cadherin down-regulation and human colorectal cancer epithelial-mesenchymal transition. *J Biol Chem,* 287**,** 5819-32.

XU, D. H., ZHU, Z., WAKEFIELD, M. R., XIAO, H., BAI, Q. & FANG, Y. 2016a. The role of IL-11 in immunity and cancer. *Cancer Lett,* 373**,** 156-63.

XU, H., LI, M., ZHOU, Y., WANG, F., LI, X., WANG, L. & FAN, Q. 2016b. S100A4 participates in epithelial-mesenchymal transition in breast cancer via targeting MMP2. *Tumour Biol,* 37**,** 2925-32.

XU, J., LAMOUILLE, S. & DERYNCK, R. 2009. TGF-beta-induced epithelial to mesenchymal transition. *Cell Res,* 19**,** 156-72.

XU, X., SU, B., XIE, C., WEI, S., ZHOU, Y., LIU, H., DAI, W., CHENG, P., WANG, F., XU, X. & GUO, C. 2014. Sonic hedgehog-Gli1 signaling pathway regulates the epithelial mesenchymal transition (EMT) by mediating a new target gene, S100A4, in pancreatic cancer cells. *PLoS One,* 9**,** e96441.

XU, X., ZHOU, Y., XIE, C., WEI, S. M., GAN, H., HE, S., WANG, F., XU, L., LU, J., DAI, W., HE, L., CHEN, P., WANG, X. & GUO, C. 2012. Genome-wide screening reveals an EMT molecular network mediated by Sonic hedgehog-Gli1 signaling in pancreatic cancer cells. *PLoS One,* 7**,** e43119.

XU, Y. 2003. Regulation of p53 responses by post-translational modifications. *Cell Death Differ,* 10**,** 400-3.

XUE, M., ZHU, F. Y., CHEN, L. & WANG, K. 2017. HoxB9 promotes the migration and invasion via TGF-beta1/Smad2/Slug signaling pathway in oral squamous cell carcinoma. *Am J Transl Res,* 9**,** 1151-1161.

YACHIDA, S., WHITE, C. M., NAITO, Y., ZHONG, Y., BROSNAN, J. A., MACGREGOR-DAS, A. M., MORGAN, R. A., SAUNDERS, T., LAHERU, D. A., HERMAN, J. M., HRUBAN, R. H., KLEIN, A. P., JONES, S., VELCULESCU, V., WOLFGANG, C. L. & IACOBUZIO-DONAHUE, C. A. 2012. Clinical significance of the genetic landscape of pancreatic cancer and implications for identification of potential long-term survivors. *Clin Cancer Res,* 18**,** 6339-47.

YADAV, A., KUMAR, B., DATTA, J., TEKNOS, T. N. & KUMAR, P. 2011. IL-6 promotes head and neck tumor metastasis by inducing epithelial-mesenchymal transition via the JAK-STAT3-SNAIL signaling pathway. *Mol Cancer Res,* 9**,** 1658-67.

YAMADA, S., FUCHS, B. C., FUJII, T., SHIMOYAMA, Y., SUGIMOTO, H., NOMOTO, S., TAKEDA, S., TANABE, K. K., KODERA, Y. & NAKAO, A. 2013. Epithelial-to-mesenchymal transition predicts prognosis of pancreatic cancer. *Surgery,* 154**,** 946-54.

YAMMANI, R. R., LONG, D. & LOESER, R. F. 2009. Interleukin-7 stimulates secretion of S100A4 by activating the JAK/STAT signaling pathway in human articular chondrocytes. *Arthritis Rheum,* 60**,** 792-800.

YAN, W., CHEN, J., CHEN, Z. & CHEN, H. 2016. Deregulated miR-296/S100A4 axis promotes tumor invasion by inducing epithelial-mesenchymal transition in human ovarian cancer. *Am J Cancer Res,* 6**,** 260-9.

YANG, J., MANI, S. A., DONAHER, J. L., RAMASWAMY, S., ITZYKSON, R. A., COME, C., SAVAGNER, P., GITELMAN, I., RICHARDSON, A. & WEINBERG, R. A. 2004. Twist, a master regulator of morphogenesis, plays an essential role in tumor metastasis. *Cell,* 117**,** 927-39.

YANG, J. & WEINBERG, R. A. 2008. Epithelial-mesenchymal transition: at the crossroads of development and tumor metastasis. *Dev Cell,* 14**,** 818-29.

YANG, X. J., CUI, W., GU, A., XU, C., YU, S. C., LI, T. T., CUI, Y. H., ZHANG, X. & BIAN, X. W. 2013. A novel zebrafish xenotransplantation model for study of glioma stem cell invasion. *PLoS One,* 8**,** e61801.

YANG, Y., ZHANG, N., ZHU, J., HONG, X. T., LIU, H., OU, Y. R., SU, F., WANG, R., LI, Y. M. & WU, Q. 2017. Downregulated connexin32 promotes EMT through the Wnt/beta-catenin pathway by targeting Snail expression in hepatocellular carcinoma. *Int J Oncol*.

YANG, Z., SUN, B., LI, Y., ZHAO, X., ZHAO, X., GU, Q., AN, J., DONG, X., LIU, F. & WANG, Y. 2015. ZEB2 promotes vasculogenic mimicry by TGF-beta1 induced epithelial-to-mesenchymal transition in hepatocellular carcinoma. *Exp Mol Pathol,* 98**,** 352-9.

YILMAZ, M. & CHRISTOFORI, G. 2009. EMT, the cytoskeleton, and cancer cell invasion. *Cancer Metastasis Rev,* 28**,** 15-33.

YOSHIDA, R., MORITA, M., SHOJI, F., NAKASHIMA, Y., MIURA, N., YOSHINAGA, K., KOGA, T., TOKUNAGA, E., SAEKI, H., OKI, E., ODA, Y. & MAEHARA, Y. 2015. Clinical Significance of SIP1 and E-cadherin in Patients with Esophageal Squamous Cell Carcinoma. *Ann Surg Oncol,* 22**,** 2608-14.

YOU, Y., SHAN, Y., CHEN, J., YUE, H., YOU, B., SHI, S., LI, X. & CAO, X. 2015. Matrix metalloproteinase 13-containing exosomes promote nasopharyngeal carcinoma metastasis. *Cancer Sci,* 106**,** 1669-77.

YU, H., PARDOLL, D. & JOVE, R. 2009. STATs in cancer inflammation and immunity: a leading role for STAT3. *Nat Rev Cancer,* 9**,** 798-809.

YU, S., CAO, H., SHEN, B. & FENG, J. 2015. Tumor-derived exosomes in cancer progression and treatment failure. *Oncotarget,* 6**,** 37151-68.

YUAN, J., ZHANG, F. & NIU, R. 2015. Multiple regulation pathways and pivotal biological functions of STAT3 in cancer. *Sci Rep,* 5**,** 17663.

YUAN, T. M., LIANG, R. Y., HSIAO, N. W. & CHUANG, S. M. 2014. The S100A4 D10V polymorphism is related to cell migration ability but not drug resistance in gastric cancer cells. *Oncol Rep,* 32**,** 2307-18.

YUNIS, A. A., ARIMURA, G. K. & RUSSIN, D. J. 1977. Human pancreatic carcinoma (MIA PaCa-2) in continuous culture: sensitivity to asparaginase. *Int J Cancer,* 19**,** 128-35.

YUSUP, A., HUJI, B., FANG, C., WANG, F., DADIHAN, T., WANG, H. J. & UPUR, H. 2017. Expression of trefoil factors and TWIST1 in colorectal cancer and their correlation with metastatic potential and prognosis. *World J Gastroenterol,* 23**,** 110-120.

ZHA, C., JIANG, X. H. & PENG, S. F. 2015. iTRAQ-based quantitative proteomic analysis on S100 calcium binding protein A2 in metastasis of laryngeal cancer. *PLoS One,* 10**,** e0122322.

ZHAI, X., ZHU, H., WANG, W., ZHANG, S., ZHANG, Y. & MAO, G. 2014. Abnormal expression of EMT-related proteins, S100A4, Vimentin and E-cadherin, is correlated with clinicopathological features and prognosis in HCC. *Med Oncol,* 31**,** 970.

ZHANG, B., XUAN, C., JI, Y., ZHANG, W. & WANG, D. 2015a. Zebrafish xenotransplantation as a tool for in vivo cancer study. *Fam Cancer,* 14**,** 487-93.

ZHANG, F., LU, Y. X., CHEN, Q., ZOU, H. M., ZHANG, J. M., HU, Y. H., LI, X. M., ZHANG, W. J., ZHANG, W., LIN, C. & LI, X. N. 2017a. Identification of NCK1 as a novel downstream effector of STAT3 in colorectal cancer metastasis and angiogenesis. *Cell Signal,* 36**,** 67-78.

ZHANG, H. Y., ZHENG, X. Z., WANG, X. H., XUAN, X. Y., WANG, F. & LI, S. S. 2012. S100A4 mediated cell invasion and metastasis of esophageal squamous cell carcinoma via the regulation of MMP-2 and E-cadherin activity. *Mol Biol Rep,* 39**,** 199-208.

ZHANG, J., LIU, C., SHI, W., YANG, L., ZHANG, Q., CUI, J., FANG, Y., LI, Y., REN, G., YANG, S. & XIANG, R. 2016. The novel VEGF receptor 2 inhibitor YLL545 inhibits angiogenesis and growth in breast cancer. *Oncotarget,* 7**,** 41067-41080.

ZHANG, J. M. & AN, J. 2007. Cytokines, inflammation, and pain. *Int Anesthesiol Clin,* 45**,** 27-37.

ZHANG, W., LIU, Y. & WANG, C. W. 2014. S100A4 promotes squamous cell laryngeal cancer Hep-2 cell invasion via NF-kB/MMP-9 signal. *Eur Rev Med Pharmacol Sci,* 18**,** 1361-7.

ZHANG, X., YANG, M., SHI, H., HU, J., WANG, Y., SUN, Z. & XU, S. 2017b. Reduced E-cadherin facilitates renal cell carcinoma progression by WNT/beta-catenin signaling activation. *Oncotarget,* 8**,** 19566-19576.

ZHANG, X., YUAN, X., SHI, H., WU, L., QIAN, H. & XU, W. 2015b. Exosomes in cancer: small particle, big player. *J Hematol Oncol,* 8**,** 83.

ZHANG, X., ZHENG, K., LI, C., ZHAO, Y., LI, H., LIU, X., LONG, Y. & YAO, J. 2017c. Nobiletin inhibits invasion via inhibiting AKT/GSK3beta/beta-catenin signaling pathway in Slug-expressing glioma cells. *Oncol Rep,* 37**,** 2847-2856.

ZHAO, F. T., JIA, Z. S., YANG, Q., SONG, L. & JIANG, X. J. 2013. S100A14 promotes the growth and metastasis of hepatocellular carcinoma. *Asian Pac J Cancer Prev,* 14**,** 3831-6.

ZHAO, P., MENG, M., XU, B., DONG, A., NI, G. & LU, L. 2017. Decreased expression of MUC1 induces apoptosis and inhibits migration in pancreatic cancer PANC-1 cells via regulation of Slug pathway. *Cancer Biomark.*

ZHAO, S., HUANG, J. & YE, J. 2015. A fresh look at zebrafish from the perspective of cancer research. *J Exp Clin Cancer Res,* 34**,** 80.

ZHAO, Z., CHENG, X., WANG, Y., HAN, R., LI, L., XIANG, T., HE, L., LONG, H., ZHU, B. & HE, Y. 2014. Metformin inhibits the IL-6-induced epithelial-mesenchymal transition and lung adenocarcinoma growth and metastasis. *PLoS One,* 9**,** e95884.

ZHENG, C., JIA, W., TANG, Y., ZHAO, H., JIANG, Y. & SUN, S. 2012. Mesothelin regulates growth and apoptosis in pancreatic cancer cells through p53-dependent and -independent signal pathway. *J Exp Clin Cancer Res,* 31**,** 84.

ZHENG, H., YANG, Y., HAN, J., JIANG, W. H., CHEN, C., WANG, M. C., GAO, R., LI, S., TIAN, T., WANG, J., MA, L. J., REN, H. & ZHOU, W. P. 2016. TMED3 promotes hepatocellular carcinoma progression via IL-11/STAT3 signaling. *Sci Rep,* 6**,** 37070.

ZHONG, L., YANG, J., CAO, Z., CHEN, X., HU, Y., LI, L. & YANG, S. 2017. Preclinical pharmacodynamic evaluation of drug candidate SKLB-178 in the treatment of non-small cell lung cancer. *Oncotarget,* 8**,** 12843-12854.

ZHOU, H., HUANG, Z., CHEN, X. & CHEN, S. 2017a. miR-98 inhibits expression of TWIST to prevent progression of non-small cell lung cancers. *Biomed Pharmacother,* 89**,** 1453-1461.

ZHOU, J., ZHANG, C., PAN, J., CHEN, L. & QI, S. T. 2017b. Interleukin6 induces an epithelialmesenchymal transition phenotype in human adamantinomatous craniopharyngioma cells and promotes tumor cell migration. *Mol Med Rep*.

ZHOU, Q. X., JIANG, X. M., WANG, Z. D., LI, C. L. & CUI, Y. F. 2015. Enhanced expression of suppresser of cytokine signaling 3 inhibits the IL-6-induced epithelial-to-mesenchymal transition and cholangiocarcinoma cell metastasis. *Med Oncol,* 32**,** 105.

ZHOU, W., PAN, H., XIA, T., XUE, J., CHENG, L., FAN, P., ZHANG, Y., ZHU, W., XUE, Y., LIU, X., DING, Q., LIU, Y. & WANG, S. 2014. Up-regulation of S100A16 expression promotes epithelial-mesenchymal transition via Notch1 pathway in breast cancer. *J Biomed Sci,* 21**,** 97.

ZHU, W., XUE, Y., LIANG, C., ZHANG, R., ZHANG, Z., LI, H., SU, D., LIANG, X., ZHANG, Y., HUANG, Q., LIU, M., LI, L., LI, D., ZHAO, A. Z. & LIU, Y. 2016. S100A16 promotes cell proliferation and metastasis via AKT and ERK cell signaling pathways in human prostate cancer. *Tumour Biol,* 37**,** 12241-12250.

ZHU, X., SHEN, H., YIN, X., LONG, L., CHEN, X., FENG, F., LIU, Y., ZHAO, P., XU, Y., LI, M., XU, W. & LI, Y. 2017. IL-6R/STAT3/miR-204 feedback loop contributes to cisplatin resistance of epithelial ovarian cancer cells. *Oncotarget*.

ZONI, E., CHEN, L., KARKAMPOUNA, S., GRANCHI, Z., VERHOEF, E. I., LA MANNA, F., KELBER, J., PELGER, R. C., HENRY, M. D., SNAAR-JAGALSKA, E., VAN LEENDERS, G. J., BEIMERS, L., KLOEN, P., GRAY, P. C., VAN DER PLUIJM, G. & KRUITHOF-DE JULIO, M. 2017. CRIPTO and its signaling partner GRP78 drive the metastatic phenotype in human osteotropic prostate cancer. *Oncogene*.

http://www.cancerresearchuk.org/about-cancer/pancreatic-cancer

https://www.cancer.org/cancer/pancreatic-cancer/about/key-statistics.html

https://en.wikipedia.org/wiki/Cadherin

http://www.western-blot.us/western-blot-protocol/wet-western-blot.